Best Available
Copy
for all Pictures

AD-782 276

# PROCEEDINGS OF THE PRAIRIE SMOKE V RF MEASUREMENTS DATA WORKSHOP HELD ON 8-9 NOVEMBER 1973

P. A. Fialer

Stanford Research Institute

Prepared for:

Office of Naval Research
Advanced Research Projects Agency

March 1974

DISTRIBUTED BY:

NTIS

National Technical Information Service
U. S. DEPARTMENT OF COMMERCE
5285 Port Royal Road, Springfield Va. 22151

SECURITY CLASSIFICATION OF THIS PAGE (When Data Entered)

# REPORT DOCUMENTATION PAGE

READ INSTRUCTIONS BEFORE COMPLETING FORM

| | |
|---|---|
| 1. REPORT NUMBER | 2. GOVT ACCESSION NO. |
| 3. RECIPIENT'S CATALOG NUMBER | AD-782 276 |
| 4. TITLE (and Subtitle) | PROCEEDINGS OF THE PRAIRIE SMOKE V RF MEASUREMENTS DATA WORKSHOP--8, 9 November 1973 |
| 5. TYPE OF REPORT & PERIOD COVERED | Proceedings |
| 6. PERFORMING ORG. REPORT NUMBER | SRI Project 8727 |
| 7. AUTHOR(s) | Compiled by P. A. Fialer |
| 8. CONTRACT OR GRANT NUMBER(s) | N00014-70-C-0413<br>ARPA Order 1656 |
| 9. PERFORMING ORGANIZATION NAME AND ADDRESS | Stanford Research Institute<br>Menlo Park, California 94025 |
| 10. PROGRAM ELEMENT, PROJECT, TASK AREA & WORK UNIT NUMBERS | ONR NR 088-047 |
| 11. CONTROLLING OFFICE NAME AND ADDRESS | Defense Advanced Research Projects Agency<br>Arlington, Virginia 22209 |
| 12. REPORT DATE | March 1974 |
| 13. NO. OF PAGES | 208 |
| 14. MONITORING AGENCY NAME & ADDRESS (if diff. from Controlling Office) | Office of Naval Research, Code 464<br>Arlington, Virginia 22217 |
| 15. SECURITY CLASS. (of this report) | UNCLASSIFIED |
| 15a. DECLASSIFICATION/DOWNGRADING SCHEDULE | |

16. DISTRIBUTION STATEMENT (of this report)

Approved for public release; distribution unlimited.

17. DISTRIBUTION STATEMENT (of the abstract entered in Block 20, if different from report)

18. SUPPLEMENTARY NOTES

19. KEY WORDS (Continue on reverse side if necessary and identify by block number)

Ionospheric modification
Ionospheric heating
Ionospheric irregularities
Ionospheric scatter propagation
(continued)

20. ABSTRACT (Continue on reverse side if necessary and identify by block number)

Project PRAIRIE SMOKE is a series of coordinated field experiments investigating the effects of HF heating on the ionosphere. These proceedings describe results from various experiments conducted during the PRAIRIE SMOKE V test series. PRAIRIE SMOKE V was carried out during the period 10 September to 10 October 1973. Its primary purpose was to collect data regarding the efficiency of ionospheric heating, including the dependences of the various
(continued)



DD FORM 1 JAN 73 1473 EDITION OF 1 NOV 65 IS OBSOLETE

SECURITY CLASSIFICATION OF THIS PAGE (When Data Entered)

19. KEY WORDS (Continued)

Field-aligned scattering
Electron-density fluctuations
Plasma waves
Ion acoustic waves
Plasma instabilities

20 ABSTRACT (Continued)

observable effects of heating on the frequency, power, and modulation of the heater.

The papers included in these proceedings present some of the data from the PRAIRIE SMOKE V tests together with analyses of these data that have been completed at this time. Although a comprehensive "yield model" for ionospheric heating is not available at present, most of the major characteristics of heater yield have been determined. In many cases, a more complete model may be obtained from further analysis of the data obtained during the PRAIRIE SMOKE V tests.

Included also in these proceedings are papers describing previously unpublished experimental and analytical results derived from earlier test data and analyses.

March 1974

PROCEEDINGS OF THE

# Prairie Smoke V

RF MEASUREMENTS DATA WORKSHOP

8, 9 NOVEMBER 1973


*Compiled by:*

P. A. FIALER



THESE PROCEEDINGS WERE SPONSORED BY THE DEFENSE ADVANCED RESEARCH PROJECTS AGENCY OF THE DEPARTMENT OF DEFENSE AND WERE MONITORED BY ONR UNDER CONTRACT NO. N00014-70-C-0413; ARPA ORDER 1656, PROGRAM CODE 3E30.




*Copy No.* ......8.....

## FOREWORD

The PRAIRIE SMOKE V field experiments are the last of a series of tests whose major objective has been to obtain a basic understanding of many of the interesting phenomena produced by ionospheric heating. The program has been successful in accomplishing this objective and in revealing many new and unexpected phenomena. The usefulness of ionospheric heating has been demonstrated, both as a means of gaining new insights into ionospheric physics and as a tool for research in basic plasma physics. It appears that future work in both these areas bears promise of additional important results.

On behalf of all of the participants in the PRAIRIE SMOKE program, it seems appropriate at this time to express our thanks to Dr. William F. Utlaut, Deputy Director of the Office of Telecommunications/Institute for Telecommunication Sciences (ITS), whose foresight and planning transformed the possibility of significant ionospheric modification by high powered radio waves into a reality. The operating procedures requested by many of the experimentors in the PRAIRIE SMOKE program have frequently demanded extraordinary efforts on the part of those involved with operating the Platteville heating facility. Many ITS personnel worked long, hard hours to make the program a success, and the help provided by Dr. Utlaut and his staff has been greatly appreciated. Special thanks are due to Mr. Edmond J. Violette, Mr. John C. Carroll, Mr. Richard Chavez, Mr. Donald H. Layton, Mr. Laurence L. Melanson, Mr. Albert R. Mitz, and Mr. Gene E. Wasson for their considerable efforts on behalf of the program.

CONTENTS



**Preceding page blank**

# INTRODUCTION

Project PRAIRIE SMOKE is a series of coordinated field experiments investigating the effects of HF heating on the ionosphere. These proceedings describe results from various experiments conducted during the PRAIRIE SMOKE V test series. PRAIRIE SMOKE V was carried out during the period 10 September to 10 October 1973. Its primary purpose was to collect data regarding the efficiency of ionospheric heating, including the dependences of the various observable effects of heating on the frequency, power, and modulation of the heater.

The papers included in these proceedings present some of the data from the PRAIRIE SMOKE V tests together with analyses of these data that have been completed at this time. Although a comprehensive "yield model" for ionospheric heating is not available at present, most of the major characteristics of heater yield have been determined. In many cases, a more complete model may be obtained from further analysis of the data obtained during the PRAIRIE SMOKE V tests.

Included also in these proceedings are papers describing previously unpublished experimental and analytical results derived from earlier test data and analyses.

**Preceding page blank**

# RRI PRAIRIE SMOKE V RESULTS

J. Minkoff R. Kreppel M. Laviola

Riverside Research Institute
New York City, N.Y.

ABSTRACT

Measurements of field-aligned scattering from the F region of the ionosphere were made using the RTMS radar at the White Sands Missile Range at frequencies of 150.31 MHz and 354.90 MHz. The scattering irregularities were produced by operation of the Institute for Telecommunication Sciences' ionospheric heating facility at Platteville, Colorado.

A series of tests were made in which the effective radiated power of the heating transmitter was stepped through a number of power levels. Measurements of the backscattering cross section at 150 MHz indicate that the change in scattered power $\Delta P_R$ (expressed in dB), may be related to the change in heater power, $\Delta P_H$ (also in dB), by an expression of the form

$$\Delta P_R = k \Delta P_H$$

where k is a number between 0.57 and 0.65.

Measurements of the size of the heated region show that for heater frequencies below the F-region critical frequency ($f_oF2$), the east-west extent of the region is closely comparable to the calculated heater-antenna beamwidth. For heating frequencies above $f_oF2$, the east-west extent is larger by about a factor of 2.



Pages 1 and 2 are blank

## I INTRODUCTION

This report summarizes the RRI results of the PRAIRIE SMOKE (PS) V experiments which were carried out during mid-September 1973 using the RTMS radar at the White Sands Missile Range (WSMR). The major purpose of the RRI measurements was to determine the dependence of the VHF (150.31 MHz) and UHF (354.90 and 448.89 MHz) backscatter cross sections of the heated volume over Platteville, Colorado, on the value of the transmitted HF power of the Platteville Heater. These measurements fall under the general category of yield experiments, in which it is the purpose to determine the magnitude of the RF scattering cross section of the heated volume as a function of heater operating parameters such as antenna configuration and time of day, as well as HF power. The PS V experiments employed for the first time a newly installed antenna at Platteville covering the frequency range 2.6 to 3.4 MHz. The other Platteville heater antenna, which has been used on all previous PS experiments, covered the frequency range 4.6 to 10 MHz. Thus, with the use of both antennas, essentially 24-hour operation was possible. In addition to the yield measurements, experiments were also carried out for the purpose of measuring the east-west beamwidth of the heater antenna.

The RRI yield data include a considerable number of VHF measurements as well as a measurement carried out at the lower UHF frequency. Earlier yield measurements obtained during PS IV[1*] showed a definite tendency toward saturation of the RF cross section in the region of maximum heater power. The RRI PS V results, however, show little if any evidence of such saturation effects. The most probable reason for this difference is that, for PS V, the values of the HF heater power levels were determined much more accurately than was possible during

---

*References are listed at the end of the paper.

PS IV. The apparent saturation in the PS IV data may therefore be due to incorrect values of heater power used in plotting the results. A composite of the PS V yield results at VHF shows that $\Delta P_R$, the change in dB relative to the peak value of the measured RF cross section, and $\Delta P_H$, the change in dB relative to the peak value of the HF heater power, are related by the expression $\Delta P_R = k\Delta P_H$, where k is a number between 0.57 and 0.65.

With regard to measurements of the spatial extent of the heated volume, earlier experiments[2] have shown that, for $f_h/f_oF2 < 1$, where $f_h$ is the HF heater frequency and $f_oF2$ is the ordinary-ray critical frequency for the F2 layer, the heated volume is essentially confined to the beamwidth of the heater antenna. For $f_h/f_oF2 > 1$, however, the heated volume is observed to become significantly spread out, say by a factor of 2, in the east-west direction. As expected, these same effects were observed during PS V. In addition, use of PS V data for $f_h/f_oF2 < 1$ permitted making a much more accurate determination of the heater beamwidth than was feasible using data from earlier experiments. It was found, for the high-frequency heater antenna operating at 4.9 MHz, that the east-west extent of the volume can be modeled quite accurately using a gaussian function of the form, $\exp - (\phi^2/2\sigma_H^2)$ where $\phi$ is the angle measured from the perpendicular to the earth's surface at Platteville in the east-west direction, and $\sigma_H = 8.75°$. For other $f_h$ values, $\sigma_H$ must of course be scaled accordingly. This value of $\sigma_H$ corresponds to a 3-dB heater beamwidth of 24°. For $f_h = 4.9$ MHz this value of half-power beamwidth is in good agreement with reported[3] values.

## II YIELD MEASUREMENTS

The RTMS radar is located approximately 6 miles northwest of the RAM radar, for which the scattering geometry has been described in an earlier report.[2] During the yield experiments the basic mode of heater

operation was to maintain a given reference level, r, for 2 min, change the power by n dB and maintain at r + n for one min, and then switch back to r and maintain for 2 min, with this cycle being repeated a sufficient number of times to cover all the n-values specified for a given test. Using this basic procedure, two different yield tests were carried out (Test 2 and Test 3); these are depicted in Figures 1 and 2. Because in these experiments the variation in heater power rather than the absolute value is the parameter of interest, and since the $P_H$ values corresponding to the different values of n were measured with respect to the neighboring reference levels, this mode of operation served to

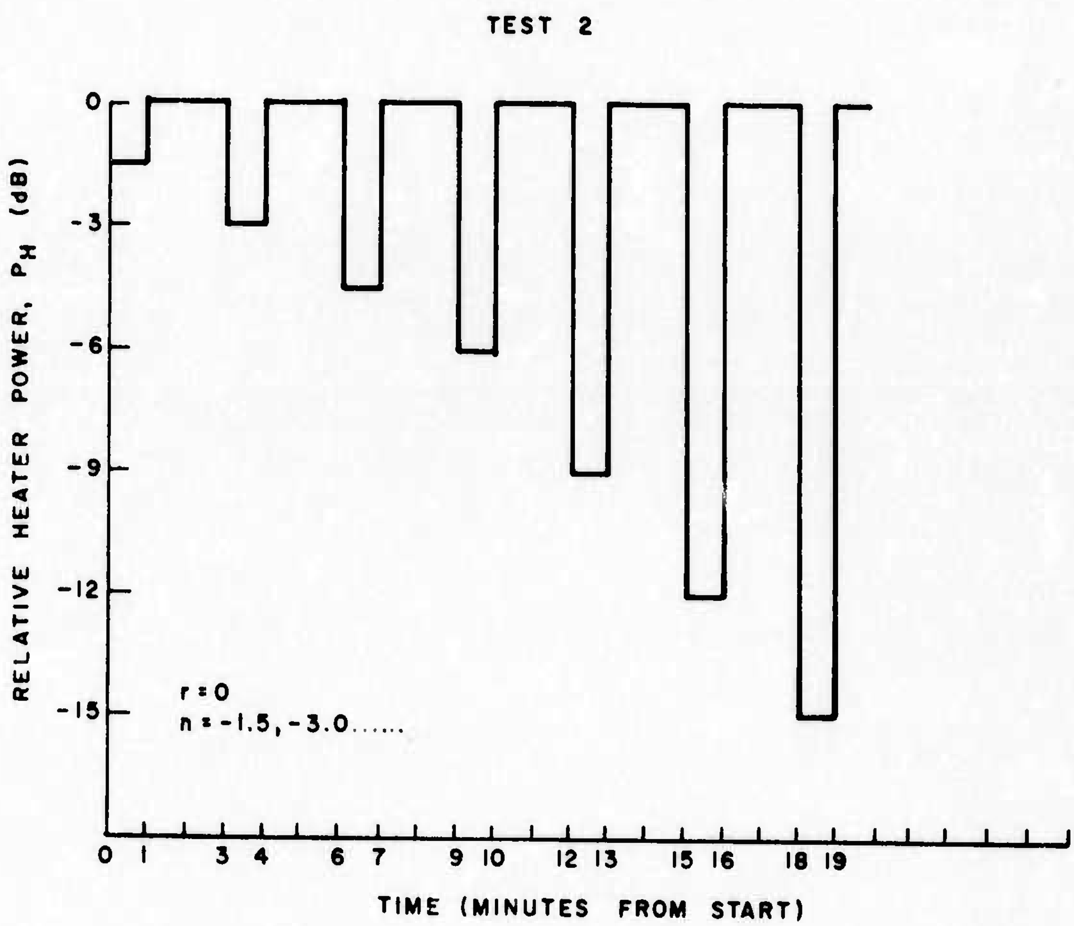


FIGURE 1 YIELD TEST (0 dB reference level)

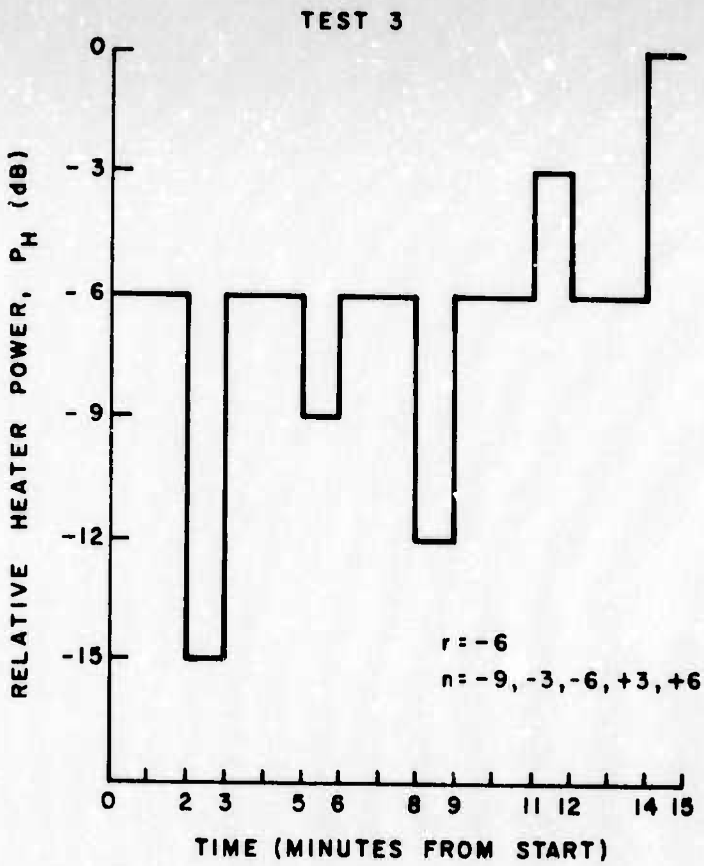


FIGURE 2 YIELD TEST (-6 dB reference level)

eliminate the effects of ionospheric changes taking place over time scales greater than ~1 min. As it turned out, however, ionospheric conditions during the time of the RRI experiments were extremely stable and very little variation in the reference levels was observed.

Plots of $P_R$ versus $P_H$ for all the RRI PS V observations at VHF are presented in Figures 3 through 11; the UHF measurements are presented in Figure 12. It is seen that, in contrast with the results of PS IV,[1] none of the PS V results shows evidence of saturation of $P_R$ in the neighborhood of $P_H = 0$. In these figures, the true values of $P_H$ used during the tests are seen to differ somewhat from the prescribed

values of n given in Figures 1 and 2. These true $P_H$ values were obtained by Stanford Research Institute (SRI) as the result of a detailed post-experiment analysis of the actual heater power levels during the experiment. As mentioned in Section I, the apparent saturation observed during PS IV may actually have been due to differences between the actual $P_H$ values and the specified values at the time of the experiments; unfortunately the necessary data for a similar post-experiment analysis on PS IV were not available.

In Figure 13 a composite of all the RRI PS V yield data, excluding the UHF results, is presented in a single scatter diagram. It is seen that the general result can be described by the expression $\Delta P_R = k\Delta P_H$, where k is between 0.57 and 0.65.

## III AZIMUTHAL TARGET EXTENT

As mentioned in Section I, it has been observed[2] on numerous occasions during the IVORY CORAL program that the heated volume is confined essentially to the HF heater beamwidth for $f_h/f_oF2 < 1$, and is observed to become significantly spread out in the east-west direction for $f_h/f_oF2 > 1$. These observations have been made from WSMR, using both the RAM and RTMS radars, by sweeping the antenna beam along an east-west line at a fixed elevation angle and measuring the received signal as a function of the azimuth angle. It is possible that spreading-out in the north-south direction also occurs, but this is not directly visible from WSMR because of the aspect sensitivity.

Similar measurements were made using RTMS during PS V. Unfortunately, because of extreme spreading of the ionogram traces it is not possible to determine to sufficient accuracy what the $f_oF2$ values were at the time of these measurements. Presumably, on the basis of previous observations, the results presented in Figures 14 and 15 represent

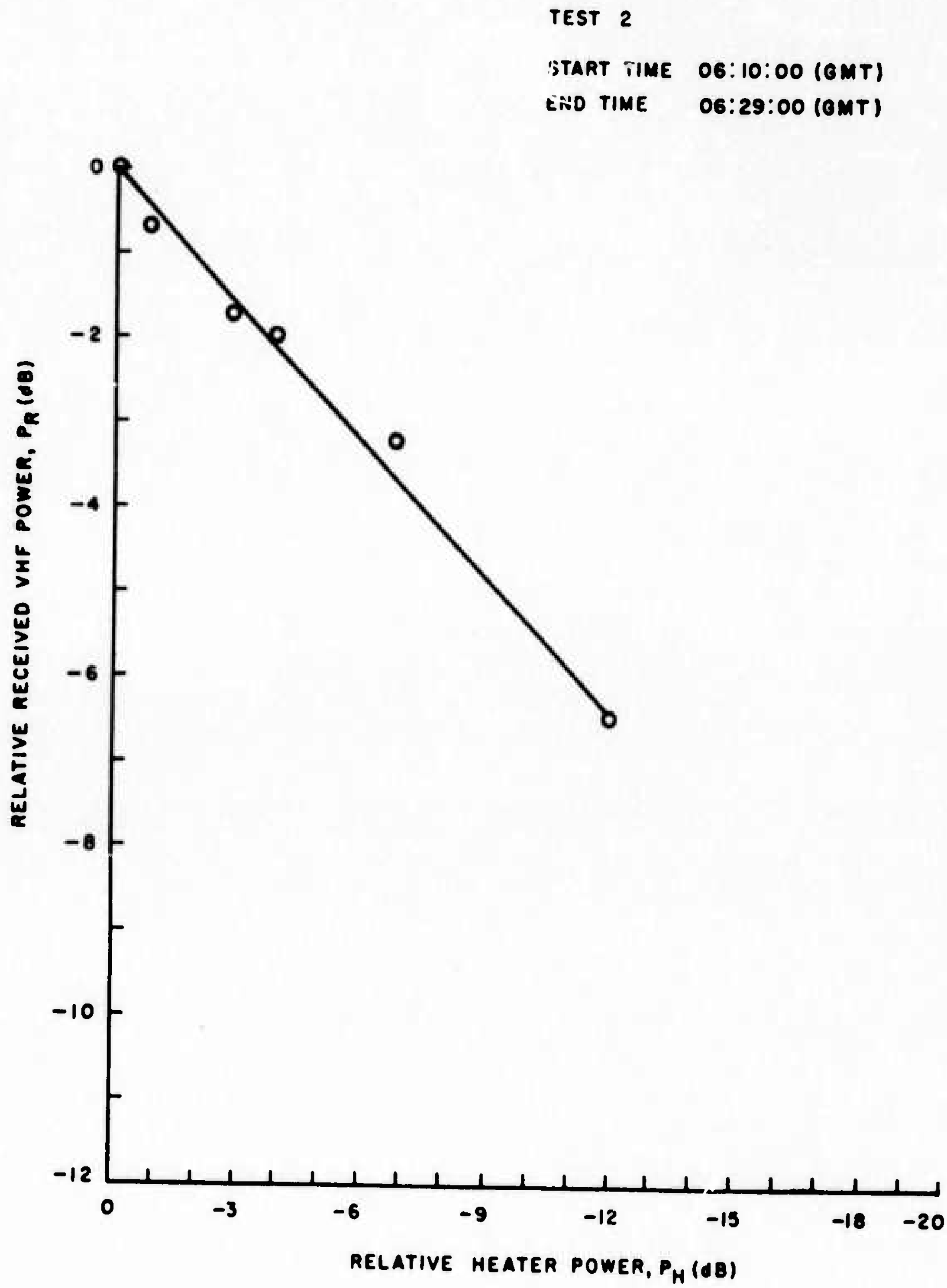


FIGURE 3 YIELD EXPERIMENT, 19 SEPTEMBER 1973 (GMT)

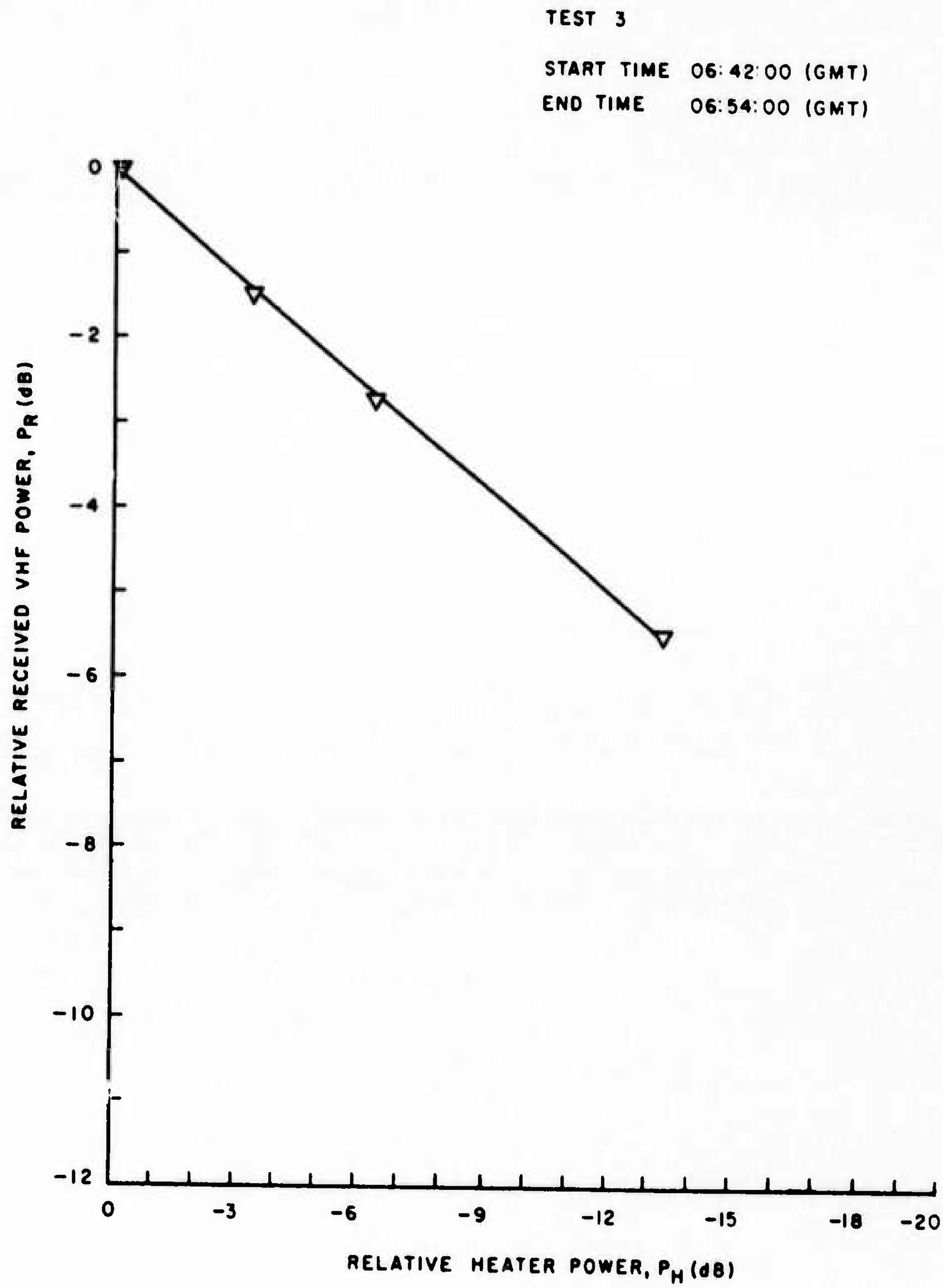


FIGURE 4 YIELD EXPERIMENT, 19 SEPTEMBER 1973 (GMT)

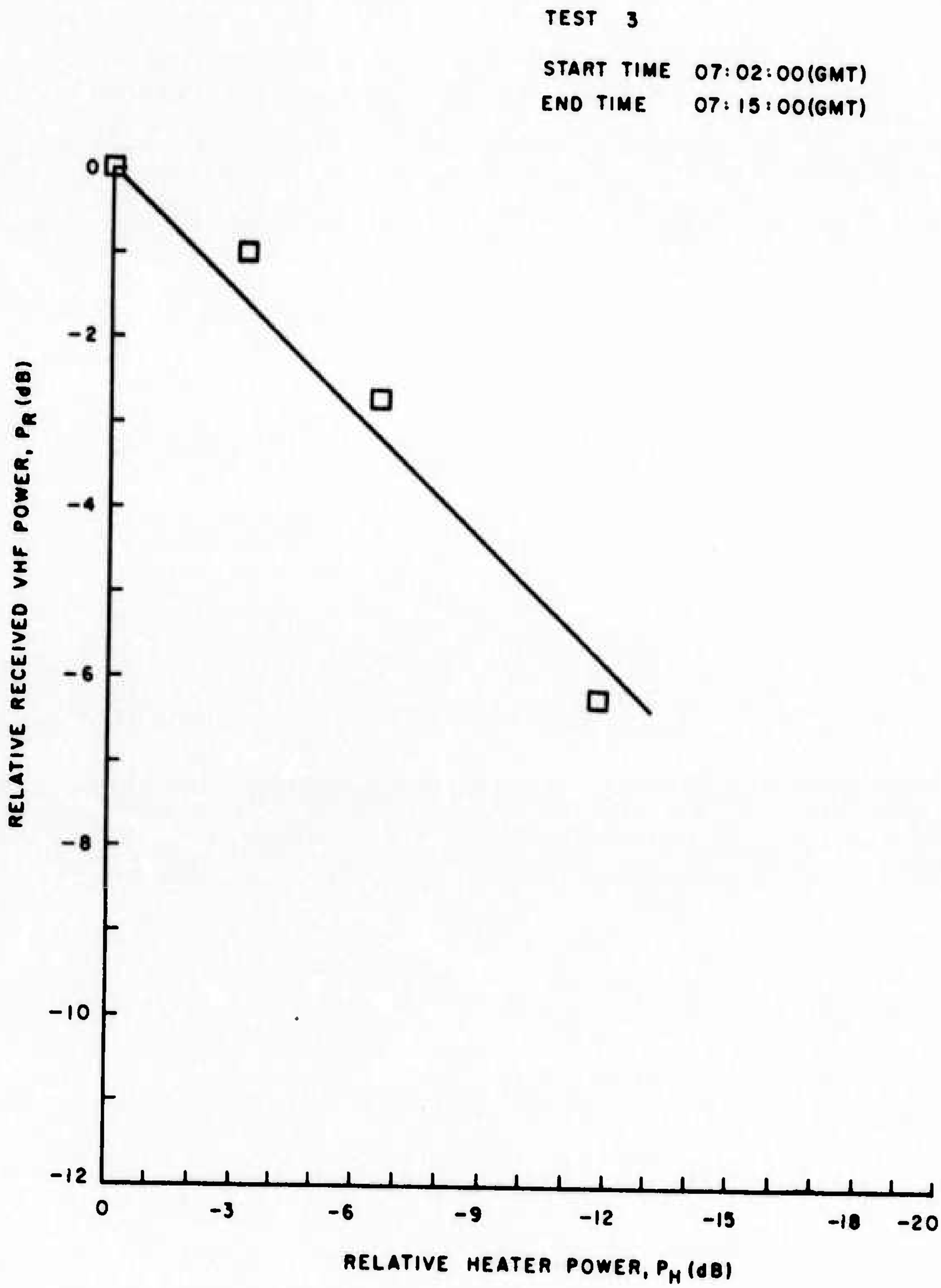


FIGURE 5 YIELD EXPERIMENT, 19 SEPTEMBER 1973 (GMT)

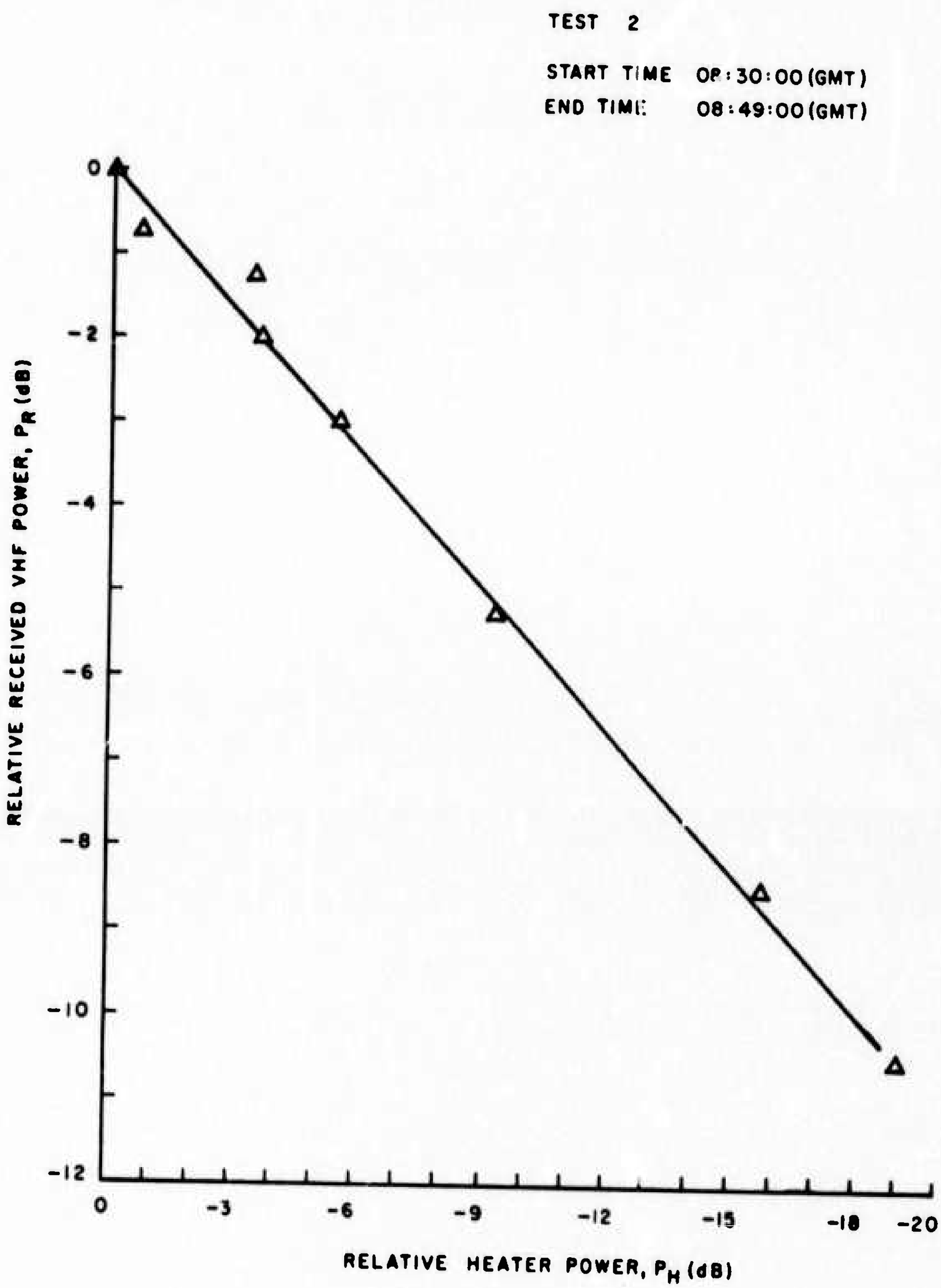


FIGURE 6 YIELD EXPERIMENT, 19 SEPTEMBER 1973 (GMT)

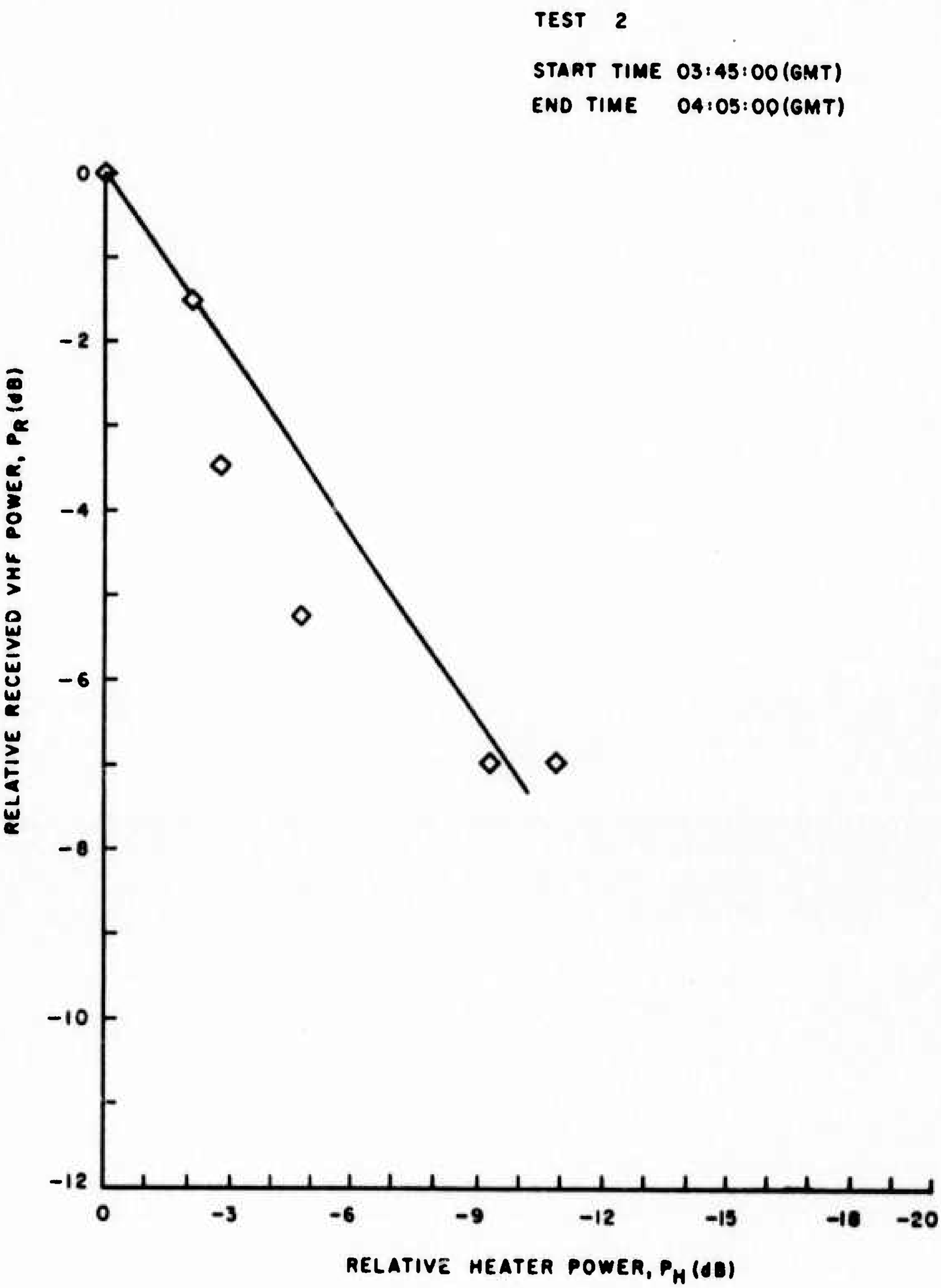


FIGURE 7 YIELD EXPERIMENT, 20 SEPTEMBER 1973 (GMT)

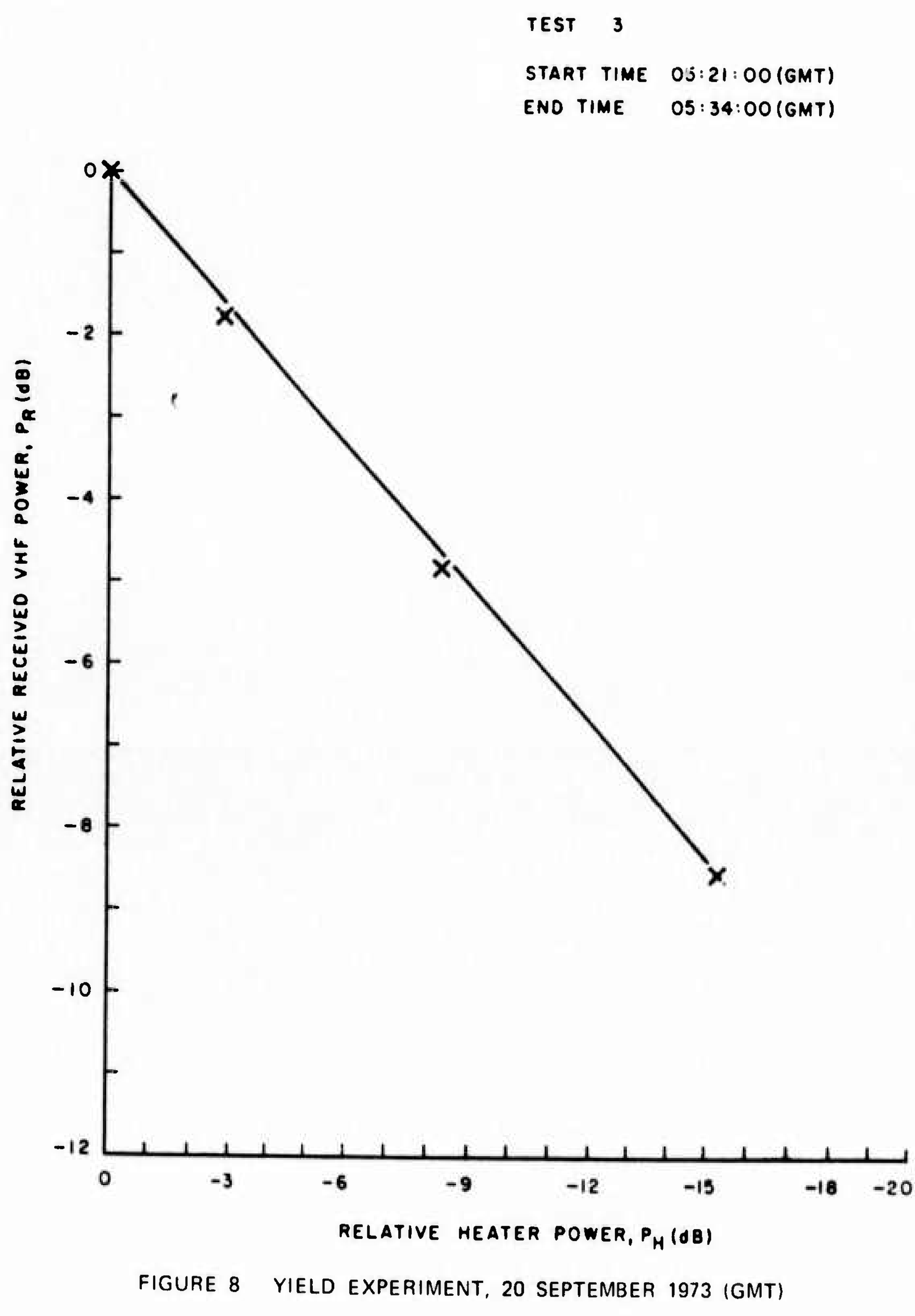


FIGURE 8 YIELD EXPERIMENT, 20 SEPTEMBER 1973 (GMT)

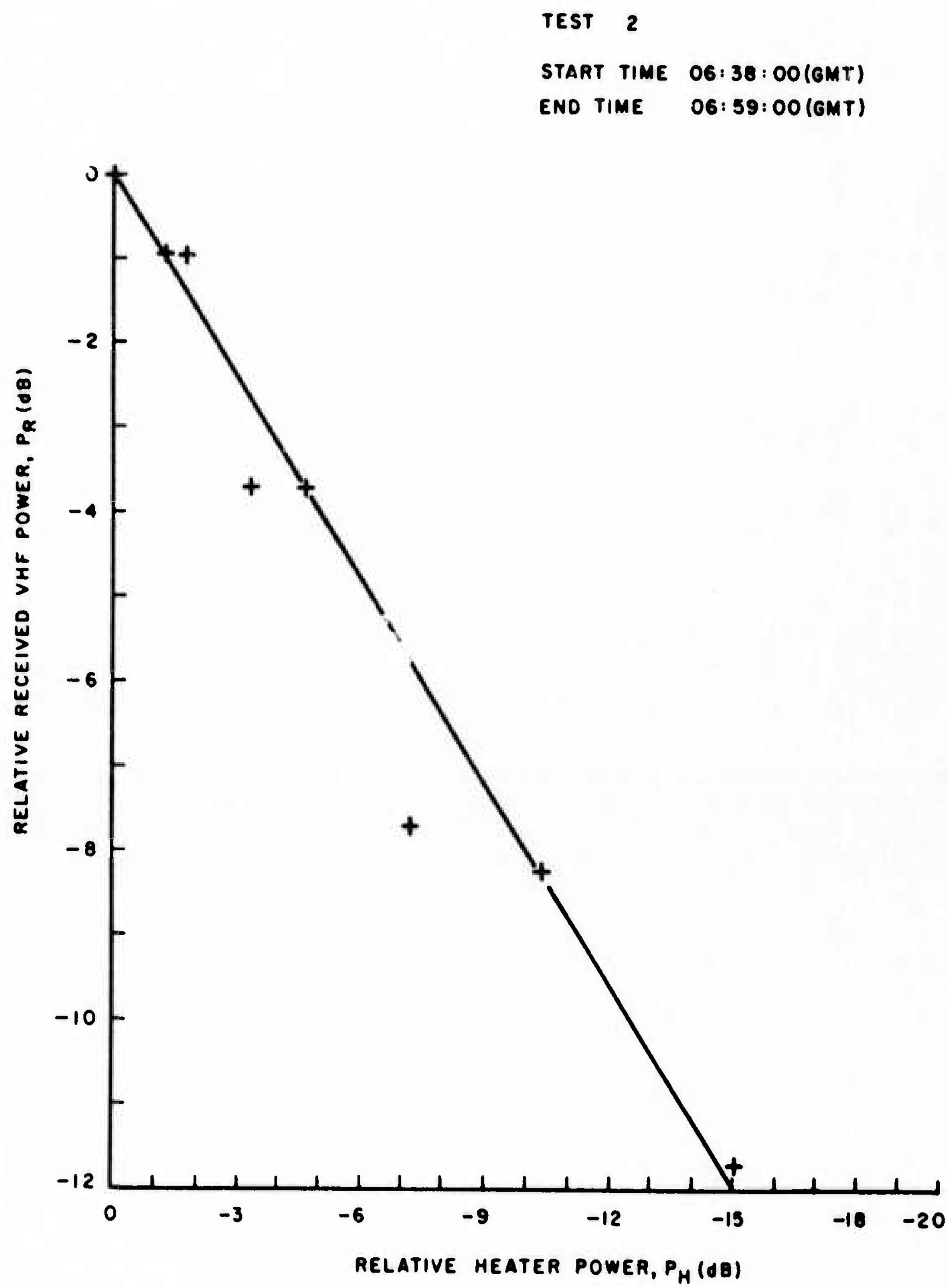


FIGURE 9 YIELD EXPERIMENT, 20 SEPTEMBER 1973 (GMT)

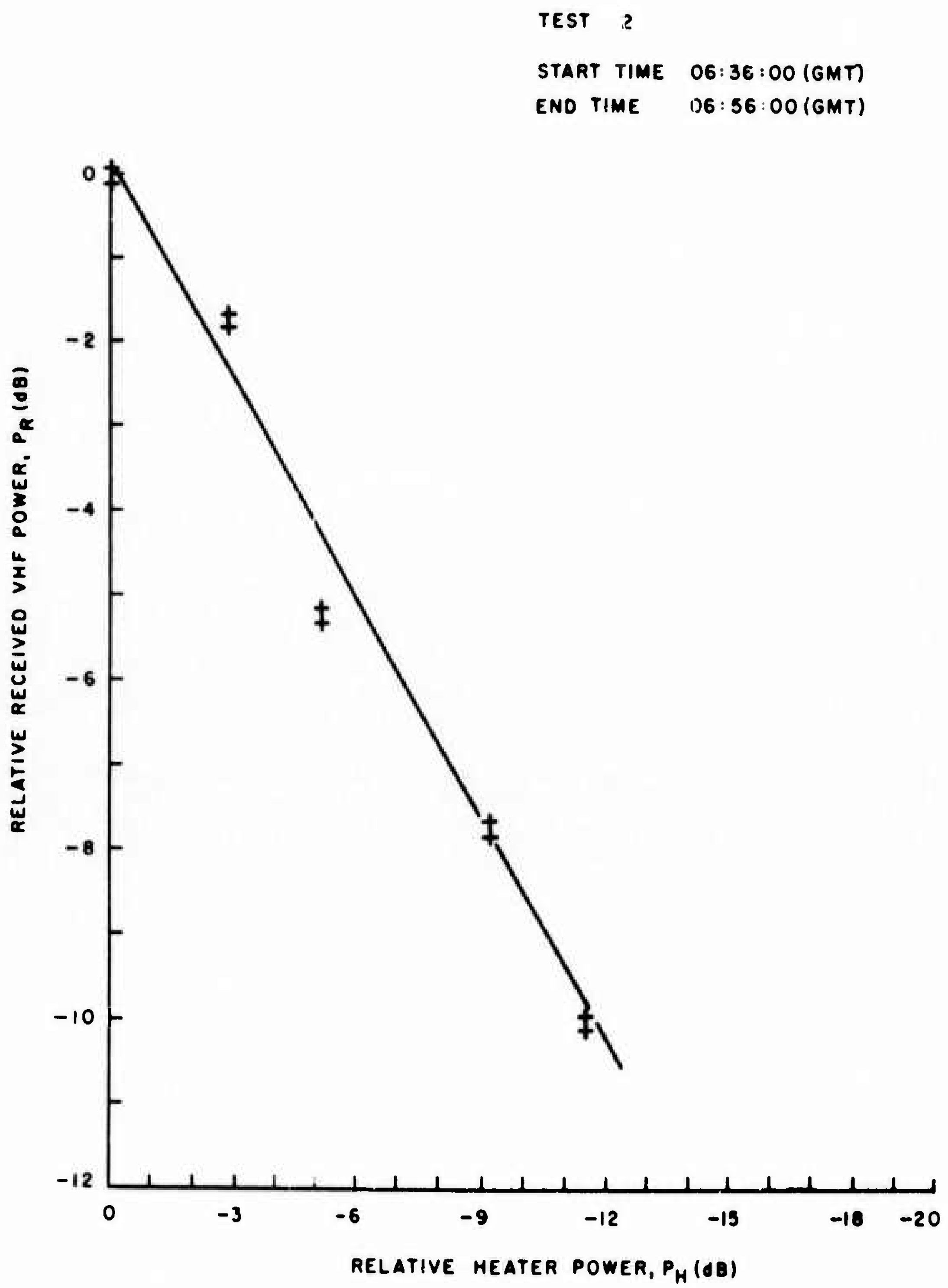


FIGURE 10 YIELD EXPERIMENT, 21 SEPTEMBER 1973 (GMT)

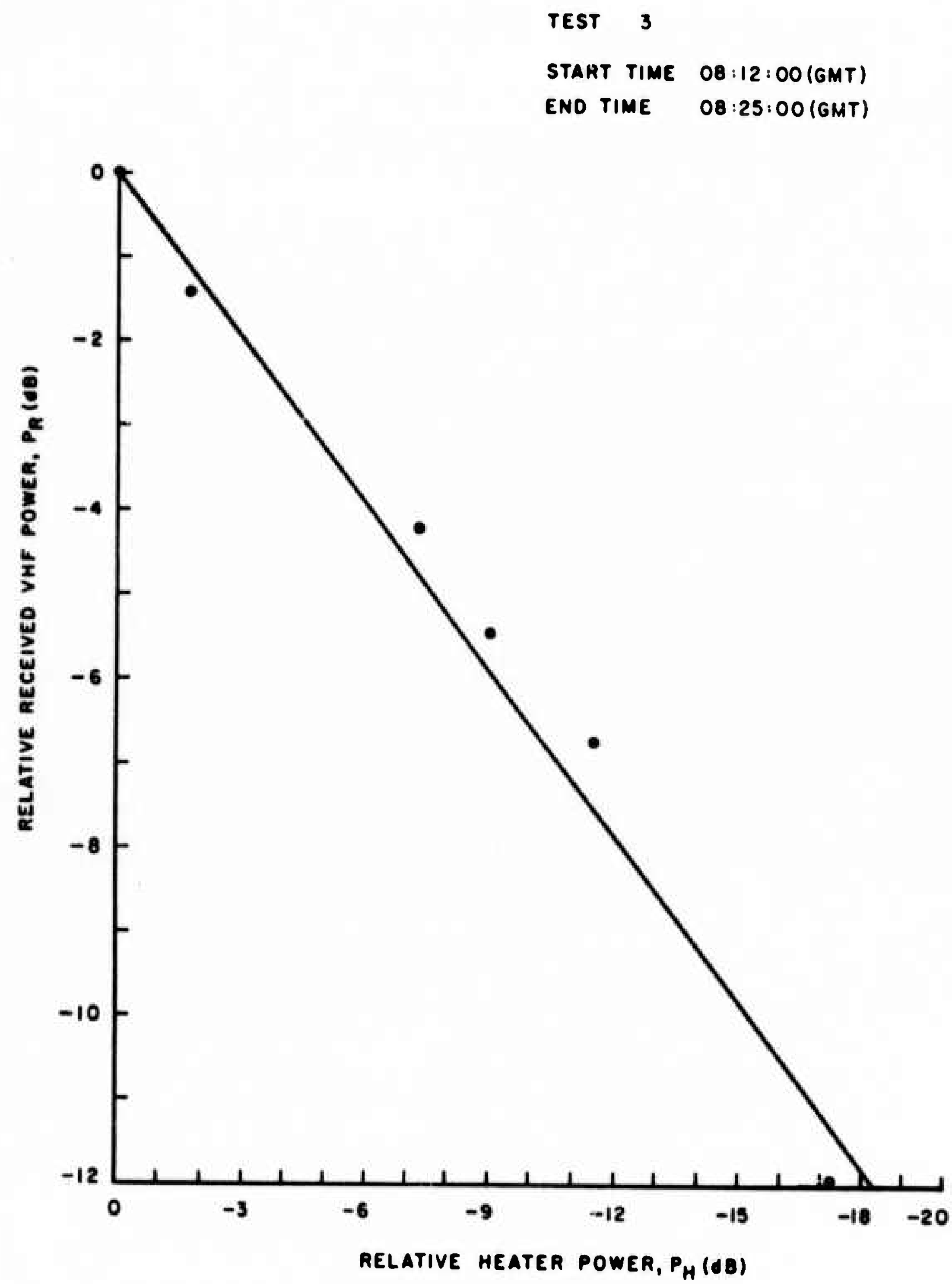


FIGURE 11 YIELD EXPERIMENT, 21 SEPTEMBER 1973 (GMT)

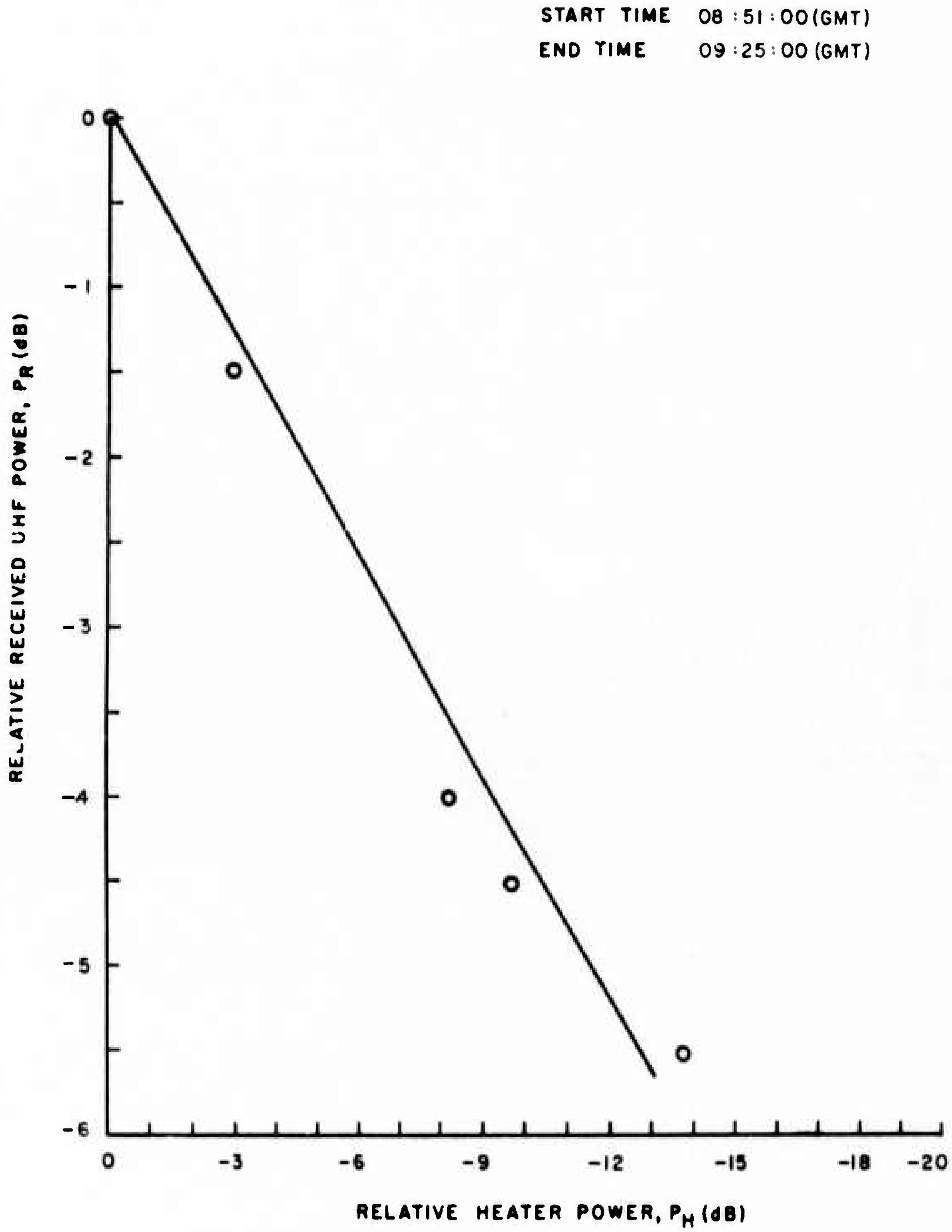


FIGURE 12 YIELD EXPERIMENT, 21 SEPTEMBER 1973 (GMT)

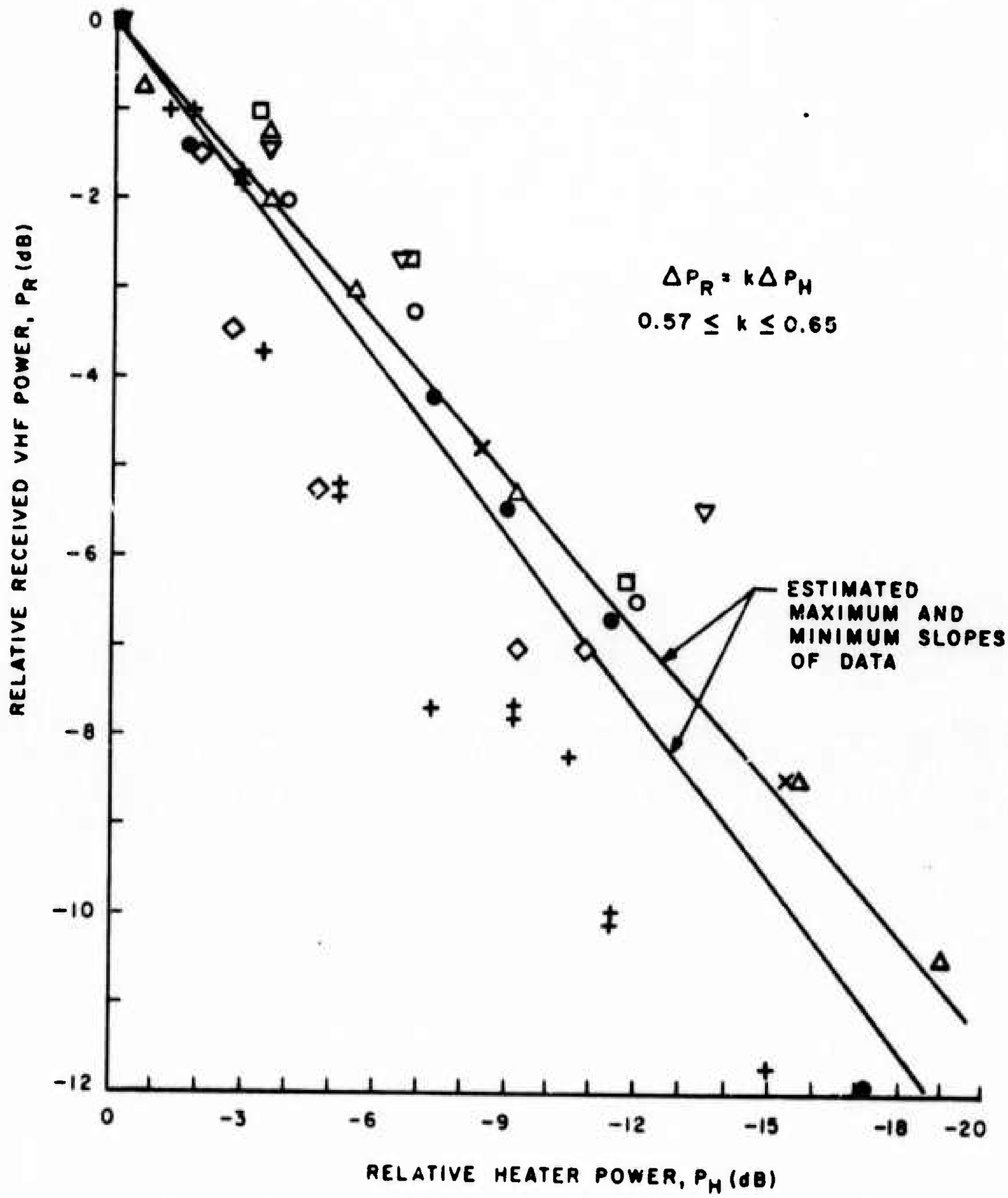


FIGURE 13 COMPOSITE RESULTS OF YIELD EXPERIMENTS

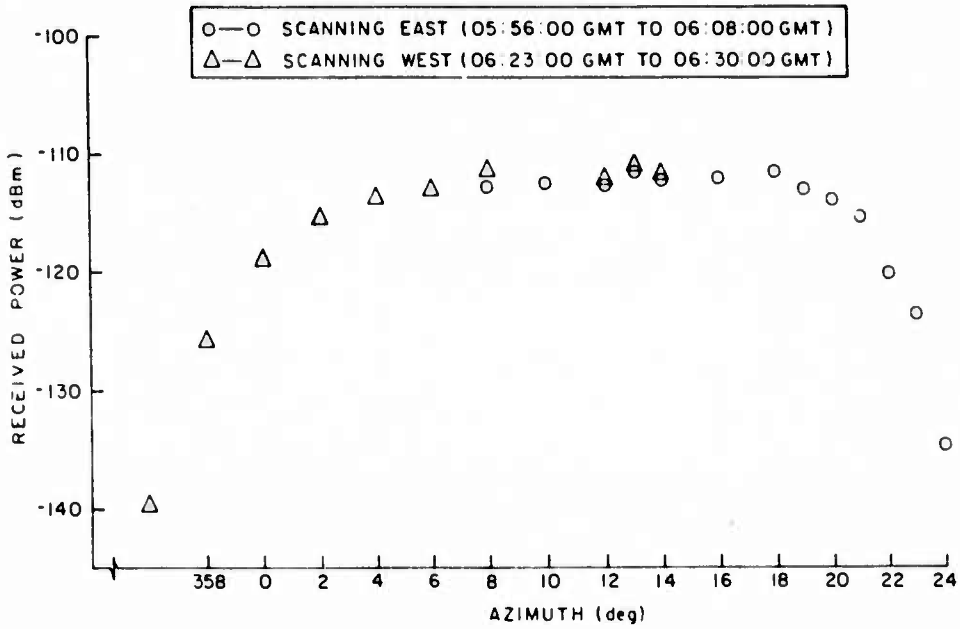


FIGURE 14 AZIMUTH SCAN, 20 SEPTEMBER 1973 (GMT)

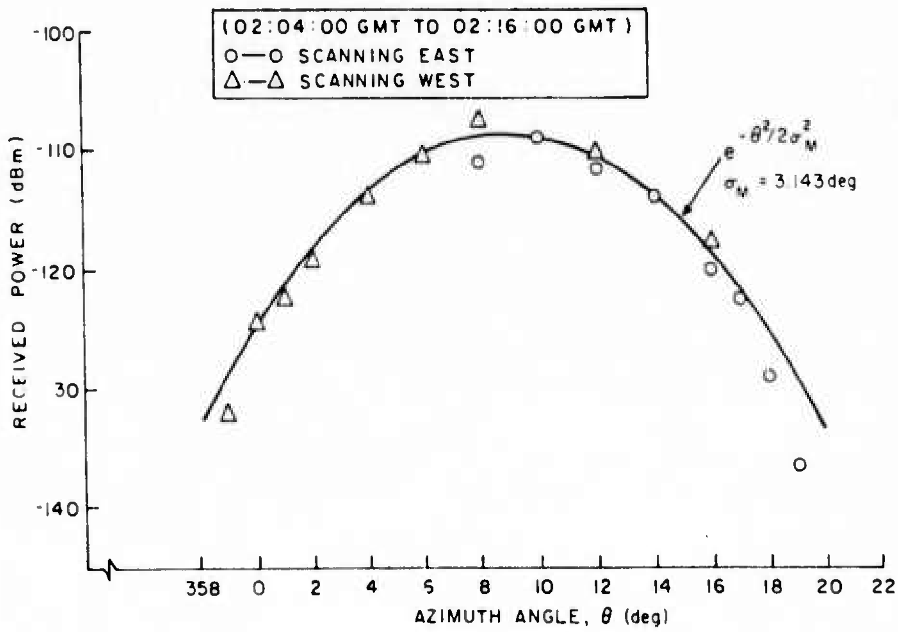


FIGURE 15 AZIMUTH SCAN, 20 SEPTEMBER 1973 (GMT)

conditions for which $f_h/f_oF2$ was, respectively, greater and less than unity. The extreme difference in the azimuthal extent of the heated volume for these two observations is evident.

The results shown in Figure 15 are seen to be a very good fit to a gaussian, $\exp -\left(\theta^2/2\sigma_M^2\right)$, where $\sigma_M = 3.143^\circ$ and $\theta$ is the azimuth angle. Assuming that $f_h/f_oF2 < 1$ at the time of these measurements, this result permits an accurate determination of the shape of the beamwidth of the Platteville heater antenna. That is, the measured result is a convolution of the square of the RTMS antenna beam with the azimuthal beam pattern of the heater antenna. By means of antenna-pattern measurements, the square of the RTMS antenna beam has been found to be, to a very good approximation, a gaussian, $\exp -\left(\theta^2/2\sigma_\alpha^2\right)$, where $\sigma_\alpha = 1.575$. This implies that, to a good approximation, the heater beamwidth can also be described by a gaussian function, since the convolution of two gaussians is also gaussian. Furthermore, if $\bar{\sigma}_H^2$ is the variance of the gaussian heater beamwidth as seen from WSMR, we have

$$\sigma_M^2 = \bar{\sigma}_H^2 + \sigma_\alpha^2$$

from which, using the number stated above, $\bar{\sigma}_H = 2.72^\circ$; at the time of this measurement the heater frequency was 4.9 MHz. Now this describes the angular width of the heater beam as seen from WSMR ($\sim$900 km). For heating at $\sim$280 km, the beamwidth seen from the ground would be approximately three times as large as this so we get, as a model of the Platteville low-frequency antenna beam, the function $\exp -\left(\phi^2/2\sigma_H^2\right)$, where $\phi$ is the angle measured from the perpendicular to the earth's surface at Platteville and $\sigma_H = 8.75^\circ$. This value of $\sigma_H$ corresponds to a 3-dB heater beamwidth of $24^\circ$, which is in very good agreement with reported values[3] scaled to the heater frequency (4.9 MHz) at the time of this measurement.

## REFERENCES


1. J. Minkoff, R. Kreppel, and M. Laviola, "RRI Results of PRAIRIE SMOKE IV Experiment (U)," Research Memorandum M-4/174-4-50, Riverside Research Institute, New York, N.Y. (4 May 1973), SECRET.

2. J. Minkoff and P. Kugelman, "Preliminary Summary of Results of IVORY CORAL Experiments (U)," Technical Memorandum TM-38/174-4-50, Riverside Research Institute, New York, N.Y. (29 December 1971), SECRET.

3. W. F. Utlaut, "Radio Wave Modification of the Ionosphere," J. Geophys. Res., Space Physics, Vol. 75, No. 31 (1 November 1970), UNCLASSIFIED.

# HF AND VHF OBSERVATIONS OF FIELD-ALIGNED SCATTERING

P. A. Fialer

Stanford Research Institute
Menlo Park, California

ABSTRACT

This paper presents results from the PRAIRIE SMOKE V test series that show the variation of field-aligned-scatter cross-section with various operating parameters of the ITS ionospheric-modification transmitter facility at Platteville, Colorado. Results of these experiments suggest that the plasma instabilities previously postulated are not the primary mechanism responsible for the production of field-aligned scattering. It was observed for the first time during this experiment that operation of the ionospheric modifier at frequencies slightly in excess of twice the electron gyrofrequency produces ≈ 10-to-15-dB enhancements of the field-aligned-scatter cross section.

It is possible, with the new low-frequency heating capability (2.7 MHz), to create field-aligned irregularities in the F region through the day and night, and even with frequencies as much as 20% in excess of $f_oF2$ at night. It was found that when the heating height and specular surfaces are matched, the diurnal variation in FAS cross section is less than ±5 dB. It was further found that field-aligned-scatter cross sections for matched heights in excess of 260 km are about 10 to 15 dB greater than those for matched heights under 245 km.

Yield experiments proved highly variable, as during previous experiments; however, it was determined that this variability is a real phenomenon. It was found that the



Pages 23 and 24 are blank

field-aligned-scatter cross section is proportional to $P^n$, where P is the average effective radiated power and n is an exponent, between 1/2 and 1 for CW and other 100%-duty-cycle waveforms, and equal to 1 for pulsed emissions.

## I INTRODUCTION

The principal objective of the PRAIRIE SMOKE V test series was to determine how variations in the operating parameters of the Platteville heating transmitter affected the production of various observable phenomena in the ionosphere. The results presented in this paper address specifically the influence of heating-transmitter parameters on the production of field-aligned scatterers. The parameters of the heating facility available for manipulation during these tests included the power output, modulation form, operating frequency and associated height of interaction, time of day, and to a limited extent the antenna pattern of the heating facility.

The results of previous power-variation (yield) tests have proven difficult to interpret, due primarily to the many variables of the ionospheric environment which are not under the control of the experimental observers. Therefore various tests were designed and repeated several times in order to acquire a reasonably significant data base for analysis. Special attention was given to monitoring hardware and ionospheric parameters that might influence the interpretation of the data. Specifically, a power monitor was installed at the Platteville facility to provide an independent verification of the actual transmitted heater power. Several new diagnostics were employed to determine the influence of linear and nonlinear D-region absorption on the production of F-region phenomena. Also, during the latter portion of the PRAIRIE SMOKE V tests a new capability was incorporated into the Erie

vertical-incidence ionospheric sounder to permit near-real-time reductions of ionospheric true-height profiles. This enabled maintaining a closer control over the effective heating altitude.

The results of a number of the tests performed, particularly those involving variations in the CW power output of the heating transmitter, continued to be highly variable as they had been during previous tests. However, the quantity of data now available indicates that this variability is due to an actual variability in the observed phenomena. Considerable attention has been paid to attempts to determine the parameters responsible for the observed variability. To date, however, these attempts have met with little success and it must be concluded that the causes of this variability are not yet understood.

Several new and in some cases unanticipated phenomena were observed during the PRAIRIE SMOKE V tests. Among the most interesting are the following:

- The recently completed modification of the Platteville facility permitted effective heating to be accomplished at all hours of the day.
- Because the F-region critical frequency dropped below the lowest operating frequency of the Platteville heater on several occasions during the nighttime hours, heating tests were conducted using operating frequencies as much as 20% above the F-region critical frequency. During these periods substantial field-aligned-scattering cross sections were still observed, indicating that at least during nighttime hours operation at frequencies substantially above the F-region critical frequency is still relatively efficient in generating field-aligned scatterers.
- Very strong evidence was obtained during nighttime operations for a substantial enhancement of the observed field-aligned-scattering cross section when the heating transmitter is operated very close to a frequency equal to twice the electron gyrofrequency in the F region.

- A substantial quantity of data was collected under similar conditions over two paths that were sensitive to field-aligned scatterers at two different altitudes in the ionosphere. This permits a more quantitative assessment of the effect of heating altitude on the observed field-aligned-scattering cross section.

## II EXPERIMENTAL ARRANGEMENTS

### A. Operation of the Heater

In order to obtain a significant quantity of test data under controlled conditions, a number of specific test procedures were designed prior to the start of operations and repeated a number of times during the operation. Table 1 provides a brief description of the objectives of each of the tests performed and indicates the number of times that that test was performed successfully. More detail on the exact test procedures used is provided when necessary in the discussion of the results of specific tests. In the presentation of test results all references to changes in the heater-power output refer to values measured using the independent power monitor at Platteville, unless otherwise indicated. A simplified block diagram of this power monitor is shown in Figure 1. Quoted values of power output relative to full Platteville transmitter output are determined by summing the voltage output from each of the ten Platteville transmitter modules and squaring the results. This should indicate the effective radiated power in the vertical direction for the full facility.

Because of the configuration of the power supply for the Platteville facility, it is frequently difficult to control the relative output levels of the ten modules, particularly at power levels 10 or more dB below the full output capability of the facility. Figure 2 shows some typical records from the power monitor. Figure 2(a) shows the normal

Table 1

SUMMARY OF PRAIRIE SMOKE V TESTS

| Test No. | Test | Description | No. of Times Run |
|---|---|---|---|
| 1 | Yield--Long Term | CW output at -20 (1 Tx), -12, -6, -3, 0, and -6 dB. 6 to 10 min each level. | 4 |
| 2 | Yield--High-Level Reference | CW output at -1.5, -3, -4.5, -6, -9, -12, and -15 dB. Full-power (0 dB) reference level of 2 min duration between 1-min reduced-power intervals. | 21 |
| 3 | Yield--Medium-Level Reference | CW output at -15, -9, -12, -3, and 0 dB. -6 dB reference level of 2 min duration between 1-min changed power intervals. | 7 |
| 4 | Yield--Pulse | 25%-duty-cycle pulses at 100, 300, 1,000, 3,000, and 10,000 pps. 2-min CW reference between 1-min pulse intervals. | 5 |
| 5 | Yield--Double Resonance | Two-frequency operation with $\Delta f$ = 0 to 10 kHz. | 3 |
| 6 | Yield--Pulse Compression | Heater frequency swept to permit pulse compression by ionospheric dispersion. | 4 |
| 7 | Yield--Pump Bandwidth | Noise modulation with 300, 1-, 3-, and 10-kHz bandwidths. | 4 |
| 8 | Yield--Rise/Decay Times | Slow Pulsing--5 s on/5 s off. | 3 |
| 9 | Acoustic-Wave Generation | Slow Pulsing--3 min on/3 min off. | 3 |
| 10 | Gravity-Wave Generation | Slow Pulsing--6 min on/6 min off. | 2 |
| 11 | Gravity-Wave Generation | Slow Pulsing--10 min on/10 min off. | 2 |
| 12 | Scattering-Region Thickness | Frequency changes to heat at altitudes between 15 km above and 15 km below from optimum. | 2 |
| 13 | Specular Matching | Heating at altitudes between 15 km above and 15 km below optimum. Antenna 0°, 10° N and 10° S from zenith. | 2 |
| 14 | D-Region Absorption--Short-Term Effects | 1 s on/29 s off. Various power levels. | 2 |
| 15 | D-Region Absorption--Long-Term Effects | 10 min on/10 min off. Various power levels. | ? |
| 16 | D-Region Modification--Short-Term | Similar to No. 14. | ? |
| 17 | D-Region Modification--Long-Term | Similar to No. 15. | ? |
| 18 | D-Region Diagnostic Check | 5 min on/5 min off. Various power levels. | 1 |
| 19 | Extended Height-Range Heating | Simultaneous operation on two frequencies whose reflection heights differ by 3 to 15 km. | 2 |

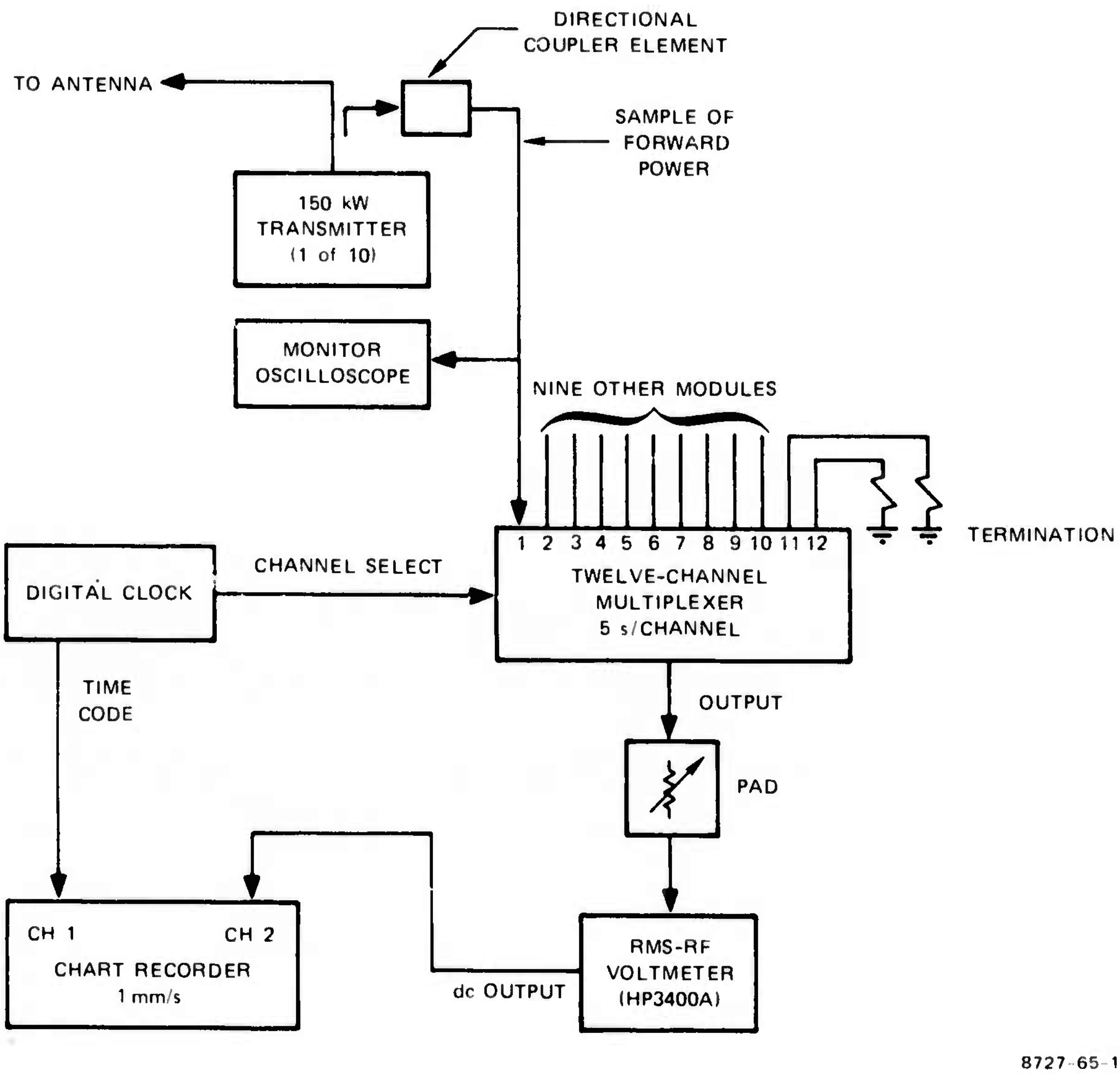


FIGURE 1 PLATTEVILLE POWER MONITOR

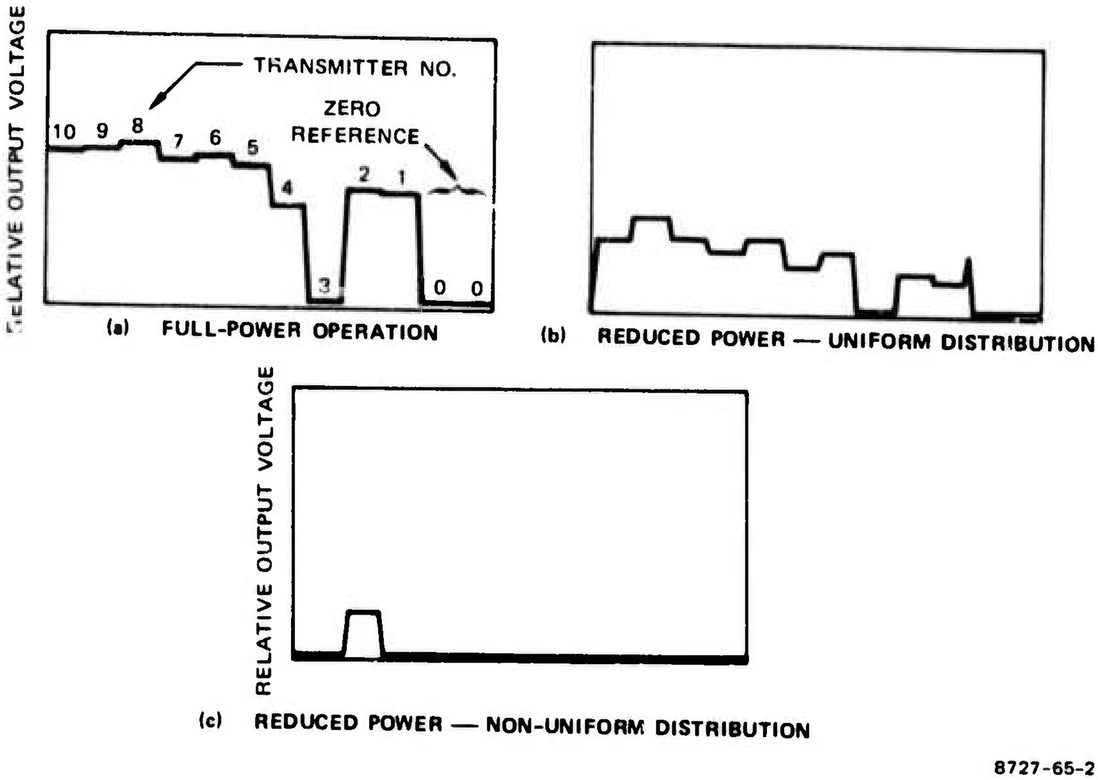


FIGURE 2 PLATTEVILLE POWER-MONITOR RECORDS

full-power indication with all of the transmitter modules operating at nearly the same power level. Figure 2(b) indicates operation at a reduced power level where all of the transmitter power outputs have remained comparable one to another. Figure 2(c) is a record for a period of reduced-power operation when most of the power output was being supplied by one of the transmitter modules. Under this last condition it is clear that the antenna pattern is highly distorted from the pattern obtained at full power or at reduced power with all modules providing similar output. This difference may be involved in some of the variability observed in the data.

## B. Field-Aligned-Scattering Measurements

The diagnostics used in gathering the data to be presented here were basically the same as has been used in previous PRAIRIE SMOKE experimental exercises.[1]* They consist of a bistatic FM CW radar capable of operating in several modes and covering the frequency range from 5 to 210 MHz. As shown in Figure 3, one transmitter site, at Los Lunas, New Mexico, and two receiver sites, at Socorro, New Mexico and Fort Huachuca, Arizona, were used for the PRAIRIE SMOKE V tests. An additional receiver site at Haswell, Colorado was used for making measurements of field-aligned scattering in the E region. These results are described in a paper by V. Frank elsewhere in these Proceedings. The sensitivity of the system is described by the plot of minimum detectable signal shown in Figure 4 for the two receiver sites. Most of the data to be presented here were taken near frequencies of 15, 35, 55, 75, 95, and 115 MHz. For some tests, however, nearly complete coverage of the 10-to-210-MHz frequency range was employed.

A critical parameter in analyzing data on field-aligned scattering is the area in space from which a given transmitter/receiver combination will observe scattering from highly aspect-sensitive irregularities aligned with the magnetic field. Figure 5 presents, in the form of a contour map, the altitude for which perfect specular reflections from field-aligned scatterers are obtained for the two paths employed for this work. These contours were computed for VHF ray propagation through a typical ionosphere. To the extent that the raypaths are curved by atmospheric or ionospheric refraction, the actual heights where specular-reflection conditions are met will be somewhat greater than those shown in the contour plots. For frequencies in the HF range the actual

---

* References are listed at the end of the paper.

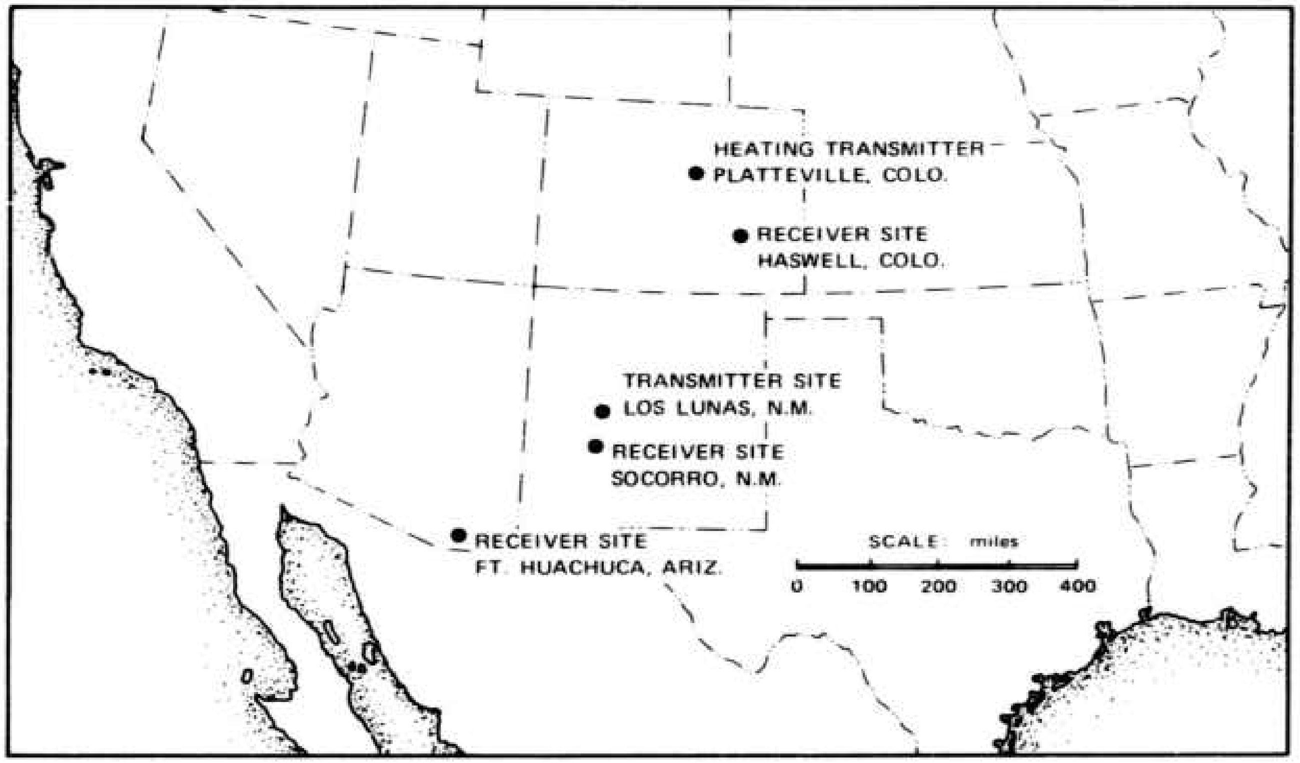


8727-65-3

FIGURE 3 FAS RADAR SITE LOCATIONS

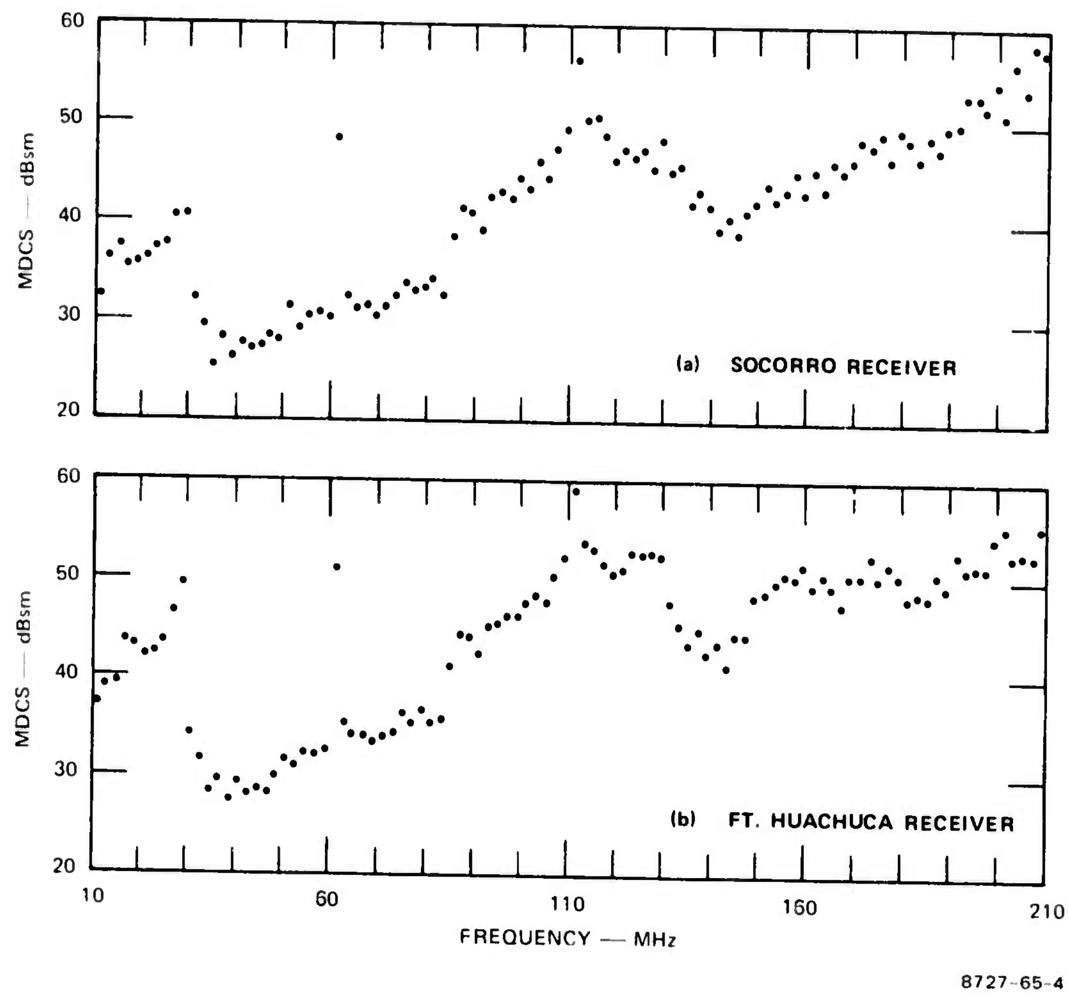


FIGURE 4 FAS RADAR MINIMUM DETECTABLE CROSS SECTION (MDCS) AS A FUNCTION OF RADIO FREQUENCY

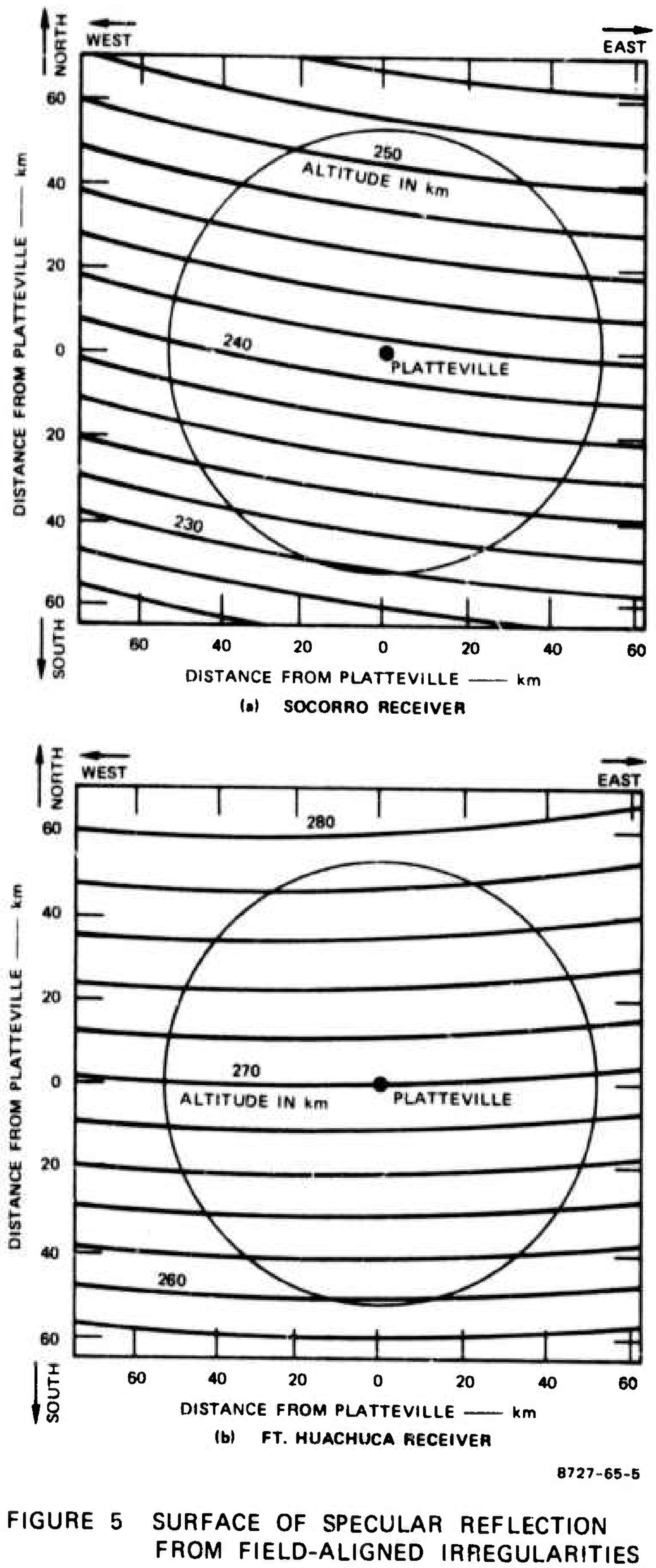


FIGURE 5 SURFACE OF SPECULAR REFLECTION FROM FIELD-ALIGNED IRREGULARITIES

specular-reflection height will be higher than the heights indicated, by as much as 60 km.

In analysis of the data to be presented, comparisons are frequently drawn between the so-called optimum height, or height for which specular-reflection conditions are met, and the heating height--i.e., the height at which the heater frequency is equal to the local plasma frequency. The values of heating height used in these analyses are obtained from post-test reduction to the true-height form of ionograms from both the Erie, Colorado and Boulder, Colorado vertical-incidence sounders.

## III EXPERIMENTAL RESULTS

### A. CW Power Variations

One of the primary objectives of the PRAIRIE SMOKE V tests was to determine the relationships between the power output of the heating transmitter and the observed cross section for field-aligned scattering. A significant fraction of the total available test time was devoted to this objective. Three types of test were performed in which the power output of the Platteville facility was varied according to different schedules, as shown in Figure 6. These tests will be referred to, as they are in the Figure, as Type 1, 2, and 3 tests. The Type 2 and 3 tests were arranged to permit observations of changes in the field-aligned scattering cross section that occurred with time constants short compared to the time constants required for gross structural changes in the ionosphere. The Type 1 test was arranged to determine the effects of such gross structural changes. The Type 2 and 3 tests are differentiated from each other by the reference level used from which changes were measured. The rationale for the use of the two different reference levels was to assure that the data obtained would

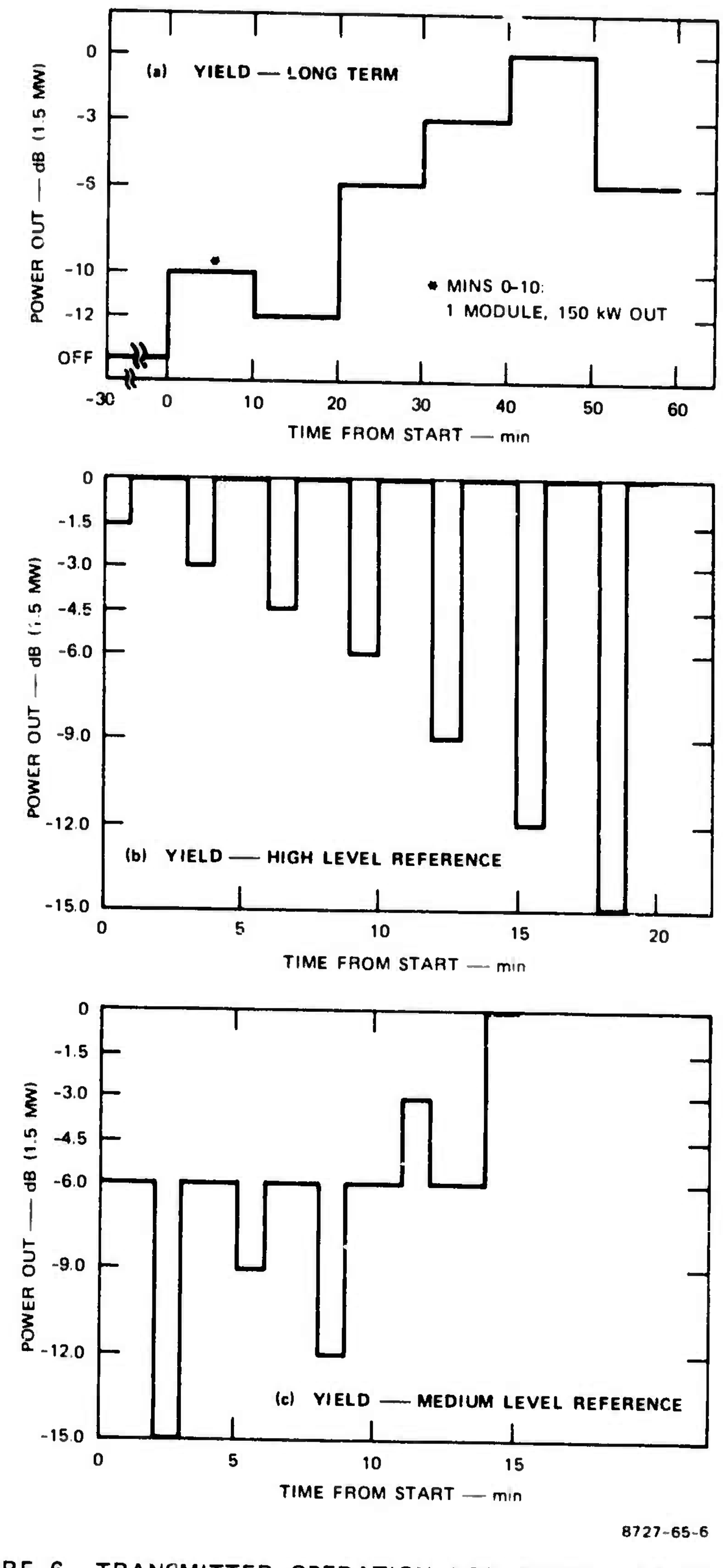


FIGURE 6 TRANSMITTER OPERATION FOR POWER-VARIATION TESTS

be valid if applied to heating facilities having substantially less maximum power capability than the Platteville facility.

In reducing the cross-section data from these power-variation tests, the technique employed was dictated by the general natural variability of the ionosphere. Figure 7 is a plot of cross-section versus time as it was observed during a Type 2 test. This plot illustrates the rather rapid changes in observed scattering cross section produced by changes in the heater-power output, as well as a slow natural variation in the observed cross section produced by changes in the ambient ionosphere. The latter effect reveals itself as a variation in the observed cross section for the referent heater-power output level during the period of the test. In reducing the cross-section data for the Type 2 and 3 tests the change in observed cross section was always measured relative to the average reference value for the period immediately before and after the power change. While this procedure may have some potential pitfalls, no other satisfactory technique for eliminating the effects of natural ionospheric variability could be devised. As one might surmise from the data shown in Figure 7, the observed variability in the reference level severely hampers the reduction of data from the Type 1, long-time-constant tests. It is almost impossible to determine with certainty whether observed cross-section changes occurring over periods of several minutes are produced by a heating-induced restructuring of the ionosphere or by natural changes in the ionosphere--e.g., changes in the heater reflection height. A discussion of the results of the Type 1 test will be postponed until the end of this section.

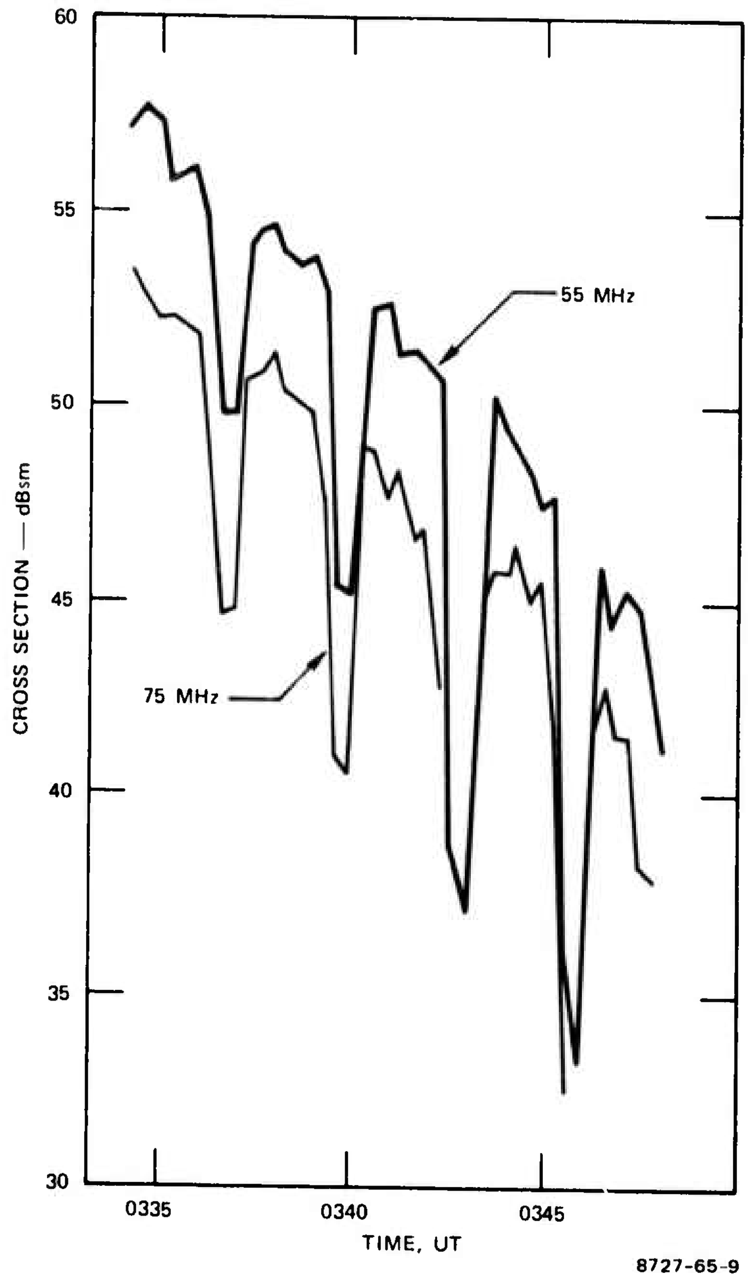


FIGURE 7 MEASURED FAS CROSS SECTION DURING A TYPE 2 TEST (Socorro, 19 September 1973)

1. Results of Type 2 and 3 Tests

The most striking characteristic of the results of these tests is the apparent variability of the relationship between heater power and observed scattering cross section. In Figure 8 the results of all of the successful Type 2 tests have been superimposed on a single plot. The format of this plot (which will be used again later) presents the observed change in cross section, relative to the reference cross section immediately preceding and following the change, as a function of the heater-power change that produced it. We note again that, in most cases, the reference level of observed cross section may well have changed significantly during the course of the test.

While Figure 8 does not give much insight into the data, it does indicate the type of variability with which the analysis is confronted, and the bounds of that variability. The data of Figure 8 are a composite of approximately 20 Type 2 tests observed over two different paths on up to four different radar frequencies.

Figure 9 shows a similar plot of the data from six Type 3 tests. Here the variability does not appear so great, although this may simply reflect the smaller number of tests performed. We will now attempt to examine some of the data more closely in an effort to get more insight into the test results.

The first point worth noting is that the variability in the data cannot be attributed to measurement uncertainties. As can be seen from the data of Figure 7, random data fluctuations are quite small. This is as expected, since each plotted data point represents a value averaged over several seconds and over the entire range spread of the scattering region. Considerable additional support for the observed variability being a result of an actual variability in the response of the ionosphere is provided by examining the results of

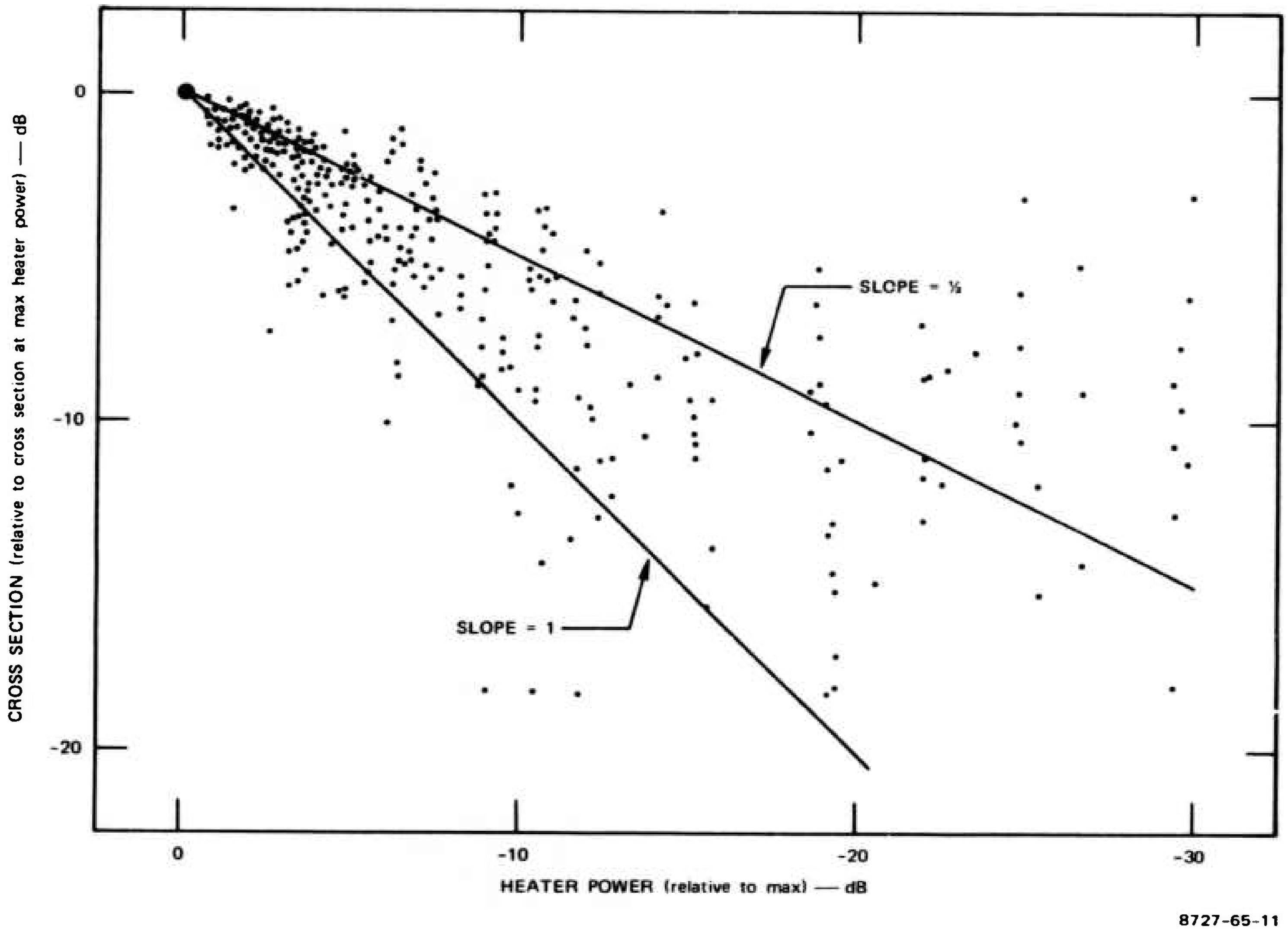


FIGURE 8 CROSS-SECTION VARIATION FOR CHANGES IN HEATER-POWER RESULTS OF 21 NO. 2 YIELD TESTS

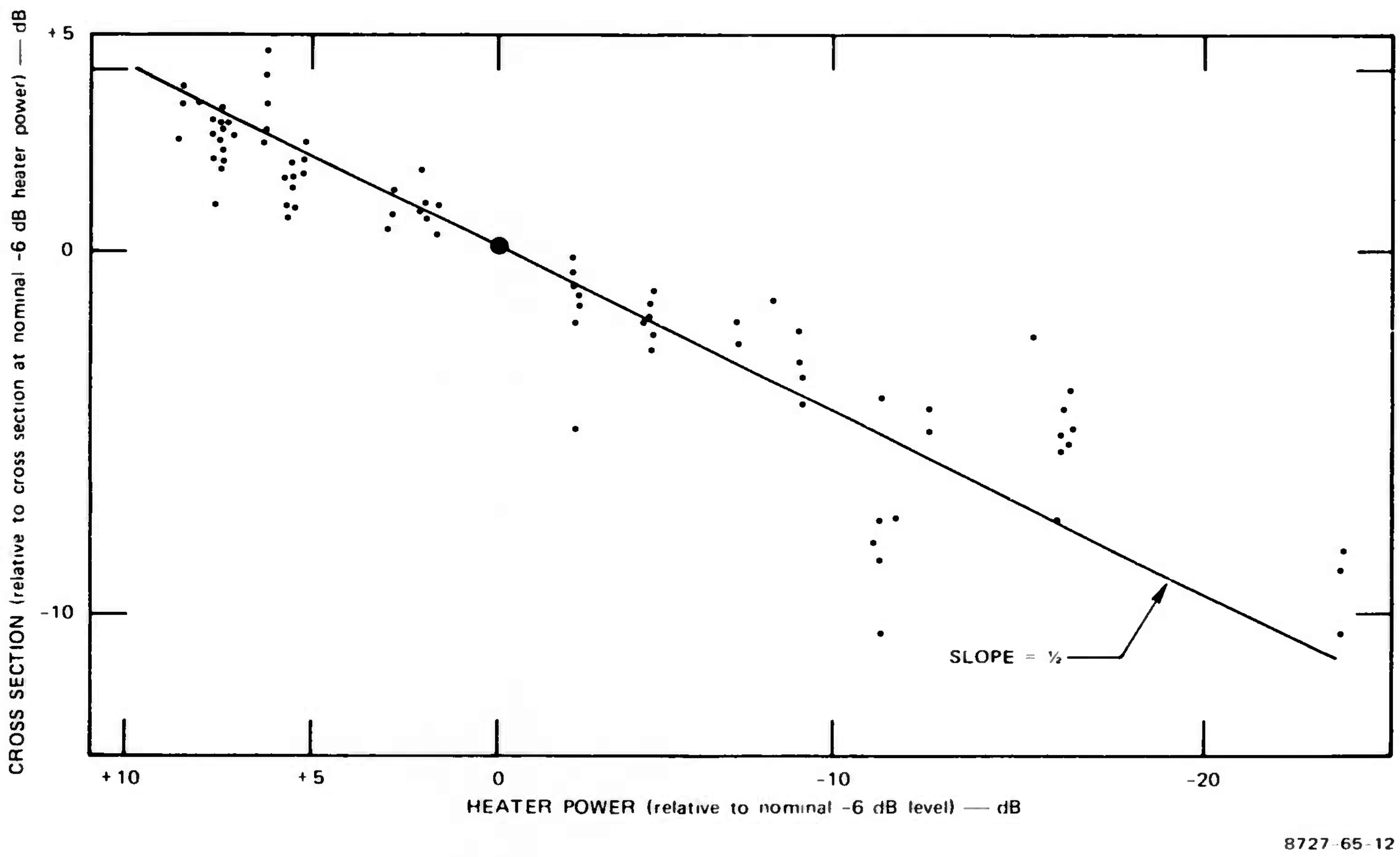


FIGURE 9 CROSS-SECTION VARIATION FOR CHANGES IN HEATER-POWER RESULTS OF SIX NO. 3 TESTS

several individual tests. In Figure 10 the results of two tests are presented. In one case, simultaneous observations from two sites are shown. Several representative important characteristics of the data can be seen in these curves. In all cases the data points can be approximated fairly closely by a straight line (on a log-log plot). This characteristic is generally descriptive of the available data. Different slopes observed during different test runs are the primary contributor to the variability observed in Figure 8. During any single run the responses observed at different sites and on different radar frequencies are quite similar in terms of being amenable to approximation by straight lines of the same slope. We therefore feel that the observed differences in curves of cross section versus heater power are truly representative of a real, although not yet understood, variability in the response of the ionosphere.

In an effort to relate the observed ionospheric response to some known or measurable ionospheric or heating-transmitter parameter we attempted to correlate particularly steeply sloping or particularly shallowly sloping responses with the following parameters: time of day, heating frequency, effective heating altitude, electron-density gradient at the effective heating altitude, heater frequency as a percentage of F-region critical frequency, and the absolute magnitudes of the observed cross sections during the run. In all cases no significant relationship could be established. This is not to say that none exists or that the relationship of cross section to heater power might not be influenced by one or more of these parameters, but that for the available data no such relation has been found.

As mentioned earlier in Section II of this paper it has been observed that the Platteville heating facility, when operating at reduced power, under some circumstances produces a relatively uniform energy distribution to the transmitting-antenna elements and under

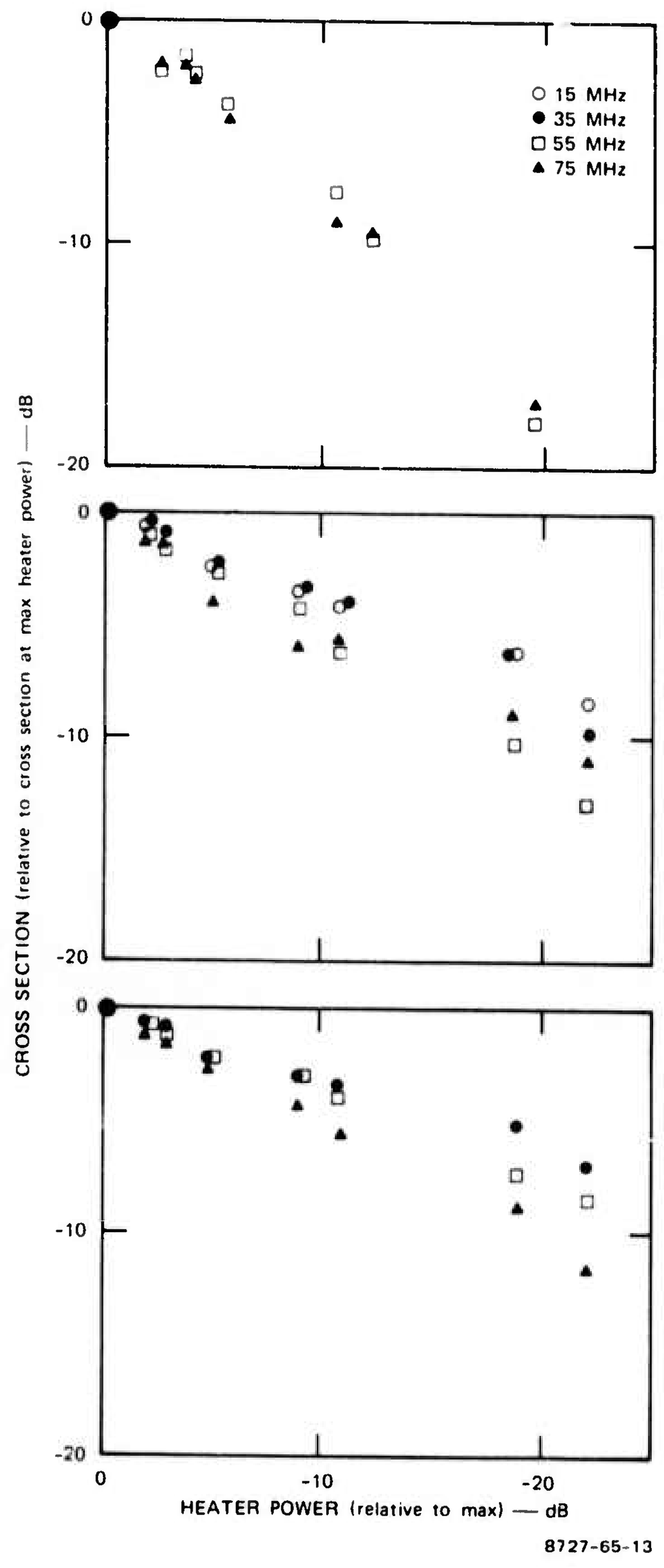


FIGURE 10 FAS CROSS SECTIONS FOR THREE TYPE 2 TESTS

other circumstances produces a very nonuniform distribution. Although insufficient data are available at this time to confirm a relation between the observed ionospheric response and the aperture or antenna distribution of energy there is some indication that this parameter may be correlated with the observed ionospheric response characteristics. Cross-section curves having steep slopes--i.e., large changes in cross section for a given change in heater power--generally coincided with tests during which, for low power levels, nearly all of the heater output was being supplied by one or two transmitter modules. Conversely, low slopes were associated with runs during which the Platteville power output was reduced more or less uniformly over a majority of the transmitter modules. This suggests that there may be some relation between changing antenna patterns and changes in the slope of the cross-section-versus-heater-power curves. At the present time no good explanation for this behavior can be provided.

The suggestion of a relationship between ionospheric response and antenna-pattern changes in the heating transmitter may be a clue to the possible existence of pitfalls either in the technique used to measure scattering cross section or in the technique used to interpret the Platteville transmitter power output. For several reasons of a practical nature we have chosen, as our measurement of scattering cross section, the cross section provided by the entire observed heated region. This choice was made because the values of cross section obtained in this manner may be interpreted directly in terms of system application--that is, they represent the effective cross section that would be available for communication-type applications. The choice was made also, because the values so obtained are somewhat more stable statistically, since each individual measurement is averaged over the entire range interval.

It appears that a complete understanding of the CW heater-yield question will be produced only by a more microscopic examination of the scattering region. This has been done to a very limited extent due to time constraints for some of the PRAIRIE SMOKE V data. In Figure 11 we have plotted data from two Type 2 tests in several different formats. Plots of observed cross section versus heater power have been made for the total cross section, as used in the majority of our analysis, and for the cross section observed at two small, fixed range intervals within the scattering region. In addition, the resulting plots of cross section versus heater power are presented for each of the cross-section curves. Note that the cross sections measured at a fixed range are produced in a relatively large region of space due to the fact that no angular resolution is employed by the radar. The variations in the reference cross section observed are typical and illustrate both the dynamic behavior of the whole region and of individual parts of that region. This dynamic behavior is clearly seen in Figure 12, which shows the rise and decay of centers of strong field-aligned scattering within the heated region. Previous examples of such scattering centers during turn-on of the heater have been presented elsewhere.[2] Although these strongly scattering regions are not so obvious or well defined after long periods of heater operation, they appear to be a part of the normal state of the heated region.

Returning to the data presented in Figure 11, it appears that substantially different changes in cross section can occur at different points in the heated region. This is noticeable in Figure 11(a). On other occasions similar changes can be observed at different points within the region, as seen in Figure 11(b). Although very little data has been reduced and examined in this form, there is some suggestion that a nonlinear relationship exists between incident heater field and field-aligned-scattering cross section, and that what is being observed

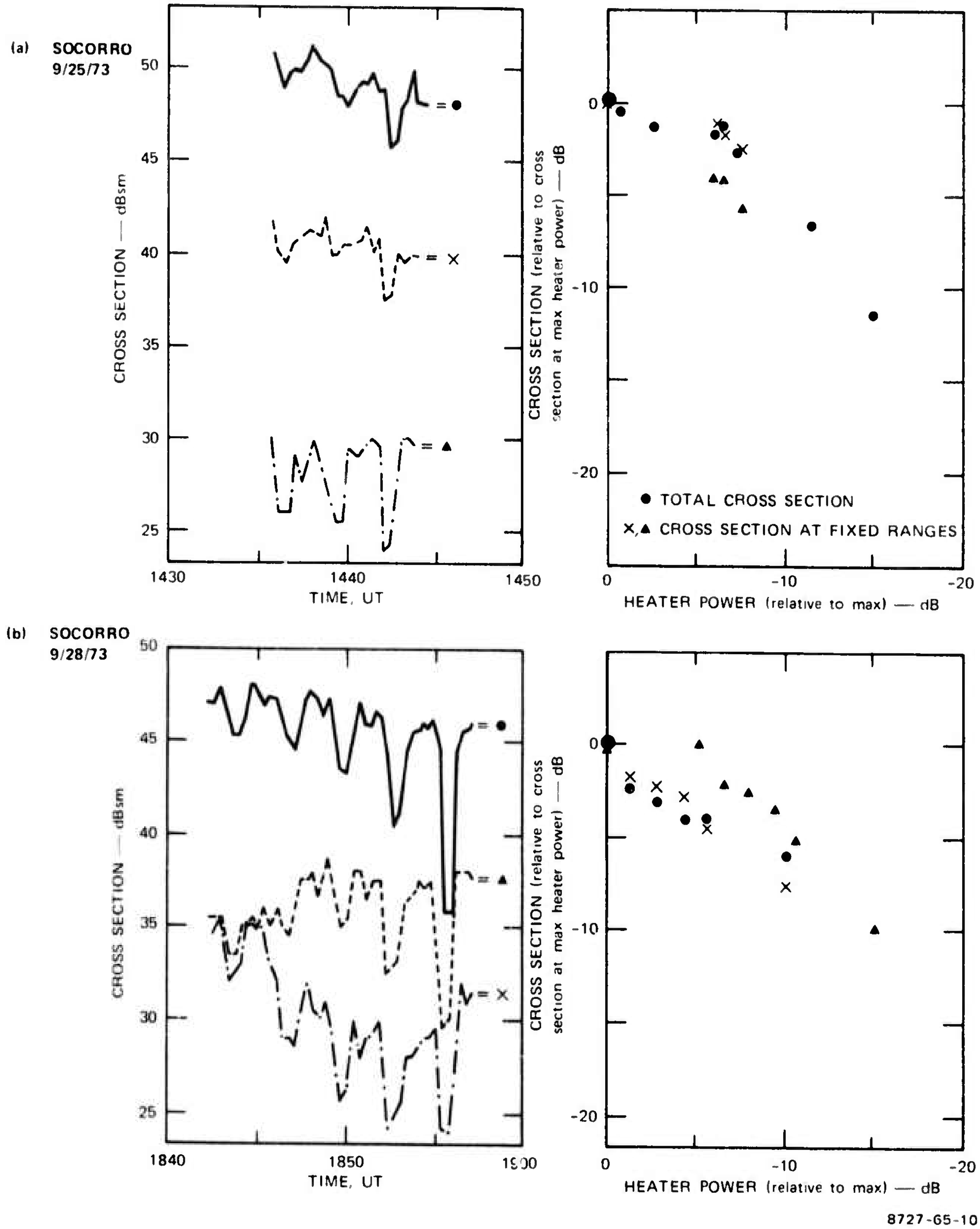


FIGURE 11 COMPARISON OF YIELD DATA FOR TOTAL CROSS SECTION AND FIXED-RANGE CROSS SECTION

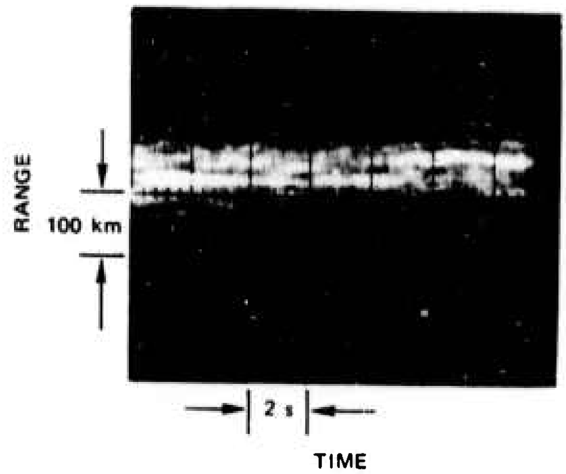


FIGURE 12 STRUCTURE WITHIN THE HEATED REGION

is an integrated effect over regions having substantially different incident-power densities. The differences in incident-power density are a function of the heater antenna pattern and possibly of focusing by large structures within the heated region. Such a process could explain the wide variability in the observed behavior of total field-aligned-scattering cross section. Further analysis of such data should probably be sufficient to uncover the basic relationship between heater power and FAS cross section.

2. Results of Type 1 Tests

During the Type 1 tests the heater power output was maintained at a constant value for 6 min, as opposed to 1-min intervals used in the Type 2 and Type 3 tests. The objective of the Type 1 tests was to determine the effect of longer-term structural changes in the heated region on the FAS cross section. An analysis of such effects on the observed cross section is difficult, due to natural variations in the observed cross section as mentioned above. Because of these natural variations no quantitative results have been derived from the Type 1

test data. In various Type 1 tests, cross sections during the 6-min power-step intervals were observed in some cases to increase, in some cases to decrease, and in some cases to remain essentially constant during the 6-min intervals. During one Type 1 test in which cross section was relatively constant during the 6-min interval of each power level, the changes in cross section were approximately equal to the changes in the incident heater power. It also appears that illumination by a single transmitter (producing an incident field 20 dB below the field produced at maximum power) resulted in a scattering cross section of value comparable to that produced by the full 10-element array operating at a -20 dB power level. This result would be expected if the heating height was fairly well matched to the specular-reflection surface.

At this point it appears that further analysis of such long-term variations should be attempted only when the short-term response of the ionosphere is better understood. There is no indication that long-term, high-power operation of the heater preconditions the ionosphere to produce either higher or lower cross sections than would be observed without such preconditioning.

## B. Pulsed Heater Operation

During previous PRAIRIE SMOKE tests,[3] the Platteville transmitters have been pulsed at various rates and duty cycles. In general the observed cross section has been proportional to the average power output of the transmitters. During PRAIRIE SMOKE V, pulsed operations were conducted in which the cross section observed when pulsing with a 25% duty cycle pulse at pulse rates between 100 pps and 10,000 pps were compared with the CW cross section. The objective of these tests was to determine whether the pulse rate affected the cross section observed.

Over the range of pulse rates used, the observed scattering cross section does not appear to depend significantly upon the pulse rate employed. This result, together with previous pulsed heating results, indicates that the observed cross section is directly proportional to the average heater-power output for pulse rates between 100 and 10,000 pps and for duty cycles between 10% and 100%.

## C. Modulations of the Heating Transmitter

Several different techniques were employed in attempts to enhance the observed FAS cross sections or to gain insight into the mechanisms responsible for FAS generation.

The possibility of enhancing FAS cross section by using two heater frequencies, separated by a frequency near the ion-acoustic frequency range in the ionosphere, was suggested on the basis of laboratory results obtained earlier in the program. Such a test using frequency spacings from zero to 10 kHz was attempted during PRAIRIE SMOKE V. No enhancements of the FAS cross sections were observed as a result of this mode of operation.

In an attempt to determine the role of plasma instabilities in the production of field-aligned scattering, tests were performed in which the heater was operated alternately with a monochromatic (CW) signal and with a broadband noise signal. The broadband noise modulation was adjustable to provide 3-dB bandwidths between 100 Hz and 10 kHz. The expectation, from plasma theory was that if plasma instabilities are a primary mechanism responsible for the production of field-aligned scatterers, then the heater signal must be coherent for time periods similar to the growth rate of plasma waves. If such time coherence is not maintained, plasma waves would not be expected to be excited in the ionosphere. The predicted growth rates are of the order of 1 ms. The

noise bandwidths used provide coherence times ranging from 1/10 ms to 10 ms. We would expect to observe a decrease in the FAS cross sections for the wider bandwidth or shorter-coherence-time random noise excitations. Data were obtained from this test on a number of runs. The observed FAS cross section remained quite constant regardless of the noise-modulation bandwidth employed and was the same as the cross section observed for CW operation. This result indicates that the excitation of plasma waves is not the primary mechanism responsible for the production of field-aligned scatterers.

Two other test types performed during PRAIRIE SMOKE V will be mentioned here. The first involved a pulse-compression experiment in which the frequency of operation of the Platteville heater was rapidly swept in a controlled manner that might permit ionospheric dispersion to compress the sweep and produce substantially higher field intensities in the ionosphere. The results of this experiment are reported elsewhere in these proceedings. The second test type involved 5-s-on/5-s-off heater operation. The objective was to study the FAS rise and decay time as a function of frequency. These data have not been analyzed to date, due to time limitations.

### D. Variations in FAS Cross Section with Time of Day and with Heating Altitude

The new lower-frequency capability of the Platteville facility permitted the generation of field-aligned scatterers at all hours of the day and night. Some of the nighttime operations included periods when the F-region critical frequency was somewhat below the low-frequency limit of the Platteville transmitter. Field-aligned scattering was still observed under these conditions and is discussed in Section III-G below. The absolute values of cross section observed at 55 MHz, for

conditions when the heating height was matched to the specular-reflection height, ranged from 48 to 55 dBsm at the Socorro receiver site and from 60 and 70 dBsm at the Fort Huachuca receiver site. The amount of data available from these tests provides strong evidence of a 10-to-15-dB difference in cross sections at 55 MHz that is produced primarily by the difference in heating altitudes. No consistent day/night differences were observed and, if they exist, they are less ±5 dB. The observed cross sections are enhanced from the values given above by approximately 5 dB when the heating frequency (which must remain matched to the desired heating altitude) is very close to the F-region critical frequency.

In addition, an unexpected source of enhancement was observed with heater operation at frequencies near the second harmonic of the electron gyrofrequency in the ionosphere. These effects are described in Section III-F below.

## E. Heater-Frequency Optimization and Antenna Steering

Raytracing analyses performed by Meltz et al.[4] indicate that some improvement in energy density in the ionosphere should be attainable by tilting the heater beam to the north by about 10°. In addition, it is anticipated from the scattering-model development work[5] that by controlling both the heating frequency and the direction of the heater beam, additional flexibility in controlling and optimizing the field-aligned-scattering geometry should be available.

Several antenna-tilt and frequency-changing tests were performed during the PRAIRIE SMOKE V series. The results indicated a general agreement with the scattering-model predictions for optimum performance at a given heater energy output. The changes produced by such operations are generally of the order of 5 dB or less. At some times no discernible changes in FAS cross section were seen for antenna tilts of 10° to 20°

away from the zenith. Frequently, however, a tilt of 10° to the north produced a significant (approximately 5 dB) increase in the observed FAS cross section. One significant departure from this behavior was that when Platteville was operating using the low-frequency (2.7 to 3.3 MHz) antenna, no cross-section changes were observed during antenna steering operations. This may be attributable to the wider beamwidth of the low-frequency array.

## F. Operation at Heater Frequencies Near the Second Harmonic of the Electron Gyrofrequency

In this subsection we describe an unexpected result obtained during PRAIRIE SMOKE V operations. A substantial enhancement of the FAS cross section has been observed when the heater is operated at frequencies approximately twice the electron gyrofrequency in the F region. Few phenomena observed in the field-aligned-scattering measurements have been so clearly demonstrated as this effect. A continuous set of observations made during a frequency-changing and antenna-tilting test provided data from two receiver sites on several frequencies simultaneously.

In Figure 13 we have plotted a set of observed-cross-section data from two receiving sites and at several different frequencies from each site. (Some of the data--for example, the 35-MHz Fort Huachuca data--are not completely valid because of receiver saturation effects at high signal levels.) In addition, the peak heater power at all operating frequencies was constant within approximately 1 dB, so power variations are not plotted and may be assumed to have negligible influence on the data except during the actual heater tuning intervals.

The electron gyrofrequency at 240 km over Platteville is very nearly 1.40 MHz (1.3935 MHz, computed from standard field models). The data in Figure 13 show a very strong enhancement of the field-aligned-scattering cross section when the heater is operating at a frequency of 2.85 MHz

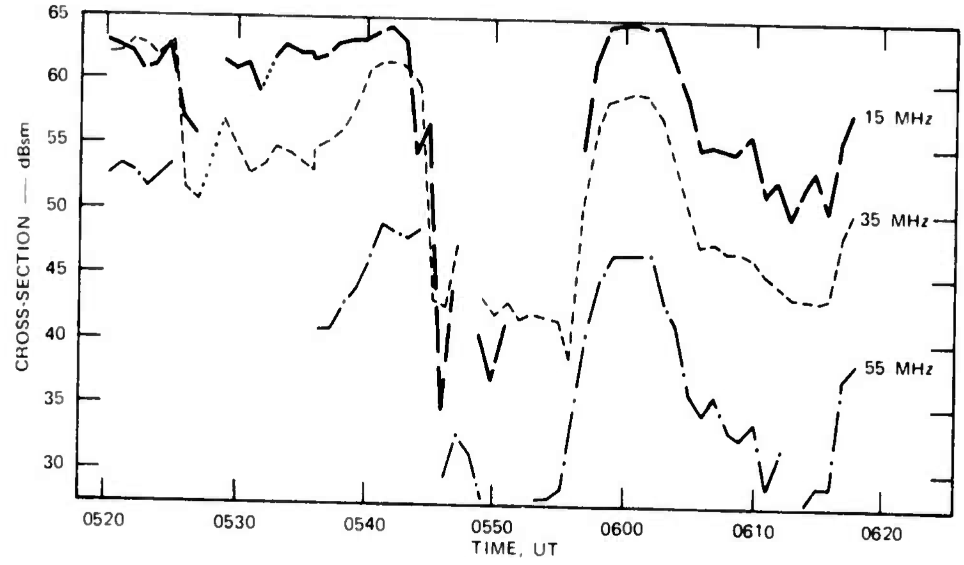


(a) SOCORRO RECEIVER SITE

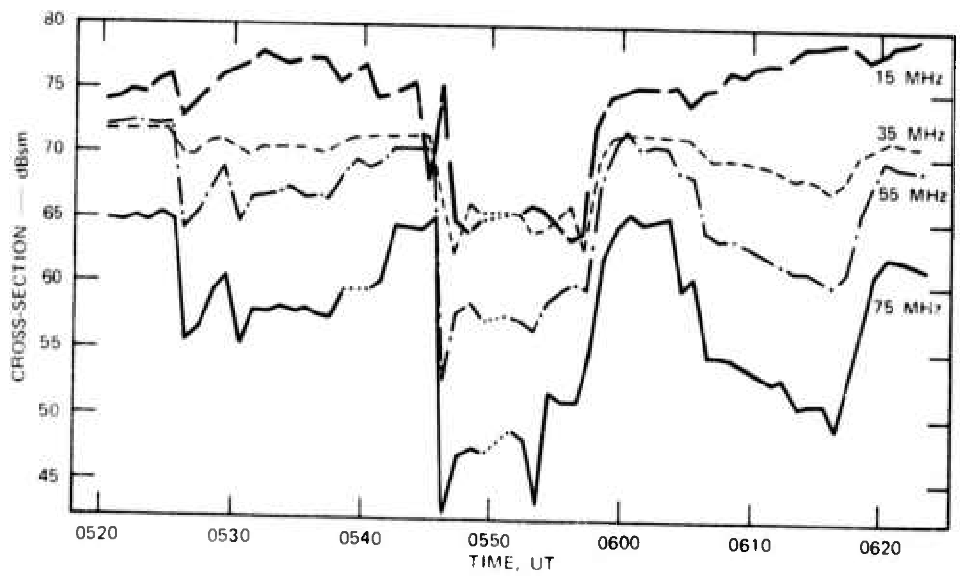


(b) FT. HUACHUCA RECEIVER SITE

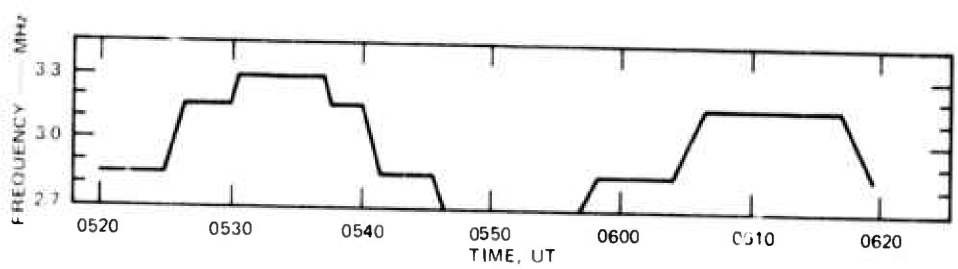


(c) HEATER FREQUENCY

8727-65-17

FIGURE 13 FAS CROSS SECTIONS FOR HEATING FREQUENCIES NEAR TWO TIMES THE ELECTRON GYROFREQUENCY

relative to the cross section observed for heater operation at 2.7, 3.16, and 3.3 MHz. The 2.85-MHz frequency is very nearly twice the electron gyrofrequency. We can also see that the cross sections observed for the 3.16-MHz heater frequency may be somewhat higher than those observed for the 3.3-MHz heater frequency. The availability of data from two different receiving sites appears to eliminate the possibility that the observed enhancement is an effect of changes in the effective heating altitude. Note that the influence of the changing heating altitude can be observed on the 15-MHz Fort Huachuca data. At 0605 GMT, when the heater frequency is increased from 2.85 to 3.16 MHz, thereby raising the effective heating altitude, this signal increases in strength rather than decreasing as do all the other signals. This results from the fact that the specular matching conditions are now better satisfied for the 15-MHz rays, which are substantially refracted within the ionosphere.

These data lead to the conclusion that a strong enhancement in observed FAS cross section is associated with operation of the heater at a frequency of approximately twice the local electron gyrofrequency. There is some indication that the enhancement may be a maximum for frequencies slightly above twice the gyrofrequency.

Other data from various PRAIRIE SMOKE V tests have been examined briefly in an effort to determine whether other higher multiples of the electron gyrofrequency might also produce enhancements in the FAS cross section. There is a slight indication that this may be the case. However an insufficient number of examples are available to draw any firm conclusions on this point. Because of the strong enhancement observed at twice the gyrofrequency, it would be desirable to make controlled tests in attempts to observe enhancements at other higher multiples of the gyrofrequency. Additionally, the observation at twice

the gyrofrequency should provide a better understanding of at least one of the mechanisms by which heating produces field-aligned scattering.

## G. Heater Operation at Frequencies Above the F-Region Penetration Frequency

One of the major objectives of the PRAIRIE SMOKE V tests was to determine the capability of heating to generate field-aligned scattering at all hours of the day and night. During a number of occasions during the late-night and early-morning hours the critical frequency dropped below the low-frequency limit of the heater (2.7 MHz). Operations were conducted with heating frequencies up to 120% of the critical frequency. Field-aligned scattering was still clearly observable. During these periods the critical frequency was almost always above 2 MHz. Therefore the heating frequency was still below the X-mode critical frequency in the ionosphere. This leads to the possibility that it is the X-mode radiation from the heater that is actually causing the observed field-aligned scattering. A test of this possibility was made on 18 September at 0800 when the critical frequency was 2.6 MHz, the heating frequency was 2.75 MHz, and the heater was operated first with X-mode polarization then with O-mode polarization. The field-aligned-scattering cross sections observed with O-mode heating were 15 dB greater than those observed with X-mode heating, indicating that the O-mode heater energy is responsible for producing the observed field-aligned scattering. It is indeed possible that when the heater is operating in X-mode it is actually leaking O-mode energy, which is producing the observed field-aligned scattering.

The overall effects of the ratio of heating frequency to F-region O-mode penetration frequency are now nearly completely known. During daylight hours there is a small increase in observed cross section (approximately 5 dB) when the heater frequency approaches the F-region

critical frequency. This 5-dB increase is associated with heater operation at about 0.98 to 1.0 times the F-region critical frequency. During daytime hours, operation above the F-region critical frequency causes field-aligned-scattering cross sections to drop below the observation limits (a decrease of greater than 20 dB). At night the effects are similar, with the exception that operation at frequencies above the F-region critical appears to result in only about a 10-dB decrease in FAS cross section.

## IV CONCLUSIONS

The major conclusions that can be drawn from the F-region field-aligned-scattering observations during PRAIRIE SMOKE V aje given below. Unless otherwise stated, these conclusions apply to FAS at frequencies in the HF and VHF bands. The conclusions are as follows:

- Field-aligned scattering is producible by the Platteville facility at all hours of the day and night.
- Observed FAS cross sections do not exhibit a diurnal dependence greater than ±5 dB from average values.
- At night, heater operation at frequencies as much as 20% above $f_oF2$ produces FAS cross sections about 10 dB below those observed with heater frequencies below $f_oF2$. This suggests that, at least at night, oblique heating might produce useful FAS cross sections.
- FAS cross sections observed in the upper F region (above 260 km) are generally 10 to 15 dB greater than those observed in the lower F region (below 245 km). It is not known whether thi; difference always exists, nor whether it is a primary effect or a secondary effect--i.e., a result of using higher heater frequencies at higher altitudes with attendant narrower heater beamwidths and lower D-region absorption.

- FAS yield can usually be described as approximately a linear relation (on a log-log plot) between heater power and FAS cross section. The slope of the linear approximation is usually between 1/2 and 1 where

$$\text{Slope} \equiv \frac{\text{Change in FAS cross section}}{\text{Change in heater-power output}} .$$

  This relation has been observed to apply for the Platteville heater at power output levels of 15 kW to 1.5 MW.

- Considerable structure is present within the heated region, resulting in localized regions of strong FAS. These structures grow and decay over time intervals of a few seconds and longer.

- The FAS yield of different portions of the heated region is quite dissimilar, indicating that the roughly linear variations of total cross section for the region may be the result of smoothing of a basic nonlinear yield relation observed at numerous different local intensities. Data gathered during PRAIRIE SMOKE V, but not analyzed in a manner suitable to examining the basic relation, probably could be used to determine the basic relation.

- For the Platteville antenna configuration, backscatter FAS is similar when using a single transmitter module at full power and when using all 10 modules, each operating near 20 dB below full power. This indicates that <u>backscatter</u> FAS cross section is governed by <u>ERP</u> rather than total power, at least for heater beamwidths as wide as or wider than the full Platteville array. This relation probably would <u>not</u> hold for oblique-scatter paths where the surface of specular reflections slopes less rapidly.

- For pulsed heater operation, at pulse rates from 100 to 10,000 pps and a duty cycle from 10% to 100%, FAS cross section is linearly proportional to heater <u>average</u> power.

- Operation of the heater at frequencies near twice the electron gyrofrequency produces strong (10-to-15-dB) enhancements in the FAS cross section. There is some possibility that operation at other multiples of the electron gyrofrequency may also enhance the FAS cross section. No other techniques for enhancing FAS cross section have been found to date.

- The application of the PRAIRIE SMOKE scattering model[5] and of heater-beam raytracing is adequate to explain the general observed behavior of the heated region in response to heater-frequency changes and to heater-antenna steering.

## REFERENCES


1. P. A. Fialer, and J. M. Lomasney, "PRAIRIE SMOKE I Sweep Frequency Backscatter Observations (U)," Proceedings of PRAIRIE SMOKE I RF Measurements Data Workshop, 25, 26, 27 January 1972 (U), SRI 2-4335, Stanford Research Institute, Menlo Park, Calif. (March 1972), SECRET.

2. P. A. Fialer, "SFCW Observations of Field Aligned Scattering (U)," Proceedings of the IVORY CORAL 1973 Technical Review Meeting (U), Vol. II, Experiments, SRI 3-4534, Stanford Research Institute, Menlo Park, Calif. (April 1973), SECRET.

3. V. R. Frank, and P. A. Fialer, "PRAIRIE SMOKE IV SFCW Observations (U)," Proceedings of the PRAIRIE SMOKE IV RF Measurements Data Workshop, 7 March 1973 (U), SRI 3-4836, Stanford Research Institute, Menlo Park, Calif. (June 1973), SECRET.

4. G. Meltz, S. J. Boak, and B. R. Pendyala, "The Relationship Between Energy Density Distribution and the Strength of Field Aligned Scattering (U)," Proceedings of the PRAIRIE SMOKE Yield-Model Workshop, 17, 18 July 1973 (U), SRI 3-5193, Stanford Research Institute, Menlo Park, Calif. (October 1973), SECRET.

5. Proceedings of the PRAIRIE SMOKE RF-Scattering-Model Workshop, 18, 19 July 1972 (U), SRI 2-5200, Stanford Research Institute, Menlo Park, Calif. (September 1972), SECRET.

# THE GEOSTATIONARY YIELD EXPERIMENT

E. K. Walton   D. R. Ward   S. A. Bowhill

Aeronomy Corporation
Champaign, Illinois

ABSTRACT

Observations of the scintillation of the 136-MHz signals from the ATS-5 geostationary satellite were made during most of the PRAIRIE SMOKE V test series. The Type 1 power-stepping experiment, which called for 10-min steps in power of the Platteville transmitter, was used to perform a yield experiment. In this experiment, it was shown that the yield, defined in terms of scintillation index, was linearly proportional to the transmitter power. Evidence of a saturation effect for a transmitter power of 0.97 MW is presented.

A nighttime experiment was also performed during which the geostationary satellite was received by two stations separated by 57 km. Scintillation indices have been computed over a 4-hour period for signals received at both stations. A large variability in the yield during periods of very stable ionospheric conditions may be seen.

## I EXPERIMENTAL PROCEDURE

An experiment was performed on 20 September 1973 that may be used to perform a yield study using geostationary data. The geostationary observation station, which was essentially the same as used in PRAIRIE SMOKE IV, was used to receive the 136-MHz transmission from ATS-5. The



Pages 60, 61 and 62 are blank

receiving station was located (in Lusk, Wyoming) so that the LOS to the geostationary satellite passed over Platteville at 275 km. The signal used in this study was received, and mixed with the local receiver beat-frequency oscillator (BFO). The beat note was detected, filtered, converted to digital form, and stored on digital magnetic tape for later analysis. This is the same technique as used in PRAIRIE SMOKE IV.[1*]

The scintillation index, S, was then calculated from the amplitude measurements, A, by the expression[1]

$$\langle A^2 \rangle / \langle A \rangle^2 = S^2 + 1 \quad .$$

In this study, the scintillation index will be chosen to represent heater yield. Since the time response of the scintillation index to a change in power is on the order of a minute, the yield study was performed using the 10-min power steps available during the Type 1 experiment.

## II DATA

The most reliable Type 1 experiment with respect to heater transmitter operation, power calibration, and geostationary data reliability was performed on 20 September 1973 from 2100 MST to 2200 MST (21 September 1973, 0400 to 0500 GMT). The scintillation index and the transmitter power as a function of time for this experiment are shown in Figure 1. As can be seen, the scintillation index increases as the power is increased.

---

* References are listed at the end of the paper.

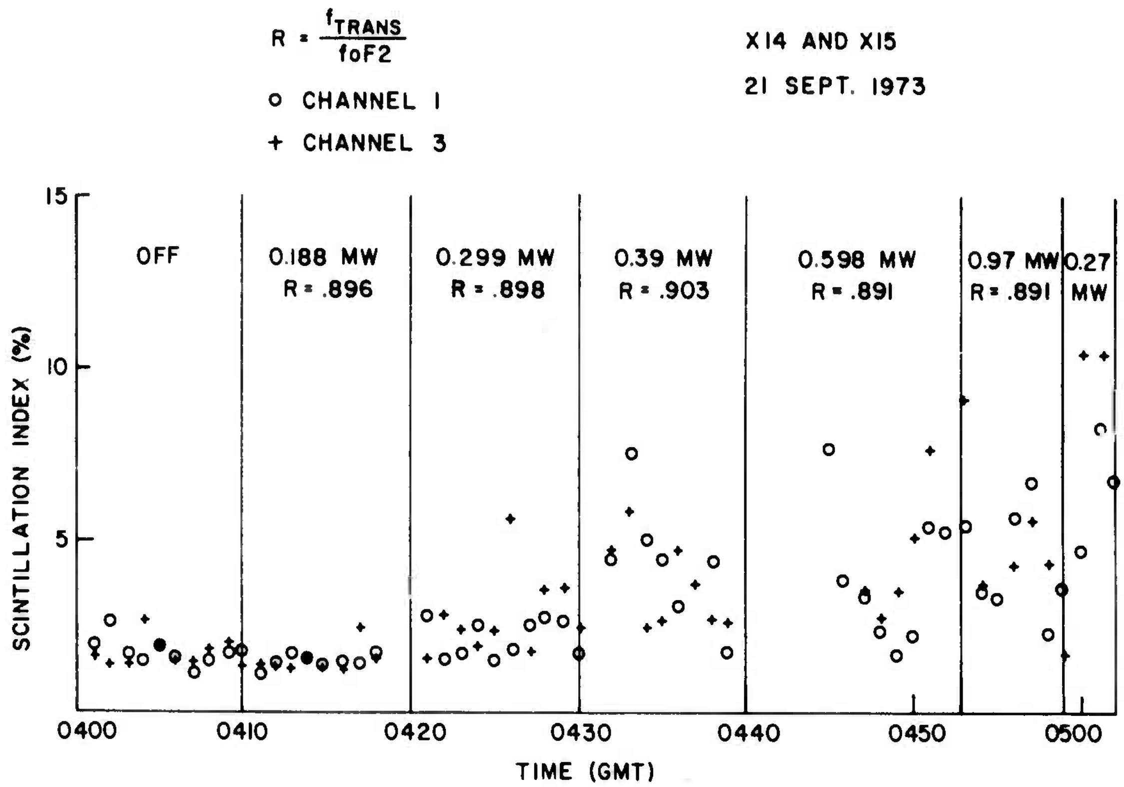


FIGURE 1 SCINTILLATION INDEX AND TRANSMITTER POWER vs. TIME FOR 21 SEPTEMBER 1973

## III ANALYSIS

In an attempt to determine the relationship between the scintillation index and the transmitter power, the data shown in Table 1 were tabulated. The value of the mean scintillation index is determined by omitting the first minute from each group and averaging the remaining data. The power was determined from the Platteville transmitter logs. These data were next plotted on log-log paper to determine the quantity x in the relationship $S \propto P^x$. The results are shown in Figure 2. As can be seen, data points 2 through 5 lie approximately on a line of slope x = 1.0. Data point 1 with power = 0 cannot be shown on a logarithmic scale. Point 6 for the highest value of power (0.970 MW) seems to exhibit a saturation effect, while Point 7 is derived from a short group of data

Table 1

TABULATION OF POWER AND SCINTILLATION INDEX FOR THE 20 SEPTEMBER 1973 TYPE 1 YIELD EXPERIMENT

| Point | Time (GMT) | Mean Scintillation Index | | Power (MW) |
|---|---|---|---|---|
| | | Ch. 1 | Ch. 3 | |
| 1 | 0400-0410 | 1.75 | 1.77 | Off |
| 2 | 0410-0420 | 1.51 | 1.56 | 0.188 |
| 3 | 0420-0430 | 2.14 | 3.00 | 0.299 |
| 4 | 0430-0440 | 4.36 | 3.75 | 0.390 |
| 5 | 0440-0453 | 4.11 | 5.33 | 0.598 |
| 6 | 0453-0459 | 4.36 | 3.92 | 0.970 |
| 7 | 0459-0502 | 7.50 | 10.05 | 0.270 |

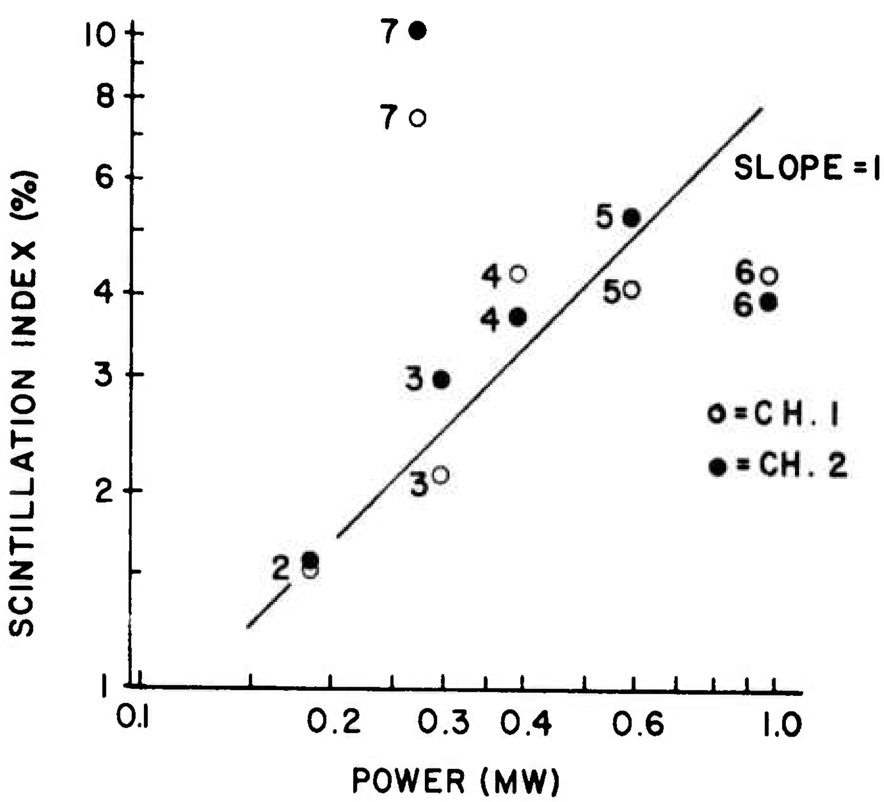


FIGURE 2 SCINTILLATION INDEX vs. POWER FOR THE 21 SEPTEMBER 1973 DATA

following the 0.970-MW sequence. It should be pointed out that this yield result ($S \propto P^1$) differs from an earlier PRAIRIE SMOKE result showing ($S \propto P^{1/2})^2$. The earlier data, however, were based on a scatter plot of data collected over a long period of time rather than a power-stepping experiment as described here. Also, the earlier power calibrations were less reliable than the power data presented here.

## IV THE REDBIRD EXPERIMENT

A second experiment has been performed that gives some insight into the yield-versus-power question. On the night of 18 September 1973 (19 September GMT date), the geostationary satellite ATS-6 was received by two stations. One station was the Lusk receiving station described earlier in this report. The other receiving station used a single receiver mounted in the mobile Winnebago shell. This receiving station was located 57.4 km north of the Lusk station in Redbird, Wyoming. The LOS from Lusk to ATS-5 passed over Platteville at 275 km height, while the LOS from Redbird passed over Platteville at 328 km (a difference of 53 km). The elevation angle of the geostationary satellite was 42.5°.

The scintillation index computed during the Redbird geostationary experiment is shown in Figures 3, 4, and 5. These figures show the scintillation index computed from the signal received at both Lusk, Wyoming, and Redbird, Wyoming from 0600 to 1020 GMT on 19 September 1973. The scintillation index of the signal received at the Lusk site was computed from data stored on digital magnetic tape in the same manner as described earlier in this section. The scintillation index of the signal received at Redbird was computed by detecting, filtering, and digitizing the analog tape records of the signal that were made during this experiment.

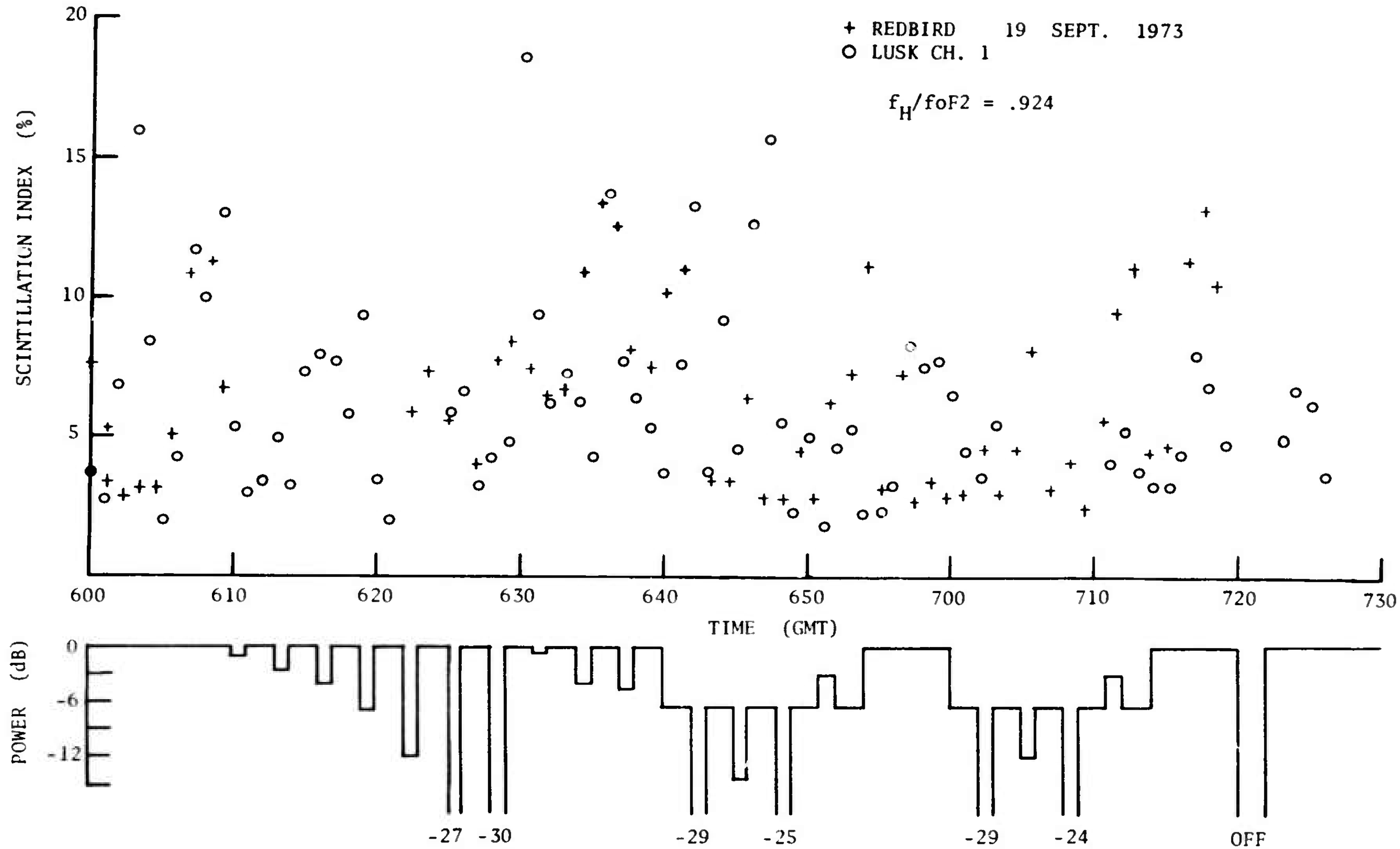


FIGURE 3 SCINTILLATION INDEX FOR THE LUSK AND REDBIRD DATA 0600 TO 0730 GMT

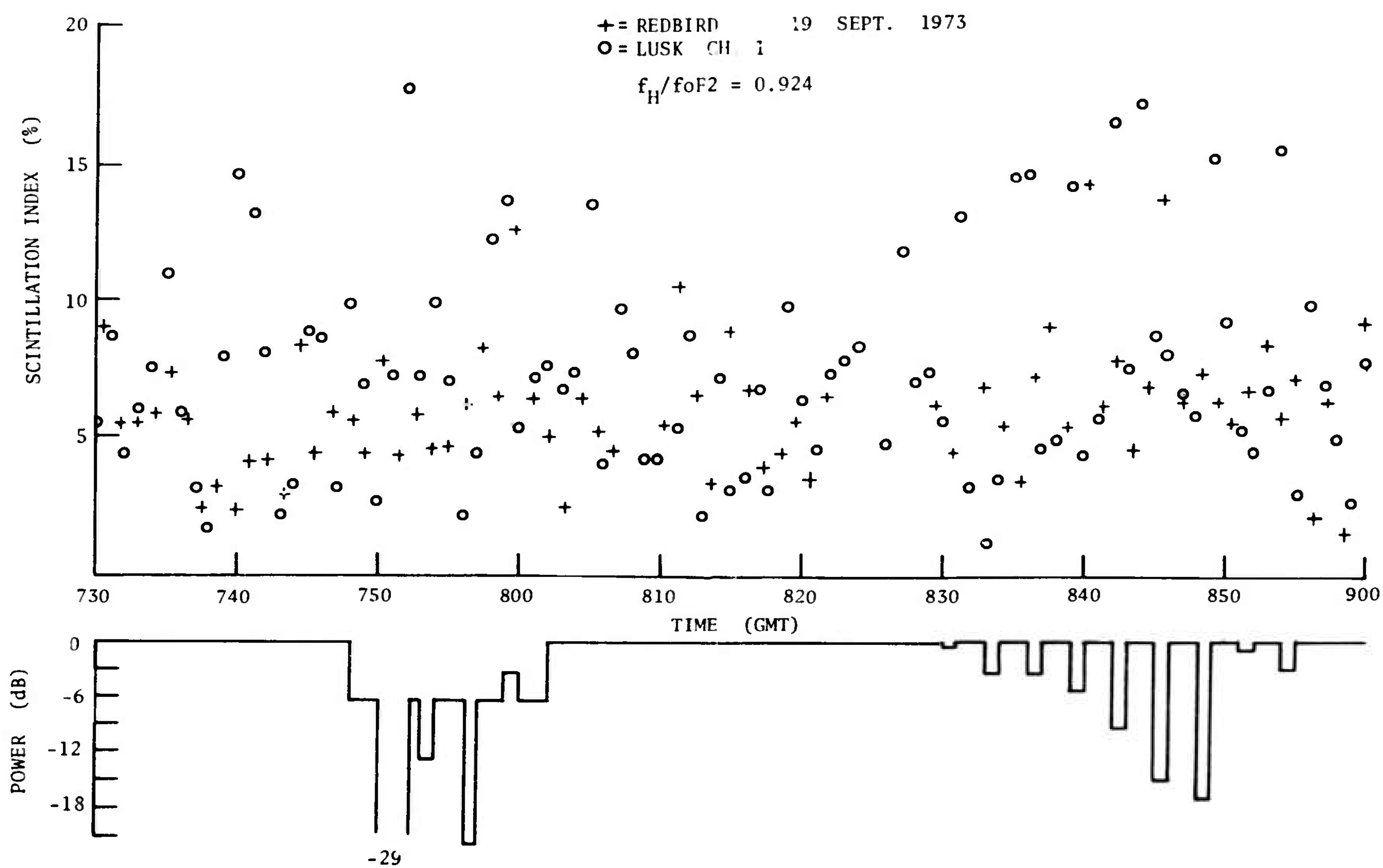


FIGURE 4 SCINTILLATION INDEX FOR THE LUSK AND REDBIRD DATA 0730 TO 0900 GMT

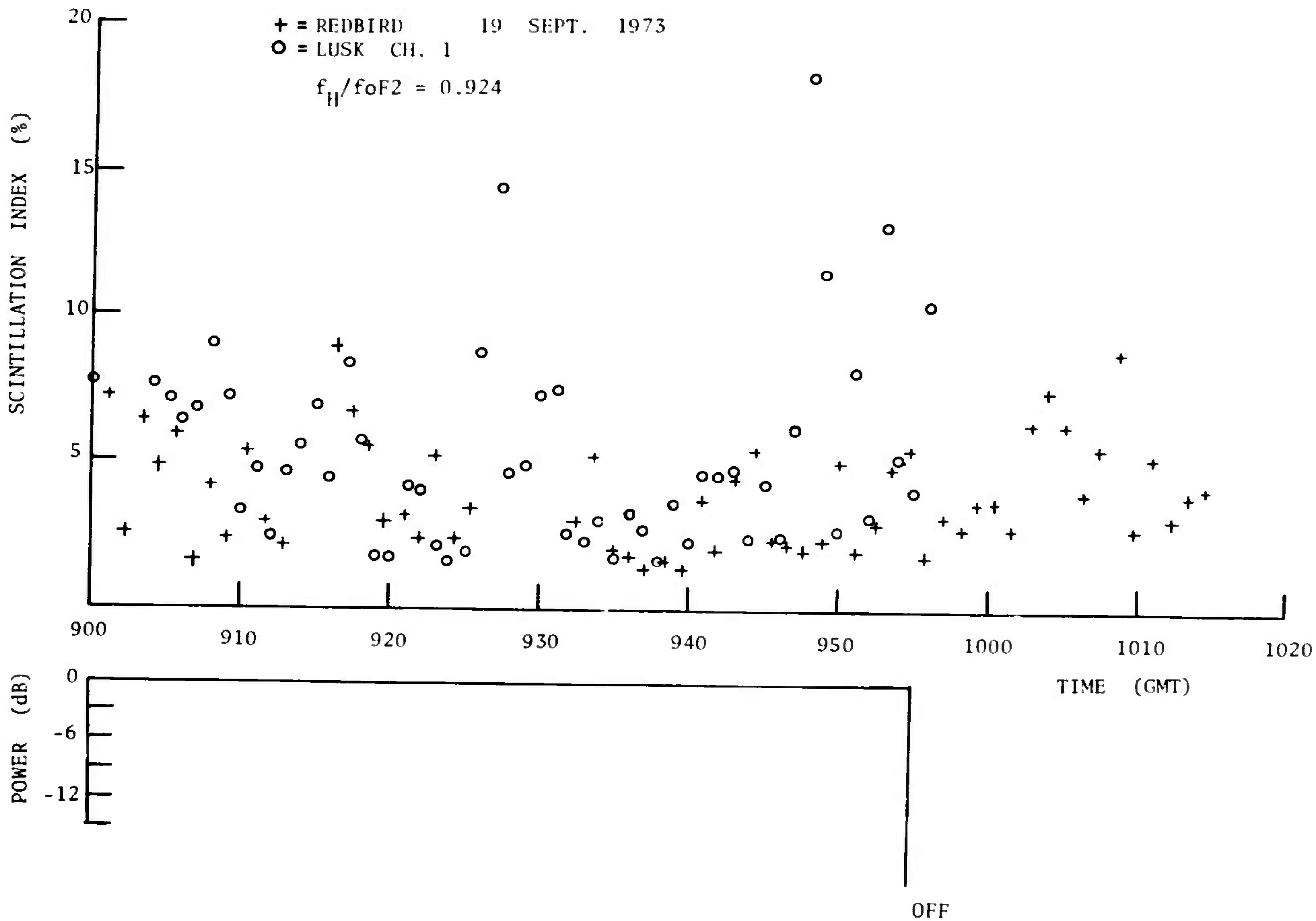


FIGURE 5 SCINTILLATION INDEX FOR THE LUSK AND REDBIRD DATA 0900 TO 1020 GMT

The power data shown in Figures 3, 4, and 5 were prepared from the "log of measured transmitter output" supplied by SRI for these times. The value of $f_oF2 = 3.03$ MHz was reported to be constant over the entire period. The transmitter frequency was also held constant during this time at 2.8 MHz. This gives a ratio $F_H/f_oF2 = 0.924$ for the entire period.

The scintillation data, in spite of the stability of the ionosphere, are quite variable with time. It can be seen that extended periods of reduced power (10 min or more) correspond to periods of reduced scintillation index. On the other hand, extended periods of constant full-power operation (Figure 5) yield large variations in the scintillation of the signal received at both Lusk and Redbird. Detailed comparison of the Redbird versus the Lusk scintillation index shows a great deal of short-term variation. There is somewhat greater long-term (15 min or more) similarity, however. This implies that there does exist a certain amount of correlation between the region probed from the Lusk site and that probed from the Redbird site.

It is clear that some further analysis of these data can be performed. A more accurate measure of the correlation between the Lusk and the Redbird data should be computed. A search should be made for time shifts between these two sets of data.

## REFERENCES


1. S. A. Bowhill and D. R. Ward, "Geostationary Transmission Experiments in PRAIRIE SMOKE IV (U)," in Proceedings of the PRAIRIE SMOKE IV RF Measurements Data Workshop, 7 March 1973 (U), SRI 3-4836, Stanford Research Institute, Menlo Park, Calif. (June 1973), SECRET.

2. E. K. Walton, D. R. Ward, and S. A. Bowhill, "Yield Studies Based on Geostationary-Satellite Transmissions (U)," in Proceedings of the PRAIRIE SMOKE Yield-Model Workshop 17, 18 July 1973 (U), SRI 3-5193, Stanford Research Institute, Menlo Park, Calif. (October 1973), SECRET.

# E-REGION SCATTER OBSERVED AT HASWELL, COLORADO

V. R. Frank

Stanford Research Institute
Menlo Park, California

ABSTRACT

The experiment reported herein concerns the detection of field-aligned irregularities produced in the E region during daylight hours by operation of a high-power ground-based transmitter near a frequency of 3 MHz. Sweep-frequency backscatter soundings showed that the irregularities could be detected at frequencies between 14 and 200 MHz, and that over much of this range they provided radar cross sections as high as 65 dBsm. The sweep-frequency soundings provided samples of scattering from most of the disturbed region, since the area of the intersection of the specular surface and the heated region moves southward with decreasing sounding frequency, as a result of ionospheric refraction. Plots of field-aligned scatter cross section versus modifier transmitter power (yield curves) show a knee. For heater powers below the knee the change in cross section in dB is three or more times the change in heater power in dB. At sounding frequencies in excess of 110 MHz the measurements indicated a decrease of radar cross section with frequency of -20 to -30 dB per octave.

Pages 72, 73 and 74 are blank

# I INTRODUCTION

During two days of the PRAIRIE SMOKE V experiments the Institute for Telecommunication Sciences (ITS) operated their ionospheric modification facility at Platteville, Colorado, at frequencies in the vicinity of 3 MHz during daylight hours to produce HF heating at E-region heights. As a part of these experiments Stanford Research Institute (SRI) operated a sweep frequency CW (SFCW) receiver at the DoC, ITS facility at Haswell, Colorado, using their 60-ft parabolic dish antenna. The sounding transmitter was located at Los Lunas, New Mexico, and has been used during previous experiments of the PRAIRIE SMOKE series. Los Lunas and Haswell are so located as to be linked by specular scattering from field-aligned ionization at E-region heights over Platteville.

Strong field-aligned echoes believed to be from the E region were observed during the experiment. Echoes were observed as high in frequency as 200 MHz. This paper will illustrate the types of echoes observed and their variation in cross section with frequency, heater power, heater-antenna polarization, and steering of the heating antenna beam.

Field-alignment of the scatterers was established by simultaneous observations made on 2 and 3 October 1973 at Haswell and at our receiving field site at Socorro, New Mexico. The appearance of echoes at the two sites was mutually exclusive. That is, when the heater was heating the E region, echoes were observed at Haswell but not at Socorro, and when the heater was heating the F region, echoes were observed at Socorro, but only marginally, if at all, at Haswell.

## II EXPERIMENTAL CONSIDERATIONS

### A. Geometry

Figure 1 is a map showing parts of New Mexico and Colorado, the locations of the SFCW transmitter and receivers, and a 100-km-diameter circle indicating the scattering region over the ionospheric modification facility at Platteville, Colorado. The 60-ft parabolic antenna at Haswell (Figure 2) has a calculated beamwidth of about $6^\circ$ at 150 MHz. For frequencies this high (and higher), the dish probably does not illuminate all of the scattering volume. This effect can be seen in Figure 3(a), which shows the azimuth from Haswell to different points in the heated region.

### B. Raytracing and Specular Surfaces

The height of the specular surface was determined by raytracing through a model ionosphere derived from true-height analysis of a Boulder, Colorado ionogram taken the previous year, near noon. The effects of ionospheric refraction are quite evident in the contours of Figure 3. These contours show specular height, time delay, and elevation angle from Haswell for sounding frequencies of 160 MHz (almost no refraction), 70 MHz, 30 MHz, and 20 MHz.

For the lower sounding frequencies, refraction (especially on the longer path from Los Lunas) causes a change in the magnetic aspect angles [see Figure 3(f)], and an increase in specular heights. For some ranges, at frequencies of 30 MHz and below, specularity is obtained at as many as three heights.

Ultimately the ionosphere will prevent rays launches from the more distant site from reaching a specular height, and a low-frequency cutoff will be observed. We see from the contours of Figure 3 that for this close-in asymmetrical geometry the specular surfaces are highly inclined.

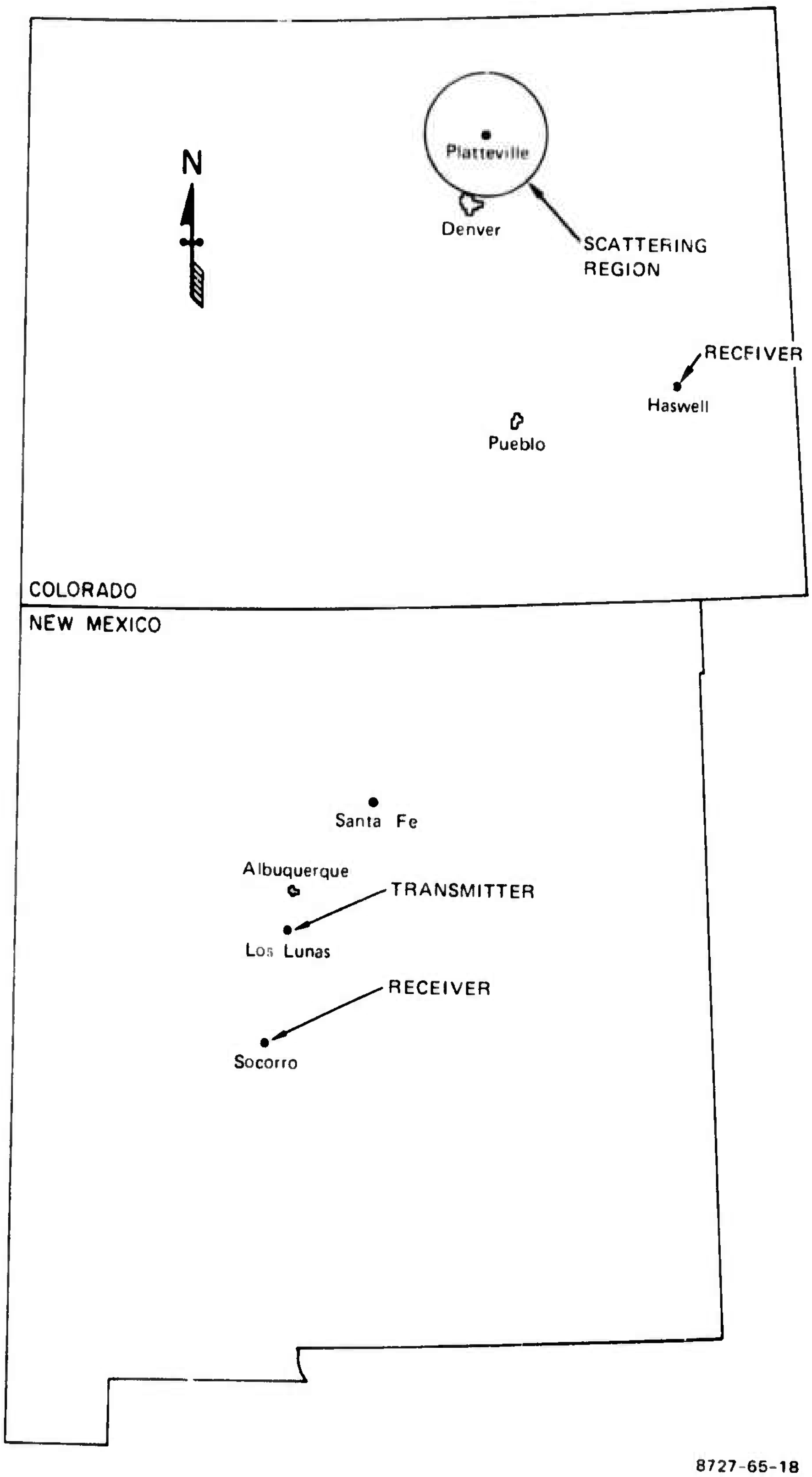


FIGURE 1 MAP SHOWING GEOMETRY OF THE EXPERIMENT

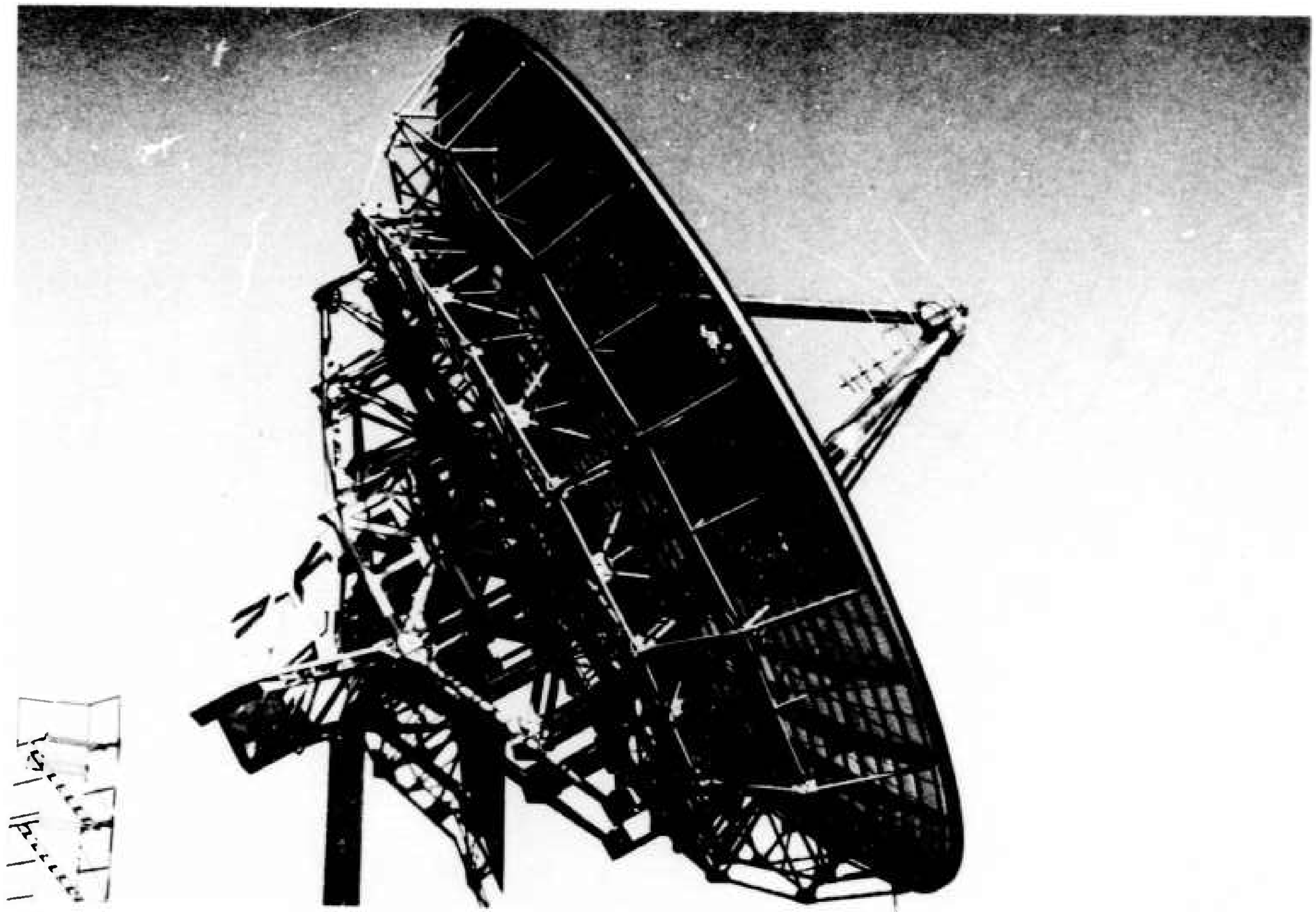

8727-65-19

FIGURE 2 PHOTOGRAPH OF 60-FOOT PARABOLIC DISH ANTENNA AT HASWELL, COLORADO

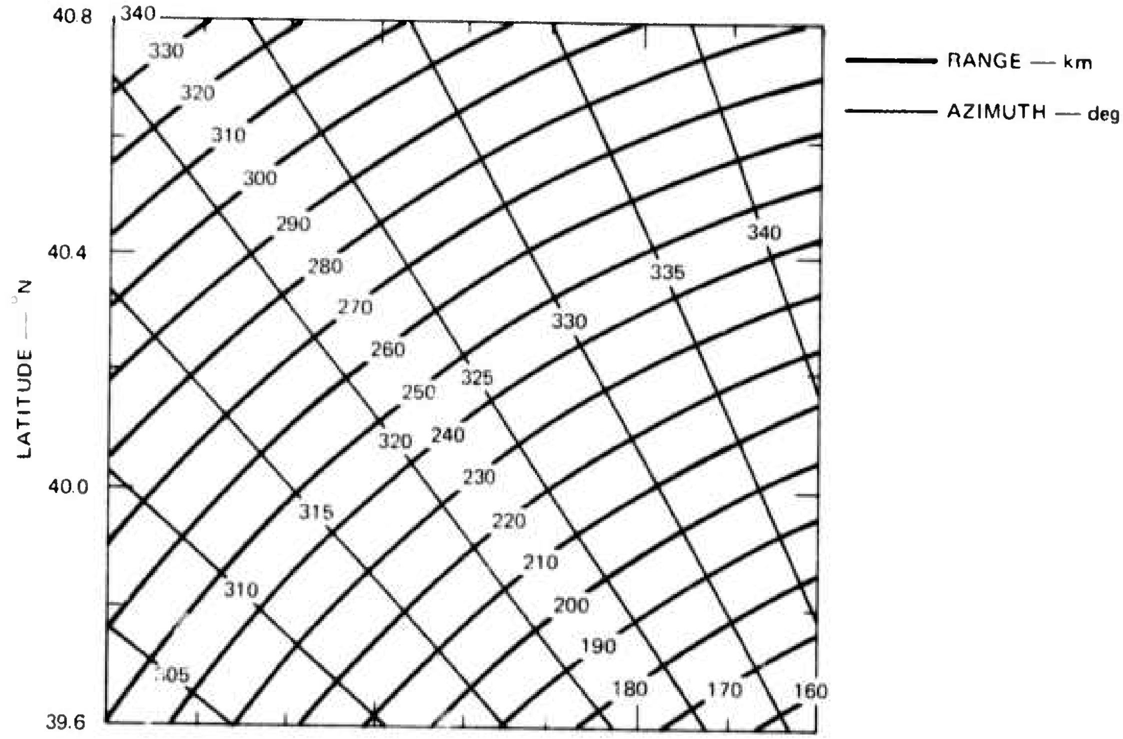


FIGURE 3(a) PLOTS OF GROUND RANGE AND AZIMUTH OF THE HEATED REGION FROM HASWELL

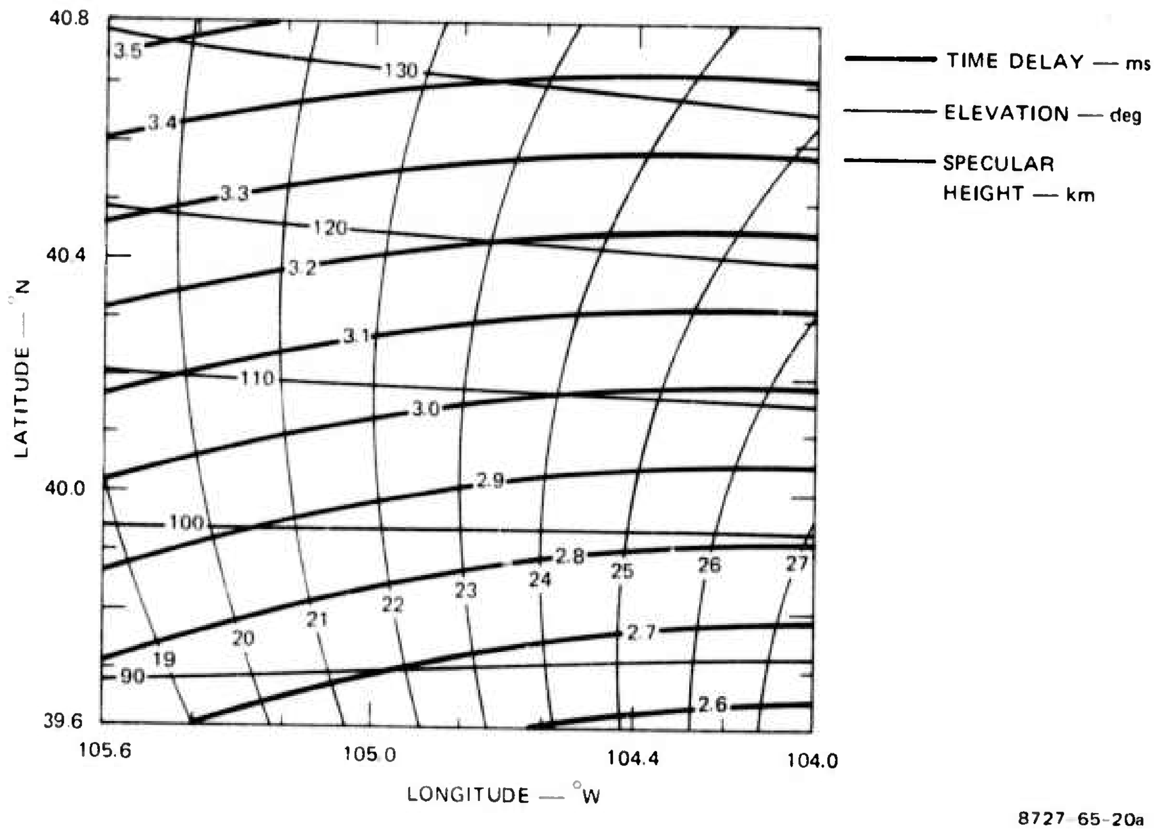


FIGURE 3(b) CONTOUR PLOTS OF SPECULAR HEIGHT, TIME DELAY, AND ELEVATION ANGLE AT HASWELL FOR A SOUNDING FREQUENCY OF 160 MHz

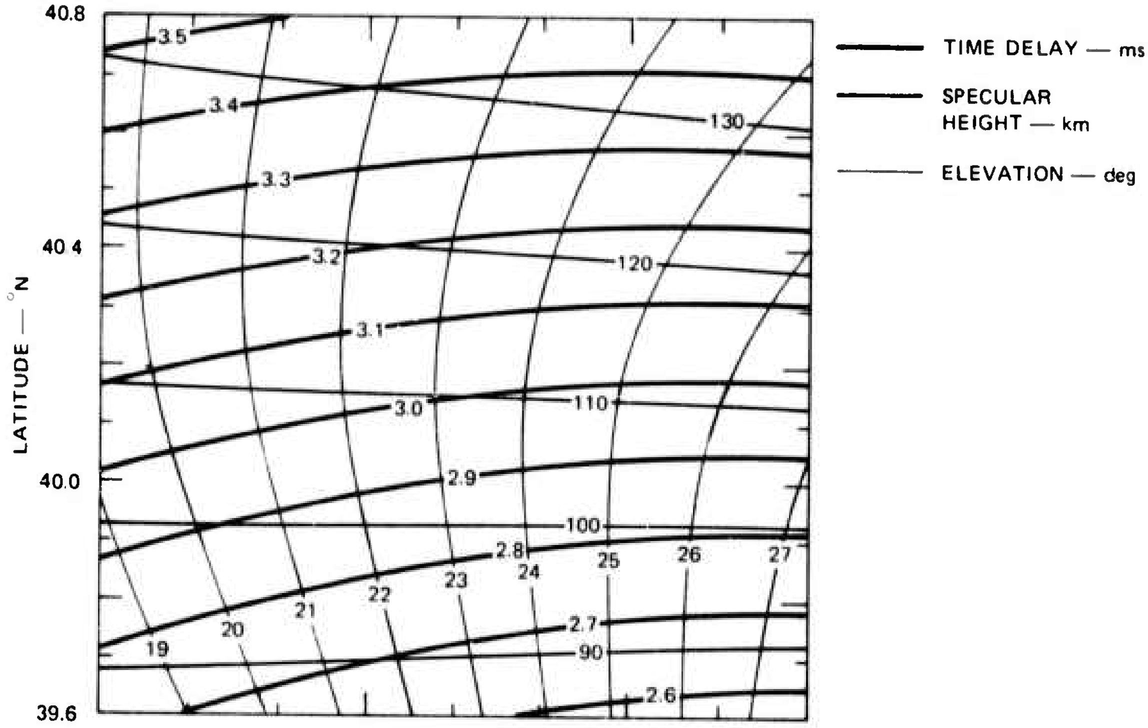


FIGURE 3(c) CONTOUR PLOTS OF SPECULAR HEIGHT, TIME DELAY, AND ELEVATION ANGLE AT HASWELL FOR A SOUNDING FREQUENCY OF 70 MHz

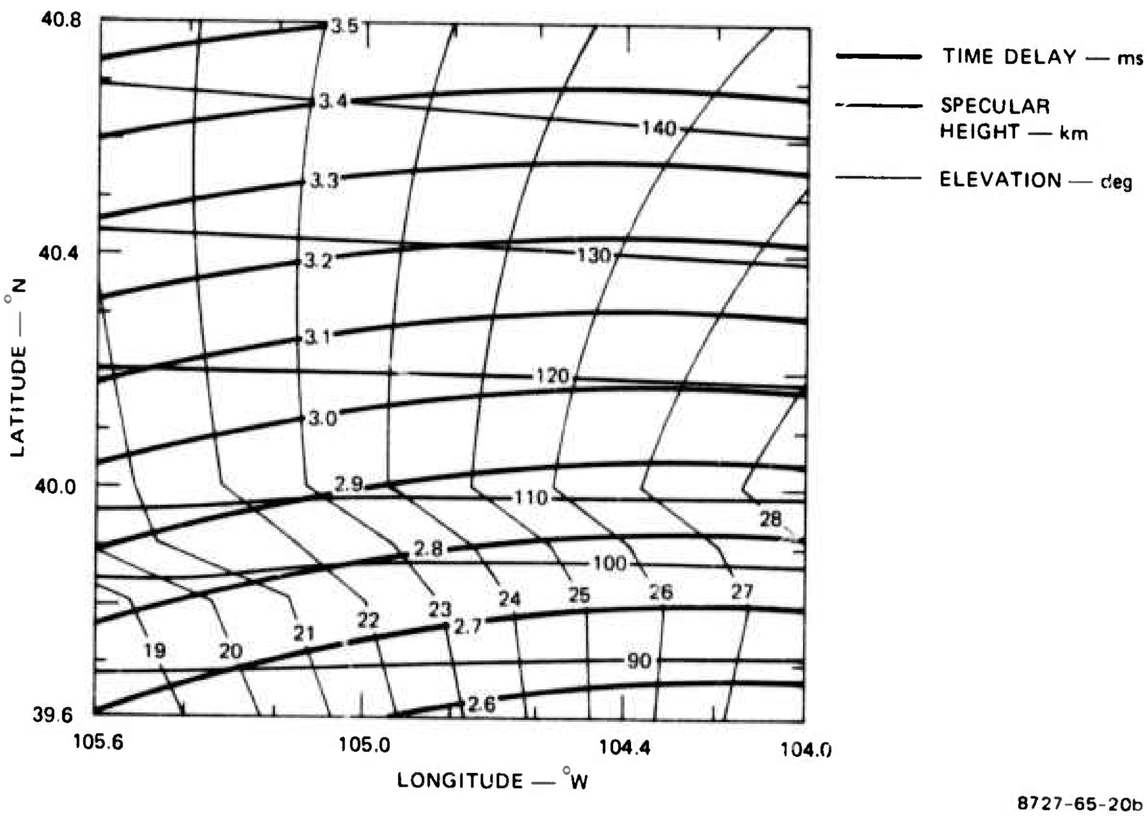


FIGURE 3(d) CONTOUR PLOTS OF SPECULAR HEIGHT, TIME DELAY, AND ELEVATION ANGLE AT HASWELL FOR A SOUNDING FREQUENCY OF 30 MHz

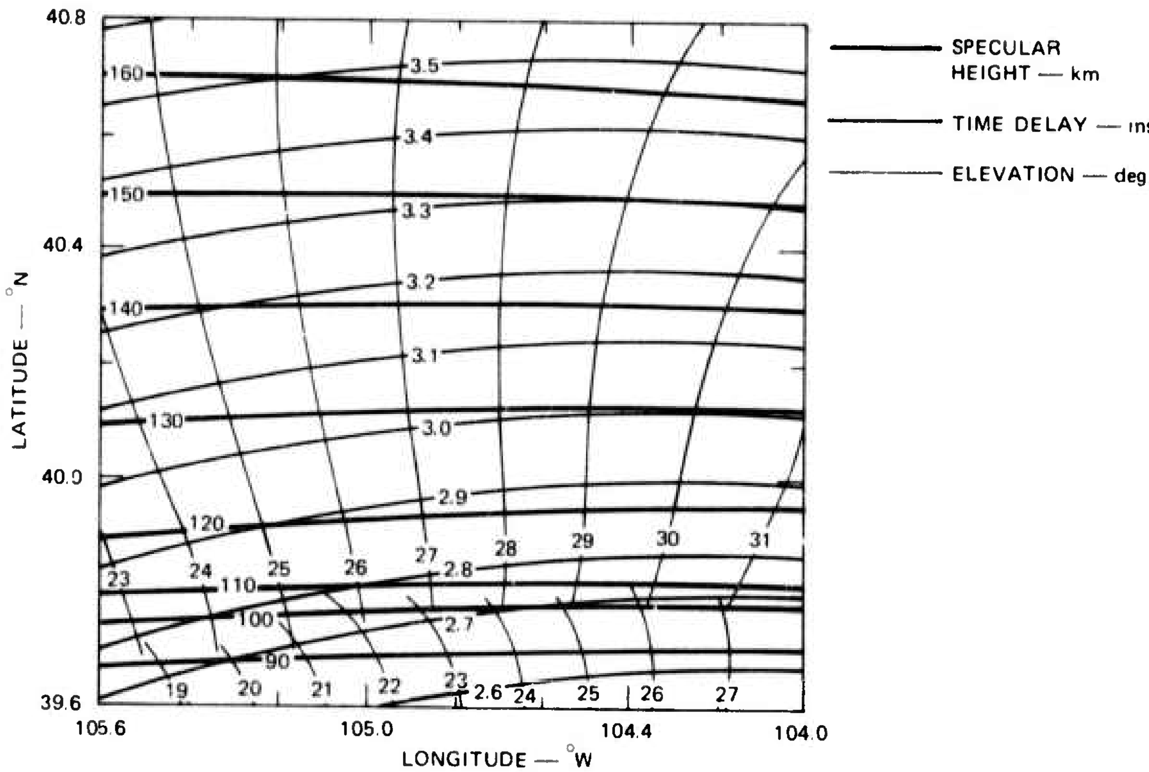


FIGURE 3(e) CONTOUR PLOTS OF SPECULAR HEIGHT, TIME DELAY, AND ELEVATION ANGLE AT HASWELL FOR A SOUNDING FREQUENCY OF 20 MHz

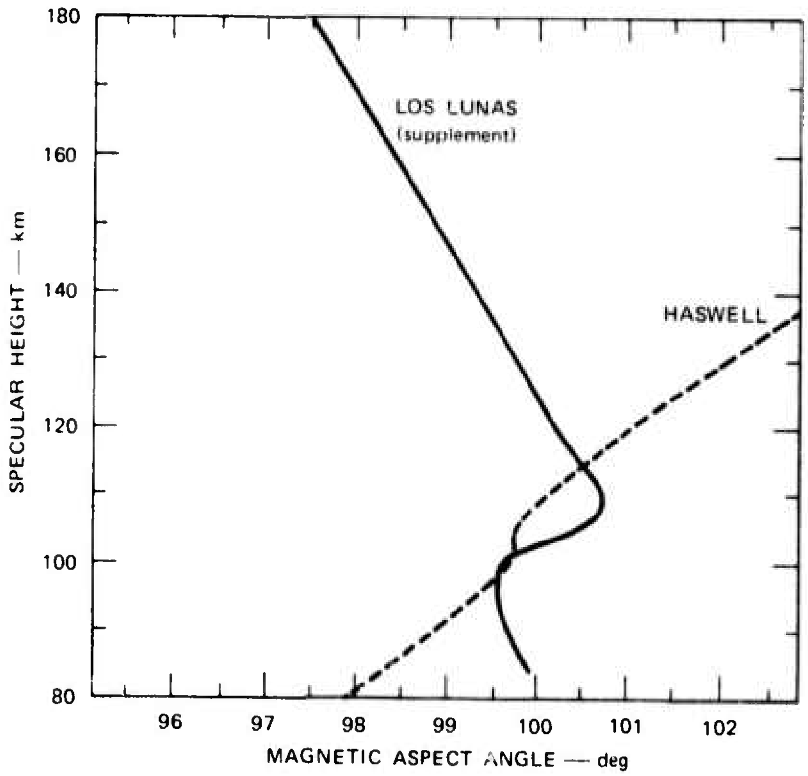


8727-65-20c

FIGURE 3(f) PLOT OF ASPECT ANGLE vs. HEIGHT FOR HASWELL AND LOS LUNAS (Supplement) TO A FIELD-ALIGNED SCATTERER AT 39.8°N, 105.2°W SHOWING MULTIPLE SPECULAR HEIGHTS

If field-aligned scattering is produced over a narrow height range, near the height at which the heating frequency is equal to the local plasma frequency, then only a small portion of the total heated volume, a narrow strip running east-west, will be usable for field-aligned scattering between the two sites. The above considerations will reduce the effective cross sections. Also, the time-delay spread in the echo will be reduced, with a resultant increase in the usable communication bandwidth.

## C. The Background Ionosphere

Figure 4 shows contours of constant plasma frequency as a function of height and time of day for the two days of operations at Haswell. These were derived from true-height analyses of ionograms from Erie and

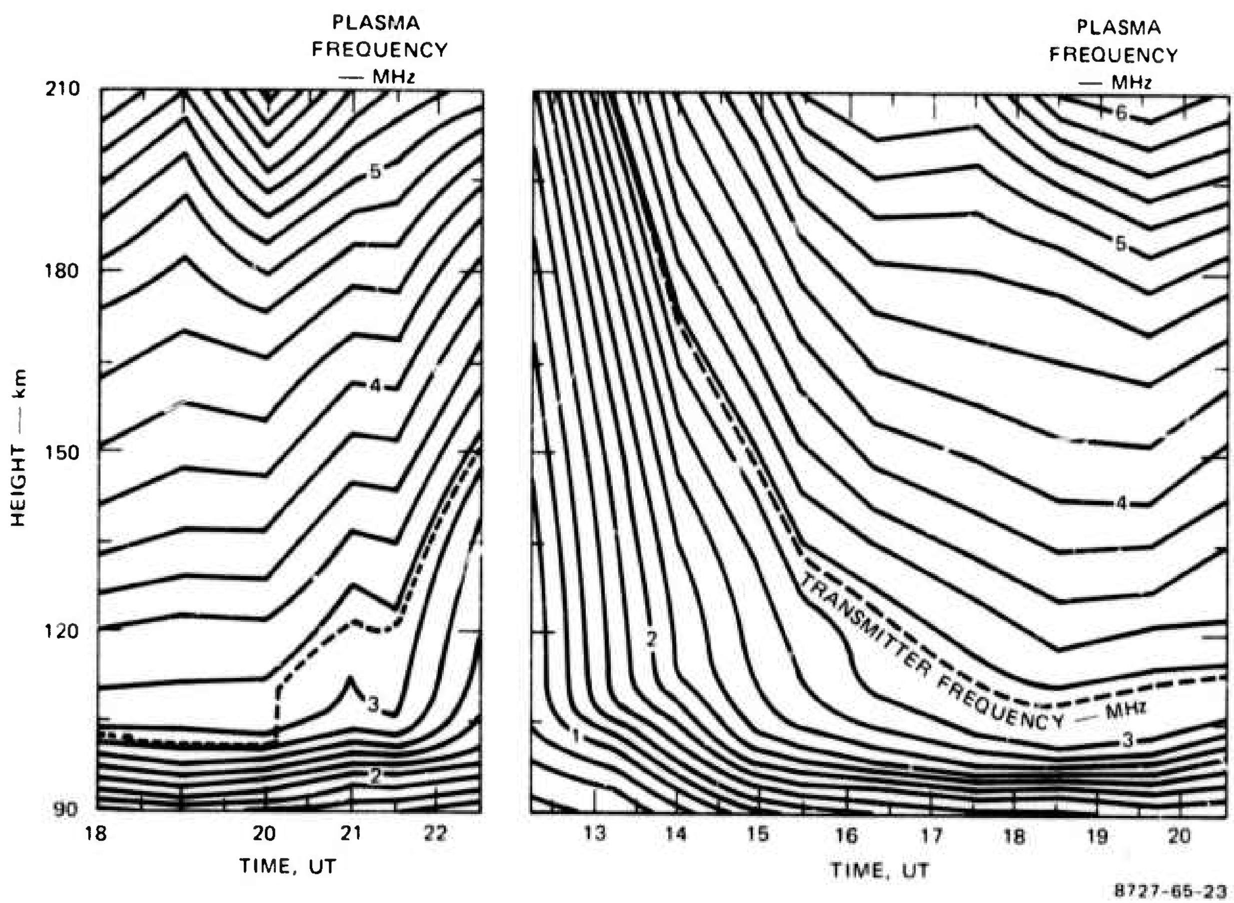


FIGURE 4 CONTOURS OF PLASMA FREQUENCY AS A FUNCTION OF HEIGHT AND TIME OF DAY FOR THE EXPERIMENTAL PERIOD

Boulder, Colorado which were supplied to us by the World Data Center (WDC) at Boulder, Colorado. The usual caveats about true-height reductions are especially pertinent in the E- and F1-region height regime (90 to 210 km).

The dashed line in Figure 4 indicates the contour corresponding to the frequency in use by the Platteville transmitter.

D. Effects of an Ionospheric Valley

As is well known, at times (especially during midday) there may be a valley above the E-region peak in which the electron density is lower than that at higher and lower altitudes. Information about the distribution of electrons in this valley cannot be obtained by vertical-incidence sounders. The WDC true-height reductions produce monotonically increasing profiles. That is, height is a single-valued continuous function of plasma frequency up to the peak of the F2 region.

The importance of the possible existence of a valley above the peak of the E region can be illustrated by the following example. Suppose that the frequency of operation of the modifier transmitter was just slightly in excess of the $f_oE$ and that a valley of 20% or so was located above the E region. Then ionospheric heating would be expected at two heights--i.e., near the peak of the E region, and at a height in the F region at which the local plasma frequency was nearly equal to the modifier transmitter frequency. Thus, field-aligned ionization could be produced at heights around 110 km and also at, say, 150 km or higher.

Also, since rays launched vertically from Platteville will penetrate more deeply into the ionosphere than rays that are launched obliquely, the shape of the heated region is not exactly that of a flat disk centered over the modifier transmitter (although in practice this model

will come quite close in the E region. If the modifier frequency is slightly in excess of the local $f_oE$, the E-region heating is likely to take the form of a doughnut, while the energy escaping up the hole in the middle produces field-aligned ionization in the F1 region.

Figure 5, a north-south cut through the specular surfaces of Figure 3, shows the height of the specular surface along 104.8° W versus distance in kilometers north and south of the latitude of Platteville. It is seen that the specular surface is inclined approximately 27° to the horizontal, and is multivalued in some areas.

Also shown in Figure 5 are the loci of reflection points for rays of frequencies of 3.0 MHz and 4.2 MHz. The loci form dome-shaped curves.

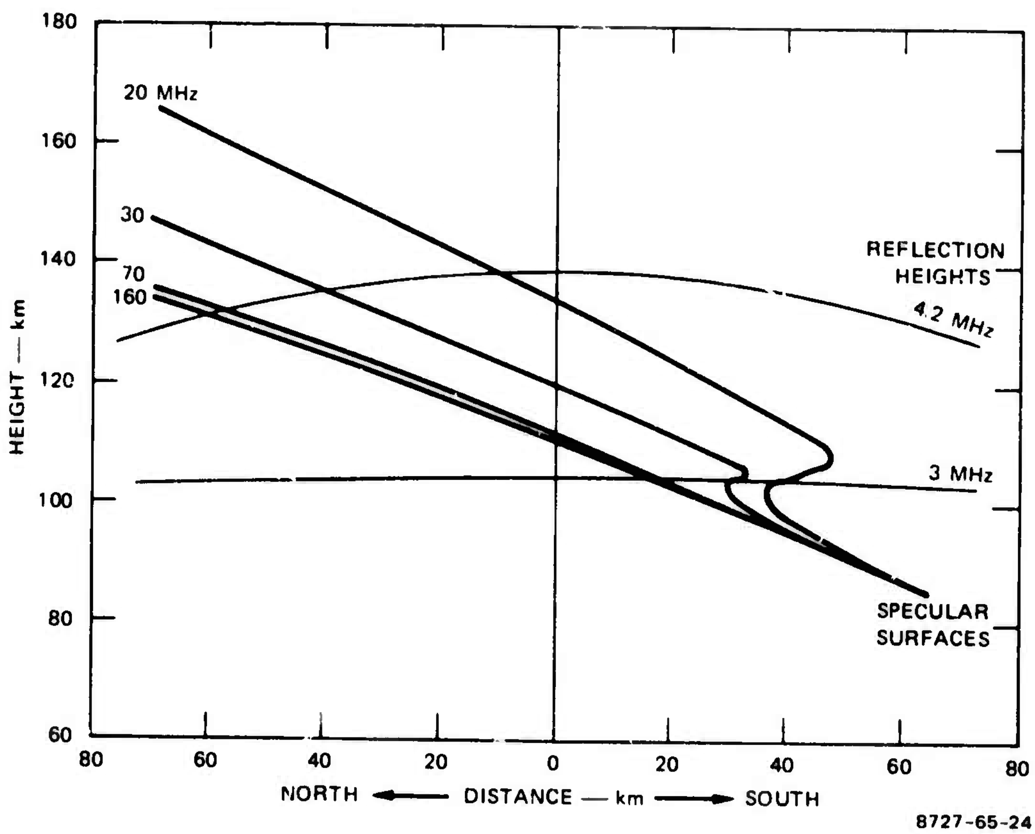


FIGURE 5 NORTH-SOUTH CUT ALONG 104.8°W SHOWING SPECULAR SURFACES AND MATCHED REFLECTION HEIGHTS FOR MODEL IONOSPHERE

(With a lower vertical gradient of ionization above the E layer, the locus would be bell-shaped.) It is interesting to note that, even with the no-magnetic field raytracing used, rays within a circle of some 75 km diameter can reach within a few kilometers of their maximum penetration anywhere. The 75-km diameter corresponds to rays launched from Platteville at an elevation angle of 80°.

If, as it is believed, heating takes place within a few kilometers of the reflection height, then at any particular radar probing frequency, field-aligned scattered echoes will be obtained from those regions where the slanted specular surface intersects the dome-shaped heater region. In Figure 5 it may be seen that the lowest sounding frequencies will be reflected from the southern edge of the dome while the higher sounding frequencies are reflected from further north. Note also that for a doughnut-shaped heated region (a bell with the top blown off), there may be two separated E-region areas giving rise to scattering, one at the south end of the doughnut, scattering the lower sounding frequencies and low time delays, and the other at the north end of the bell, with higher time delays. Such echo patterns have in fact been observed and may be seen in Figure 6.

Figure 6 also illustrates the format of a number of the records presented in this paper. Echo amplitude is represented by the intensity (whiteness) of the data. The sounder frequency is swept linearly over the frequency range indicated (in this case, 10 MHz to 210 MHz). The sharp gaps in the data (e.g., 66 to 72 MHz) are a result of disabling the sounder transmitter to avoid interfering with TV broadcasts and other critical portions of the spectrum. The x-axis (frequency) also is a time axis. For this example, 5 min are required to sweep the entire frequency range. When good temporal resolution is required, continuous sweeps are not used. Instead, the frequency is stepped as rapidly as

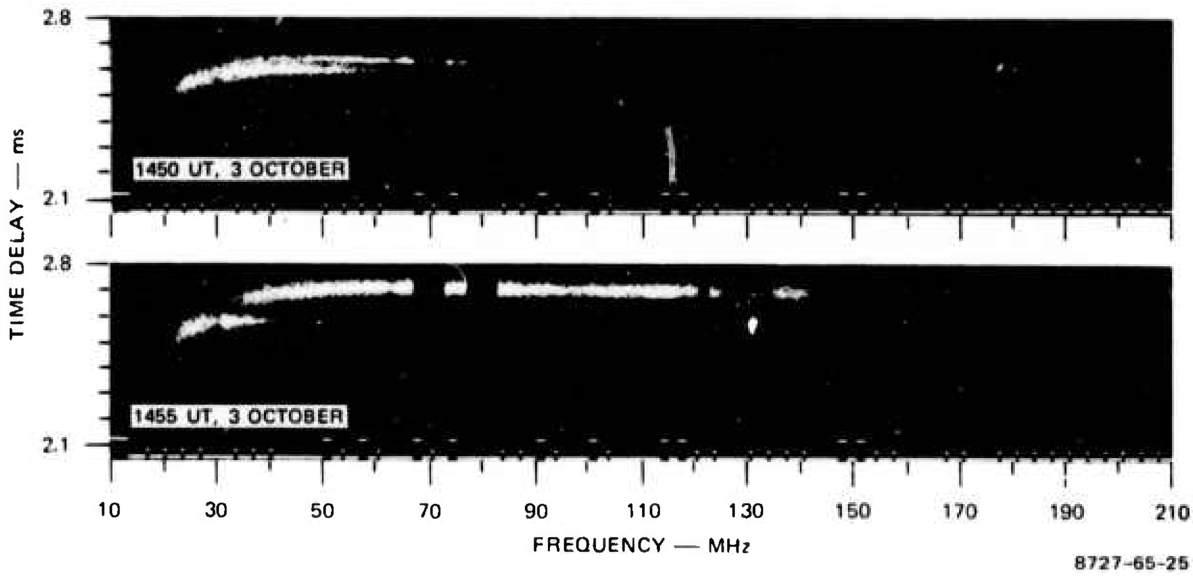


FIGURE 6 CONSECUTIVE SWEEP-FREQUENCY SOUNDINGS SHOWING SEPARATED SCATTERERS

necessary in 20-MHz steps. When the maximum temporal resolution is required, observations are made on only one or two frequencies.

The y-axis of these records indicates echo time delay. The great-circle distance between Los Lunas and Haswell is 505.9 km, corresponding to a delay time of 1.686 ms. Direct signals from Los Lunas to Haswell, apparently diffracted over the intervening hills, were available both days. This should permit absolute calibration of the time delay between the sites. Based on these time delays, the location of the scatterers is apparently some 120 km south of Platteville. We now believe that the signals used for clock synchronization must have traveled by some non-direct route, reflecting off various mountains, which added some 400 μs of time delay. This would place the scattering region nearly over Platteville. (The figures in this paper that have time-delay scales have not been corrected for this extra time delay.) The direction of arrival of the energy scattered from the heated region indicates that the region is indeed over Platteville.

## III EXPERIMENTAL RESULTS

### A. General Characteristics of E-Region FAS

There are some notable differences in characteristics of field-aligned scatter observed during this experiment, compared to earlier experiments using the F region. Some of these are due to actual changes with height and some are due to the experimental geometry (path assymetry). First, as will be shown in the figures of the following sections, the time-delay spread of the E-region echo at VHF is small, less than 150 $\mu$s, corresponding to about 20 km in range. F-region echoes, are spread as much as 1 ms. Some of this difference is due to the heated region being smaller in the E region, and some is due to the greater inclination of the specular surface for this path, as discussed in Section II-B.

The E-layer time-delay spread corresponds to a range of heights of only 8 km in which specularity conditions are satisfied.

The low-frequency tail of the echo, sloping down in time delay, indicates that the heated region is at least 50 km in north-south extent (and probably double that, since the bulk of the VHF echo is believed to originate from directly over the heater).

Another characteristic of E-region field-aligned-scatter echoes is a lack of Faraday rotation of the plane of polarization. Thus, the same polarization should be employed at both receiver and transmitter, and if the bistatic scattering angle is greater than, say, 45°, the polarization should be vertical.

The third unique characteristic is an extended high-frequency cutoff (under optimum conditions), of 110 MHz, about 1-1/2 times that observed in the F region. Below this frequency, the cross section is about 50 to 65 dBsm; above it the cross section drops -20 to -30 dB per octave. The data appear in Section III-C and later sections.

A fourth unique characteristic is a knee in the yield curve. For modifier powers below the knee, the field-aligned scatter drops rapidly. These data appear in Section III-G.

## B. Delayed Effects

Although there is little time delay (under one second) between turn-on of the ionospheric-modification transmitter and reception of field-aligned scattered energy once the ionosphere has been initially excited, some unique effects become evident only after a minute or two of sustained ionospheric heating at high power levels. Figure 7 shows a sequence of sweep-frequency soundings made over the Los Lunas-to-Haswell

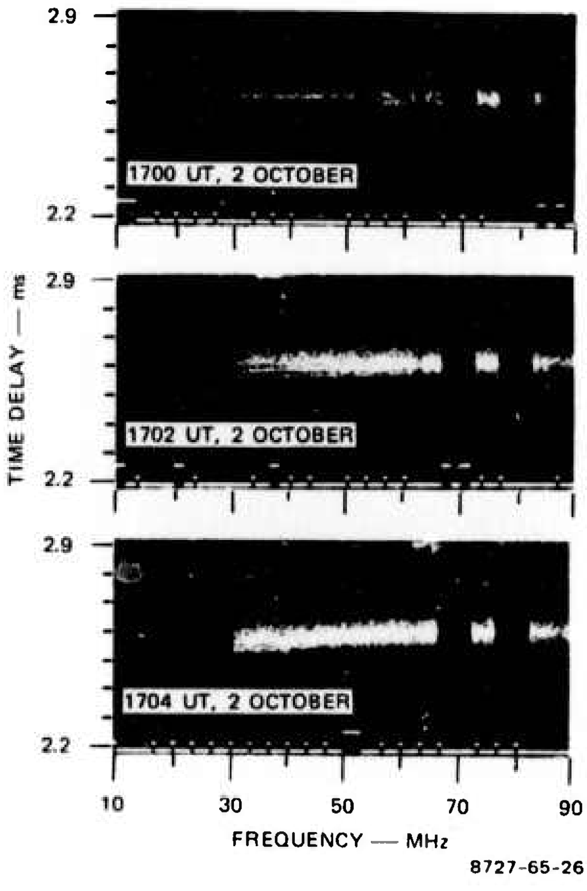


FIGURE 7 CONSECUTIVE SWEEP-FREQUENCY SOUNDINGS SHOWING DEVELOPMENT OF SCATTERING FROM A COLD START AT LOW POWER

path during commencement of Platteville operations on 2 October 1973. This was a cold start. The heater transmitter does not, however, come to full power immediately, and, according to the log, was turned on at 1700 UT at a frequency of 2.9 MHz at some low initial power. The first of the soundings shows the rather small echoes that were produced. According to the Platteville transmitter log, just prior to 1708 GMT power was increased to 0.78 MW with ten transmitters, and full power input was reached just after 1715 GMT. It is our belief that this sequence (Figure 7) shows that when one starts with a cold ionosphere and low excitation levels, heating takes place first in separated areas where focussing allows the electric fields to exceed some threshold level. The heat thus produced is distributed by convection and the affected area fills in and spreads in size.

Figure 8 shows the scattering observed during a series consisting of 10 min of operation at full-power level followed by 10 min of silence. Note that the time-delay spread of the echo is noticeably greater on the second 5-min sounding made during each on interval. This effect has also been observed for F-region heating.[1]*

## C. Other Temporal Effects

The strength and character of the field-aligned scattered signals received at Haswell changed with time. This should be no surprise since the background ionosphere varies greatly with time. In fact, in order to match the E-region critical frequencies at night, a heater frequency of as low as 600 kHz would be required.

Since the ionospheric modification facility was limited to a lower frequency of 2600 kHz, heating of the normal E layer could be accomplished

---

* References are listed at the end of the paper.

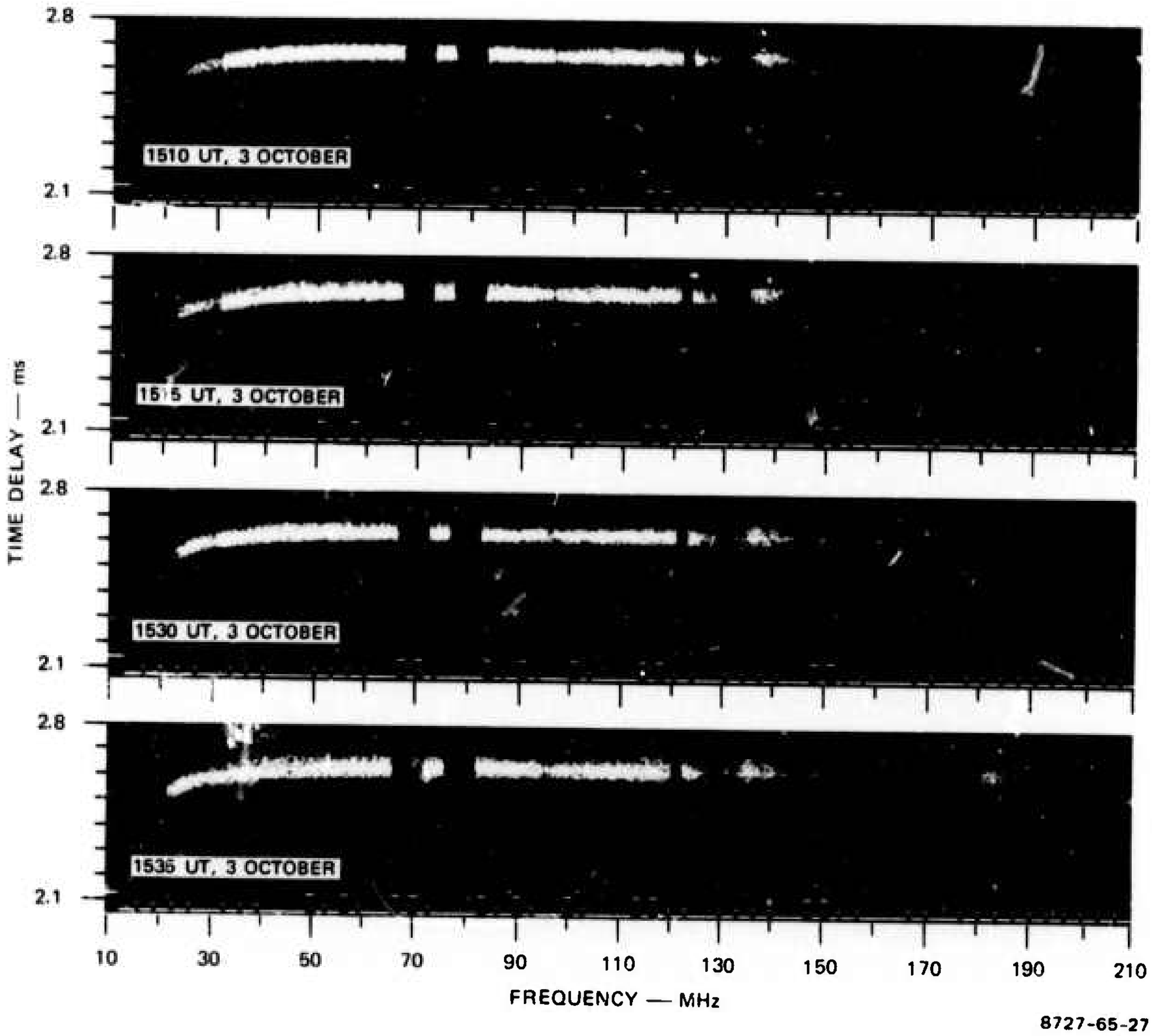


FIGURE 8 SERIES OF SWEEP-FREQUENCY SOUNDINGS SHOWING INCREASED RANGE SPREADING AFTER FIVE MINUTES OF OPERATION. The modifier transmitter was turned on at the beginning of the first and third soundings.

only during daylight hours. Radar-cross-section data indicate a decrease in cross section for heating frequencies whose matched reflection height is much below the peak of the E layer.

Figure 9 shows the results of two sweep-frequency soudings separated by 15 min. On the first sounding the heater frequency was 2.85 MHz, corresponding to a reflection height of 101 km. The dc power input at this time was 1.66 MW. The heater frequency was then moved to 3.15 MHz, with

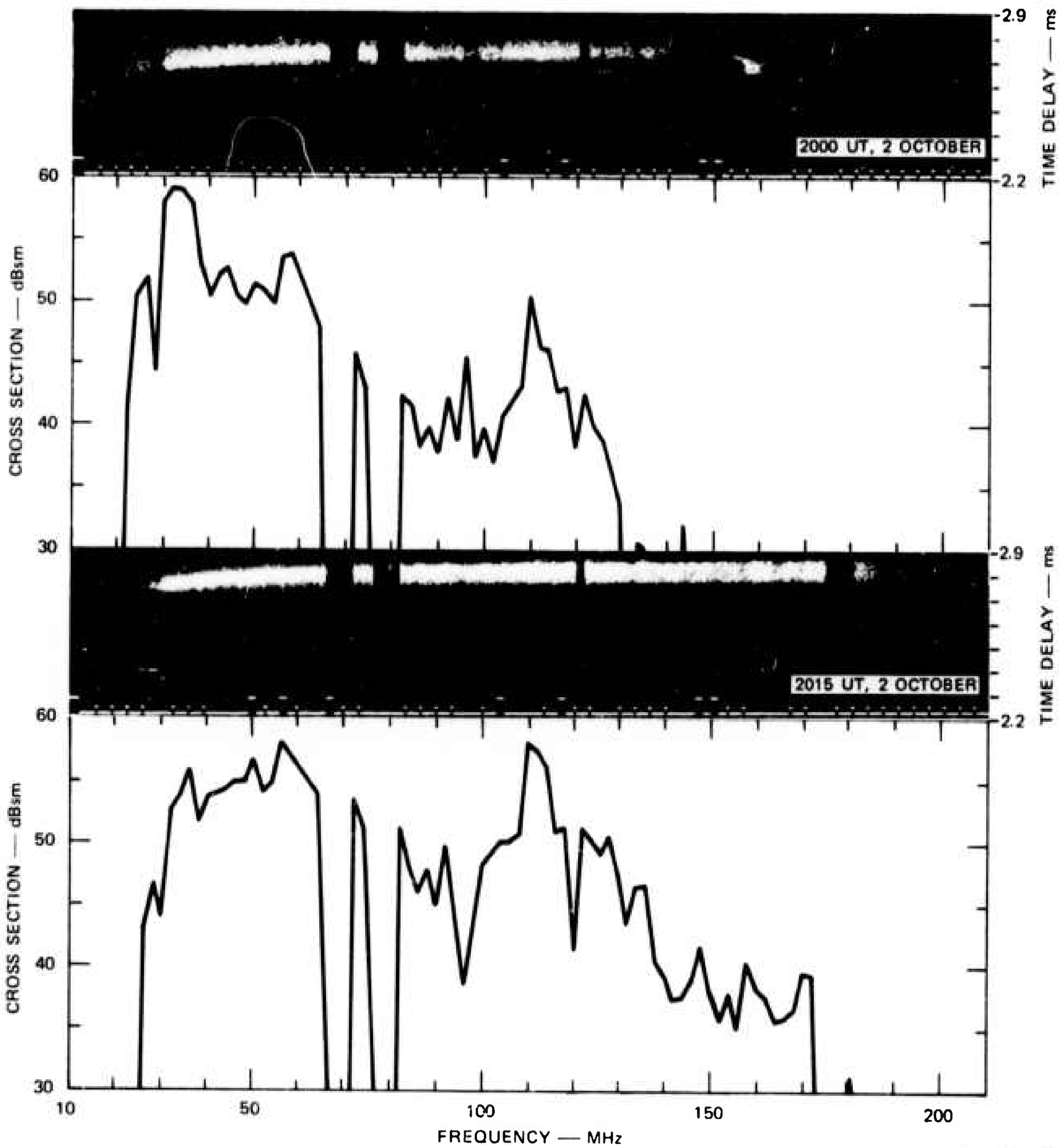


FIGURE 9 TWO SWEEP-FREQUENCY SOUNDINGS AND CORRESPONDING CROSS SECTIONS SHOWING EFFECT OF CHANGING MODIFIER FREQUENCY FROM 2.85 TO 3.15 MHz (resulting in change of reflection height from 101 to 109 km)

a reflection height of 109 km. Although the dc power input was only 0.72 MW, the VHF cross sections are about 8 dB stronger for the second sounding. It is doubtful that changes in D-layer nondeviative absorption between these two frequencies would account for such a large change in cross section. It may be, as Fialer has pointed out,[2] that there is a resonance with the second harmonic of the gyrofrequency (1480 kHz) in this region, or it may simply be that the irregularities were produced at a height where the electron density was greater and thus the RMS variations in the refractive index were greater.

On this date (2 October 1973) the largest cross sections were observed in mid-afternoon when the matched reflection height was between 125 and 150 km. On 3 October 1973 the largest cross sections were observed in mid-morning when the matched reflection height was between 125 and 130 km. Clearly, however, the experiment was much too brief to obtain reliable statistics on diurnal behavior.

## D. Effects of Beam Steering

Our measurements at Haswell strongly suggest that scattering from a heated E region is field-aligned with aspect sensitivity similar to scattering observed from a heated F region. One piece of evidence leading us to this conclusion is the shape of the backscattered radar return in time delay versus frequency, with the lowest frequencies appearing at the shortest time delays (see Figures 6 through 9). An echo from a hard target fixed in range would have the opposite character due to ionospheric refraction--e.g., the lowest frequencies would suffer retardation and refraction and would thus have higher time delays than the higher frequencies. This retardation is present on our soundings; note, for instance, that between 100 and 200 MHz the average time delay

decreases by up to 50 μs.* The reason for the shorter delay time of the HF return (10 to 30 MHz) is that the specular surface is farther south for the lower frequencies. This real change in range to the specular surface is greater than the change in apparent range due to retardation.

As mentioned earlier, the heated region is larger than the beamwidth of the parabolic dish antenna at the higher observing frequencies. In order to measure this, we operated the sounding system in a narrow-band mode wherein the frequency was swept over a 1.33-MHz band in the vicinity of 144 MHz every two seconds. The dish antenna was then slewed either in elevation or in azimuth. Even during sweeping over a frequency range this narrow there was a considerable change in average time delay with sounding frequency. However, as shown in Figure 10, it is quite

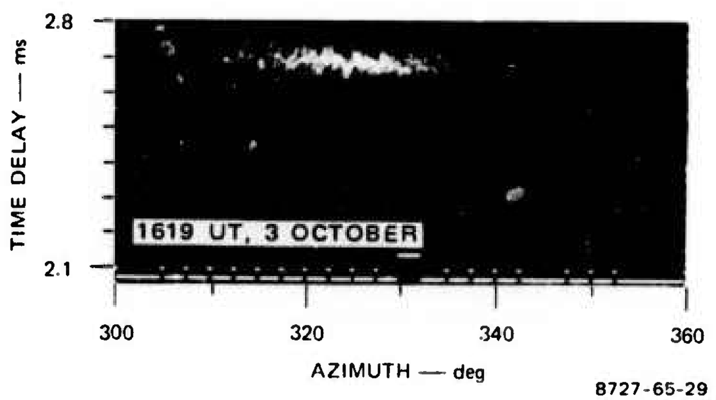


FIGURE 10 TIME DELAY-INTENSITY-AZIMUTH PLOT OBTAINED BY SFCW SOUNDER NEAR 144 MHz AS THE HASWELL DISH WAS STEERED IN AZIMUTH. The serrated return is due to decreased time delay with increasing radar frequency. The overall pattern shows decreasing time delay as the beam is steered to the north. The echo spread in azimuth is greater than the antenna beamwidth.

---

* This characteristic could be caused by a Doppler shift corresponding to a radially receding target; however, since it is usually seen only in this direction (decreasing time delay with increasing frequency) it is now thought to be due more to retardation rather than to Doppler shift.

evident that there is an increased time delay as the parabolic dish antenna is steered to the west as opposed to steering to the north. This behavior can be explained only by a scattering region wider in east-west extent than in north-south extent, such as would be produced by the field-aligned scattering that was discussed in the previous section and shown in Figure 3.

An elevation scan (Figure 11) shows, on the other hand, very little change in time delay with elevation angle. This would also be expected from Figure 3, since the intersection of the heated region with the specular surface is narrow in vertical extent--i.e., does not fill the antenna beam. Figure 12 shows a sequence of three soundings and three cross-section-versus-frequency plots taken on the morning of 3 October 1973. The first sounding was taken with the receiving antenna raised to an elevation angle of 45°. The second was taken 8 min later with the receiving antenna elevation at 35°, while the third sounding was taken at an elevation angle of 25°. The records show a decreasing time delay with decreasing elevation angle. During this period ionospheric critical frequencies were rising rapidly, and the height at which the

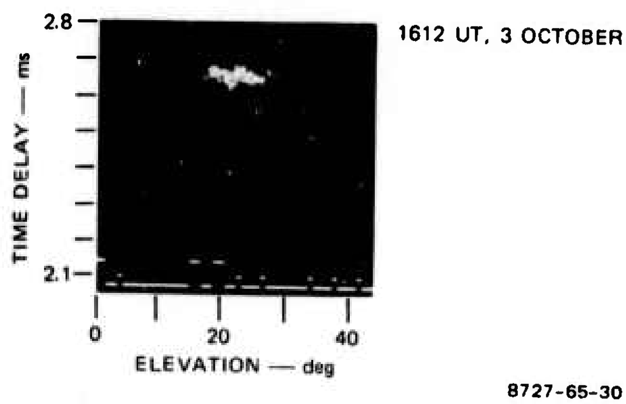


FIGURE 11 TIME DELAY-INTENSITY-ELEVATION ANGLE PLOT OBTAINED UNDER SAME CONDITIONS AS PREVIOUS PLOT. No obvious change in time delay is evident. The echo is spread in elevation angle by somewhat more than the antenna beamwidth.

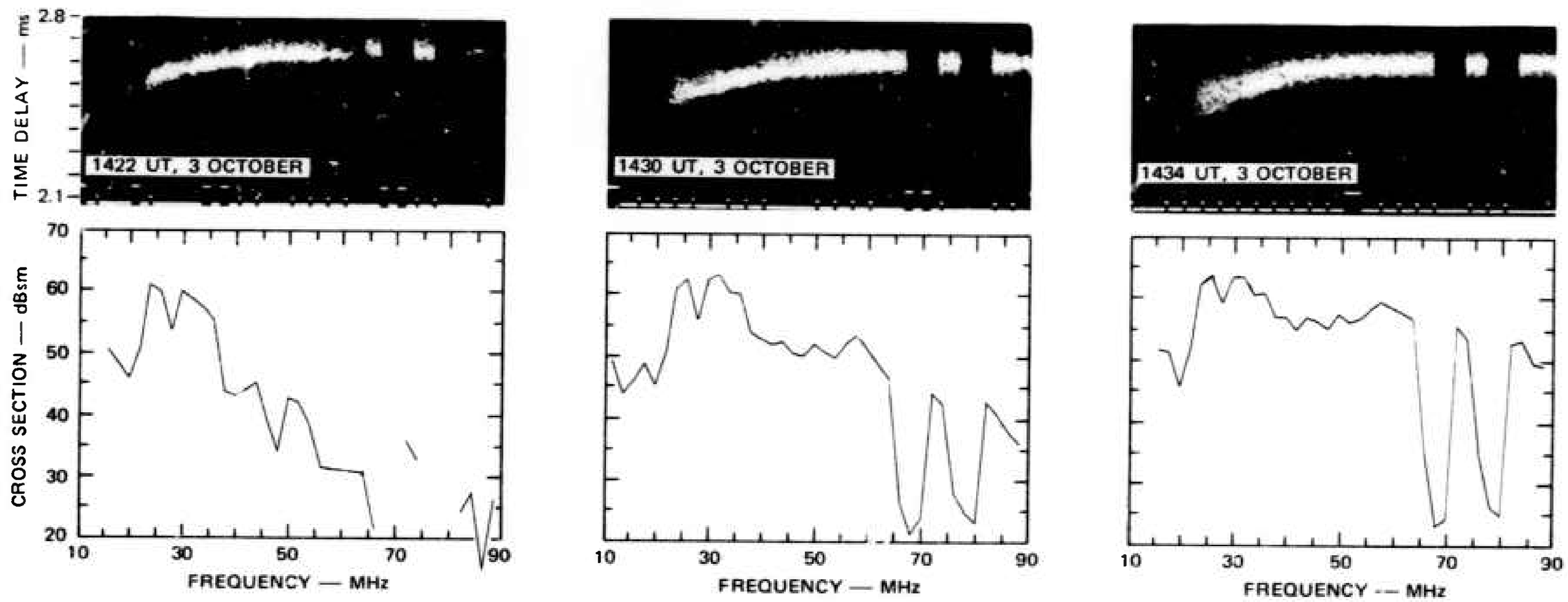


FIGURE 12 SERIES OF SWEEP-FREQUENCY SOUNDINGS SHOWING CHANGE IN TIME DELAY AND CROSS SECTION FOR ELEVATION STEERING ANGLES OF 45°, 35°, AND 25°. The matched reflection heights were dropping rapidly during the series, and that is believed to be the major reason for the range change.

plasma frequency was equal to the heater frequency dropped from 162 km on the first sounding to 157 km on the third. At frequencies near 25 MHz, the lowest elevation angle is preferred, but by only a few decibels. At 60 MHz, where the receiving antenna has more directivity, the cross-section difference between the first and last soundings is on the order of 25 dB.

From Figure 3 it may be seen that the specular surface for a frequency of 70 MHz is some 20 km or more below the heating height, and then only at the northern rim of the heated region. If scatterers were being produced only very near the heating height, and if the scattering was not field-aligned, then the strongest cross sections would be observed at an elevation of 35°. But the strongest cross sections were observed at 25°, corresponding to E-region heights, indicating that a disturbance near 160 km traveled down about 40 to 50 km to produce the effects seen.

The preceding arguments have neglected one important factor--sporadic-E--which often takes the form of a thin ledge of enhanced ionization near the peak of the E region. Sporadic-E frequently produces critical frequencies of 6 or 7 MHz or more. The layer is frequently thin and/or patchy enough to allow reception of vertical-incidence echoes from the F-layer simultaneously. One effect of E-region heating was the formation of strong sporadic-E. An entry in the Platteville transmitter log noted at 1423 UT, 3 October 1973, that strong sporadic-E was evident on vertical-incidence soundings at Erie as a result of ionospheric heating.

The combination of vertical-incidence sporadic-E echoes and FAS from the E region rather than higher suggests (1) that a sporadic-E layer can be disturbed by ionospheric heating so as to produce field-aligned ionization, and/or (2) strong RF fields at frequencies on the order of 3 MHz (about 600 kHz higher than the normal E-layer plasma frequency at this time) can create sporadic-E.

It is well known that there are localized trails of ionization in the E region having critical frequencies much greater than the ambient plasma. These are created by the passage of meteors. It is also quite possible that these too can be affected by ionospheric modification, although previous experiments conducted by this laboratory that set out to detect this process produced negative results.

## E. Effect of Slewing Heater Beam

Figure 13 shows a sequence of three cross-section-versus-frequency plots, before, during, and after a tilt of the ionospheric modifier beam at 20° away from the zenith at an azimuth of 270°. The effect was a small (3-to-6-dB) reduction in cross section observed fairly uniformly across the frequency band. However, the power input of the ionospheric-modification transmitter was only 0.98 MW during the tilt, compared to 1.37 MW before and after. Thus, some, if not all, of the change may be attributed to the reduction in transmitter power rather than the steering of the transmitter beam.

## F. Effect of Using Extraordinary Polarization

One new capability of the low-frequency heating array at Platteville was the ability to make almost instantaneous changes in the sense of circular polarization transmitted. Earlier experiments indicated a pronounced preference for the polarization favoring transmission of the ordinary magnetoionic-component ray in the ionosphere. This is believed to be due to a resonance phenomenon between the exciting RF wave and the ambient plasma. (The extraordinary component, of course, is reflected at a lower height than the ordinary component.) The observations made in this experiment do nothing to discredit the earlier view.

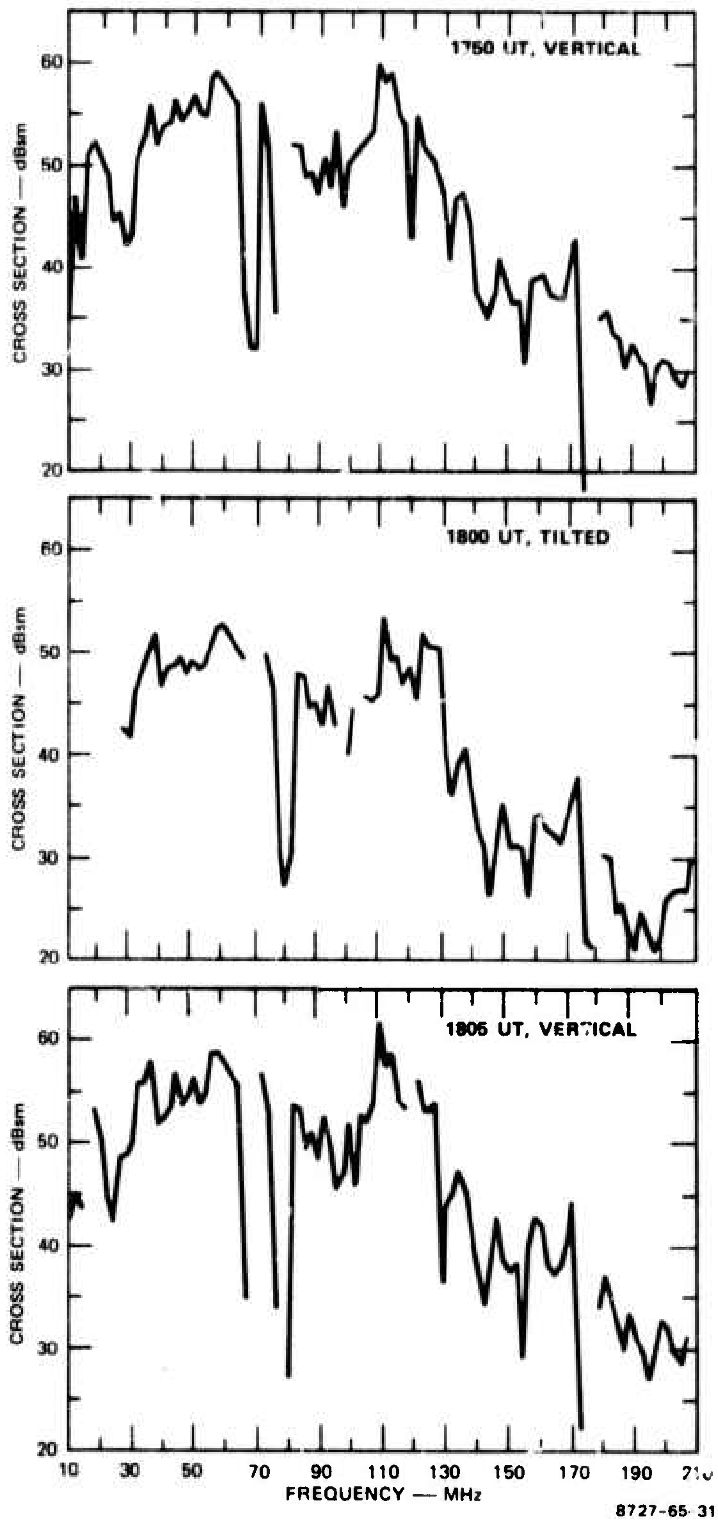


FIGURE 13 SERIES OF CROSS-SECTION-vs.-FREQUENCY PLOTS SHOWING EFFECT OF TILTING THE IONOSPHERIC MODIFIER BEAM 20° AWAY FROM THE ZENITH AT AN AZIMUTH OF 270°. However, the power input during tilt was 0.98 MW compared to 1.37 MW before and after.

A fixed heating frequency of 3.15 MHz was used, corresponding to a reflection height of 110 km for the ordinary ray and 96.5 km for the extraordinary ray. Four soundings taken during an O-, X-, O-mode sequence are shown in Figure 14.

A comparison of the change from X-mode back to O-mode polarization shows cross sections some 30 dB improved with O-mode polarization. Thus, as far as E-region heating goes, either it does not pay to heat below 100 km, or (the more likely explanation) extraordinary-mode heating does not work well in the E region either. Another possible explanation is that non-deviative D-region absorption of the heater signal, which is much greater for X-mode polarization, may be responsible for some of the observed difference.

## G. Effect of Reducing Ionospheric-Modification Transmitter Power

There appears to be a threshold effect in producing field-aligned irregularities in the E region. For ionospheric modification powers below a knee in the yield curve, scattered VHF power varies with the modifier power raised to the third or higher powers. It appears that the Platteville facility is not quite capable of producing saturation of field-aligned scatterers in the E region.

Figure 15 shows three plots of scattered VHF power versus ionospheric modifier power. At the time of the first of these yield tests, the modifier transmissions on a frequency of 2.85 MHz were reflected from a height of 101 km. For the second plot, modifier transmissions on a frequency of 3.15 MHz were reflected from a height of 100 km; and for the third plot the modifier transmissions on a frequency of 3.15 MHz were reflected from a height of 125 to 150 km. If one overlays these plots one finds that the curves are similar, with an offset in heater power (compared to the 101-km plot) of +2.3 dB for 110 km and +3.3 dB

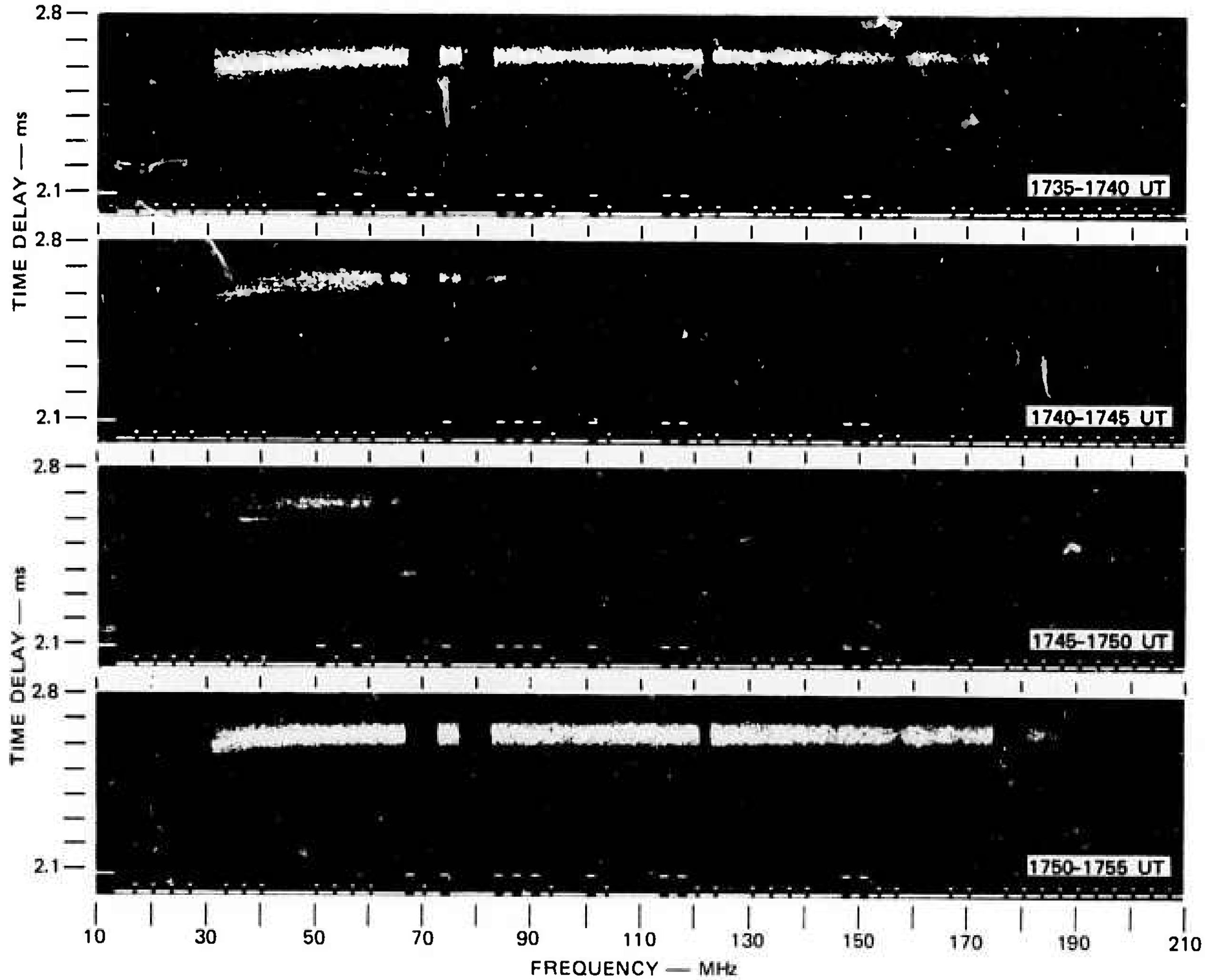


| | |
|---|---|
| 1735:00 | OFF |
| 1735:30 | ON, HAVING DIFFICULTY CHANGING TO X-MODE, POWER INPUT = 0.73 MW |
| 1739:07 | COMPLETED X-MODE CHANGE |
| 1744:00 | GOING UP IN POWER |
| 1744:16 | POWER INPUT = 1.37 MW |
| 1750:50 | COMPLETED SETUP FOR O-MODE, POWER INPUT = 1.37 MW |

8727-65-32

FIGURE 14 FOUR SWEEP-FREQUENCY SOUNDINGS SHOWING EFFECT OF CHANGING HEATER-ANTENNA POLARIZATION FROM ORDINARY RAY (first and last soundings) TO EXTRAORDINARY RAY

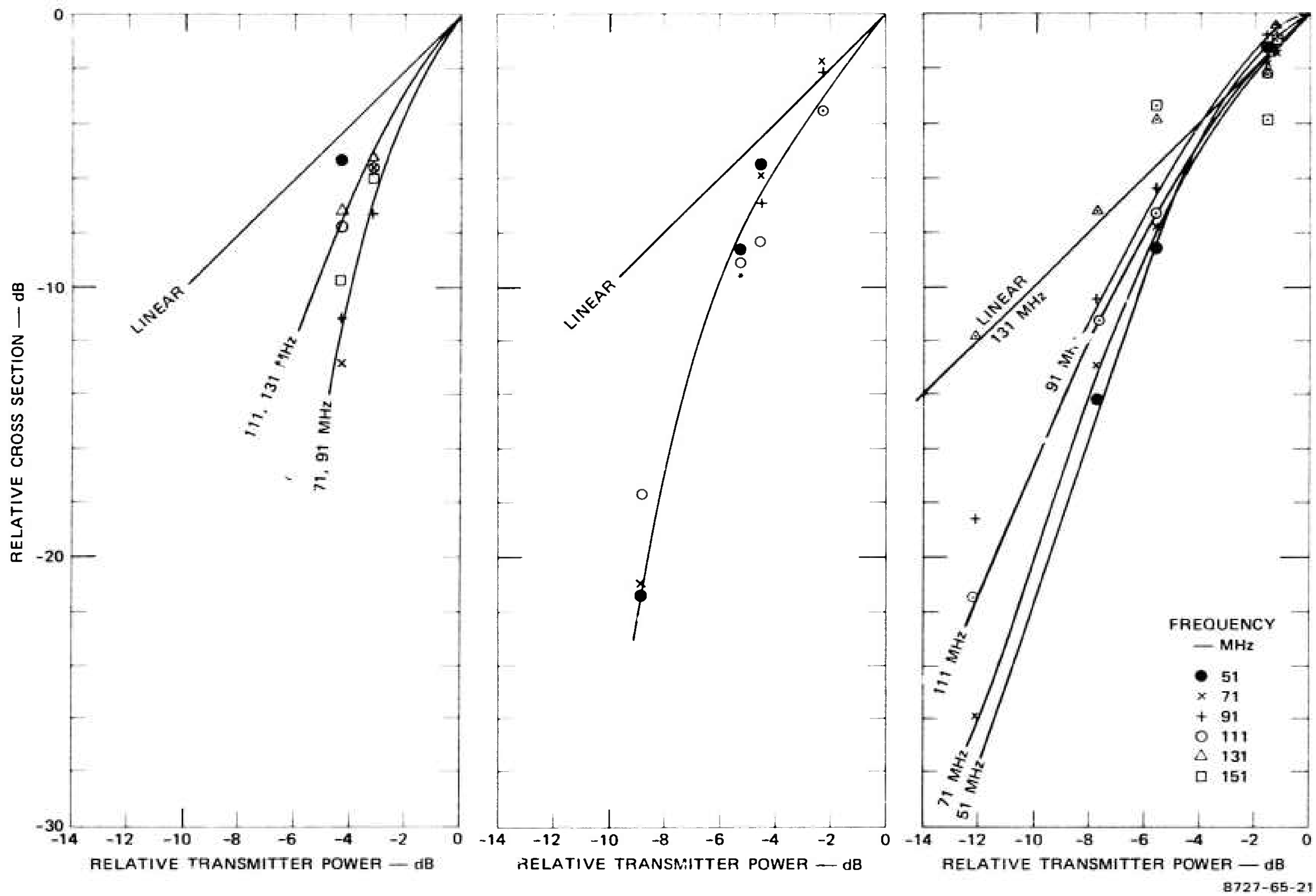


FIGURE 15 THREE PLOTS OF CROSS SECTION-vs.-HEATER-POWER OUTPUT SHOWING THRESHOLD POWERS THAT INCREASE WITH DECREASING MATCHED REFLECTION HEIGHTS (101, 110, 125-150 km left to right)

for 125 to 135 km--values that could well correspond to changes in nondeviative D-layer absorption for the different cases.

There may well also be deviative absorption and some influence of operation near harmonics of the gyrofrequency.[2] However, these latter effects are believed to be the ones that transfer the modifier energy to the scattering irregularities, while the former effect represents a loss mechanism in the D region that may or may not produce irregularities there.

## IV CONCLUSIONS

VHF scattering was observed over a backscatter path between Los Lunas, New Mexico and Haswell, Colorado from field aligned-irregularities in the E region produced by and over the ITS ionospheric modification facility at Platteville, Colorado. These echoes were observed with modifier transmitter frequencies between 2.85 and 3.15 MHz and ordinary-ray vertical-incidence reflection heights of 100 to 160 km. The observations indicated a maximum scattering-region size of 100 km diameter at E-region heights and a thickness under 10 km.

The specular surface for this path is inclined at an angle of approximately 27° (rising toward the north). The use of the sweep-frequency soundings allowed reception of echoes at frequencies as low as 14 MHz and as high as 200 MHz, and the refraction of these signals allowed sampling the heated region over much of its north-south extent.

Radar cross sections as high as 65 dBsm were observed in this experiment at frequencies between 25 and 100 MHz. For frequencies in excess of 110 MHz, the radar cross section was observed to decrease with frequency at 20 to 30 dB per octave. However, some of this reduction may be due to a deterioration of sounder-antenna performance at the high

end of the frequency range. Most if not all of the scattered energy received over this path actually came from the E region, even though the matched reflection height (determined by true-height analysis) was at times as much as 50 km higher.

As with F-region heating, extraordinary-mode E-region heating appears to produce very little field-aligned-irregularity scattering. Results of varying the ionospheric-modifier transmitter power (yield tests) indicate that a knee exists in the yield curve for E-region heating, and that for powers below this knee, scattered energy is proportional to the heater power raised to the third or higher powers.

Ionospheric heating at frequencies in the vicinity of 3 MHz during midday can produce returns on vertical-incidence sounders that appear to be sporadic-E. It is yet to be seen whether this heater-produced sporadic-E will support great-circle-path oblique propagation at very high frequencies similar to the natural type of sporadic-E.

## V RECOMMENDATIONS

Insufficient time has been allowed for completion of the analysis of the data obtained during these two days. There remain two areas of investigation that may prove fruitful; they are range-Doppler soundings, and determination of the rise and decay time constants in response to pulsing of the ionospheric-modification transmitter.

Further experimental work might (1) determine if sporadic-E, capable of forward-scattering great-circle-path VHF signals, is produced by ionospheric heating, and what its characteristics are, (2) determine if there is a scattering enhancement when the E-region is illuminated at twice the gyrofrequency, and (3) confirm that the scatterers really are centered over the heater and are at E-region heights.

## REFERENCES


1. P. A. Fialer, "SFCW Observations of Field-Aligned Scattering (U)," Proceedings of the 1973 Technical Review Meeting (U), Vol. II, Experiments, 20-21 March 1973, p. 34, SRI 3-4534, Stanford Research Institute, Menlo Park, Calif. (April 1973), SECRET.

2. P. A. Fialer, "HF and VHF Observations of Field-Aligned Scattering (U)," these proceedings.

# IONOSPHERIC D-REGION MODIFICATION

W. F. Utlaut

Institute for Telecommunication Sciences
Boulder, Colorado

ABSTRACT

Radio energy traveling upward from the high-powered Platteville transmitter passes through the lower D and E regions of the ionosphere. Before the energy arrives at the location in the F region where the main modification is intended, some modification of these lower regions is to be expected. Such modification had previously been confirmed by cross-modulation observations made by the Institute for Telecommunication Sciences.

Three types of measurements have been made to further explore D-region modification. These are: changes in amplitude of reflected 2.667-MHz signals ($A_1$-type measurement), partial reflection, and 30-MHz riometer measurements.

The A -type measurement showed prompt (<40 ms) decrease in reflected signal strength of up to 6 dB coincident with full-power pulses of heating energy. The prompt onset of increased attenuation is in agreement with conventional D-region theory, although the results available to date do not provide a full description of the D-region effects.

The limited quantity of partial-reflection data analyzed to date indicates that the conventional theory of partial reflections, applicable to the unmodified D region, is not adequate to explain the results observed during ionospheric modification. Finally, the riometer measurements showed no observable changes in absorption associated with operation of the heating transmitter.



Pages 106, 107 and 108 are blank

The radio energy traveling upward from the high-power Platteville transmitter passes through the lower D and E regions of the ionosphere. Before the energy arrives at the location in the F region where the main modification is intended, some modification of these lower regions is to be expected also. Such modification had been confirmed by cross-modulation observations made by the Institute for Telecommunication Sciences. These observations[1, 2*] utilized 20-kHz (WWVL), 60-kHz (WWVB), and 2.5-MHz (WWV) transmissions received at a location so that the signals reflected from the ionosphere over Platteville. With the Platteville transmitter modulated on and off, it was observed that an amplitude modulation was impressed on the signals passing over the heating transmitter and that this modulation exceeded 8% at 2.5 MHz, 12% at 60 kHz, and a few percent at 20 kHz. The 2.5-MHz signal was reflected from the E region at an altitude of about 110 km, while the lower-frequency signals were reflected from D-region altitudes of perhaps 80 to 85 km for 60 kHz and appreciably lower for 20 kHz. These measurements and theoretical estimates of the increase in electron temperature and hence in electron collision frequency in the D-region raised questions relating to how much additional absorption the high-power wave would induce in the lower ionosphere. Such questions are of interest not only in understanding the aeronomy of the D region but also in determining how much of the radiated power from the transmitter is effective in modifying the higher ionosphere. They are also useful in the effort to discover whether there is a limit to the amount of power that can be used if, for example, the D-region absorption increases at a rate such that it nearly consumes most of any increase in transmitter power beyond some level (a saturation effect). The latter had been suggested as a possible explanation for the nonlinear increase of the reflecting cross section of the modified ionosphere region as modifier power was increased.

---

* References are listed at the end of the paper.

Because of the concentration to date on understanding the phenomena associated with F-region modification, only limited data have been obtained pertaining to D-region modification effects. Some results from cross-modulation measurements were cited above. In addition, three other types of measurements have been made to explore D-region modification. These included: change in amplitude of reflected signals ($A_1$ type measurement), partial reflection, and riometer measurements.

A 30-MHz riometer was operated by SRI at the ITS Table Mountain field site near Boulder, Colorado. A relatively narrow-beamwidth antenna array was arranged to provide an intersection of the riometer beam and the heater beam at D-region heights over Platteville. The data analyzed to date have shown no indication of attenuation associated with the operation of the heating transmitter.

The limited number of partial-reflection measurements that were made gave erratic results when analyzed using conventional theory. In the usual analysis procedure a "standard" collision-frequency-versus-height profile is assumed, and calculations of electron-density profiles are made using the partial-reflection amplitude-ratio measurements of the ordinary to extraordinary magnetoionic components of the signals that are weakly reflected from the same heights in the lower ionosphere. This procedure, which presumably provides correct results for most of the natural small perturbations of the D region, seems to fail in the case of artificial modification because the collision-frequency profile is modified in an unknown way as is, also, the electron-density profile. It appears that it might be possible to sort out these two phenomena, with measurements that have not yet been made, and to obtain partial-reflection measurements that would provide a correct interpretation of the changes caused in the D region by the high-power transmitter. The change in collision-frequency profile might be measured by comparing,

for a sequence of heights, partial-reflection amplitude changes during the on and off times of the modifier, with the modifier on for only a second or less. During this short on-time it would be assumed that absorption changes would result from a change in collision frequency, which has a short time constant, and not from a change in electron density, which should not occur during the short on-period. With the modified collision-frequency profile obtained in this way, and with partial-reflection measurements made during a longer turn-on of the high-power transmitter to allow time for electron-density changes to occur, analysis should provide information on the density changes.

Measurements were made of the incremental increase in attenuation produced by the Platteville transmitter in the region from the bottom of the ionosphere, up to a height of about 110 km. A 2.667-MHz X-mode diagnostic pulse signal was transmitted with a separate transmitter located at the Platteville site. The signal was reflected from the E region, about 110 km directly overhead, and received at the site. The amplitude of the once-reflected diagnostic signal was recorded on moving film as shown in Figure 1, and the two-way attenuation was measured by comparing the received signal level with Platteville on and off. A 1-s on and 29-s off period was used for these measurements. The heating transmitter was turned on for this short time so as to minimize any changes in the reflection property of the E region experienced by the diagnostic signal. Thus, the change in signal level should be attributable to increased absorption in the lower ionosphere caused by the high-power transmitter. The pulse interval shown in the record of Figure 1 is approximately 80 ms. Other records were made with pulse intervals of 40 ms, and from these it is clear that the increase in absorption occurs in less than 40 ms after Platteville is turned on. This short time constant is as predicted by theory and is attributable to a prompt increase in the electron temperature and therefore in the

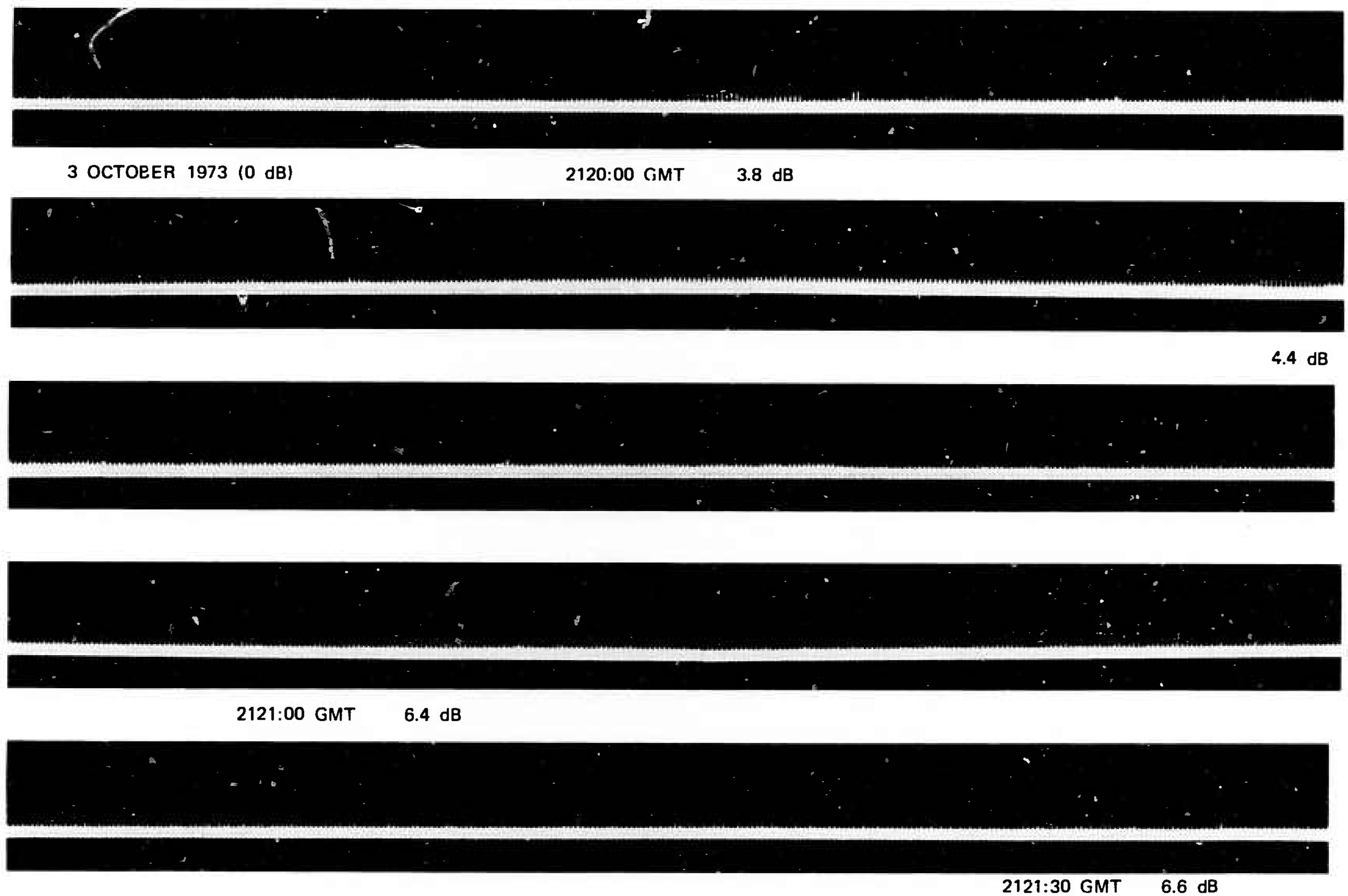


FIGURE 1 PULSE-BY-PULSE AMPLITUDE MEASUREMENTS OF ONE-REFLECTED SIGNALS FROM THE IONOSPHERE AT ABOUT 110 km OVER PLATTEVILLE TRANSMITTER SITE. Diagnostic signals at 2.667 MHz; Platteville transmitter operating with O-mode polarization at 6.21 MHz; 1 second on at full power, 29 seconds off. Incremental dB attenuation indicated near notches in pulse record caused by high-power wave from Platteville.

collision frequency in the illuminated region below the reflecting height of the diagnostic wave.

Figure 2 shows the median values of two-way additional attenuation, when Platteville is on, measured on different days and with heating being done with O-mode and with X-mode. Unfortunately, due to scheduling arrangements for a variety of IVORY CORAL tests, comparable frequencies for the O- and X-mode heating were not used, so it is not possible to sort out the affects of illumination mode and frequency from this limited set of available data made in the last days of IVORY CORAL observations. The X-mode data were obtained at about 1200 MST and the O-mode data were obtained at 1800 MST on 30 September 1973 and about 1400 MST on 3 October 1973. They show, on the relatively low frequency of 2.667 MHz, that the two-way attenuation induced by the Platteville transmitter did not exceed about 6 dB for either heating mode or frequency. Higher frequencies would experience a lesser incremental, and total, attenuation. It is somewhat surprising that the 3.15-MHz X-mode heating did not produce a greater incremental absorption than was observed with the 6.21-MHz O-mode runs. Theory would predict a greater absorption of the heating wave with decreasing frequency and also that the X-mode is absorbed to a greater extent than is the O-mode. Thus, it might have been expected that the X-mode runs would have increased the effective collision frequency a greater amount and, consequently, absorbed the diagnostic pulses to a greater extent. If, however, the electron density could have changed at a very fast rate also, then it is possible, as shown by Kissick and Ferraro,[3] that high-power waves can result in a reduction of total absorption.

In Figure 2 it may also be observed that the variation, with heater power, of the incremental absorption is different for the two modes, the X-mode resulting in a smaller increase with increased heater power.

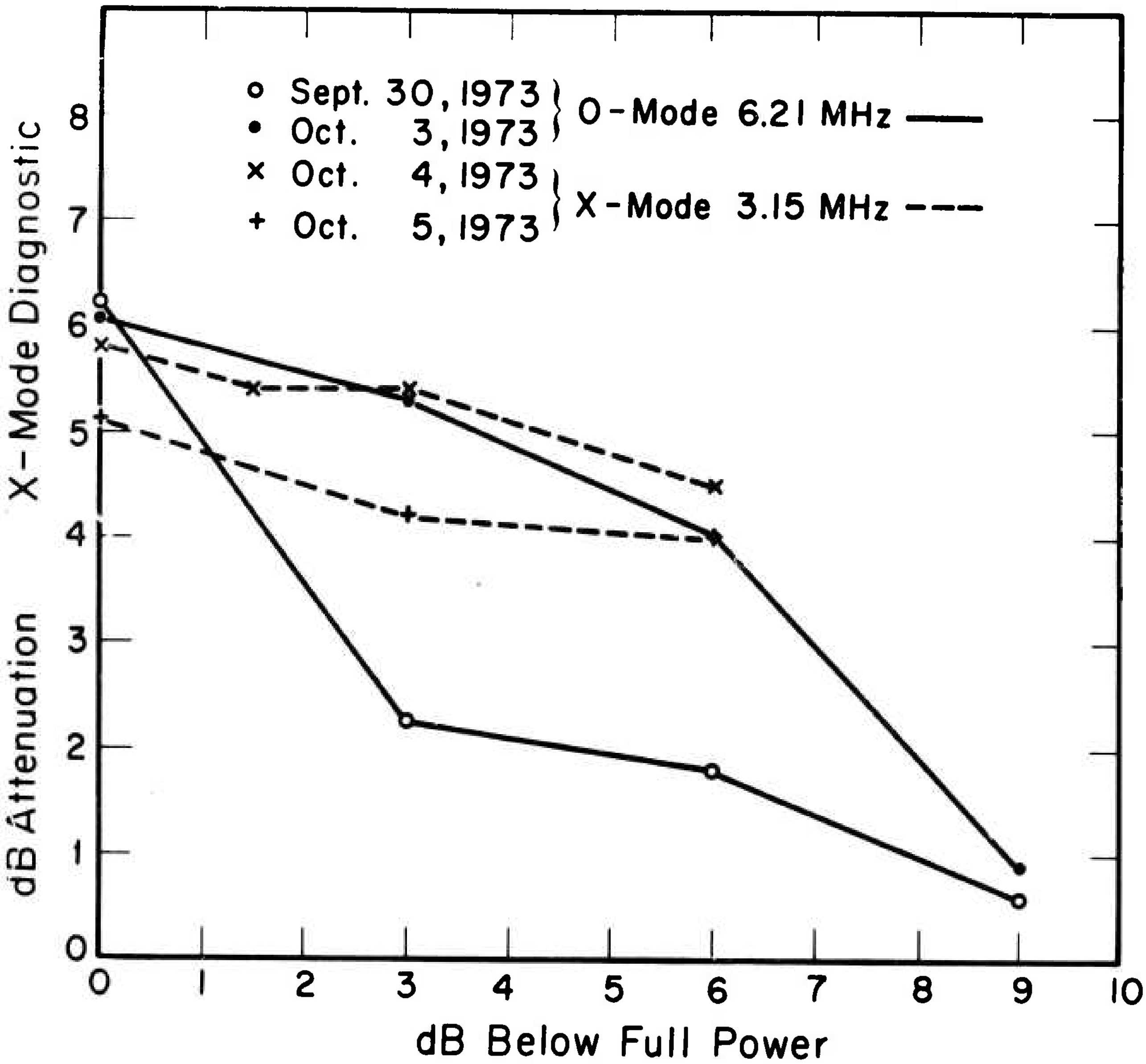


FIGURE 2 MEDIAN dB INCREMENTAL ATTENUATION IN RELATION TO PLATTEVILLE TRANSMITTER OUTPUT. Data obtained from records similar to those shown in Figure 1.

There is some evidence of a saturation effect for the X-mode heating, but not for the O-mode.

A few observations of attenuation of the 2.667-MHz diagnostic pulses were made with 10 min of heating and 10 min of no heating. Data were obtained for O-mode heating only. They show that the incremental attenuation with the heater on is about the same as was observed for the 1-s heating, around 6 dB two-way attenuation at the diagnostic frequency. Two other features were observed that need further verification and explanation. One is that while increased attenuation is produced rapidly upon turn-on of Platteville, recovery is slower and appears to continue throughout the 10-min heater-off period. The second is that the X-mode of the diagnostic signal shows a lesser incremental attenuation than does the O-mode during the time the heater is on.

In summary, the limited number of observations made of D-region effects show that significant phenomena occur and raise many questions as to what processes are going on. While there is much that needs further study in regard to modification of the lower ionosphere, a tentative conclusion relevant to F-region modification can be made. It is that within the power range available ($\sim$100 MW ERP), the incremental absorption of the heating wave caused by the heating wave probably does not exceed 1 to 3 dB during the daytime, at frequencies that would normally be used for F-region modification. This incremental absorption is additive to whatever absorption prevails in the ambient ionosphere. In addition, a saturation effect limiting the amount of power that passes through the lower ionosphere was not observed for O-mode transmission, but may have been indicated for X-mode transmission.

## REFERENCES


1. T. B. Jones, K. Davies, and B. Wieder, "Observations of D-region Modifications at Low and Very Low Frequencies," Nature, Vol. 238, p. 33-34 (1972), UNCLASSIFIED.

2. T. B. Jones, "Modification Effects in the Ionospheric D-region," AGARD Conference-CPP-138, Edinburgh, Scotland, Symposium, 12-16 November 1973, UNCLASSIFIED.

3. W. A. Kissick, and A. J. Ferraro, "Wave Interaction Using a Partially Reflected Probing Wave," AGARD Conference-CPP-138, Edinburgh, Scotland, Symposium, 12-16 November 1973, UNCLASSIFIED.

# ORBITAL EXPERIMENTS IN PRAIRIE SMOKE V

E. K. Walton D. R. Ward J. L. Long S. A. Bowhill

Aeronomy Corporation
Champaign, Illinois

ABSTRACT

Three orbital passes are described with scintillation results as the line of sight (LOS) passed through the heated region. Two orbital passes utilized a cross-field geometry in which the LOS is normal to the field-aligned region, and the third pass observed scintillations along the field line. The cross-field observations are shown to give information on the height distribution of the heated region. The observations along the field line show both sporadic-E and F-region effects of the heater. Cylindrical-model parameters describing the extent of the heated region are given for the passes and for both E- and F-region effects.

## I EXPERIMENTAL PROCEDURE

A series of experiments using the 150-MHz signals from U.S. Navy navigation satellites has been performed to study the heated region over Platteville. These experiments are similar to those described in earlier PRAIRIE SMOKE documents[1*] except that data were obtained from the far except that data were obtained from the far southern (or cross-field)

---

* References are listed at the end of the paper.



Pages 118, 119 and 120 are blank

location. Actually, three locations were chosen. The first was at Platteville itself, where the region of interest was vertically upward. The second site was near Hillsdale, Wyoming. This site was chosen as the downfield ("down the magnetic field line from the heated region") point, and was located 110 km geomagnetically north of Platteville. The third site was the cross-field site. This site, in Cimarron, N.M., was 408 km geomagnetically south of Platteville. It was on a line extending normal to the magnetic field of the heated region over Platteville.

All the equipment for these experiments was mounted in a Winnebago motor home shell. Each observation site consisted of three antennas (called Channel 1, Channel 2 and Channel 3) oriented in a right triangle. One leg of the triangle was set up in a true north-south direction, and the other in a true east-west direction. Small turnstile antennas were used, and were set at a height above the ground such that the main lobe was pointed approximately at the heated region (typically estimated as 200 to 300 km over Platteville). The antenna separation was approximately 200 ft. The signals were converted to the HF band, received with an R-390 HF receiver with a 16-kHz bandwidth (to reduce Doppler-shift problems), and recorded using a 2-channel chart recorder (detected audio) and a 4-channel magnetic tape recorder (audio beat note). The system is described in more detail in earlier PRAIRIE SMOKE documents.[1] Table 1 shows the time, location, and configuration of the various experiments.

## II DATA

Three experiments will be described at this time. The two Cimarron experiments are of particular interest since this is the first time that cross-field data from a southerly site such as this have been available.

Table 1

TABULATION OF ORBITAL EXPERIMENTS FOR PRAIRIE SMOKE V

| Location Day/Date GMT | Time of Interest (GMT) | Distance from Reference Antenna | | Transmitter Power | $f_h/f_oF2$ |
|---|---|---|---|---|---|
| | | Meters N or S | Meters E or W | | |
| Platteville 12 Sept 1973 (Ref = Ch. 2) | 0024-0038 | 59.74 N (Ch. 3) | 75.64 W (Ch. 1) | -6 dB FM modulation | -- |
| Platteville 13 Sept 1973 (Ref = Ch. 1) | 0200-0220 | 59.74 N (Ch. 3) | 75.64 W (Ch. 2) | 0 dB Variable slightly | 0.96 |
| Hillsdale 18 Sept 1973 (Ref = Ch. 2) | 0850-0910 | 66.37 S (Ch. 3) | 63.73 E (Ch. $\pi$) | 0 dB | 0.99 |
| Hillsdale 20 Sept 1973 (Ref = Ch. 3) | 0543-0603 | 66.37 S (Ch. 3) | 63.73 E (Ch. $\pi$) | 0 dB | 0.78 |
| Cimarron 27 Sept 1973 (Ref = Ch. 2) | 0816-0836 | 66.37 N (Ch. 3) | 66.67 W (Ch. $\pi$) | 0 dB | 0.89* |
| Cimarron 28 Sept 1973 (Ref = Ch. 3) | 2228-2248 | 66.37 N (Ch. 3) | 66.67 W (Ch. 1) | 0.81 MW (8 trans) | 0.94 |

* $\frac{f_h}{f_xF2}$ .

The Hillsdale experiment for 20 September 1973 will also be shown for comparison. Figures 1, 2, and 3 are the vertical-incidence (V.I.) ionograms taken at the Erie site near Platteville during the time of interest for each of the three satellite passes. In each case, a considerable amount of spread F ($F_s$) may be seen. The $F_s$ is so severe in Figures 1 and 2, in fact, that it is difficult to accurately determine the critical frequencies. Figures 1 and 2 also contain sporadic-E traces. The ionograms shown in Figures 1 and 2 are nighttime data, while Figure 3 is a daytime ionogram.

The data collected during the times of interest for each of the three satellite passes are shown in Figures 4, 5, and 6. These curves were prepared by playing the analog tapes of the audio signals (i.e., the "beat notes") from the three receivers through an amplifier, a diode detector, and a 20-Hz low-pass filter. It is clear from simply observing these curves that the character of the scintillations of the signal received at Hillsdale (downfield) and at Cimarron (cross-field) is quite different. The scintillations at Hillsdale are deeper and more rapid than those seen at Cimarron. Also, it can be clearly seen that the three channels of Hillsdale data exhibit more similarity in the small-scale variations than do the Cimarron data. Many of the peaks and nulls of the Hillsdale data are clearly seen in all three channels, but this is not true with the Cimarron data. The variations of the Hillsdale signals are more rapid and larger than the variations of the Cimarron data.

## III DATA ANALYSIS

As an aid to interpretation of the data presented in Figures 4, 5, and 6, the region of interest was modeled as a field-aligned cylinder. The projection of this cylinder on the 300-km-altitude plane is a circle

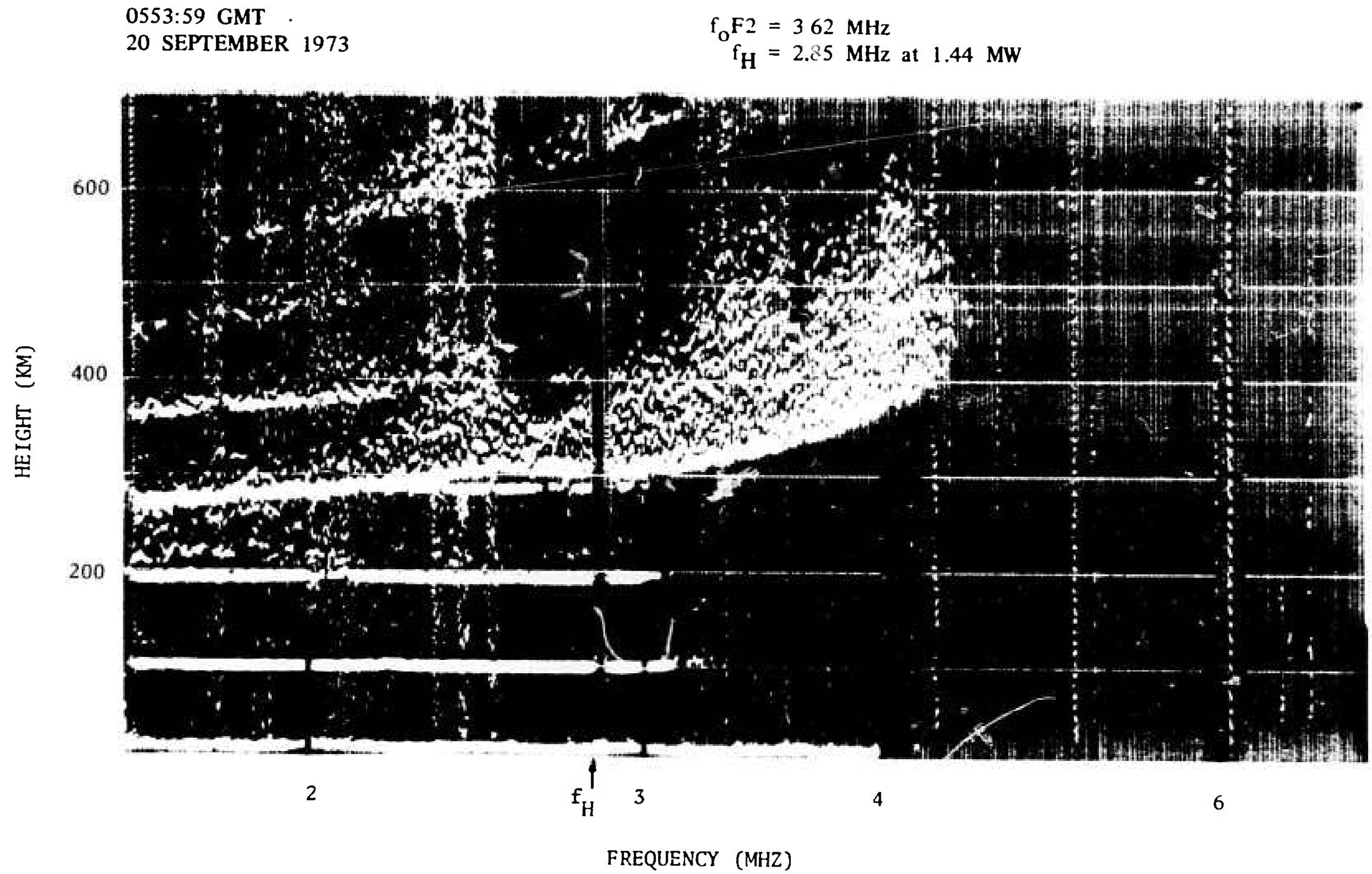


FIGURE 1    ERIE SITE V.I. IONOGRAM FOR 20 SEPTEMBER 1973 ORBITAL PASS

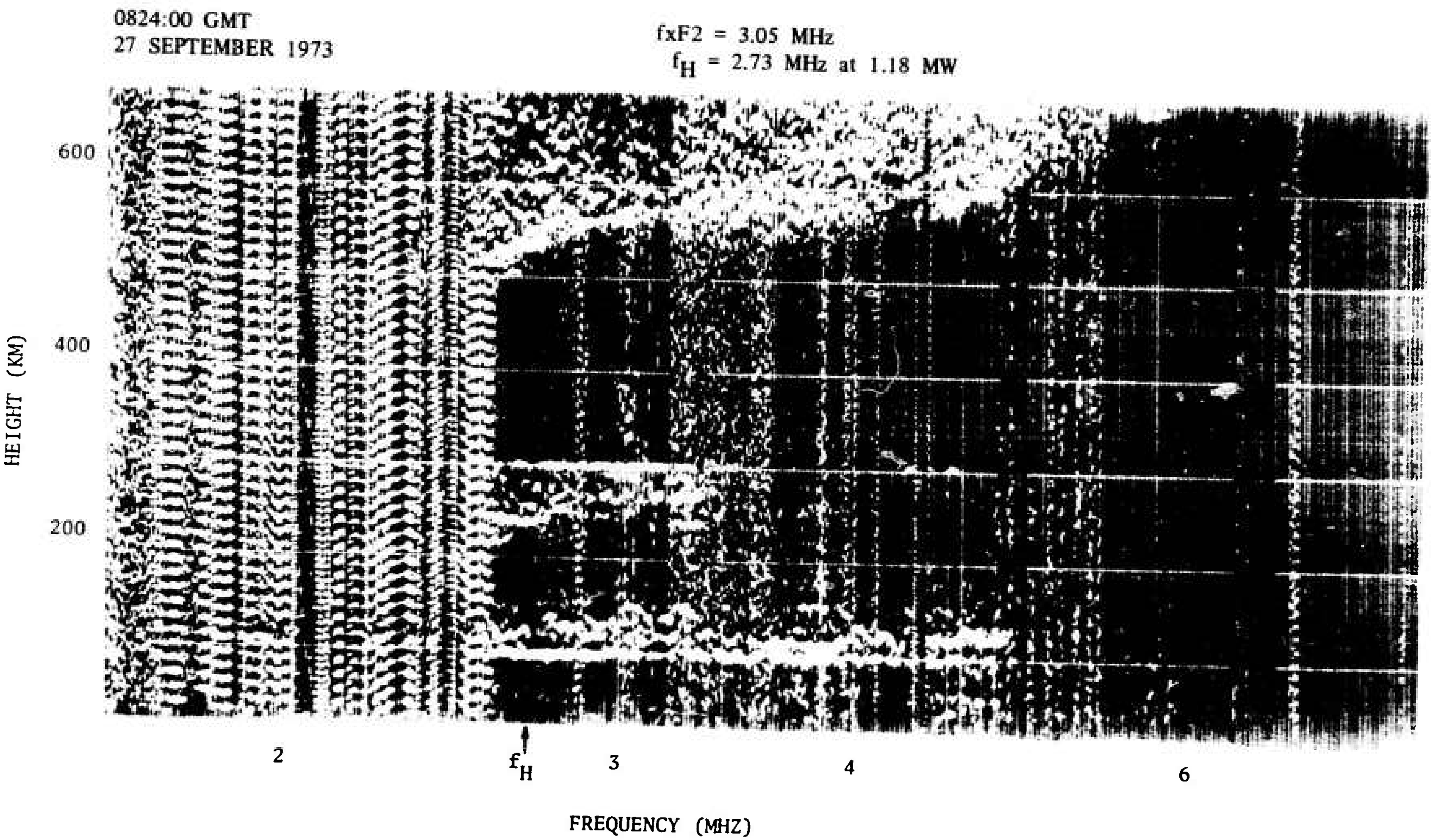


FIGURE 2 ERIE SITE V.I. IONOGRAM FOR 27 SEPTEMBER 1973 ORBITAL PASS

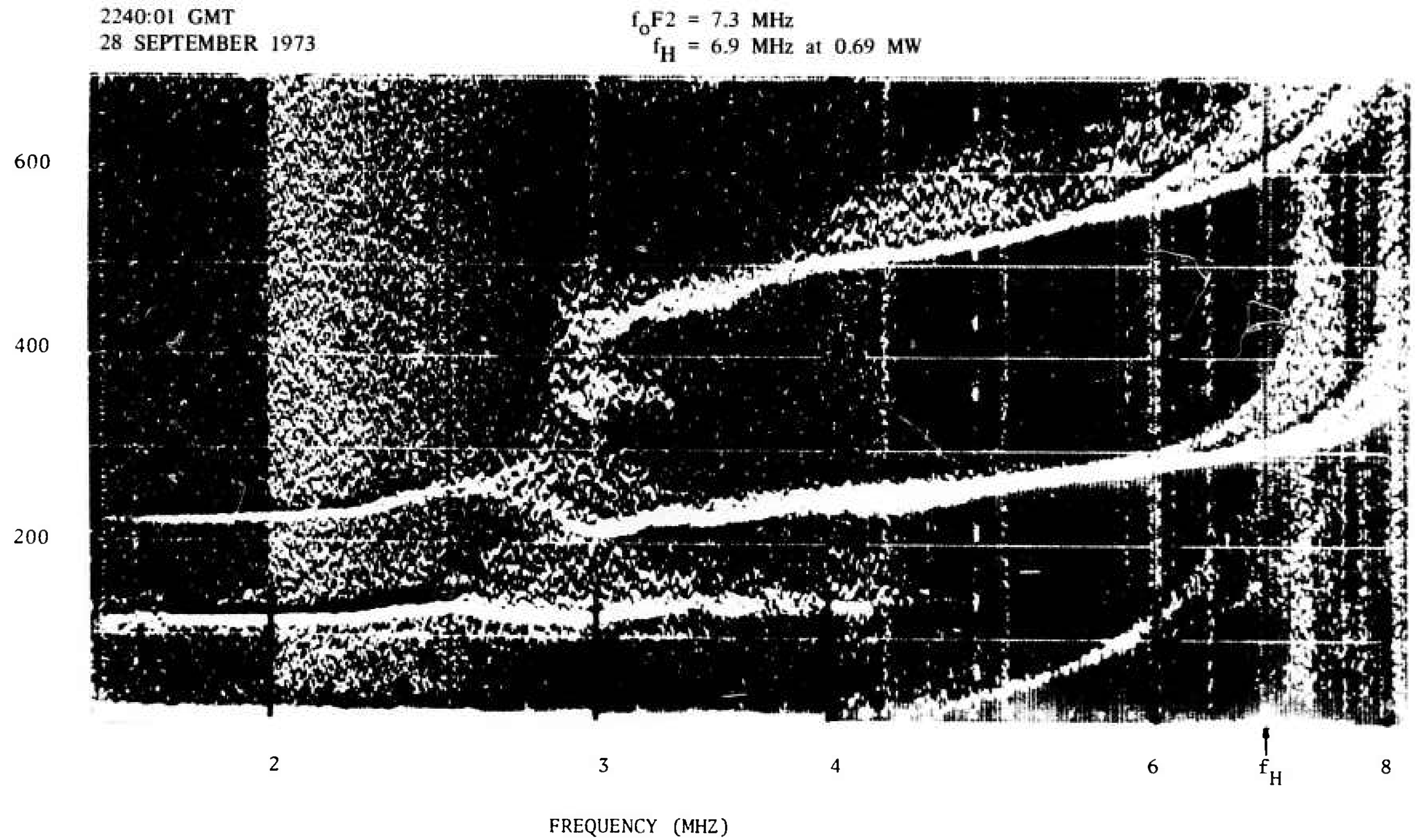


FIGURE 3 ERIE SITE V.I. IONOGRAM FOR 28 SEPTEMBER 1973 ORBITAL PASS

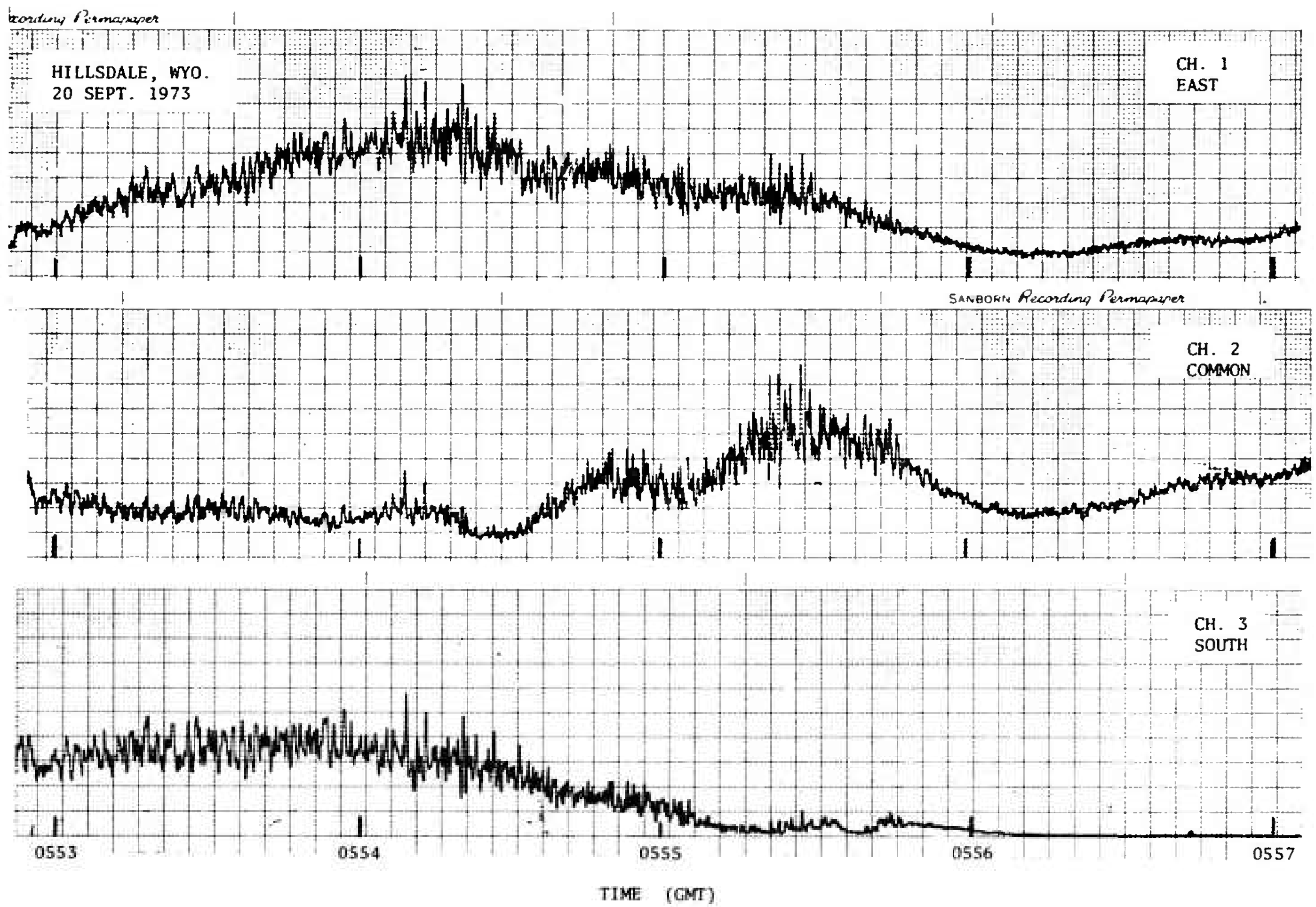


FIGURE 4 SIGNAL AMPLITUDE DATA FOR 20 SEPTEMBER 1973 ORBITAL PASS

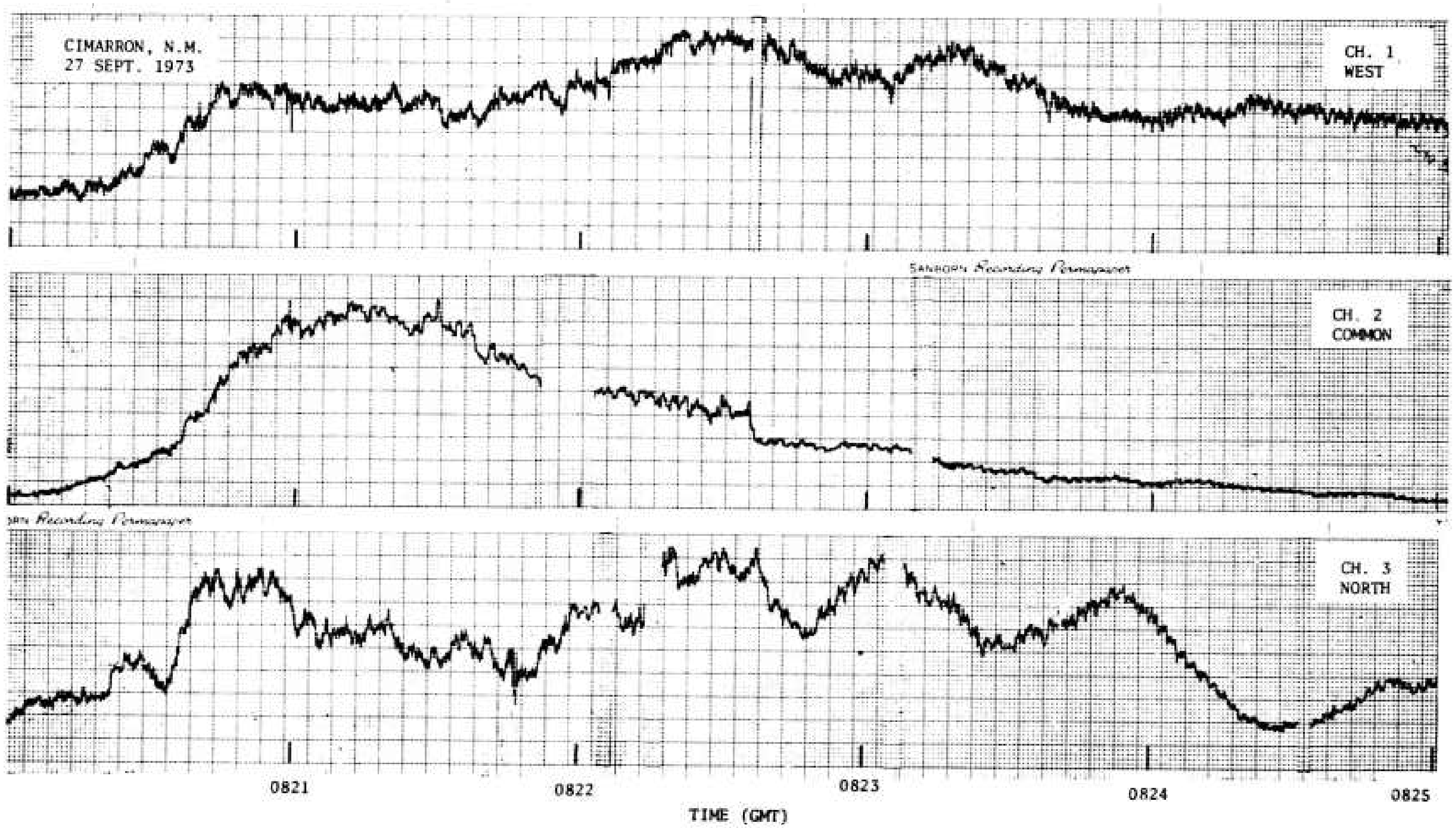


FIGURE 5 SIGNAL-AMPLITUDE DATA FOR 27 SEPTEMBER 1973 ORBITAL PASS

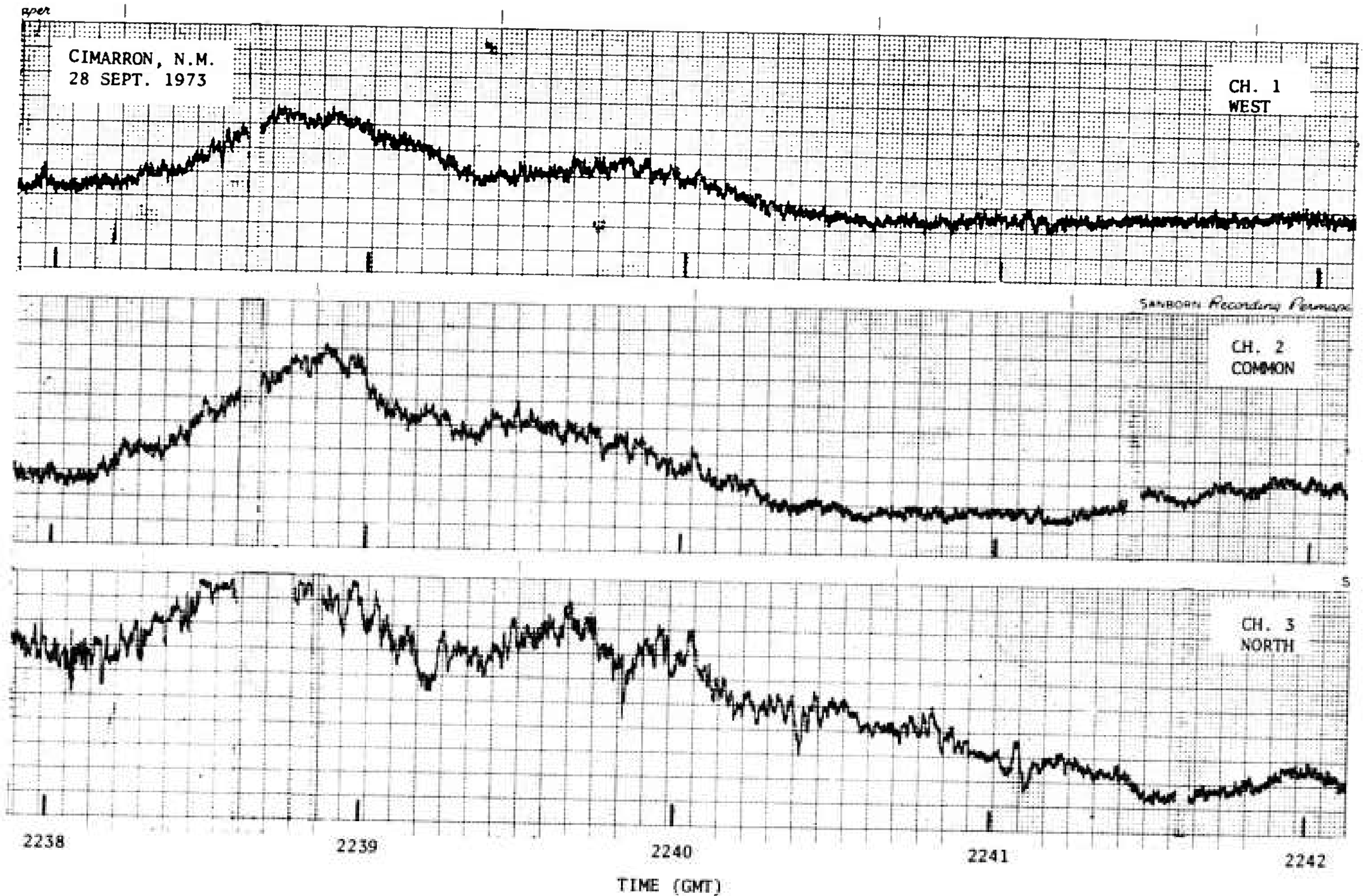


FIGURE 6 SIGNAL-AMPLITUDE DATA FOR 28 SEPTEMBER 1973 ORBITAL PASS

that may be displaced to the magnetic north or south of overhead Platteville (see page 71 of Ref. 1). The altitude of the entry and exit of the satellite LOS from the cylinder is plotted as a function of time in Figures 7, 8, 9, and 10.

Figures 7 and 8 show the data calculated with respect to Hillsdale, Wyoming for the 20 September 1973 orbital pass. The data in Figure 7 were calculated for F-region heights, and the 30-km north displacement refers to the 300-km height level. The data in Figure 8 are for the E region and the 0-, 30-, and 40-km-north numbers refer to the 100-km height level. Figures 7 and 10 also show the true height of reflection for the transmitter frequency. The true-height data are available from a set of contour plots of $f_c$ versus true-height and time of day provided by SRI. The plot for the 27th of September does not contain a true-height value. There was a magnetic disturbance on that day, and the $f_oF2$ value of 2.3 MHz was too low for an accurate calculation. As a further convenience, the elevation angle and range from the observation point to the satellite as well as the angle of the LOS to the magnetic field over Platteville are also shown on the three F-region plots.

One would expect scintillations to occur when the LOS passed through the cylinder at regions near the true height of reflection of the heater transmitter signal.

Figures 11 and 12 show scintillation indices versus time for the Hillsdale, 20 September, and for the Cimarron, 28 September, orbital passes, respectively. A description of the method used for obtaining these plots is given on page 50 of Ref. 1. In particular, the tracking filter was operated with a 200-Hz bandwidth. The scintillation indices were computed over 15-s intervals.

The crossfield location of the Cimarron site allows one to determine the horizontal extent of the heated region by utilizing the cylinder plots

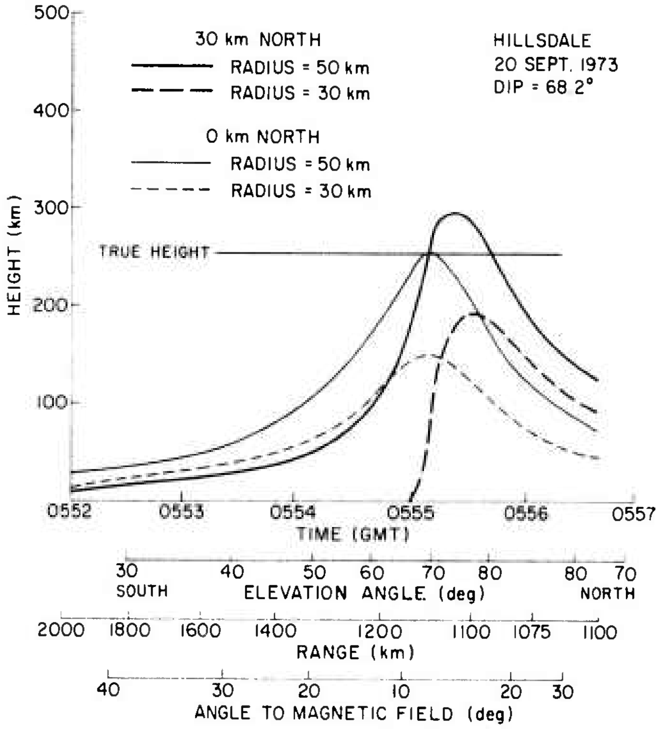


FIGURE 7 CYLINDER PLOTS FOR THE 20 SEPTEMBER 1973 ORBITAL PASS F-LAYER STUDY

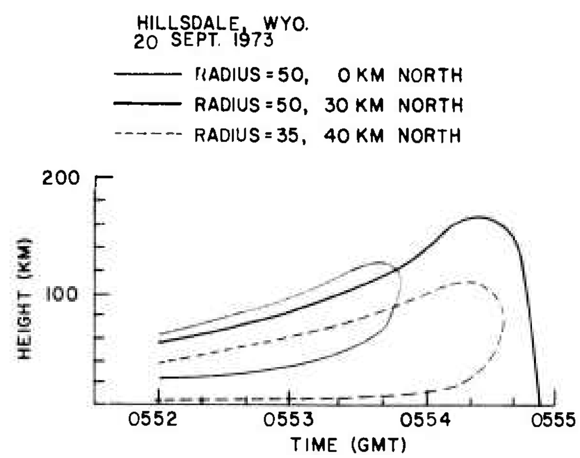


FIGURE 8 CYLINDER PLOTS FOR THE 20 SEPTEMBER 1973 ORBITAL PASS $E_s$-LAYER STUDY

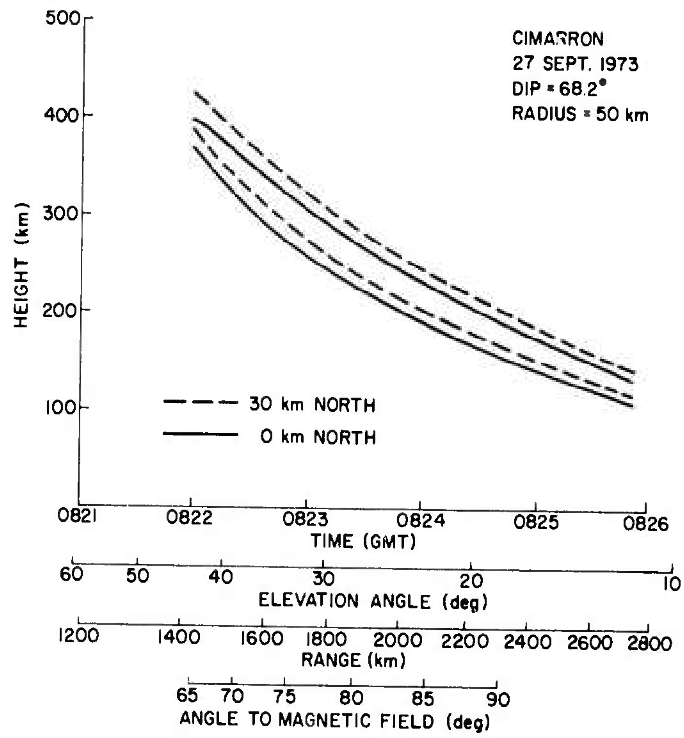


FIGURE 9 CYLINDER PLOTS FOR THE 27 SEPTEMBER 1973 ORBITAL PASS

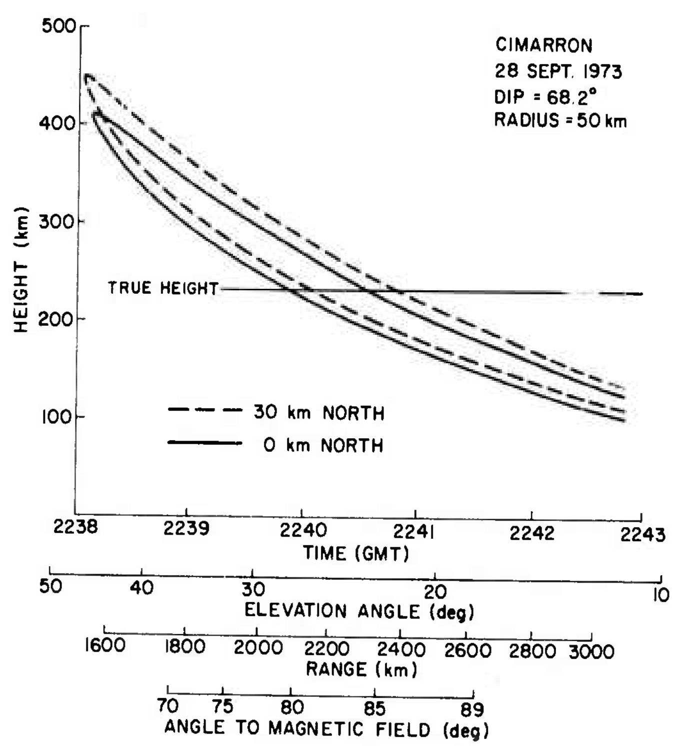


FIGURE 10 CYLINDER PLOTS FOR THE 28 SEPTEMBER 1973 ORBITAL PASS

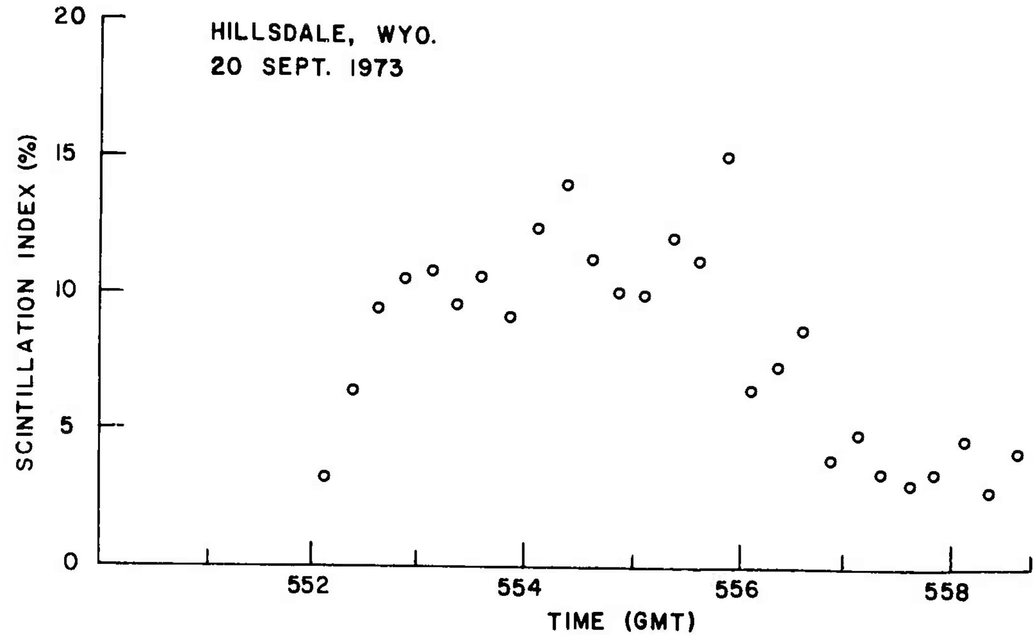


FIGURE 11 SCINTILLATION INDEX vs. TIME FOR 20 SEPTEMBER 1973

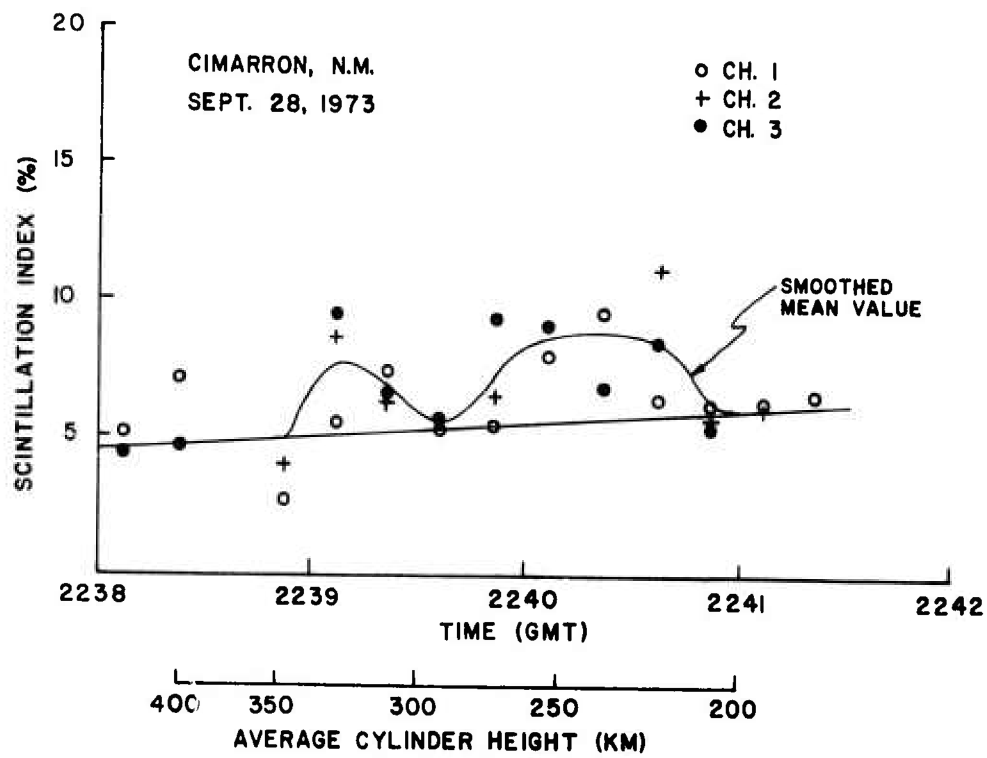


FIGURE 12 SCINTILLATION INDEX vs. TIME FOR 28 SEPTEMBER 1973

of Figure 10 and the scintillation plot of Figure 12. To determine the height, a smoothed mean-value curve (Figure 12) was plotted of scintillation indices as well as a horizontal axis calibrated in average cylinder height for a field-aligned cylinder of 50-km radius located 30-km north of Platteville. It is evident that the heated region extends from approximately 340 km to 220 km. Note that the definition of the lower height is much sharper than that of the upper height, as evidenced by a slow decrease in scintillation index in that region. The true height of reflection at $f_H$ during this period was 232 km ($f_c$ versus true-height and time of day contours supplied by SRI).

The scintillation data from the Hillsdale site are particularly interesting in that $E_s$-region as well as F-region effects are evident. The ionogram for that experiment (Figure 1) shows a very strong $E_s$ layer (at 100 km) as well as the F-region traces. The scintillation-index (S) data seen in Figures 4 and 11 may thus be interpreted with respect to both $E_s$- and F-region effects. The peak in the scintillation-index curve (Figure 11) from 0555 to 0556 GMT can be matched with an F-region cylinder 50 km in radius, 30 km north. The peak in Figure 11 from 0553:45 to 0554:30 GMT corresponds to an $E_s$ cylinder with 35 km radius shifted 40 km north of Platteville (Figure 8). The proper cylinder was determined by adjusting the radius and distance north until the cylinder model showed that the LOS passed above and below 100 km, corresponding to the start and stop of scintillations.

## IV CONCLUSIONS

The data displayed here give a general picture of the heated region as viewed from both the downfield and the cross-field angle. It was shown that the cross-field scintillations were not as severe as the downfield scintillations. The downfield observation of the $E_s$ region

is particularly interesting. The $E_s$-region scintillations are found to exist even though the heater transmitter was operated on a frequency chosen to enhance the F-region effects. Also, the cylinder model that matches the observed E-region scintillation data was smaller in radius (35 km) than the F-region cylinder (50 km). Both cylinders were displaced north of overhead Platteville (40 km north for the $E_s$ region and 30 km north for the F-region). Finally, it should be pointed out that since these are the first available cross-field data, this is the first time that the agreement with the cylinder model for such a configuration could be confirmed. A height range from 220 km to 340 km was determined for the disturbed region on 28 September 1973, when the true height of reflection of the heater signal was reported as 232 km.

## REFERENCE

1. S. A. Bowhill, E. E. Mendenhall, and D. R. Ward, "Transmission Experiments in PRAIRIE SMOKE Ib and II (U)," in Proceedings of the PRAIRIE SMOKE II RF Measurements Data Workshop--22, 23 June 1972 (U), SRI 2-5388, Stanford Research Institute, Menlo Park, Calif. (October 1972), SECRET.

# POWER-DENSITY MEASUREMENTS ON A BISTATIC PATH DURING PRAIRIE SMOKE V

G. B. Carpenter

Stanford Research Institute
Menlo Park, California

ABSTRACT

VHF (49.8 MHz) and UHF (423.3 MHz) CW transmissions radiated from the 150-ft antenna facility at Stanford, California, were monitored at a temporary receiving site at Ft. Huachuca, Arizona, during five days of the PRAIRIE SMOKE V experiment. Two modes of scatter were observed, one in which the frequency was essentially unshifted and the other in which the frequency was shifted by very nearly the frequency of the ionospheric-modification transmitter. The scattered signals were relatively narrowband and were Doppler-shifted from their nominal value. Cross-section estimates are presented.

## I INTRODUCTION

The ability of high-power high-frequency (HF) radio-wave transmitters to modify the ionosphere is now well demonstrated. Investigation of such modification is being sponsored by ARPA* under the code

---

*Defense Advanced Research Projects Agency

pages 137 and 138
are blank

name PRAIRIE SMOKE. The region of interest lies above the DoC* transmitter at Platteville, Colorado. Among the significant findings of this program are the following:

- Radio waves scatter in appreciable strength in directions that are specular with respect to the earth's magnetic field and the direction of the incident wave. Scattering is believed associated with electron-density structures whose scale lengths along the magnetic field is much greater than perpendicular to the field. Such scattering is usually referred to as field-aligned scatter (FAS), and an empirical model has been developed[1]† that accounts for most of the experimental data. In particular, the cross section is relatively constant with frequency up to about 80 MHz, then decreases at higher frequencies (but is still measurable up to at least 435 MHz). The frequency of the scattered signal is unchanged from that of the incident wave except for a small Doppler shift. Definitive measurement of the power density of FAS has been made at HF and low VHF by Fialer.[2] Measurements by Minkoff[3] at VHF (157.5 MHz) also suggest a narrow power-density distribution, but analysis was limited to a 100-Hz window. The power density of measurements at UHF (435 MHz) by Minkoff cannot be estimated because the transmissions were not coherent from pulse to pulse.

- Radio waves scatter in measurable strength in directions that are nearly specular with respect to the earth's magnetic field and the direction of the incident wave. The interesting feature of this mode is that the scattered signals are shifted by very nearly the frequency of the modifying HF transmitter. This mode is usually referred to as plasma-line scatter (PLS), and its character is not well defined experimentally. A theoretical foundation for scatter from planes perpendicular to the earth's magnetic field is well established,[4] while that for scatter from planes parallel to the field is now emerging.[5] The most extensive measurement of the PLS power density comes from Arecibo where the scatter is neither parallel nor perpendicular to the earth's field. The UHF (430-MHz) backscatter measurements at Arecibo show[6] a very interesting density distribution in which only a small amount of energy

---

* Department of Commerce

† References are listed at the end of the paper.

is concentrated at the nominal offset frequency and the major energy is contained in broader spectral peaks shifted by multiples of the ion acoustic frequency (a few kilohertz). Definitive power-density information is not available for PLS from planes parallel to the earth's field (PRAIRIE SMOKE geometry). The measurements at VHF ($\approx$160 MHz) by Minkoff[3] suggest that the energy is concentrated near the nominal offset frequency, but the analysis window was unambiguous over only 100 Hz. Minkoff also made PLS measurements at UHF ($\approx$435 MHz) but the transmissions were not coherent from pulse to pulse. The sensitivity of the HF and low-VHF measurements carried out by Fialer[2] apparently was not sufficient to observe PLS during his extensive PRAIRIE SMOKE measurements.

## II AN EXPERIMENT

The PRAIRIE SMOKE IV experiment scheduled* for September 1973 represented perhaps the last opportunity to obtain definitive power-density information for PLS from planes parallel to the earth's magnetic field. In planning such an experiment it was apparent that the sensitivity and resolution desired could best be achieved using a high-power CW transmitter associated with a large-aperture antenna. Further, the location of the transmitter and receiver (also employing a large-aperture antenna) would have to be such that the incident and scattered waves achieved near-specularity with respect to planes parallel to the earth's magnetic field. Selection of the SRI facility at Stanford, California, for transmission was based on its high-power CW capability, its large antenna aperture, and its availability. In making this selection it was realized that a ridge of hills some 50 km from the antenna limited illumination of low-elevation targets (e.g., less than 210 km above Platteville). Initial plans called for reception at one of the large parabolic

*Actually conducted from 10 September to 5 October 1973.

antennas at the White Sands Missile Range in New Mexico. Measurements had been made[7] over the reciprocal of this path and extrapolation of these earlier results gave promise of favorable signal-to-noise ratio (SNR). When it became apparent that an antenna would not be available at WSMR, an array of yagis was conceived and collocated at Ft. Huachuca, Arizona, with the SRI experiment* deployed to observe FAS of HF and low-VHF swept-frequency transmissions from Los Lunas, New Mexico. The signal-to-noise ratio was expected to be marginal. Figure 1 shows the relative location of the various facilities, including those involved in previous PRAIRIE SMOKE measurements. Table 1 contains a list of the experimental parameters.

A second objective was adopted during the course of the experiment. The character of low-VHF ($\approx$ 50 MHz) PLS was investigated over the same path as the UHF transmissions. This was accomplished through the kind cooperation of Stanford University (SU), which possesses a high-power CW transmitter capable of exciting the 150-ft antenna concurrent with the SRI UHF transmitter. By special request the SU transmitter was operated for several hours. At Ft. Huachuca reception was accomplished using the system normally employed for FAS at HF and low VHF.

A third objective was to participate in some of the special tests performed by the Platteville transmitter.

Because of the limited objectives of this experiment, serious measurements were conducted during only five days of the PRAIRIE SMOKE V experiment--11, 12, 13, 24, and 25 September.

---

*Results of this experiment are presented elsewhere in the Proceedings.

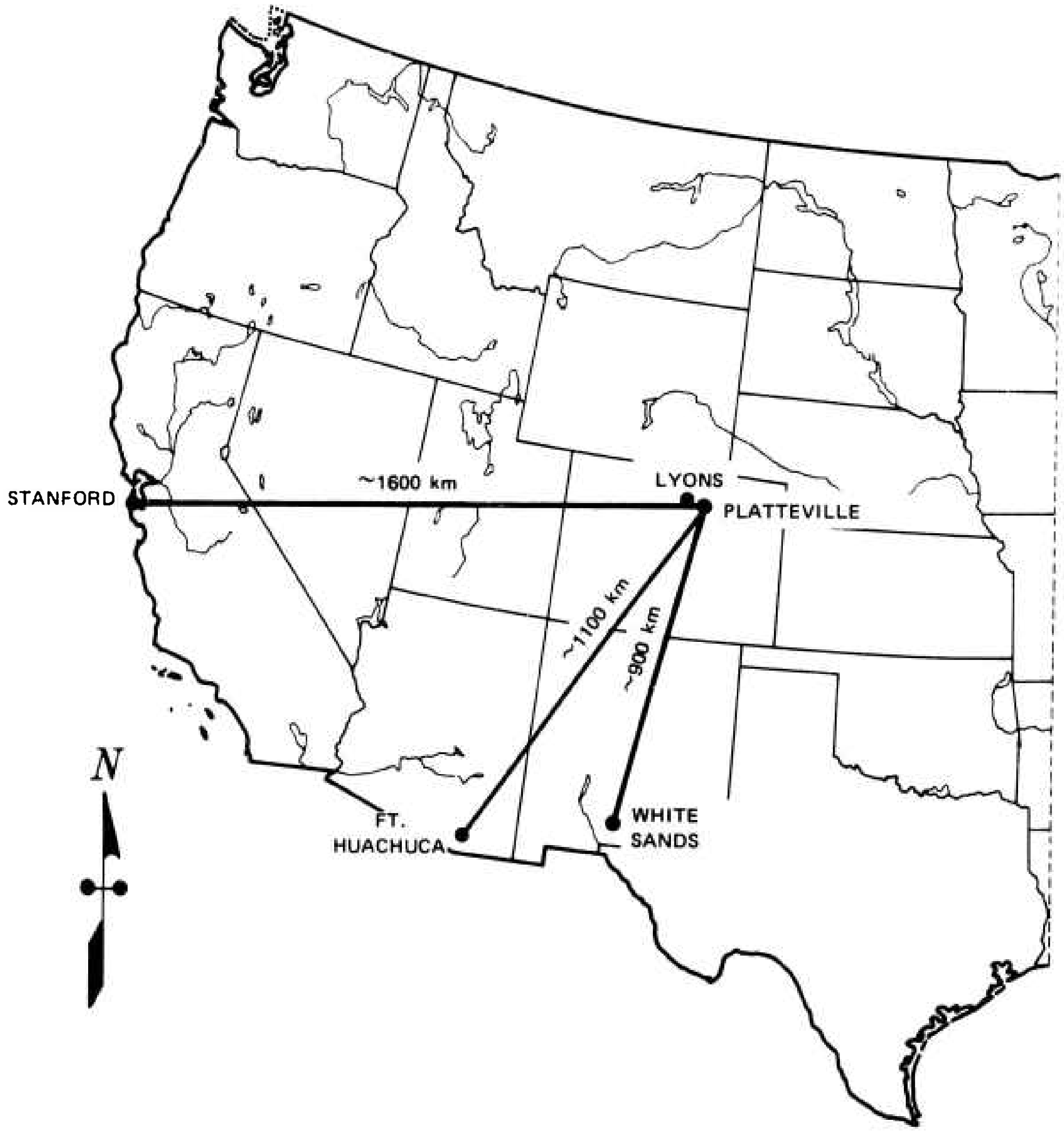


FIGURE 1 TRANSMITTER AND RECEIVER LOCATIONS

Table 1

EXPERIMENTAL PARAMETERS

| | VHF | UHF |
|---|---|---|
| **Transmitter** | | |
| Location | Stanford, California | Stanford, California |
| Frequency | 49.80 MHz | 423.30 MHz |
| Modulation | CW | CW |
| Power | 200 kW | 25 kW |
| Antenna gain | 24 dB | 44 dB |
| Beam diameter | $\approx 9^\circ$ | $1.3^\circ \times 1.6^\circ$ |
| Polarization | $\approx$circular | $\approx$circular |
| Nominal range to target | 1580 km | 1575 km |
| **Receiver** | | |
| Location | Ft. Huachuca, Arizona | Ft. Huachuca, Arizona |
| Antenna gain | $\approx$15 dB | $\approx$20 dB |
| Beam diameter | Large | Large |
| Polarization | Vertical | Vertical |
| Nominal range to target | 1120 km | 1110 km |

## III SIGNAL CHARACTERISTICS

### A. UHF Plasma-Line Scatter

As feared, reception of UHF PLS at Ft. Huachuca was marginal. Despite the low signal level (a few dB above noise), interesting signal characteristics were evident. During the early phase of measurements, repeated search of the spectrum up to several tens of kilohertz on

either side of the nominal offset frequency showed recognizable energy only in a small band centered within several tens of hertz of the nominal offset. The search conducted by systematic tuning of a 1-kHz receiver bandpass over the spectrum of interest, was abandoned later in the experiment. The bandwidth of PLS appears to be a few tens of hertz (typically 30 Hz) and the Doppler shift may be either positive or negative about the nominal offset (see list of UHF Doppler shifts in Table 2). An example of the power density observed is shown in Figure 2.

A second feature of the UHF PLS is that it always reached its strongest level when the Stanford transmitting antenna was pointed at its lowest elevation ($1.2^{\circ}$), independent of the altitude of ionospheric modification over Platteville. This is taken to mean that scatter is strongly associated with field-aligned specular geometry, as deduced by Minkoff[3] from UHF backscatter measurements at White Sands. This perhaps explains the previous[7] lack of success of bistatic measurements at Lyons, Colorado, and of monostatic and bistatic measurements at Stanford, California. The result is contrary to that deduced[7] from UHF measurements on the bistatic path from White Sands to Platteville to Stanford during PRAIRIE SMOKE II. These latter measurements clearly showed the plasma-line scatter region moving up and down with the modification altitude.

Contours of altitude where specular geometry is achieved for the UHF bistatic path have been computed and are shown in Figure 3. Note that the altitude is higher north of Platteville than it is to the south, and higher to the west than to the east. Within a radius of 50 km of Platteville (roughly the size of the modified region) the specular altitude lies as low as 187 km to the southeast and as high as 207 km to the northwest of Platteville. At no time during our measurements was modification scheduled for these altitudes, but fortunately there were numerous occasions when modification occurred

Table 2

UHF DOPPLER SHIFTS

| Date | Time (GMT) | Doppler (Hz) |
|---|---|---|
| 12 Sept | 2330 | -15 |
| | 2335 | -12 |
| | 2340 | -14 |
| | 2345 | -8 |
| | 2350 | +8 |
| | 2355 | -15 |
| 13 Sept | 0000 | -45 |
| | 0005 | -45 |
| | 0008 | -20 |
| | 0012 | 0 |
| | 0025 | -62 |
| | 0030 | -25 |
| | 0035 | -15 |
| | 0050 | -24 |
| | 2335 | +22 |
| | 2340 | +40 |
| | 2345 | +36 |
| | 2350 | +33 |
| | 2355 | +40 |
| 14 Sept | 0000 | +40 |
| | 0005 | +40 |
| | 0010 | +55 |
| | 0015 | +50 |
| | 0020 | +50 |
| | 0025 | +43 |
| 14 Sept | 0035 | +50 |
| | 0040 | +56 |
| | 0047 | +70 |
| | 0055 | +70 |
| | 0105 | +78 |
| | 0110 | +78 |
| | 0115 | +96 |
| | 0120 | +89 |
| | 0130 | +82 |
| | 0140 | +80 |
| | 0150 | +80 |
| | 0200 | +60 |
| | 0210 | +47 |
| 24 Sept | 1600 | +35 |
| | 1605 | +5 |
| | 1610 | +5 |
| | 1625 | -32 |
| | 1720 | +10 |
| | 1725 | -10 |
| | 1730 | -28 |
| | 1735 | -47 |
| | 1740 | -64 |
| | 1745 | -73 |
| 24 Sept | 1750 | -86 |
| | 1755 | -87 |
| | 1800 | -89 |
| 25 Sept | 1420 | -10 |
| | 1425 | -15 |
| | 1430 | -18 |
| | 1435 | -18 |
| | 1440 | -15 |
| | 1445 | +8 |
| | 1450 | +11 |
| | 1455 | +20 |
| | 1510 | +65 |
| | 1515 | +65 |
| | 1520 | +65 |
| | 1525 | +45 |
| | 1550 | +35 |
| | 1555 | +26 |
| | 1603 | 0 |
| | 1610 | 0 |

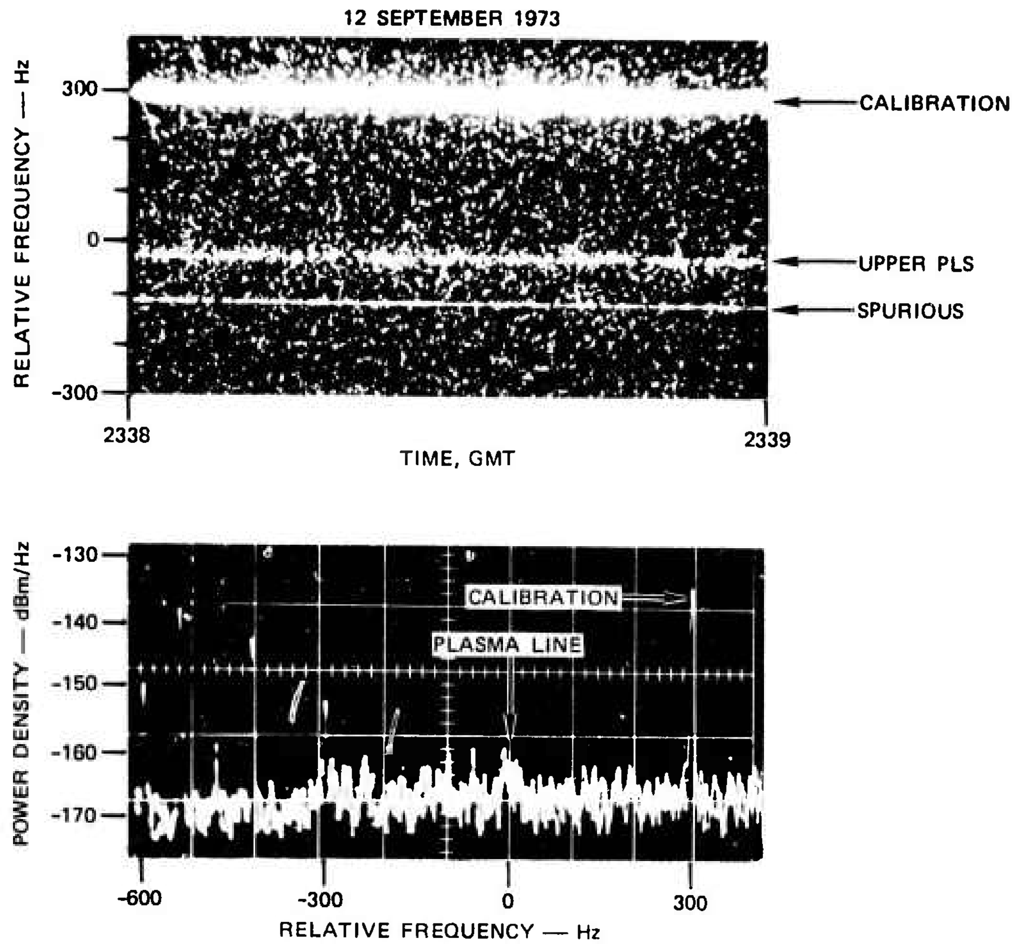


FIGURE 2 TYPICAL UHF UPPER-PLASMA-LINE OBSERVATIONS

at 210 km and below. In contrast, this region is inaccessible to direct illumination by the Stanford transmitter. Although the specular-scatter region lies below the geometric horizon of the Stanford transmitter, energy reached this region by diffraction. The degradation is believed to be roughly 12 dB for a scatter region at 207 km and 24 dB for a scatter region at 187 km.

B. UHF Field-Aligned Scatter

One of the major surprises of the experiment is that UHF FAS was observed. No such signals were observed[7] during PRAIRIE SMOKE Ib and II on a nearly reciprocal path from White Sands to Platteville to Stanford,

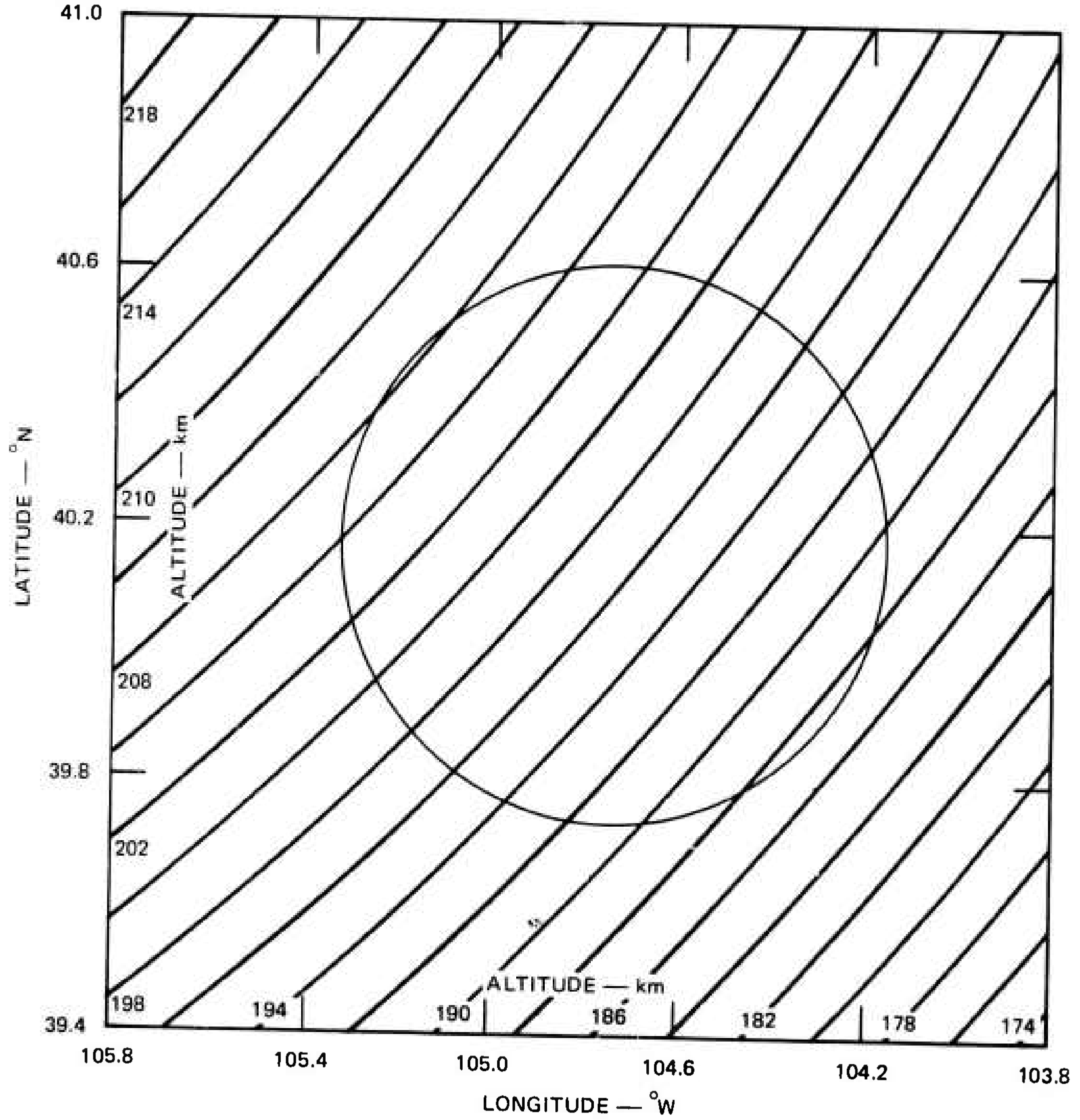


FIGURE 3 CONTOURS OF ALTITUDE AT WHICH SPECULAR SCATTER CAN BE ACHIEVED AT UHF. The circle encloses the region within 50 km of Platteville.

although PLS was observed frequently. The earlier FAS measurements at Stanford employed the same antenna and preamplifier as the PLS measurements, and the receiver was calibrated continuously by a signal injected through a directional coupler ahead of the preamplifier. The character of UHF FAS received at Ft. Huachuca is identical to that described above for PLS, except that it was about 20 dB stronger. A typical observation is shown in Figure 4.

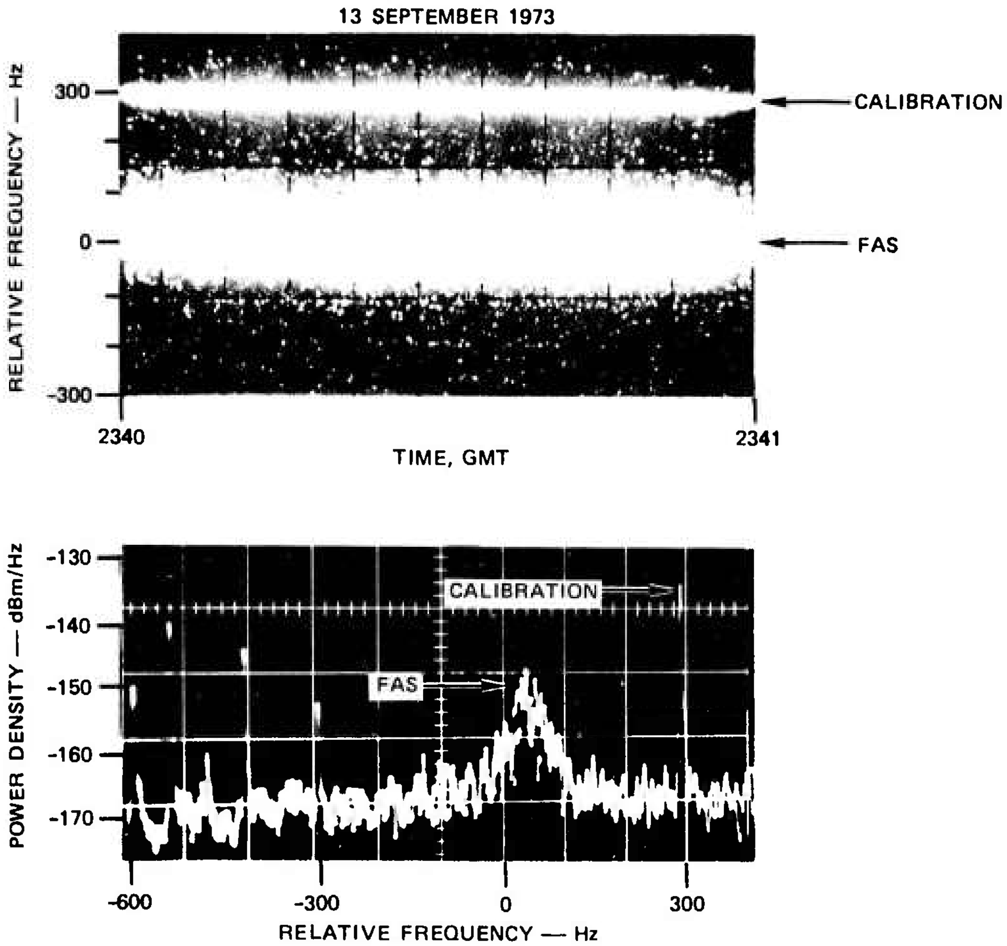


FIGURE 4 TYPICAL UHF FIELD-ALIGNED-SCATTER OBSERVATION

The UHF FAS data exist in abundance compared to the PLS data and provide a more reliable description of the scatter region and its dependence on modification parameters. The strongest scatter was always observed when the Stanford transmitting antenna was pointed at its lowest possible elevation (1.2°), a fraction of a degree above the geometric horizon (1.08°). In this position the center of the beam should have reached an altitude of about 210 km at the range of Platteville. In azimuth, the peak scatter was usually associated with a location 10 to 15 km north of the Platteville transmitter. This behavior is almost certainly an indication that this mode of scatter is supported by field-aligned electron-density fluctuations. Figure 3

shows that nearly the entire region above Platteville where field-aligned specular geometry can be achieved lies below the region that can be directly illuminated by the Stanford transmitting antenna. As indicated in the discussion of UHF PLS, the UHF energy is believed to reach the specular-scatter region by refraction and diffraction, with corresponding loss of intensity.

The importance of specular-scatter geometry is also demonstrated by the variation in scatter intensity with altitude of ionospheric modification. During our few days of operation at Ft. Huachuca the nominal altitude of modification was scheduled to be either 240 or 270 km. Fortunately, there were many periods when modification was actually much lower, down as low as 195 km. The intensity of scatter was always strongest at times when modification was in progress below 210 km. Weak scatter was usually recognized for modification at altitudes up to about 230 km (and perhaps even higher). The altitude dependence is clearly demonstrated in Figure 5, which is a frequency-time-intensity (FTI) display of data obtained during Special Test 12. During this test the frequency of the Platteville transmitter was shifted at 3-minute intervals by an amount expected to change the altitude of modification in 7.5-km steps. A first-order estimate of the modification altitudes actually achieved is shown along the top of the display. The times at which peak power was achieved are also indicated.

## C. VHF Plasma-Line Scatter

The first measurement of PLS at a frequency below 100 MHz was achieved at Ft. Huachuca. The VHF PLS had an even narrower bandwidth (a few Hz) than the UHF PLS, and the Doppler shift from the nominal offset was noticeably less (not more than about 10 to 15 Hz). The

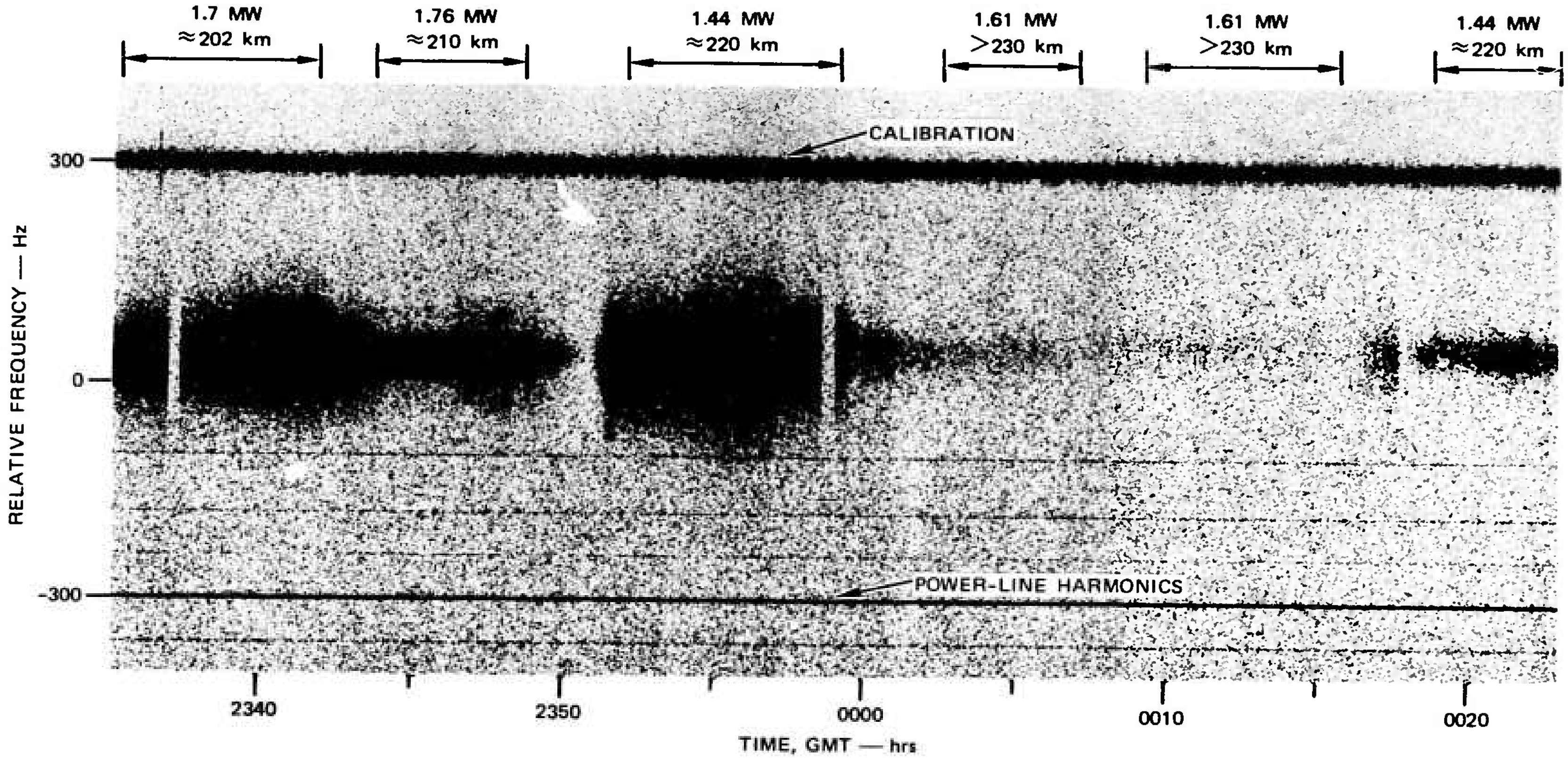


FIGURE 5 UHF FAS ͻBSERVATIONS DURING TEST NO. 12 ON 13-14 SEPTEMBER 1973

signals reached a comfortable 15 to 20 dB above noise. An example of VHF PLS power density distribution is shown in Figure 6.

The location of the region of VHF PLS is uncertain for two reasons. The beam of the Stanford transmitting antenna is so large at VHF that regions of a few tens of kilometer separation cannot be resolved. Even though the VHF transmitter was on for a few hours, only a few minutes of PLS data were obtained. During these periods of PLS data the altitude of ionospheric modification was not too different from the altitude of specular scatter. Contours of the altitude of specular scatter have been computed for the VHF bistatic path; the results are shown in Figure 7. The altitude of VHF specular scatter is nearly 30 km higher than for UHF due to ionospheric refraction, being as low as 213 km southwest and as high as 236 km northwest of Platteville (in a 50-km radius).

### D. VHF Field-Aligned Scatter

The VHF FAS signal was enormous compared to the three other types of signals observed. It was also narrowband (a few hertz) like the PLS but was approximately 70 dB larger. An example of the density distribution observed is shown in Figure 8. Except for the periods when PLS measurements were attempted, FAS was received at all times during the few hours that the VHF transmitter was operated. The nominal altitude of ionospheric modification during this time was intended to be 240 km, but actually ranged from about 240 km down to as low as 210 km.

## IV CROSS SECTIONS

Two scatter cross sections are of interest, the total cross section of the modified region and the scatter per unit volume. The total cross section can be computed directly for the VHF measurements because the

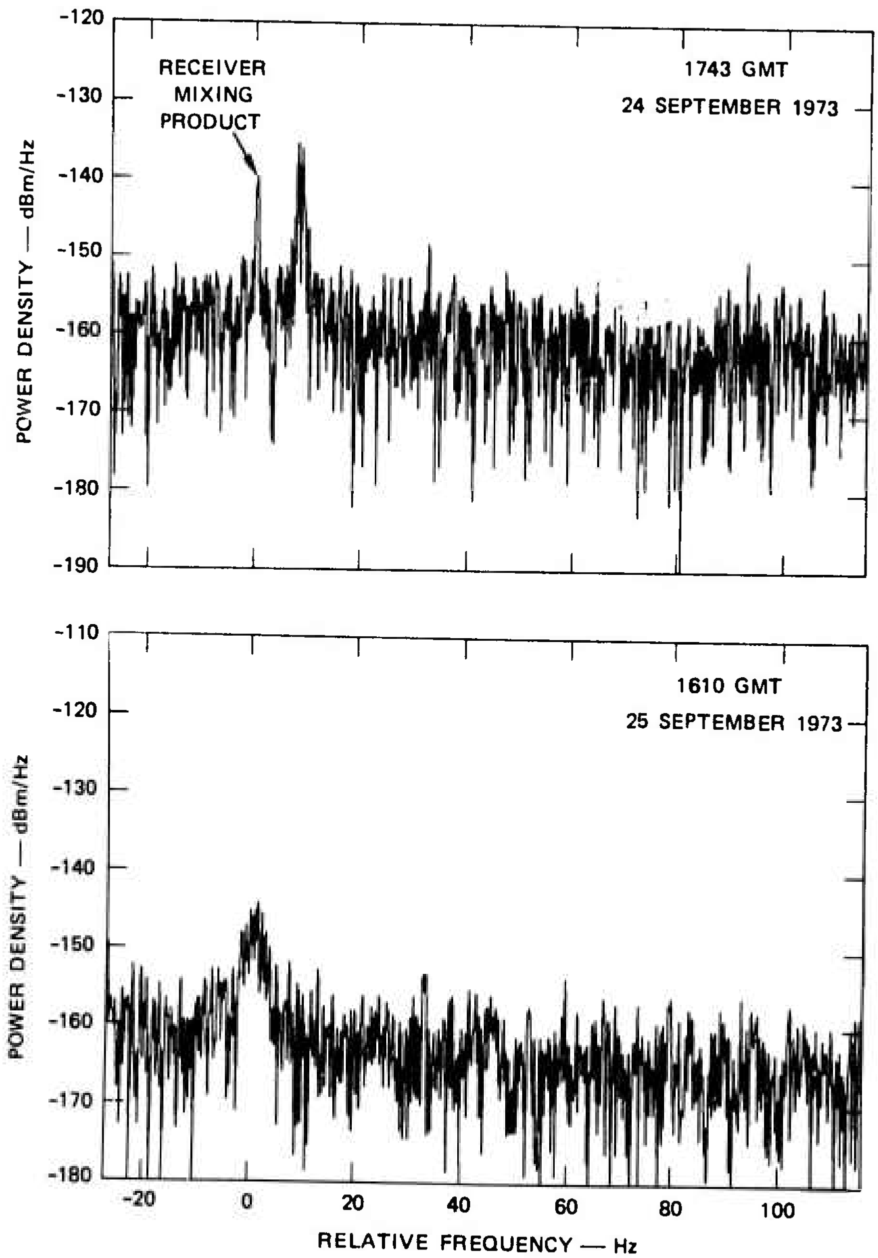


FIGURE 6 COMPUTED POWER DENSITY OF VHF PLS

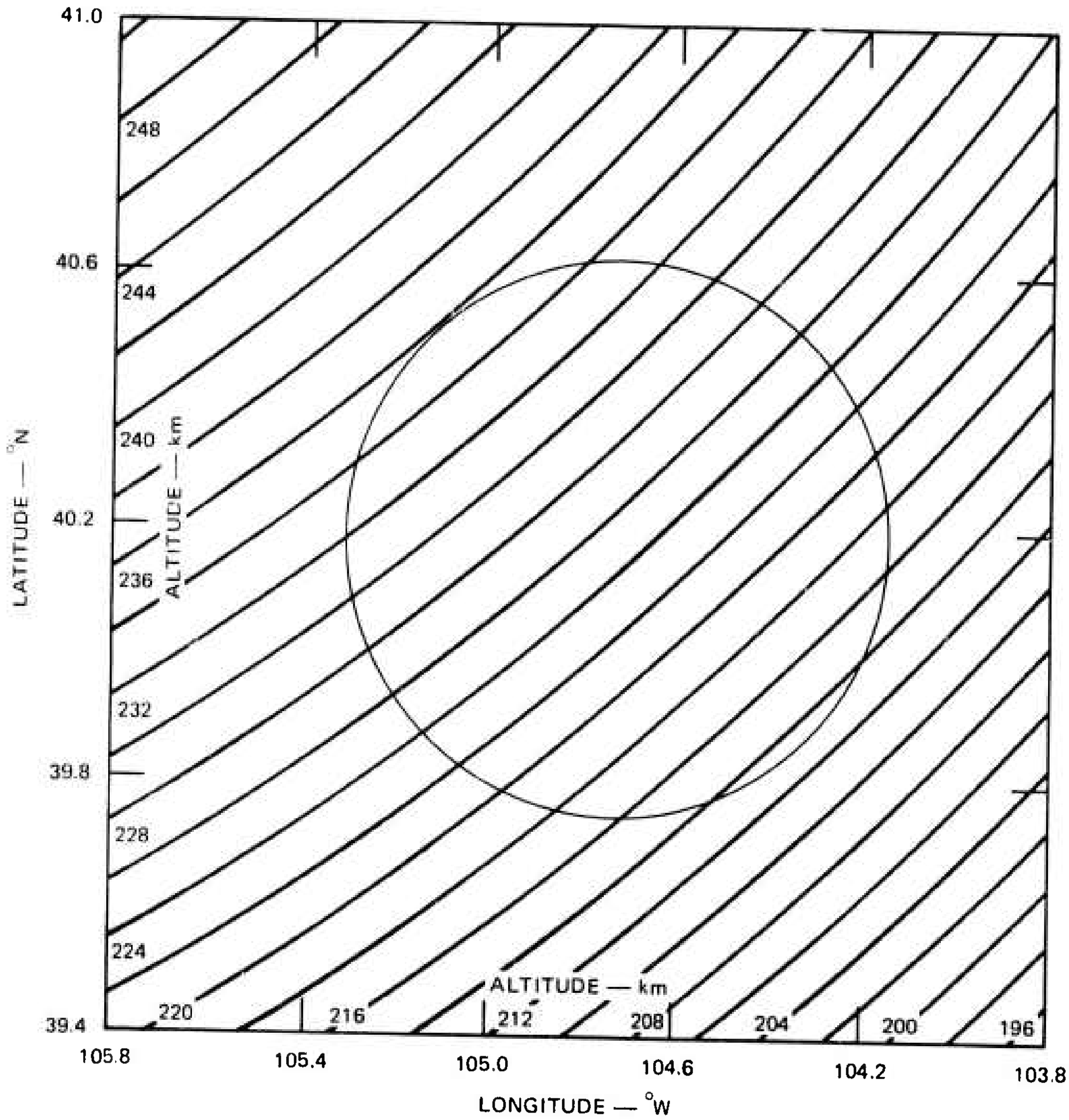


FIGURE 7 CONTOURS OF ALTITUDE AT WHICH SPECULAR SCATTER IS ACHIEVED AT VHF. The circle encloses the regions within 50 km of Platteville.

transmitting and receiving antenna beams are large with respect to the scatter region. The situation is not as simple at UHF because the 3-dB beam of the transmitting antenna has a diameter of only 45 km over Platteville. For a scatter region 100 km in diameter the measured total cross section at UHF needs to be increased by a factor of 1.9, while for a scatter region 150 km in diameter the factor is 2.7. In computing a per-unit volume cross section it is necessary to estimate the size of the scatter volume. Previous measurements suggest that the region is

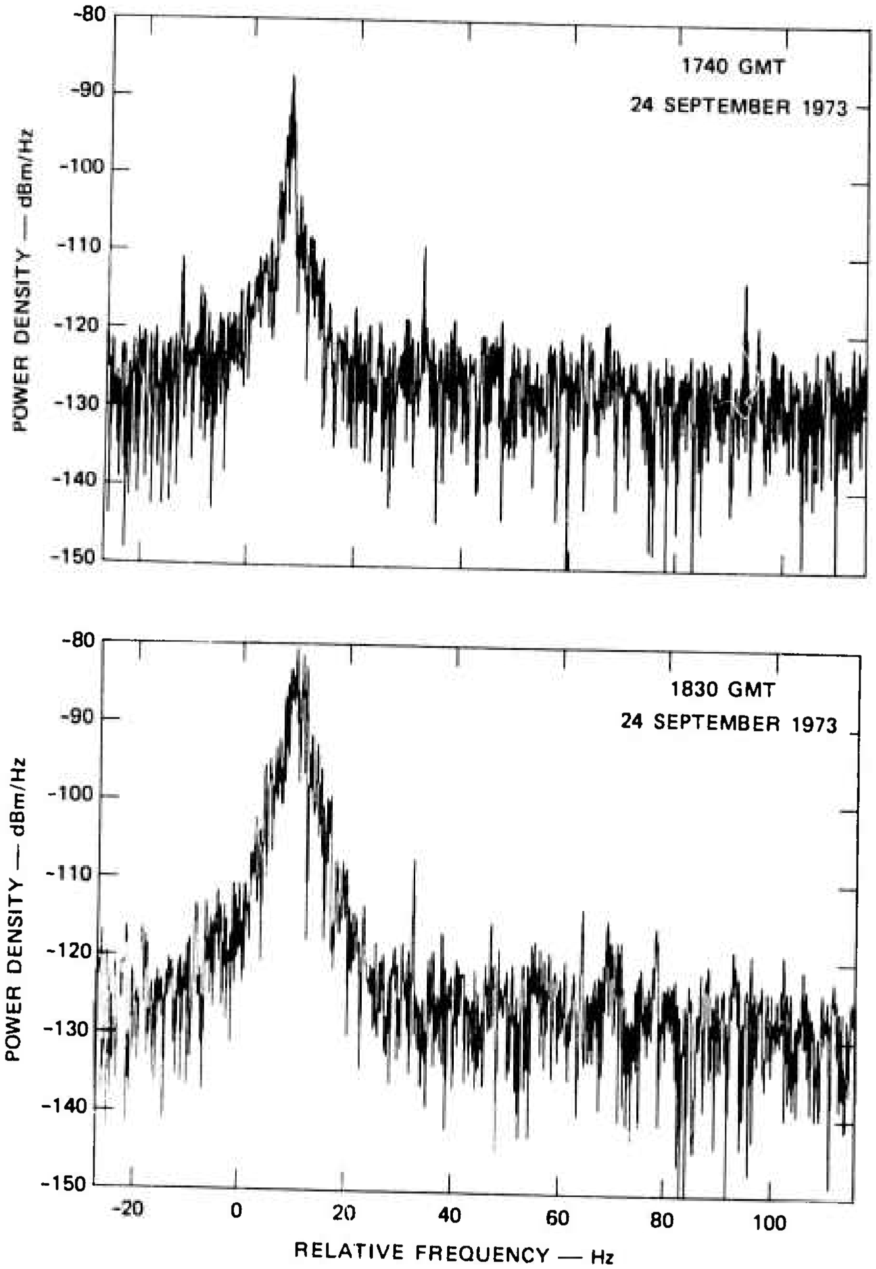


FIGURE 8 COMPUTED POWER DENSITY OF VHF FAS

roughly circular in horizontal extent, perhaps 100 to 150 km in diameter, and relatively thin in vertical extent. Lacking a reliable estimate of the vertical extent we will use $\Delta h$ km. The total volume then ranges from $7.8\ \Delta h \times 10^{12}\ m^3$ to $1.8\ \Delta h \times 10^{13}\ m^3$.

The total cross section is determined by inserting the appropriate parameters into the equation

$$\sigma = \frac{P_r (4\pi)^2 R_1^2 R_2^2}{P_t G_t A_e}$$

The per-volume cross section is determined by dividing the total cross section by the total scatter volume. Table 3 contains the results obtained by manipulating the cross-section equation. The effective area of the receiving antennas shown in Table 3 is in dB relative to $1\ m^2$. The antenna gains quoted in Table 1 have been converted to effective area using the relationship $A = G\ \lambda^2/4\pi$, and the resultant areas have been reduced by a factor of 2 to account for the mismatch in transmission and reception polarization.

The total cross section deduced for VHF FAS is compatible with previous observations.[1] The VHF PLS cross section is a new result. The volume cross section deduced for UHF FAS is within a few dB of the value associated with backscatter observations[3] at White Sands, while the PLS volume cross section is about 20 dB less than at White Sands and more like that deduced previously from bistatic measurements[7] at Stanford.

## V SPECIAL TESTS

A number of special transmission modes were employed at Platteville during the four days in which data were obtained at Ft. Huachuca. These

Table 3

CROSS-SECTION ESTIMATES

| | VHF Field-Aligned Scatter | VHF Plasma-Line Scatter | UHF Field-Aligned Scatter | UHF Plasma-Line Scatter |
|---|---|---|---|---|
| Received power, $P_r$ (dBm) | -78 | -148 | -132 | -152 |
| Path loss $(4\pi)^2 R_1^2 R_2^2$ (dB) | 267 | 267 | 267 | 267 |
| Transmitted power, $P_t$ (dBm) | 83 | 83 | 74 | 74 |
| Transmitter gain, $G_t$ (dB) | 24 | 24 | 44 | 44 |
| Reception area, $A_e$ (dB relative to 1 $m^2$) | 16 | 16 | 3 | 3 |
| Apparent cross section (dBsm) | +66 | -4 | +14 | -6 |
| Correction for beam diameter (dB) | 0 | 0 | 2.7 to 4.3 | 2.7 to 4.3 |
| Apparent total $\sigma$ (dBsm) | +66 | -4 | +17 to +18 | -3 to -2 |
| Estimated diffraction (dB) | 0 | 0 | -18 | -18 |
| Adjusted total $\sigma$ (dBsm) | +66 | -4 | +35 to +36 | +15 to +16 |
| Apparent volume $\sigma$ | $2/\Delta h$ to $5/\Delta h \times 10^{-7}$ $m^2/m^3$ | $2/\Delta h$ to $5/\Delta h \times 10^{-14}$ $m^2/m^3$ | 4 to $6 \times 10^{-12}/\Delta h$ $m^2/m^3$ | 4 to $6 \times 10^{-14}/\Delta h$ $m^2/m^3$ |
| Adjusted volume $\sigma$ | $2/\Delta h$ to $5/\Delta h \times 10^{-7}$ $m^2/m^3$ | $2/\Delta h$ to $5/\Delta h \times 10^{-14}$ $m^2/m^3$ | $2.5/\Delta h$ to $4/\Delta h \times 10^{-10}$ $m^2/m^3$ | 2.5 to $4 \times 10^{-12}/\Delta h$ $m^2/m^3$ |

modes involved primarily power and frequency shifts and are discussed in detail elsewhere in these Proceedings. A brief description of our results is given below.

- Test No. 1 (Yield, Long-Term)

  12 September, 2020 to 2100 GMT. UHF scatter was not observed. This is believed due to the relatively high (>240 km) altitude of ionospheric modification.

  13 September, 2100 to 2200 GMT. The UHF data were monitored in real time and occasionally recorded on film. Scatter was clearly recognized during full-power transmission at Platteville, but not during reduced-power transmission. The altitude of modification was approximately 210 to 215 km.

  24 September, 1520 to 1615 GMT. UHF scatter was clearly observed during the period of peak-power transmission at Platteville but not during reduced-power transmission. The absence of signal during the early part of the test is also related to the unfavorable altitude of modification; this altitude was initially about 250 km, then dropped to around 215 km.

- Test No. 2 (Yield, High Level)

  12 September, 2130 to 2150 GMT. The UHF data were monitored in real time and occasionally recorded on film. Scatter apparently was not observed. The altitude of modification exceeded 225 km.

  13 September, 0030 to 0050 GMT. The UHF data are of little use, since the receiver was tuned to the plasma line and the transmitting antenna was scanning in elevation and azimuth.

  13 September, 2230 to 2250 GMT. Data were not obtained.

  24 September, 1642 to 1713 GMT. VHF FAS data were obtained between 1700 and 1713 GMT with the following result:

| Change at Platteville Nominal | Change in VHF FAS |
|---|---|
| -6 dB | -6 to -7 dB |
| -9 | -10 to -11 |
| -12 | ≈-13 |

There are no measurements of the true power change at Platteville. UHF FAS was very weak during this period due apparently to the relatively high (≈225 km) altitude of ionospheric modification.

25 September, 0730 to 0750 GMT. UHF FAS data provide the following result:

| Change at Platteville | | Change in |
|---|---|---|
| Nominal | Actual | UHF FAS |
| -6 dB | -6.20 | ≈ -4 |
| -9 | -7.32 | ≈ -6 |
| -12 | -11.54 | ≈ -10.5 |
| -15 | -15.1 | > -12 |

- Test No. 3 (Yield, Medium Level)

  12 September, 2340 to 2355 GMT. Excellent UHF data were obtained but they have not been processed in a form suitable for amplitude scaling. The altitude of modification was roughly 210 km.

- Test No. 5 (Yield, Double Resonance)

  14 September, 0135 to 0147 GMT. UHF PLS measurements were carried out during this test; there was no recognizable improvement in scatter cross section.

- Test No. 6 (Yield, Pulse Compression)

  25 September, 1405 to 1415 GMT. Very weak UHF scatter was observed. The strength was appreciably weaker than during the CW mode about 10 minutes later. The altitudes of modification were comparable.

- Test No. 7 (Yield, Pump Bandwidth)

  12 September, 2250 to 2256 GMT. The UHF data were monitored in real time. It seems likely that scatter should have been observed (modification at ≈210 km), but none was reported.

- Test No. 8 (Yield, Rise/Decay)

  12 September, 2232 to 2240 GMT. The UHF data were monitored in real time. It seems likely that scatter should have been observed (modification at ≈210 km), but none was reported.

  14 September, 0035 to 0045 GMT. The occurrence of UHF scatter (both FAS and PLS) in alternate 5-s intervals was clearly evident. The data have not been processed in a form that permits scaling of rise and fall times.

  25 September, 1240 to 1250 GMT. Data were not obtained.

## VI CONCLUSIONS

The observations at Ft. Huachuca provide the first reliable measurements of the spectral distribution of UHF FAS, UHF PLS, and VHF PLS associated with scattering planes parallel to the earth's magnetic field in a volume modified by a high-power HF transmitter. The distribution for both modes and both frequencies was relatively narrow, in agreement with HF/VHF FAS measurements by Fialer,[2] and VHF FAS and PLS measurements by Minkoff.[3] Our PLS data are rather sparse, owing to poor SNR at UHF and a limited transmission schedule at VHF.

The region of scatter was found to be strongly tied to field-aligned specular geometry, for both FAS and PLS modes. This characteristic is consistent with all other observations of the FAS mode, but less so for the PLS mode. Minkoff[3] reported a field-aligned relationship for VHF and UHF PLS in backscatter geometry, but in bistatic measurements Carpenter[7] found the scatter region to be related to the altitude of modification. Further measurements should be conducted to resolve this inconsistency. The plasma-line scatter cross section deduced from the Ft. Huachuca measurements was about the same as deduced[7] from measurements at Stanford on a nearly reciprocal path. Both these results are about 20 dB below backscatter results obtained by Minkoff.[3]

The reception of the UHF FAS mode at Ft. Huachuca in bistatic geometry was unexpected in the light of negative results[7] on a nearly reciprocal path to Stanford. If possible, measurements should be conducted to resolve this inconsistency. The cross section observed in bistatic geometry is very nearly equal to that observed by Minkoff[3] in backscatter geometry. In making this comparison we have adjusted the bistatic data for diffraction of the beam by hills in the foreground of the transmitting antenna.


## ACKNOWLEDGMENTS

This experiment would not have been a success without the special efforts of Victor Frank, Douglas Lee, and Philip Bentley, who assisted with the design and operation of the receiving system and with data analysis. Expansion of the scope of the experiment to include VHF observations was possible only through the generous cooperation of Mr. William Faulkerson at Stanford University who coordinated use of their transmitter.


## REFERENCES


1. B. R. Pendyala and G. D. Thome, "A Model for On-Frequency Field-Aligned Scattering (U)," Proceedings of the PRAIRIE SMOKE Yield Model Workshop, 17-18 July 1973 (U), SRI 3-5193, Stanford Research Institute, Menlo Park, Calif. (October 1973), SECRET.

2. P. A. Fialer, "SFCW Observations of Field-Aligned Scattering (U)," Proceedings of the IVORY CORAL 1973 Technical Review Meeting, Vol. II: Experiments (U), SRI 3-4534, Stanford Research Institute, Menlo Park, Calif. (April 1973), SECRET.

3. J. Minkoff, "Riverside Research Institute Radar Measurements (U)," Proceedings of the IVORY CORAL 1973 Technical Review Meeting, Vol. II: Experiments (U), SRI 3-4534, Stanford Research Institute, Menlo Park, Calif. (April 1973), SECRET.

4. F. W. Perkins, C. Oberman, and E. J. Valeo, "Parametric Instabilities and Ionospheric Modification (U)," PPL-AP69, Princeton University, Princeton, New Jersey (June 1973), UNCLASSIFIED.

5. F. W. Perkins, private communication to P. A. Fialer.

6. I. J. Kantor, Plasma Waves Induced by HF Radio Waves, Ph.D. Thesis (Rice University, Houston, Texas, July 1972), UNCLASSIFIED.

7. G. B. Carpenter, "PRAIRIE SMOKE Measurements Involving the SRI 150-ft Antenna Facility (U)," Proceedings of the IVORY CORAL 1973 Technical Review Meeting, Vol. II: Experiments (U), SRI 3-4534, Stanford Research Institute, Menlo Park, Calif. (April 1973), SECRET.

# PLATTEVILLE ULF TESTS

W. H. Campbell

U.S. Geological Survey
Boulder, Colorado

ABSTRACT

The ULF tests for the Platteville antenna were scheduled for the purpose of determining whether periodic magnetic-field pulsations might be generated through E-region modification. The detection systems were three-directional induction-loop antennas (16,000 turns, 2-m diameter) with a limiting sensitivity of $\approx 0.001$ gamma-s. The Platteville transmitter, about 37 km east-northeast of the Boulder Magnetic Observatory, was operated at a 2.8-MHz fixed frequency with input powers of 0.8 to 1.9 MW. The transmitter was pulsed with a 50% duty cycle at various pulse rates.

It does not seem likely that the Platteville transmitter, operating at E-region frequencies, can generate preselected pulses at periods in the test range below 180 s. An enhancement of natural signals in the range of about 20 to 60 s does seem to occur at daylight hours with the transmitter near the $f_oE$ frequency. In such cases it appears likely that sufficient modification of the E-region conductivity has occurred to locally enhance the natural currents flowing there.

Pages 163 and 164
are blank

# I PURPOSE

The ULF tests for the Platteville antenna were scheduled for the purpose of determining whether periodic magnetic-field pulsations might be generated through E-region modification. The detection systems were three-directional induction-loop antennas (16,000 turns, 2-m diameter) with a limiting sensitivity of $\approx 0.001$ gamma-s. The Platteville transmitter, about 37 km east-northeast of the Boulder Magnetic Observatory, was operated at a 2.8-MHz fixed frequency with input powers of 0.8 to 1.9 MW. The transmitter was pulsed with a 50% duty cycle at various pulse rates. Table 1 is an abbreviated list of the scheduled transmissions. The test days were selected for low natural geomagnetic activity. The E-region critical frequency measured near the transmitter (Erie) attained 2.8 MHz during each of the three tests. Recordings of the three field components were made on rapid-run ink charts and FM magnetic tapes.

Table 1

TRANSMITTER ON 2.8 MHz
AT APPROXIMATELY 0.8 TO 1.9 MW

| Date | Start Time, UT (LMT) | End Time, UT (LMT) | Switching Periods (s) | Max K (BO) | Time $f_oE$ = 2.8 MHz |
|---|---|---|---|---|---|
| 11 Oct | 1215 (0515) | 1755 (1055) | 60, 20, 8, 0.5 | 2 | 1550 (UT) |
| 12 Oct | 1205 (0505) | 1900 (1200) | 180, 60 | 3 | 1625 |
| 17 Oct | 2009 (1309) | 2300 (1600) | 34, 10 | 2 | 2120 |

## II THE ANALYSIS

For the analysis, four procedures were used:

(1) The ink-chart records were carefully inspected for the presence of the transmitter switching frequency or natural signal modulation at the transmission schedule (Figure 1).

(2) Rayspan spectral displays were made from the magnetic-tape records to observe the changing patterns of the geomagnetic-field emission frequencies at the times of the tests.

(3) Integrated spectra were plotted for the received field changes for blocks of several hours before, during, and following the special Platteville transmissions (Figure 2).

(4) Detailed spectral analyses were made of 500-s data blocks stepped 50 s at a time through the test days and adjacent days (Figure 3).

## III THE RESULTS

Three results of the tests should be noted:

(1) In no instance could a clear appearance of the transmitter switching period be found in the received field change. There was only a faint indication of the 180-s signal that may have been present. Because of rising natural geomagnetic activity and previous Platteville commitments the tests could not be completed or be considered definitive for switching with $T < 10$ s. However, our feeling was that the longer-period switching should have been the more effective modulator. Thus we conclude from the extent of testing that the transmitter was not able to clearly generate a ULF signal of a preselected period. For example, in Figure 1, the time previous to 1900 represents a transmission of 180-s switching. Sustained periods of high-power (1.9 MW) transmission did not seem to improve the test.

(2) The integrated spectra consistently showed an enhancement of natural background field with frequencies from about 0.016 to 0.048 Hz (about a 60-to-20-s period which is called the Pc 2-3 pulsation region by geomagneticians). Figure 2 shows the best example of this enhancement. The top two spectral pairs are before sunrise. Notice the spectral

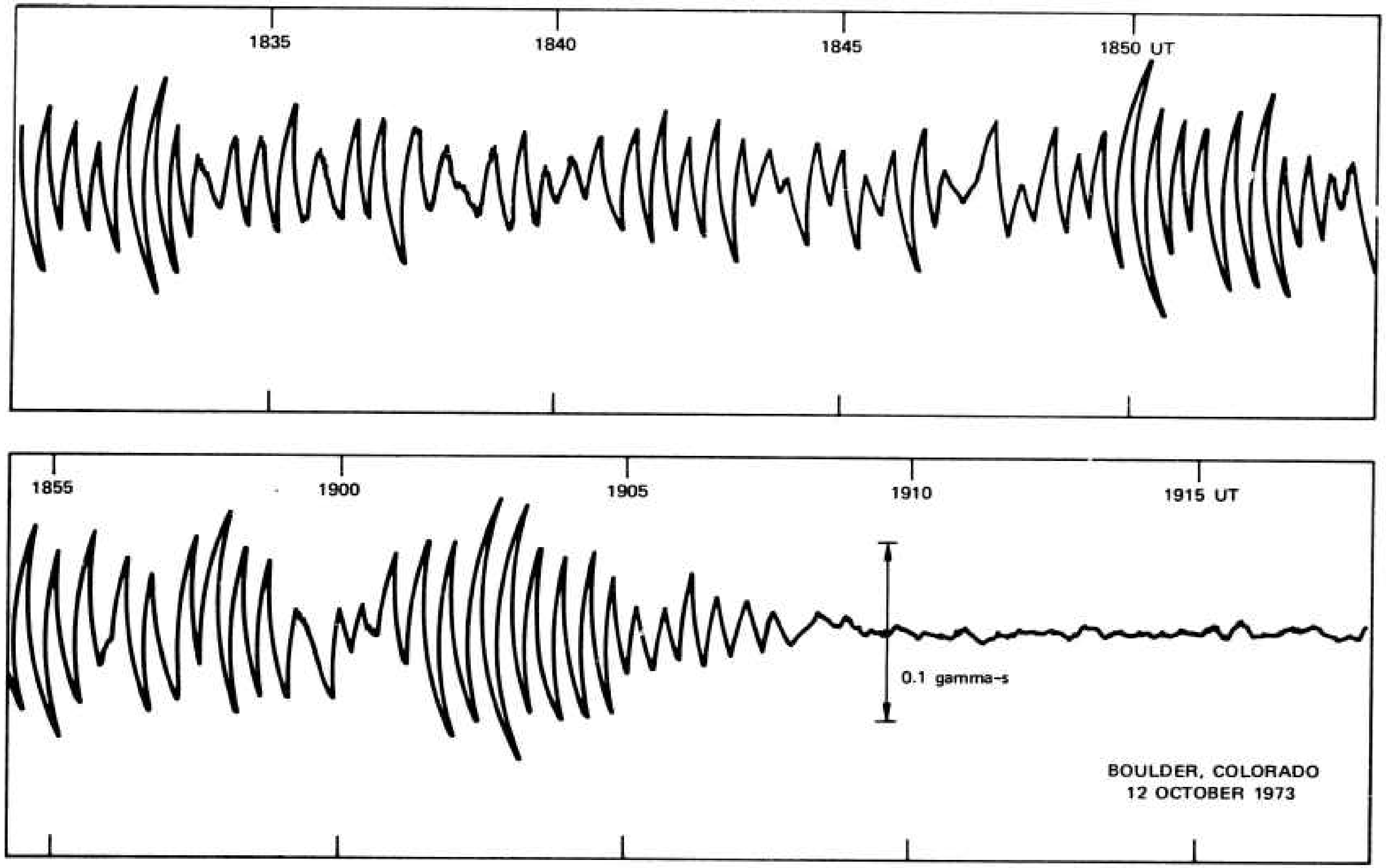


FIGURE 1 RAPID-RUN CHART RECORDS OF INDUCTION-LOOP-ANTENNA OUTPUT

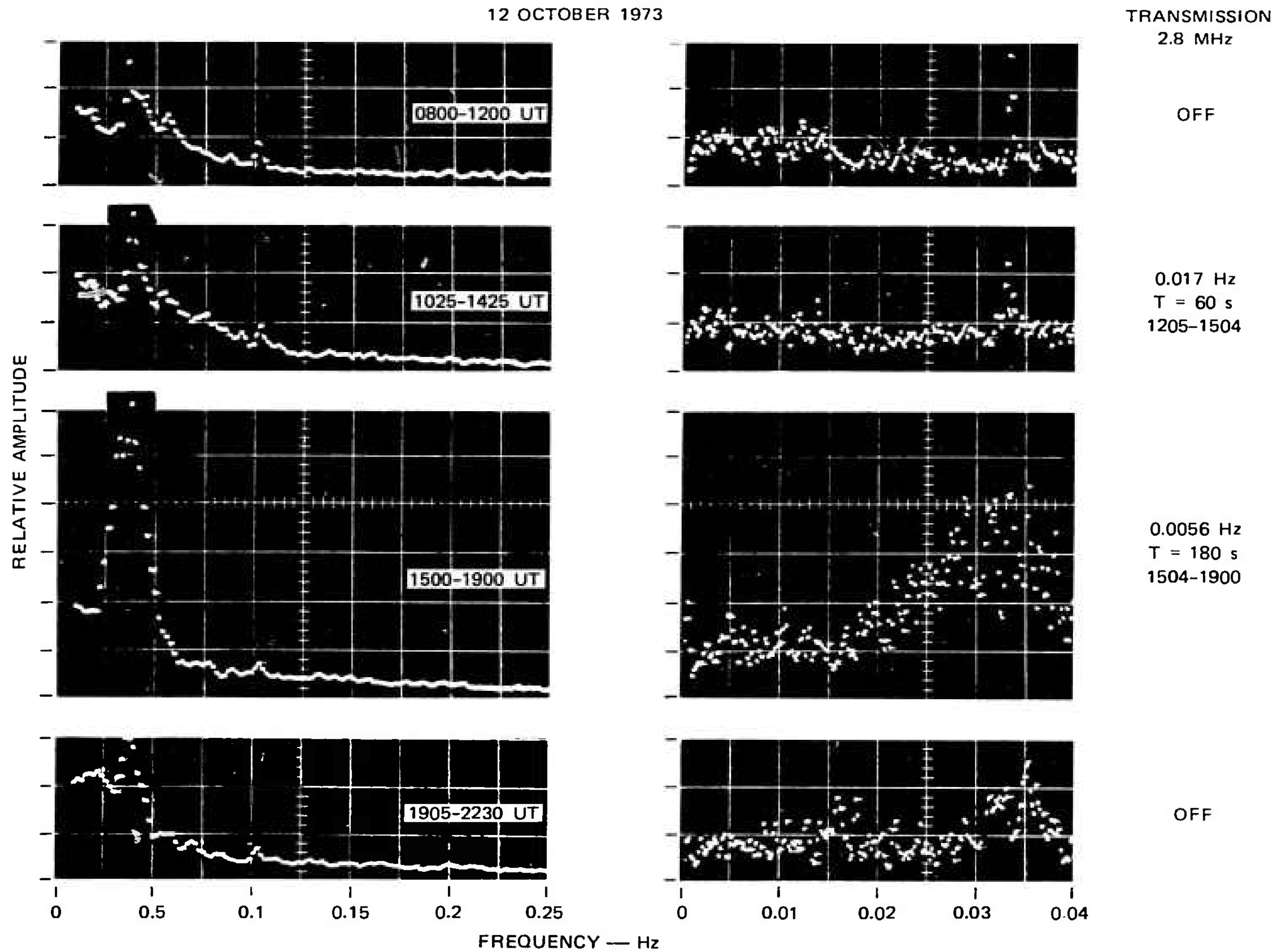


FIGURE 2 SPECTRUM vs. TIME OF THE MAGNETIC-FIELD VARIATIONS

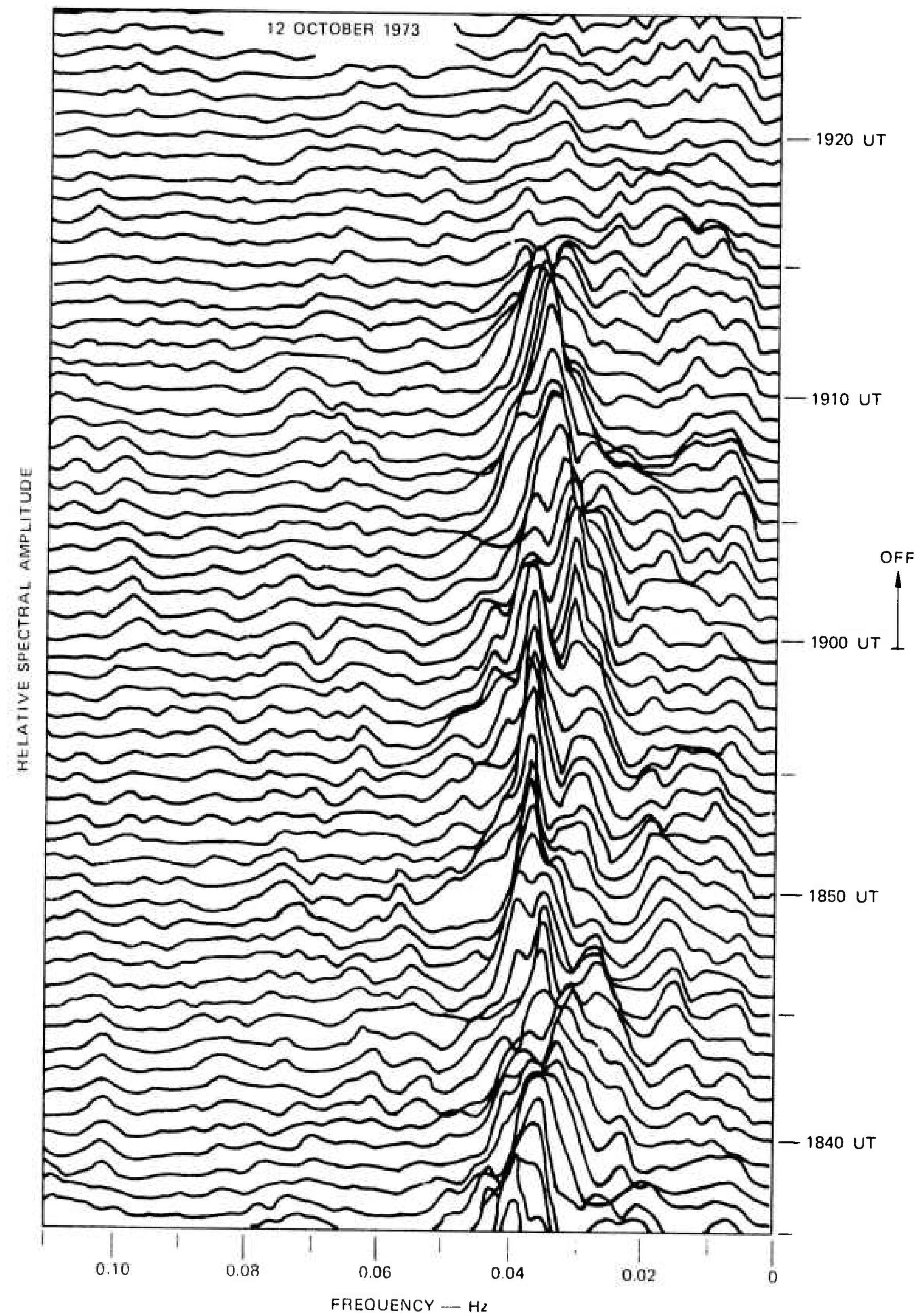


FIGURE 3 SPECTRA OF MAGNETIC-FIELD VARIATIONS

enhancement from 1500 to 1900 UT. This enhancement was noticed only for daylight portions of the run and seemed independent of the transmitter switching period even though, on the third test day, a 0.03-Hz switching was used to center on this enhancement band. Since only three test days were used, there is a possibility of natural random occurrence of this apparent enhancement. A check of transmitter-off days sustained this possibility. However, the clear coincidence of the effect with Platteville 2.8-MHz transmissions gives us the strong opinion that the effect was caused by our tests.

(3) On occasion the complete turn-off of the transmitter was followed by a drop-off of the received geomagnetic signal. Figure 3 is an example. Note that there are 500 s of data in the analyzer memory at any time; it takes ten sweeps of the display to clear this out. Figure 1 is the corresponding amplitude record. Assuming that the cutoff was caused by the transmitter shut-down at 1900, we estimate the 3-dB-level dropoff of signal enhancement to occur in about 2 min and the decay half-life to be about 5 min.

## IV CONCLUSIONS

It does not seem likely that the Platteville transmitter, operating at E-region frequencies, can generate preselected pulses at periods in the test range below 180 s. An enhancement of natural signals in the range of about 20 to 60 s does seem to occur at daylight hours with the transmitter near the $f_oE$ frequency. In such cases it appears likely that sufficient modification of the E-region conductivity has occurred to locally enhance the natural currents flowing there.

If further tests can be made, it would be good to pursue the E-region current-modification possibility that was indicated in the present results. For that purpose, a transmitter switching period of about 20 min to 1 hour would be a worthwhile starting point.

# PULSE-COMPRESSION EXPERIMENTS PERFORMED DURING THE PRAIRIE SMOKE V TEST SERIES

E. K. Walton   S. A. Bowhill

Aeronomy Corporation
Champaign, Illinois

ABSTRACT

It has been proposed that the time-delay-versus-frequency characteristics of the ionosphere near the critical frequency may be exploited to increase the yield of the heater transmitter. A downward ramp (or sawtooth) in frequency may be transmitted such that the frequency-versus-time slope of the ramp "matches" the frequency-versus-time slope at the transmitter frequency. At the height of reflection, the lower-frequency (and higher-velocity) components "catch up" with the higher-frequency components and the total signal deposits a pulse of energy much greater than that due to the average power of the transmitter.

## I THEORY

In order to obtain higher peak power in the ionosphere than the value due to maximum transmitter power, a pulse-compression technique was suggested. This idea uses the time-delay-versus-frequency characteristics of the ionosphere near the critical frequency. In this region a small increase in frequency produces a large increase in the time required for the signal to reach the reflection level. The reflection

Pages 172, 173, and 174 are blank

level is assumed to be the level at which the heating effect is produced. The actual change in height near the critical frequency due to a frequency change is considerably less than the change in the virtual height (time delay) due to such a frequency change. To take advantage of this, a frequency sweep may be transmitted such that the higher frequencies are transmitted first, followed by the lower frequencies. The lower-frequency components, with less time delay, might then "catch up" with the higher-frequency components. In fact, if the frequency sweep is carefully chosen, the total signal could arrive at the height of reflection simultaneously, and deposit a pulse of energy much greater than the average energy available. The pulse-compression experiment was performed in order to study the effect of such a frequency-sweep scheme.

## II PROCEDURE

In order to implement these ideas, the equipment shown in the block diagram of Figure 1 was set up. The bandwidth of the transmitters is 100 kHz, which limits the frequency range over which they can be swept. These transmitters are driven by an HP 5100A frequency synthesizer, which can be frequency-swept using an applied dc voltage. It was

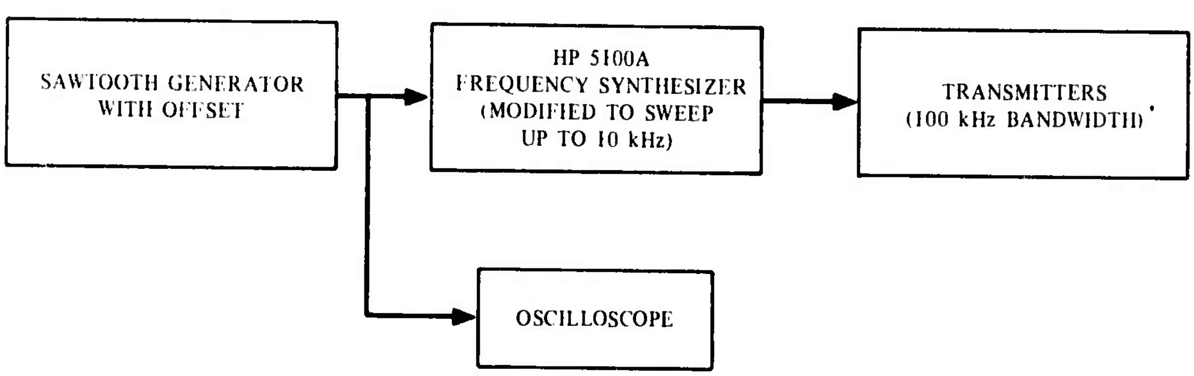


FIGURE 1 PULSE-COMPRESSION INSTRUMENTATION

modified so that it could be frequency-swept at rates up to 10 kHz. A function generator was used to generate the voltage ramp and the offset bias such that the frequency sweep rate and extent of frequency shift as well as the average (center) frequency could be adjusted. The output of the function generator was monitored using an oscilloscope.

Once the equipment was set up, the operating procedure was as follows:

| | |
|---|---|
| • 20 min before start time | Get h'(f) data from local site V.I. ionosonde. Plot data, calculate T. |
| • 1 min before start time | Get $f_oF2$ update and calculate operating frequency (96% to 99% $f_oF2$). |
| • Start time | Set $f_H$ as close to chosen operating frequency as possible. Operate with five transmitters, each at 1/2 power CW mode. |
| • Start time + 2 min | Sweep frequency 100 kHz in T seconds (sawtooth). |
| • Start time + 4 min | Sweep frequency 100 kHz in 120% of T seconds (sawtooth). |
| • Start time + 6 min | Sweep frequency 100 kHz in T seconds (sawtooth). |
| • Start time + 8 min | Sweep frequency 100 kHz in 80% of T seconds (sawtooth). |
| • Start time + 10 min | End of run. |

The variable T is the time for the frequency to sweep downward 100 kHz. The retrace time was about 1/20 T. The value of T is calculated drawing a tangent to the h'(f) curve at $f = f_H$, and determining from the slope of this line the one-way time delay for a 100-kHz change. In order to cover a wide range of values for T, the value of $f_H$ was chosen as 96% and 99% (in two cases) of $f_oF2$. The dates, times, and values of T and $f_H$ used in this series of tests are listed in Table 1.

Table 1

TRANSMITTER PARAMETERS DURING THE PULSE-COMPRESSION EXPERIMENT

| Greenwich Mean Time | | Desired $f_H$(MHz) | Actual $f_H$(MHz) | $f_oF2$(MHz) | Actual $f_H/f_oF2$ (%) | T(ms) |
|---|---|---|---|---|---|---|
| Date | Start time | | | | | |
| 11 Sept | 1826 | 5.70 | 5.949* | 5.94 | 100 | 0.094 |
| 12 Sept | 0025 | 5.94 | 5.940 | 6.16 | 96 | 0.080 |
| 21 Sept | 0740 | 2.80 | 2.80 | 2.90 | 96‡ | 0.33 |
| 25 Sept | 1405 | 4.65 | 4.60† | 4.77 | 96‡ | 0.47 |

*Unable to operate on 5.7 MHz. Closest frequency was 5.949 MHz.

†Unable to operate on 4.65 MHz. Closest frequency was 4.60 MHz.

‡The last two runs were planned to have $f_H$ = 99% of $f_oF2$. Operational and legal restrictions prevented this.

## III RESULTS

In order to display how the sweep-frequency program matched the slope of the virtual-height curve at $f_H$, the series of ionograms shown in Figures 2 through 5 was prepared. Each ionogram was taken at the Erie site near Platteville during the pulse-compression experiments. A line with slope equal to T(ms)/100 kHz used during the experiment is drawn on each ionogram. The errors in the agreement between the slope of the line and the tangent to the ordinary mode trace are caused by two factors. One factor was the ionosphere itself. The critical frequency was changing rapidly or was difficult to determine (Figure 4, for example). A further problem was that the frequency of the transmitter cannot be chosen completely arbitrarily. Operational and legal restrictions

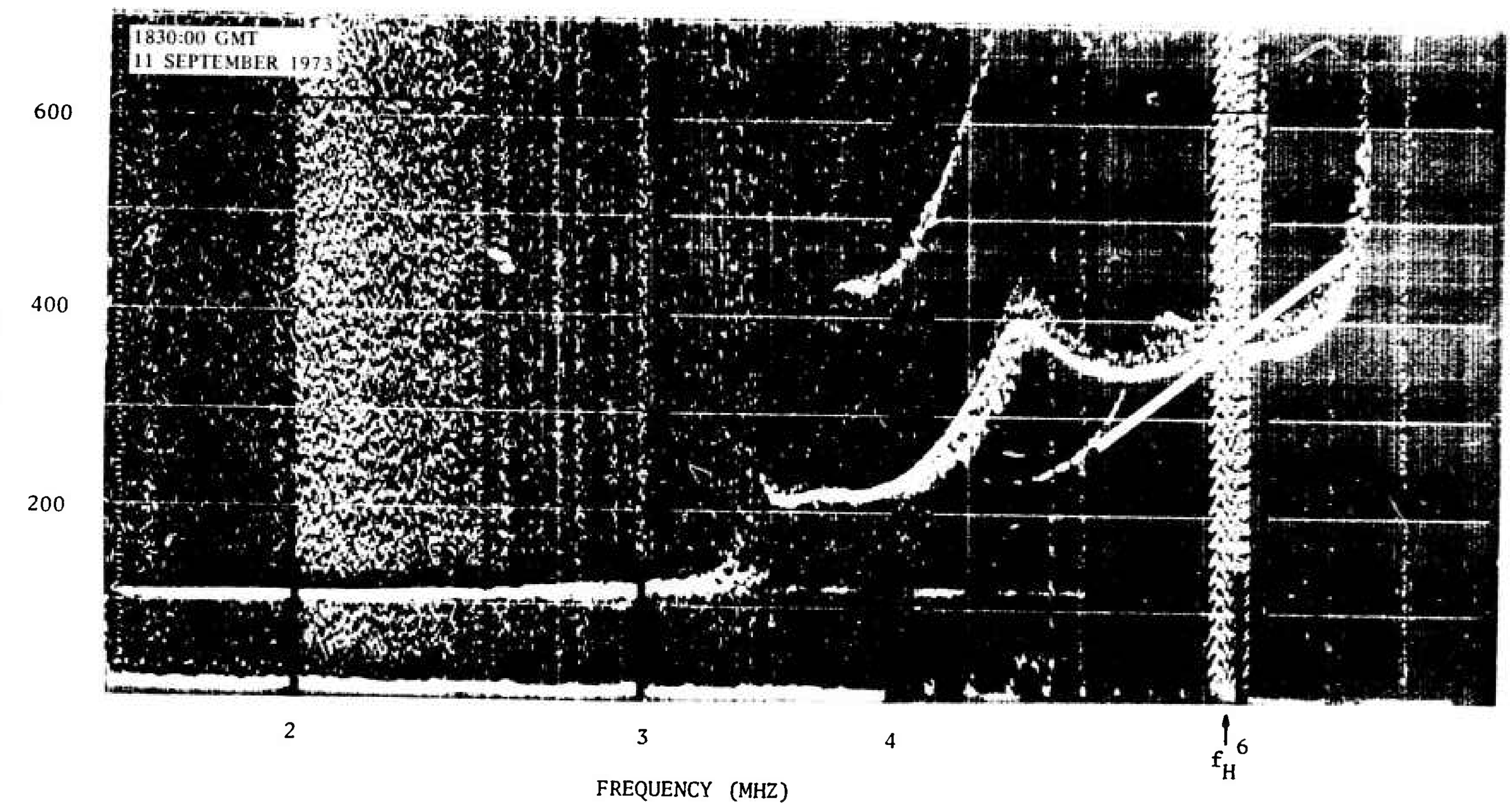


FIGURE 2 ERIE SITE V.I. IONOGRAM FOR 11 SEPTEMBER 1973

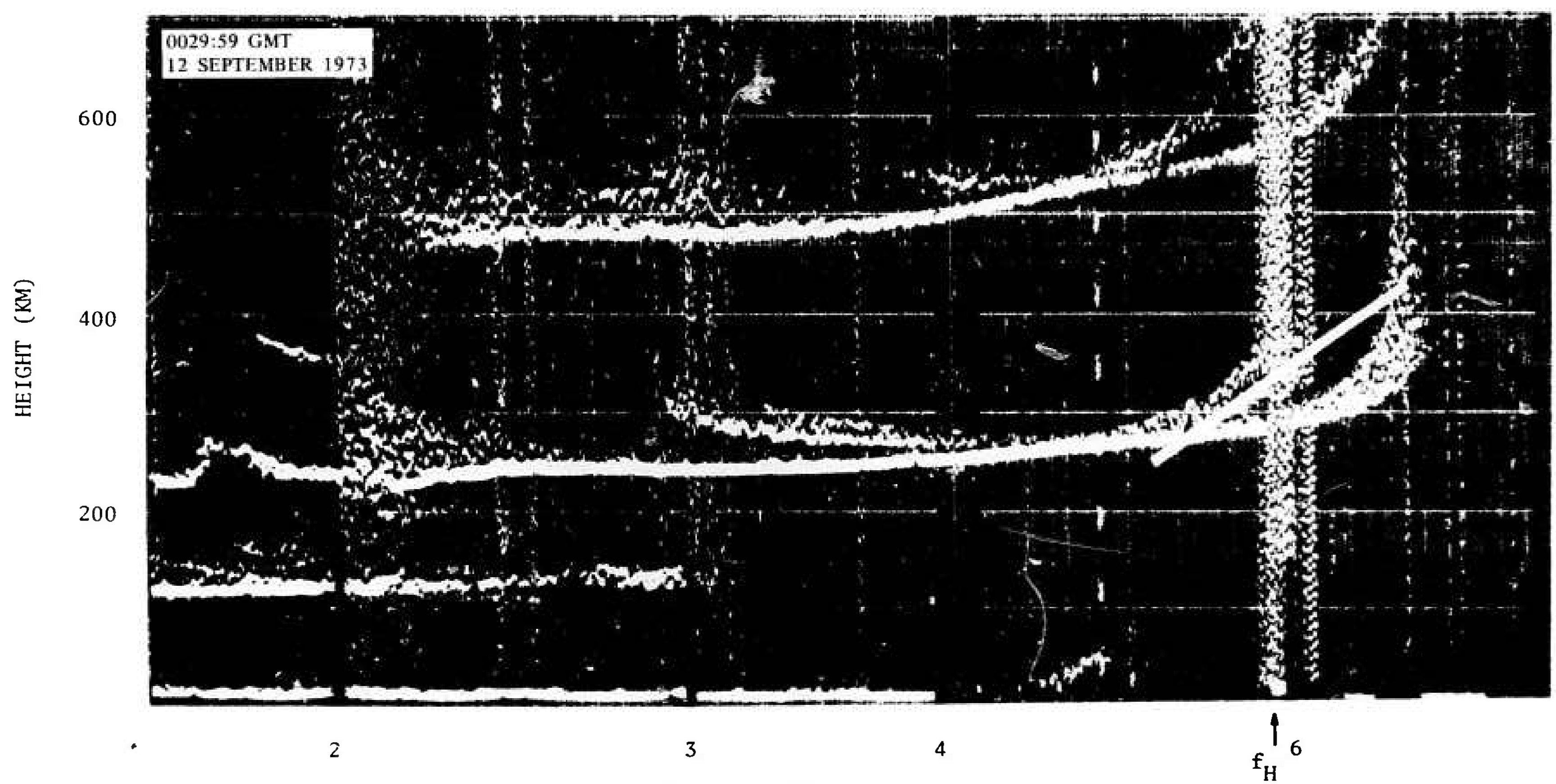


FIGURE 3 ERIE SITE V.I. IONOGRAM FOR 12 SEPTEMBER 1973

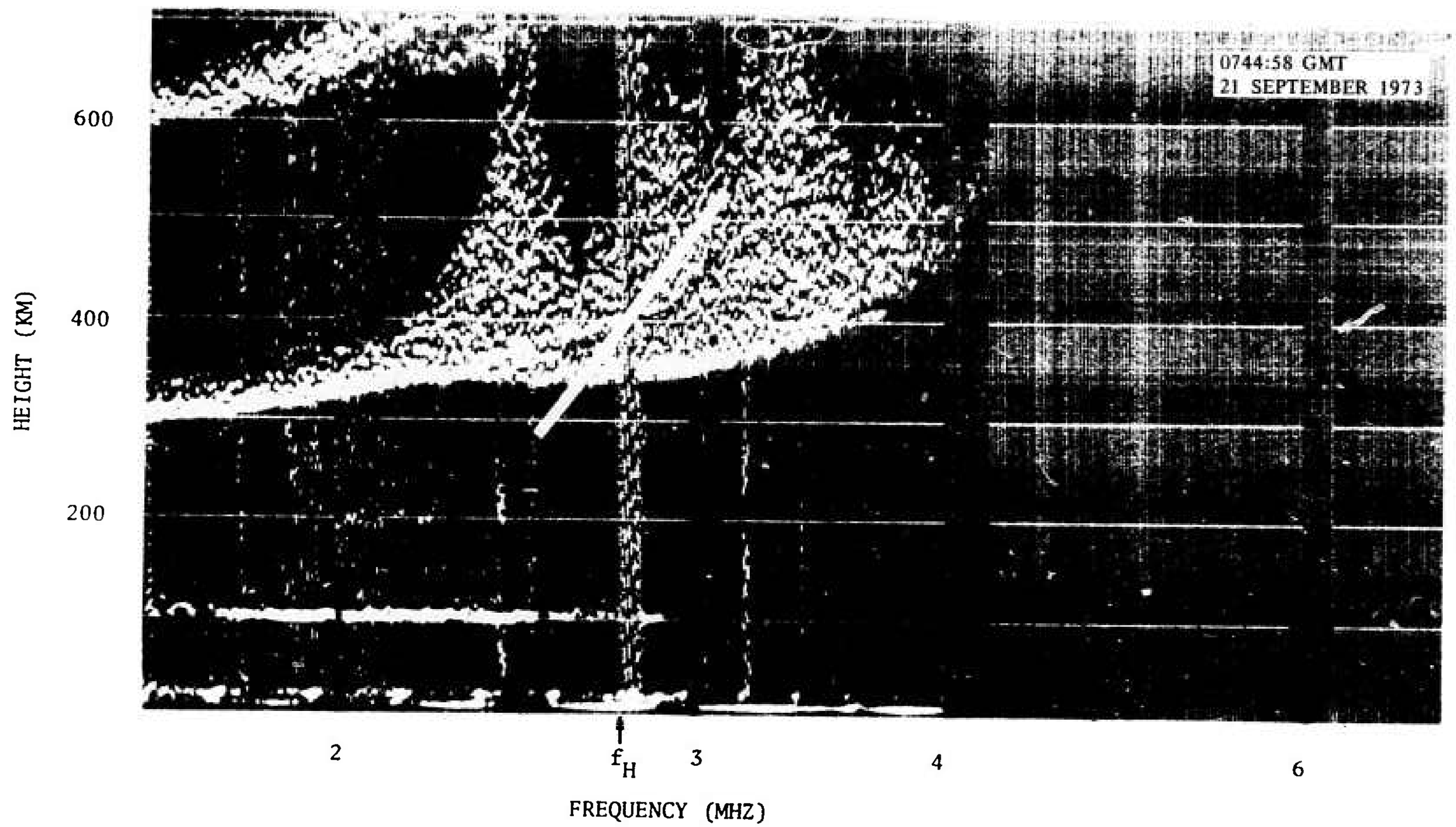


FIGURE 4 ERIE SITE V.I. IONOGRAM FOR 21 SEPTEMBER 1973

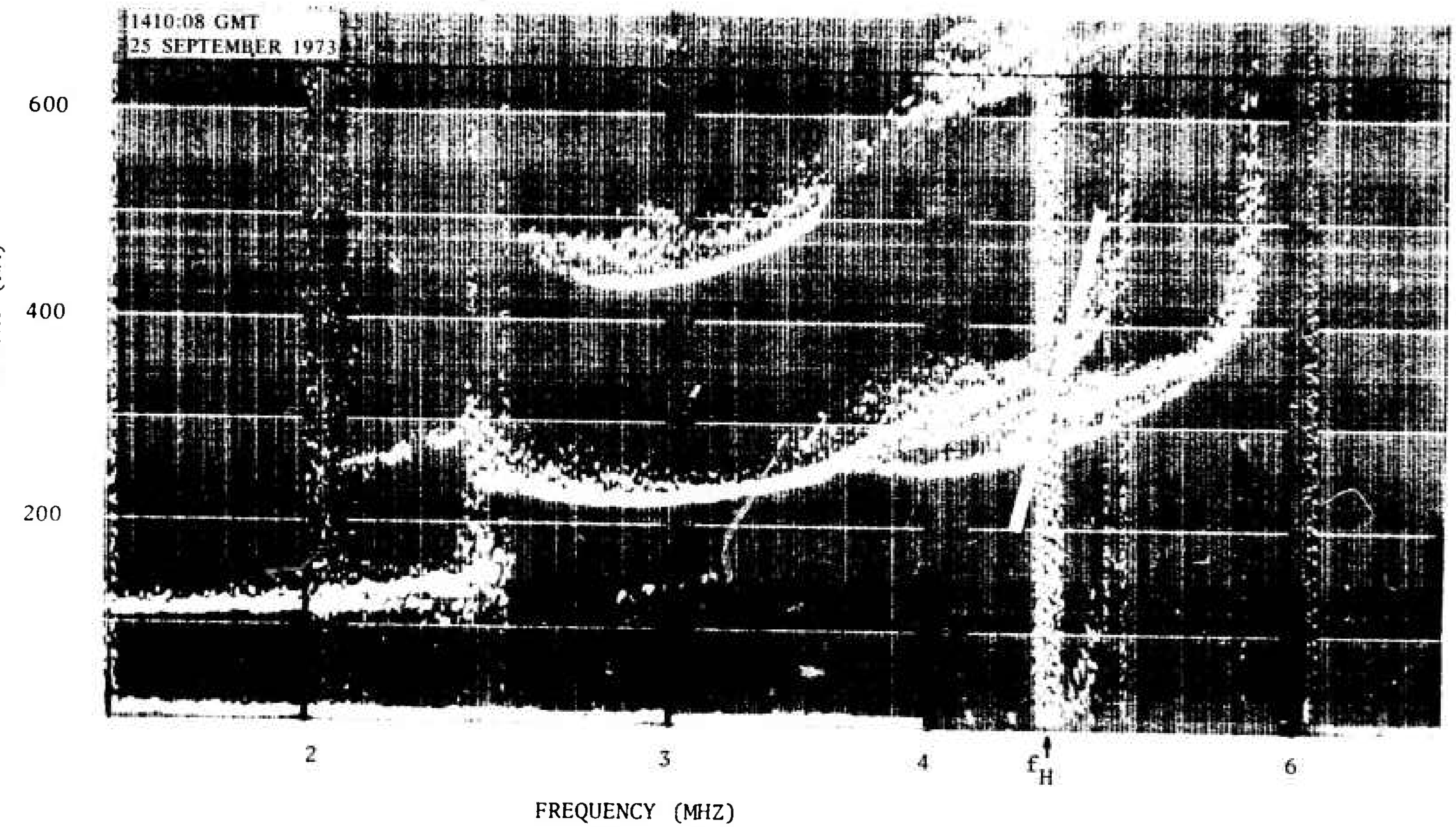


FIGURE 5 ERIE SITE V.I. IONOGRAM FOR 25 SEPTEMBER 1973

prevented the frequency shown in Figures 2 and 5 from being set at the chosen value. As can be seen from the ionograms, the experiment performed on 12 September 1973 (Figure 3) seems to have the best "match" of heater-frequency to ionospheric parameters.

Radar backscatter data are available for the 11 September 1973, 12 September 1973, and 21 September 1973 experiments. The results are shown in Figures 6, 7, and 8. The reduction in relative total cross section shown in Figures 6 and 7 may be accounted for by the reduction in transmitter power during the frequency-sweep section of data. The -6 dB and -7 dB power measurements shown in Figure 6 were calculated from a 10-channel chart recording prepared at the Platteville transmitter site. Each of the ten transmitters has a forward-power meter, and the dc voltage derived from these meters was recorded on 10-channel chart paper. Power-calibration data for Figure 7 were taken from the SRI power-monitor data.

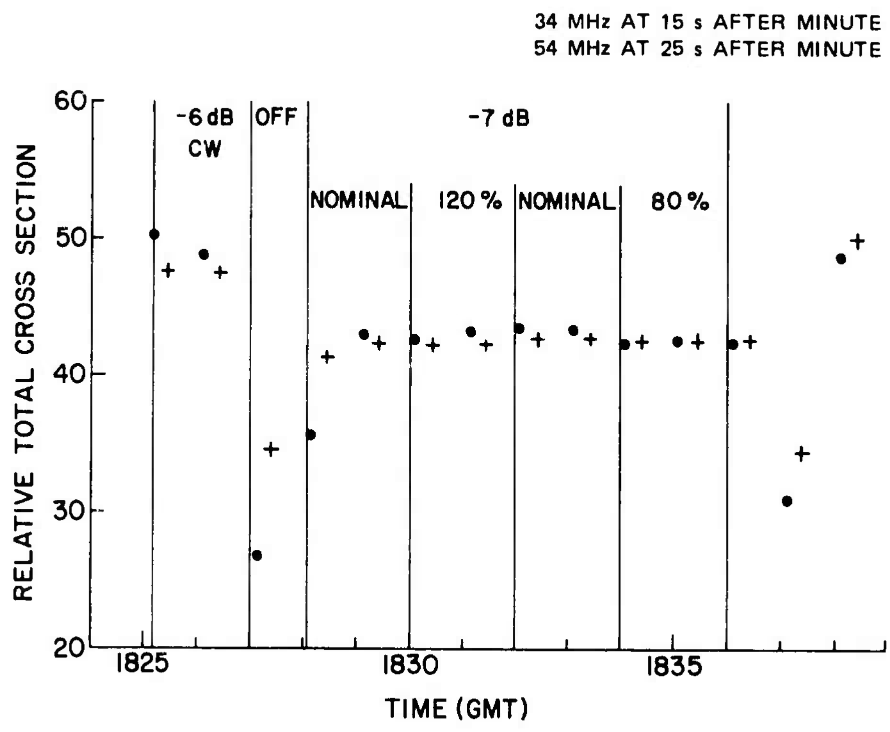


FIGURE 6 SRI RADAR BACKSCATTER DATA FOR 11 SEPTEMBER 1973

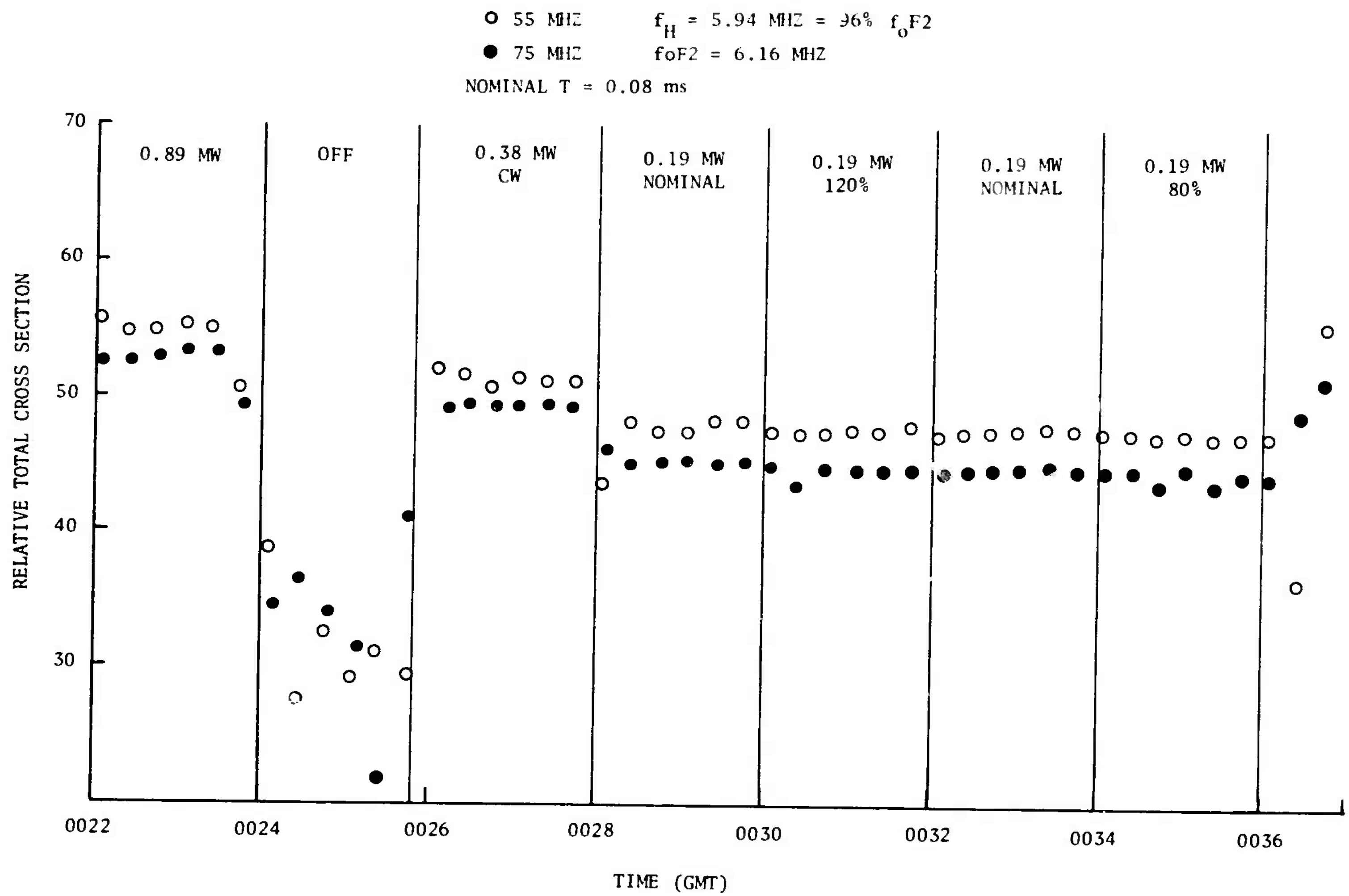


FIGURE 7 SRI RADAR BACKSCATTER DATA FOR 12 SEPTEMBER 1973

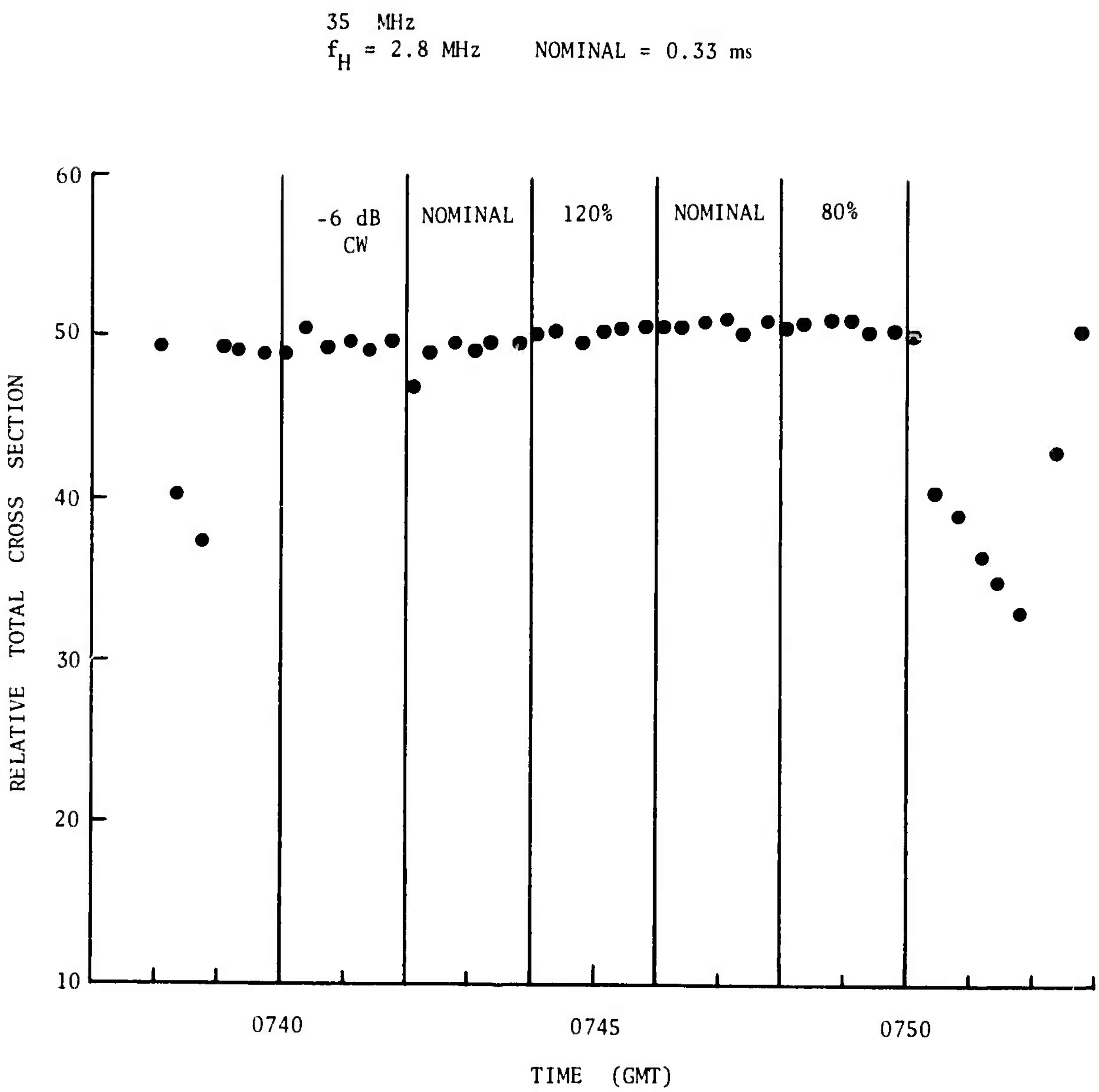


FIGURE 8 SRI RADAR BACKSCATTER DATA FOR 21 SEPTEMBER 1973

These data were provided by SRI in the form of a log of measured transmitter output. More accurate power calibration for the 21 September 1973 data is not available at this time.

It is clear from these plots that no significant change in the relative total cross section occurs due to the frequency sweeping performed during these experiments. Perhaps a more carefully controlled experiment or a different operating procedure would produce more dramatic results.

# THERMAL SELF-FOCUSING OF ELECTROMAGNETIC WAVES IN PLASMAS

F. W. Perkins E. J. Valeo*

Princeton University
Princeton, New Jersey

G. D. Thome

Raytheon Company
Sudbury, Massachusetts

ABSTRACT

An intense electromagnetic wave propagating in a collisional plasma is found to be unstable to a thermal, self-focusing instability by a self-consistent solution of the hydrodynamic, heat-conductivity, and wave-propagation equations. The results are applied to ionospheric modifications and proposed power-transmission experiments, and to laser/plasma interactions. Experimental measurements showing the development of a self-focusing instability in the ionosphere are presented.

Thermal self-focusing can occur when an intense electromagnetic wave propagates through a plasma because the wave-induced heating leads to a temperature increase which in turn causes a hydrodynamic expansion. The concomitant increase in the index of refraction concentrates the radiation in the heated region, further increasing the heating. Although

---

* Presently at Lawrence Livermore Laboratory, Livermore, Calif.

 Pages 186, 187 and 188 are blank

this phenomenon has been recognized for a number of years,[1*] the nonlocal interaction between hydrodynamic motion, thermal conductivity, and wave propagation has prevented the large literature[1] on self-focusing by local nonlinearities in the refractive index from being applied to plasmas. Self-focusing caused by the pondermotive force,[2] which occurs at higher incident intensities[3] than thermal self-focusing, has been investigated, as well as some particular thermal instabilities in plasmas[4] and gases.[5]

This paper treats linear self-focusing instabilities in both overdense and underdense bounded plasmas and applies the results in three situations of current interest: (1) ionospheric modification[6] where intense radio waves are transmitted at an overdense ionosphere, (2) satellite power-generating stations[7] that propose to beam intense microwave ($\lambda_o$ = 10 cm) power through the ionosphere, and (3) laser/plasma interactions.[8]

Our goal is to assess the stability of small-scale perturbations under the influence of heating caused by a plane electromagnetic wave incident on a nonuniform plasma slab. Figure 1 shows the geometry; the linearized equations that govern the motion of the plasma with almost isothermal electrons are

$$\partial\tilde{n}/\partial t = \gamma\tilde{n} = \vec{\nabla} \cdot \widetilde{n\vec{v}} \tag{1}$$

$$nM\gamma\tilde{\vec{v}} = -(T_e + \bar{\gamma}T_i)\vec{\nabla}\tilde{n} - n\vec{\nabla}\tilde{T}_e - nec^{-1}\tilde{\vec{\nabla}} \times \vec{B} - nM\nu_{in}\tilde{\vec{v}} \tag{2}$$

$$(\gamma + \nu_{ie})\ 3/2\ n\tilde{T}_e + nT_e\vec{\nabla} \cdot \tilde{\vec{v}} - \vec{\nabla} \cdot \overleftrightarrow{K} \cdot \vec{\nabla}\tilde{T}_e = \tilde{Q} \tag{3}$$

---

* References are listed at the end of paper.

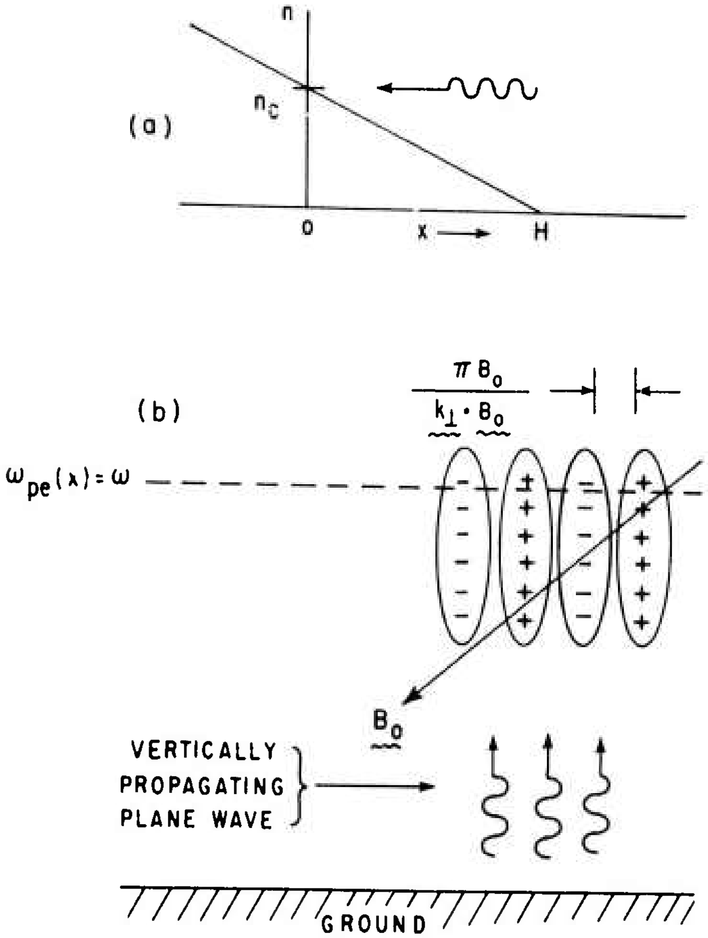


FIGURE 1 GEOMETRY OF SELF-FOCUSING CALCULATIONS. (a) The electromagnetic wave is incident from the right onto a linear density profile. In the overdense case, the critical density occurs at x = 0. (b) Unstable mode in the ionosphere. ( + ) and ( - ) refer to regions of enhanced and depressed plasma density, respectively. Only the projection of the unstable mode in the magnetic-meridian plane is shown; the component of the wave vector $\vec{k}_\perp$ out of the page is much greater.

where $\tilde{Q}$ is the electromagnetic wave heating and $\bar{\gamma}$ the "adiabatic" exponent of the ions. These equations ignore gradients in the zero-order quantities that are characterized by lengths much larger than the perturbations. The heat-conduction tensor is isotropic when $\vec{B} = 0$ (laser-plasma), and one-dimensional when $\vec{B}$ is finite (ionosphere). The last two terms of Eq. (2) enter only in the ionospheric case.

Wave propagation for an incident wave given by

$$E = \frac{1}{2} (\vec{\epsilon}_o + \vec{\epsilon}_1)(k_o/k)^{1/2} \left[\exp\left(i \int_o^x k\, dx + i\omega t\right) + cc\right] \tag{4}$$

is described by the linearized parabolic equation

$$\partial\epsilon_1/\partial x - \left(ik_\perp^2/2k\right)\epsilon_1 = -i\epsilon_o k_o^2 \tilde{n}(x)(\cos k_\perp y)(2kn_c)^{-1} \tag{5}$$

where $k^2 = k_o^2\left(1 - \omega_p^2/\omega^2\right) \equiv k_o^2(1 - n/n_c)$ and the density perturbation is $\tilde{n} = \tilde{n}(x) \cos k_\perp y$. We suppose the heat source to be entirely ohmic heating, ignore attenuation, and include the reflected wave in the overdense case to obtain

$$Q = -\nu_e \epsilon_o^2 n(16\pi n_c)^{-1}(1 - n/n_c)^{-1/2}[k_o L \cos (k_\perp y) I + \tilde{\nu}_e/\nu_e] \tag{6}$$

where

$$I = \begin{cases} \displaystyle\int_x^L \sin [D(x' - x)L^{-1}]\tilde{n}(x')L^{-1}\, dx' & (7) \\[2ex] \displaystyle\sin dV \int_\epsilon^v \cos Dv'\, \tilde{n}(v')dv' + \cos Dv \int_v^2 \sin Dv'\, \tilde{n}(v')\, dv' \quad . & (8) \end{cases}$$

Equation (7) applies to the underdense case ($n \ll n_c$), while Eq. (8) is for the overdense case [$n(0) = n_c$], and

$$\nu_e = 4(2\pi)^{1/2} ne^4 \ln \Lambda \left(3m^{1/2} T_e^{3/2}\right)^{-1} \quad , \qquad v = 2(x/L)^{1/2} \tag{9}$$

$$D = k_\perp^2 L/2k_o \quad , \qquad K = 3.16 T_e n_c/m\nu_e \quad .$$

The first term in the square brackets of Eq. (6) represents the WKB heat source (i.e., averaged over fast spatial and temporal scales) due to the interference between the pump and perturbation electromagnetic waves. The parabolic equation allows us to treat both the refraction ($D \ll 1$) and diffraction ($D \gg 1$) limits. The last term of Eq. (6) is negligible. The small cutoff length $\epsilon \sim (k_o L)^{-1/3}$ prevents divergences that arise because the WKB approximation to the heat source blows up at the reflection point.

Consider first the overdense laser/plasma case with $k_\perp \ll k_o$ and $k_\perp^2 K \gg \gamma n$. Then transverse gradients dominate x-gradients and one obtains the eigenvalue equation

$$\tilde{n}(v) = \lambda \left[1 - (v/2)^2\right]^2 v^{-1} I \tag{10}$$

where I is given by Eq. (8) and

$$\lambda = v_e \epsilon_o^2 k_o L \Big/ \left[M\left(\gamma^2 + \omega_s^2\right) 8\pi K\right] \quad ; \qquad \omega_s^2 = k_\perp^2 (T_e + \bar{\gamma} T_i) M \quad .$$

Since $\tilde{n}(v)$ is discontinuous at $v = \epsilon$, in reality there is a small region $|x| \lesssim k_\perp^{-1}$ for which the transverse derivatives do not dominate the x-derivatives; however, this region is sufficiently small to be neglected.

Substituting $\psi = \tilde{n} v \left[1 - (v/2)^2\right]^{-2}$ into Eq. (10), and using the approximation $\left[1 - (v/2)^2\right]^2 \approx 1$ (valid over most of the range of v), we recast the eigenvalue problem into a differential equation

$$\psi'' + D^2 \psi = \lambda D v^{-1} \psi \tag{11}$$

whose boundary conditions are given by Eq. (10) combined with Eq. (11):

$$\psi'(\epsilon) = 0 + O(\epsilon) \quad ; \qquad \psi(\epsilon) = \lambda \int_\epsilon^2 v^{-1}\, dv \sin Dv\, \psi(v) \quad . \tag{12}$$

The eigenvalue can be found by the following arguments. Assume $\lambda \sim |\ln(\epsilon)|^{-1/2} \ll 1$, and let the two solutions valid near $v = 0$ be

$$\psi_0 = 1 + Dv \ln v + \ldots \quad ; \quad \psi_1 = Dv + \ldots \tag{13}$$

and let $\psi = \psi_0 + A\psi_1$. Then Eq. (12) gives $A = \lambda \ln(1/\epsilon)$. Because $\lambda \ll 1$, $\psi_1 \approx \sin Dv$ and Eq. (12) yields

$$1 = \lambda^2 \ln(1/\epsilon) \int_0^2 v^{-1} dv \sin^2 Dv + \lambda \int_0^2 v'^{-1} dv \sin Dv \, \psi_0(v) \quad . \tag{14}$$

The second term on the right-hand side of Eq. (14) is of order $\lambda$, and can be ignored to obtain

$$\lambda^2 = \left[\ln(1/\epsilon) \int_0^{2D} x^{-1} dx \sin^2 x\right]^{-1} \quad . \tag{15}$$

As a rule, the thermal conduction rate exceeds the growth rate and the desired result is

$$\gamma^2 = \frac{D\nu_e^2}{3.16}\left(\frac{m}{M} k_o L\right)\left\{\frac{\epsilon_o^2}{8\pi n_c T_e}\left(\frac{1}{\lambda D}\right) - \frac{6.3\lambda_{mfp}^2}{L^2}\left(1 + \bar{\gamma}\frac{T_i}{T_e}\right)\right\} \tag{16}$$

where $\lambda_{mfp} = (T_e/m)^{1/2} \nu_e^{-1}$ .

It is evident that: (1) self-focusing instabilities can occur for weak incident fields provided $\lambda_{mfp}/L \ll 1$, and (2) the growth rate exceeds the heating rate provided $\epsilon_o^2/8\pi n_c T_e \leqslant k_o Lm/M$. Although a true laser-fusion plasma may be sufficiently collisionless to avoid self-focusing instabilities, preliminary experiments may well be collisional.

In the parlance of nonlinear optics,[5] this instability is stimulated Rayleigh scattering by the entropy mode transformed into a nonconvective instability by the reflected wave.

The satellite microwave beam[7] lacks the feedback provided by the reflected wave and instabilities change from the absolute to the spatial gain variety. Let us consider a case where $\vec{k}_\perp$ is not precisely orthogonal to $\hat{b} = \vec{B}/B$ and satisfies the inequality $\vec{k}_\perp \cdot \hat{b} \gg DL^{-1}$. Consequently, $\vec{k}_\perp$-derivatives dominate in the hydrodynamic and thermal-conductivity equations. The eigenvalue equation that results is for $\psi = \tilde{n} n_M^2 / n^2$:

$$\psi(x) = \lambda \int_x^L \sin[DL^{-1}(x - x')]\psi(x')[n(x')/n(0)]^2 \, D dx' \qquad (17)$$

where, in the limit of rapid thermal conduction,

$$\lambda = \frac{\nu_e \epsilon_o^2 k_o L}{8 K D M \nu_{in}\left[\gamma + (\vec{k}_\perp \cdot \hat{b})^2 2T/M\nu_{in}\right]} \left(\frac{n_M}{n_c}\right)^2 \qquad (18)$$

and $n_M$ is the maximum plasma density. Spatially amplifying functions that solve Eq. (17) have a spatial growth rate $\alpha = (\lambda - 1)^{1/2} D$. Letting $\lambda = 1$, $\gamma = 0$ and $\hat{k}_\perp \cdot \hat{b} = DL^{-1}$ gives the threshold field for self-focusing

$$\epsilon_o^2 c/8\pi > D^3 (n_M T_e c)\left(\lambda_o \lambda_{mfp}^2 / L^3\right)(n_c/n_M)^2 = D^3 (1 W/m^2) \qquad (19)$$

a flux substantially less than the proposed fluxes of $\sim 800$ W/m$^2$. Such a flux produces a growth rate $\gamma \sim 10^{-1}$ s$^{-1}$ (for D = 5) and can double the ionospheric temperature in $\sim 3$ s.

The ionospheric-modification configuration has a reflected wave that creates an absolute instability but the electron thermal conductivity and ion motion are field-aligned. In this case, the inequality $\vec{k}_\perp \cdot \hat{b} \gg 4D^2L^{-1}$ allows the $\vec{k}_\perp$-derivatives to dominate and the eigenvalue equation is precisely Eq. (9) but with the eigenvalue defined in the limit of rapid thermal conductivity by

$$\lambda = \frac{\nu_e \varepsilon_o^2 k_o L}{8\pi K M \nu_{in}\left[\gamma + 2T(\vec{k}_\perp \cdot \hat{b})^2/M\nu_{in}\right]} \quad . \tag{20}$$

Setting $\vec{k}_\perp \cdot \hat{b} = 4D^2L^{-1}$ and using Eq. (15), one obtains the instability condition

$$\varepsilon_o^2 c/8\pi > 20D^4\lambda(D)(n_M T_e c)\lambda_{mfp}^2\lambda_o/L^3 = D^4\lambda(D)\ 0.4 \quad , \qquad \mu W/m \quad .$$

This condition applies only for $D \geq 2$, since otherwise $\vec{k}_\perp \cdot \hat{b}$ is unrealistically small. The 50-$\mu W/m^2$ incident flux in the Boulder experiment[6] easily exceeds this threshold value, and, for $D = 2$, $\gamma \approx 0.5\ s^{-1}$, $k_\perp^{-1} \approx 4.10^2$ m, in agreement with observations.

Figures 2 and 3 present data that show the development of ionospheric field-aligned density striations initiated by intense radio-wave heating. In particular, the longer group delays associated with propagation along the magnetic field establish the field-aligned nature of the instability. On the other hand, the plasma density fluctuations in our model are vertical, but have $\vec{k} \cdot \hat{b}$ almost zero because the wave vector is very nearly in the magnetic east-west direction. Since the assumptions of our model are partially motivated by a desire for mathematical tractability, there may be lower thresholds. But we have established that unstable self-focusing modes exist.

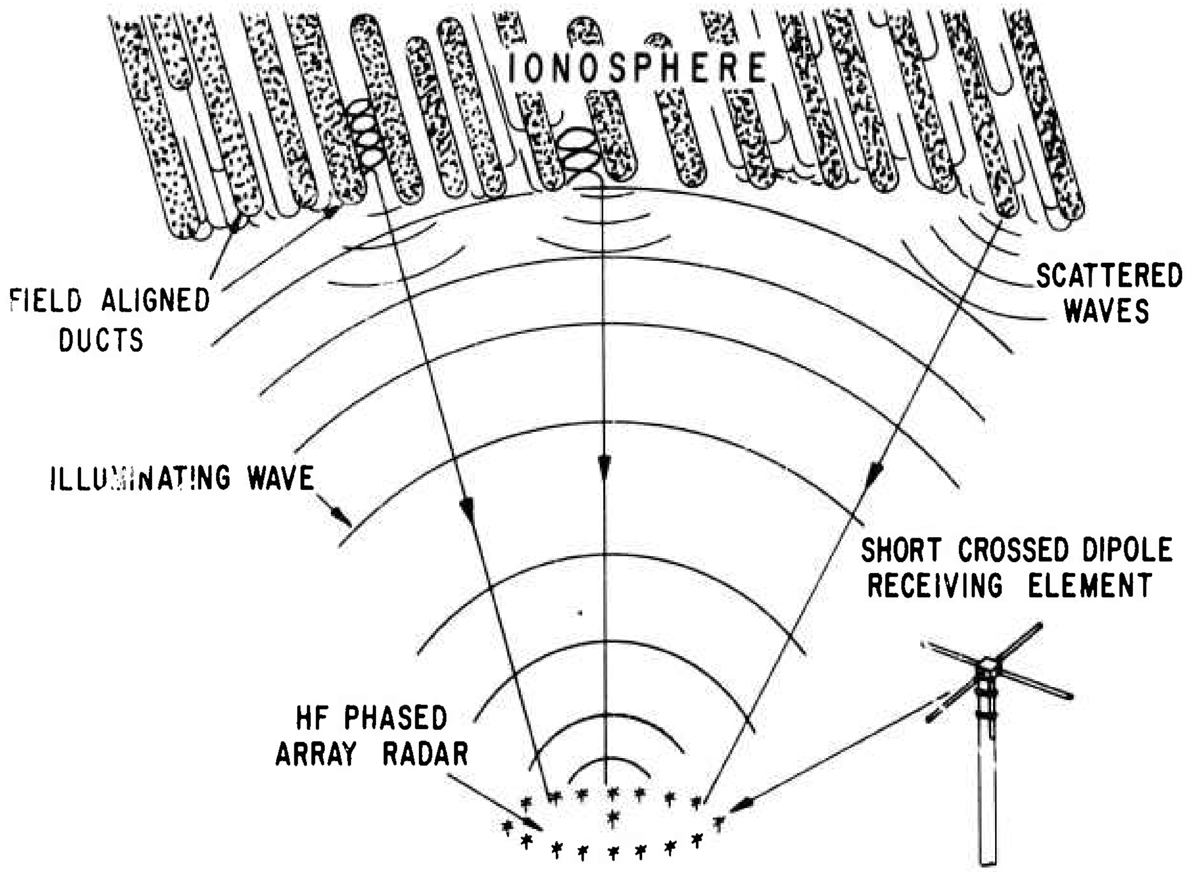


FIGURE 2 PHASED RING-ARRAY IONOSPHERIC SOUNDER. An extraordinary-mode signal is transmitted at the overdense ionosphere by the central element in a series of pulses that vary in frequency. The ring array of 32 receivers records the amplitude and phase of the echo received at a delay $\tau$. The amplitude and phases are analyzed by computer to give the echo intensity and direction of arrival.

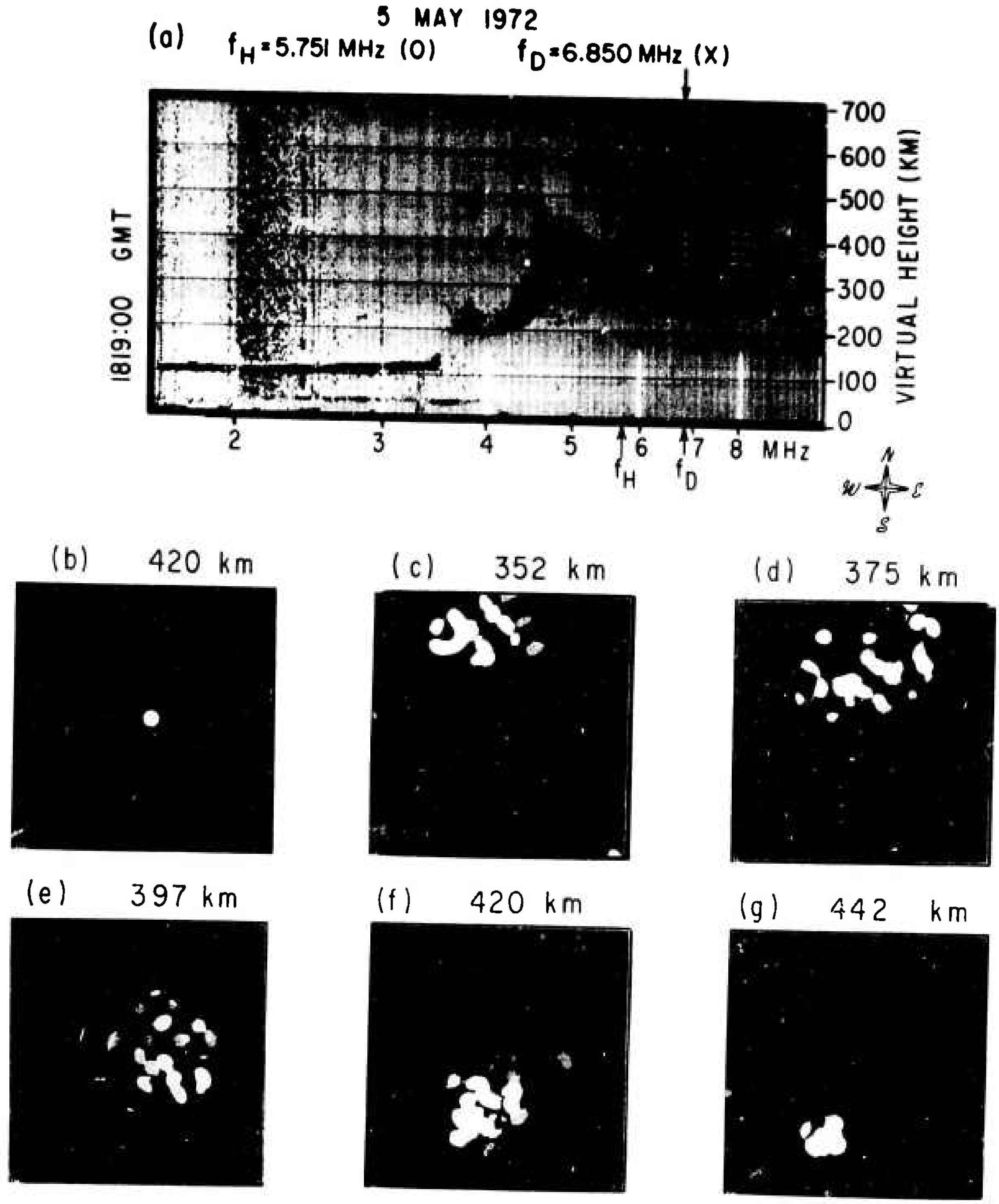


FIGURE 3 RESULTS OF THE RING-ARRAY EXPERIMENT. (a) Conventional ionosound record of the heated ionosphere. (b) Ring-array results showing intensity (whiteness) vs. zenith angle and azimuth. This result shows the ionosphere before heating; it is stratified with a slight tilt. (c) through (g) Echoes in the heated ionosphere at various "virtual" heights $h' = c\tau/2$.

In summary, overdense collisional plasmas subject to intense electromagnetic radiation develop absolute thermal self-focusing instabilities (stimulated Rayleigh scattering). We submit that ionospheric artificial Spread-F results from self-focusing and hence differs from natural Spread-F which may be caused by another instability.[9] In the laser/plasma system, self-focusing will cause ripples in the critical-density surface and increase the sideways scattering.

## ACKNOWLEDGMENTS

Informative discussions with S. Bowhill, J. Dawson, J. Fejer, P. Kaw, N. Kroll, G. Meltz, F. Tappert, and N. Tomljanovich have greatly benefited this paper. We are especially indebted to M. Rosenbluth for help with the eigenvalue problem.

This work was supported by U.S. Air Force Office of Scientific Research Contracts F44620-70-C-0033 and F44620-73-C-0026 and by the Defense Advanced Research Projects Agency.

## REFERENCES

1. S. A. Akhmanov, A. P. Sukhorukov, and R. V. Khokhlov, Usp. Fiz. Nauk, Vol. 93, No. 19 (1967), [Sov. Phys., Usp. 10, p. 609 (1968).], UNCLASSIFIED.

2. A. G. Litvak, ZhETF, Vol. 57, p. 629 (1968), [Sov. Phys. JETP, Vol. 30, p. 344 (1970)], UNCLASSIFIED.

3. F. W. Perkins, Bull. Am. Phys. Soc., Vol. 18, p. 1335 (1973), UNCLASSIFIED.

4. B. G. Eremin and A. G. Litvak, ZhETF Pis. Red., Vol. 13, p. 693 (1971), [JETP Letters, Vol. 13, p. 430 (1971)]; A. G. Litvak, "Phenomena in Ionized Gases," Contributed Papers, Vienna, 1967, p. 409, UNCLASSIFIED.

5. N. M. Kroll and P. L. Kelley, Phys. Rev., Vol. A4, p. 763 (1971), UNCLASSIFIED.

6. W. F. Utlaut and R. Cohen, Science, Vol. 174, p. 245 (1971), UNCLASSIFIED.

7. W. C. Brown, IEEE Spectrum, Vol. 10, p. 38 (1973), UNCLASSIFIED.

8. K. A. Brueckner, IEEE Trans. on Plasma Science, Vol. PS-1, No. 13 (1973); J. Nuckolls, J. Emmett, and L. Wood, Physics Today, Vol. 26, No. 8, p. 46 (August 1973), UNCLASSIFIED.

9. F. Perkins, J. Geophys. Res., Vol. 78, p. 218 (1973), UNCLASSIFIED.